THE ELECTRICAL PERFORMANCE OF CERAMIC DIELECTRICS AT ELEVATED TEMPERATURES

- o O o -

It is well known that the electrical resistance of most of the commonly used insulating materials diminishes with increasing temperature. The actual performance of ceramic insulating materials at temperatures above the normal atmospheric level, and the factors affecting the ultimate breakdown at these temperatures, has not been the subject of much investigation. Recent requirements for insulators to operate at high temperatures and high voltages have indicated the need for such information.

Apparatus and Method.

It was necessary to provide a suitable test chamber in which the specimens could be mounted and held at any desired temperature while voltage was applied. Accordingly, a thermally insulated box or furnace was built. The electrical heating elements in the back of the box were separated from the test chamber by a one inch thick thermally insulating partition in order to prevent direct heating of the specimens by radiant heat. The heated air was circulated by means of a fan thru ports at each end of the test chamber. The fan also served to maintain air turbulence in the test chamber and thus prevent stratification. Temperature measurements were by commercial gas thermometer and automatic controls were provided for holding any desired temperature between minus 100 degrees Fahrenheit and 1000 degrees Fahrenheit. With this arrangement temperatures could be held within five degrees Fahrenheit of the desired level. Provision was also made for removing the heating elements from the back of the box and substituting racks of dry ice in order to obtain low temperatures.

Most of the tests were made with d-c voltage in order to eliminate the difficulty of separating conduction currents from charging currents. The voltage source was a full wave high voltage kenetron rectifier with suitable capacitors for the elimination of the sixty cycle pulse.

The d-c voltages were measured by means of a suitable known resistance connected in series with a microammeter.

Most of the test specimens were prepared in the form of plates of various thicknesses. Some specimens were made from standard suspension insulator shells using the head section, ground down to the desired thickness, as the test area.

Electrodes of circular shapes were applied to the opposite sides of each test specimen. Guard rings were also provided to eliminate the effect of surface leakage and corona, and to preserve a more nearly uniform field thru the test zone. The electrodes and guard rings were of silver ceramically bonded to the surface of the dielectric to avoid entrapped air between the dielectric and its electrode.

Resistance measurements were made by connecting one electrode to the voltage source and grounding the opposite electrode thru a microammeter of milliammeter of proper scale range for the current involved. Suitable selector switches were provided for switching quickly from one instrument to another. The guard ring connections were shunted around the ammeters to ground. Resistance was determined from the ratio of voltage to current.

Before each measurement was made, the specimen was allowed to stand in the test chamber at zero voltage and constant temperature for a sufficient length of time to be sure that it was uniformly heated thruout its volume.

Materials:

The greater part of this investigation is concerned with porcelain, although some data has been obtained on two kinds of glass, a steatite composition, and a Zircon composition.

These are all generic names and there is considerable latitude in composition and in physical structure within each category.

The porcelain specimens involved were all made of wet process feldspathic porcelain of the type commonly known as "electrical porcelain". Samples of such porcelain as made by three different manufacturers were used.

The steatite specimens were a magnesia, alumina, silicate composition maturing at a firing temperature of about 2250 degrees Fahrenheit. The Zircon specimens were composed basically of Zirconia silicate with a calcium - zirconium - silicate flux compounded to mature at 2250 degrees Fahrenheit. This composition was developed particularly for high temperature applications.

Two types of glass specimens were included; a boro-silicate glass of the type used in the manufacture of high voltage insulators, and a lead glass also sometime used in certain classes of insulators.

Discussion of Data - Porcelain.

Many measurements were made on a variety of specimens of varying shapes and thicknesses, at temperatures ranging from minus 70 degrees Fahrenheit to 900 degrees Fahrenheit and at voltage gradients up to 700 volts per mil. A gratifying degree of consistency in results was obtained. Typical data illustrating the results obtained are presented herein. As an example, the curve, Figure 2, is typical of the measurement made to determine the variation of resistivity with temperatures and to determine the temperature at which final breakdown would occur. In plotting the curve the measured total resistances have been reduced to resistivity in megohms per inch cube. It should be noted that as the temperature was increased the resistivity steadily declined but remained stable (within the limits of measurement) at each point up to 250 degrees Fahrenheit. At 250 degrees Fahrenheit, on this particular specimen, it was found that with constant voltage the resistivity declined slowly with time, finally becoming stable at a lower level after about 45 minutes. This change in resistivity with time is indicated in Figure 2 by superimposing a time axis on the curve. The variation in resistivity with time, for a constant ambient temperature corresponding to that at zero time, is indicated by a broken line. This decline in resistance with time is undoubtedly caused by the internal heating of the specimen above the surrounding air due to the I^2R loss.

It represents an average internal temperature rise of about 20 to 25 degrees Fahrenheit.

When the test chamber temperature was raised to 300 degrees Fahrenheit and held constant, the resistivity, with constant applied voltage, diminished with increasing rapidity until after 12 minutes the specimen would no longer support voltage and had, for all practical purposes, failed electrically. At this point voltage was removed but the test chamber was still held at a constant temperature of 300 degrees Fahrenheit. At intervals of 5 minutes the same voltage was momentarily reapplied and readings were quickly taken. It should be noted that as the specimen cooled internally the resistivity recovered along a typical cooling curve.

The test chamber temperature was then raised to 325 degrees Fahrenheit and the same voltage reapplied. The resistivity again declined still more rapidly with time, and within 5 minutes reached the point where voltage could not be supported. Voltage was then removed and the piece was again allowed to recover. The test chamber temperature was raised to 350 degrees Fahrenheit and a momentary reading taken as indicated on the curve. The test chamber was allowed to cool back to room temperature and the resistivity was again measured checking the value determined at the start of the test.

On this particular specimen voltage was removed in each case as soon as a runaway condition was observed as indicated by current increasing more and more rapidly. On some other specimens voltage was not promptly removed and power was delivered to the piece for several seconds after the runaway phenomenon was observed. In such cases the dielectric was cracked or a fused path developed thru it resulting in a permanent failure.

The Curve Figure 2 illustrates the variation of resistivity with temperature for one particular porcelain specimen at a constant voltage gradient. At any temperature level the resistivity may also vary with changing voltage gradient. This effect was studied on a number of porcelain specimens and Figure 3 is a typical plot of the data obtained on one particular specimen -- the same specimen appearing in Figure 2. It should be noted that at the lower temperatures resistivity diminishes rather rapidly with increasing voltage gradient but at temperatures above 250 degrees Fahrenheit, the resistivity becomes nearly independent of voltage gradient.

The results of all measurements made on porcelain to determine the variation of resistivity with temperature was plotted on one composite curve (Figure 4). At the higher temperatures it was necessary to make all tests at relatively low voltage gradients in order to obtain stable measurements. Thus at 900 degrees Fahrenheit the measurements were made on a specimen approximately o.8 inch thick with voltage applied from a 45 volt battery equivalent to about 0.05 volts per mil. At these higher temperatures the resistivity changes but little with changing voltage gradient so this limitation does not impair the usefulness of the information contained in Figure 4.

An examination of Figure 4 shows that the data conforms with reasonable accuracy to a single curve for all temperatures above about 250 degrees or 300 degrees Fahrenheit. At lower temperatures the composite data spreads widely as indicated by the envelope shown. This spread of the data at the lower temperatures is due primarily to two factors. First the influence of voltage gradient on resistivity at lower temperatures and second the influence of specimen thickness.

In order to identify the relative influence of these two factors Figures 5 to 9 inclusive have been prepared. Each of these curves is prepared for one nominal specimen thickness and the measurements at various gradients are segregated. In a similar manner Figures 10 to 16 inclusive illustrate the variation in the resistivity of porcelain as a function of the voltage gradient for different thicknesses and temperatures. The apparent effect of thickness on resistivity is believed to be due to the variation of the true voltage gradient from the average voltage gradient. As the specimen thickness increases it becomes more and more difficult to maintain a truly uniform voltage gradient thru it.

It has been pointed out that porcelain made by three different manufacturers was used in the investigation. No significant difference was found between the three porcelains. Figure 17 shows a typical comparison of dimensionally identical pieces as made by two manufacturers. These two pieces were tested simultaneously. The change in resistivity with time (due to internal heating and cooling) is shown on the curve in the same manner as in Fugure 2. At 300 degrees Fahrenheit, voltage was applied for 10 minutes at which time the resistivity had become stable. Voltage was then removed and the specimen allowed to cool back to the test chamber temperature. Voltage was then reapplied and a duplicate heating curve was obtained. At 325 degrees Fahrenheit both specimens drifted towards breakdown. Specimen B actually refused to support voltage but specimen A was well on the way to the same condition and would doubtless have failed in another minute or two had the test been continued. It should be noted that at 325 degrees Fahrenheit, both of the resistivity drift curves pass thru a definite flex point where the shape of the drift curve changes from concave upward to concave downward. After the breakdown at 325 degrees Fahrenheit, the pieces were allowed to cool and the test chamber temperature was raised to 350 degrees Fahrenheit. At this level both specimens drifted rapidly to breakdown in about 3 minutes.

Effect of Glaze.

All data which has been discussed up to this point has been obtained on unglazed specimens. In order to determine the effect of glaze on the high temperature performance of porcelain, two cylinders were prepared 1-1/8" in diameter and 2-1/4" long. One of these cylinders was glazed with a standard glaze of the type normally applied to high voltage insulators. The other cylinder was left unglazed. Silver electrodes were applied and ceramically bonded to each end of each cylinder. The silver coatings were carried over the ends and extended down the side walls on each end for a distance of 5/16". This was done in order to place the highest voltage gradient along the outer glazed surface. Figure 18 shows the results of a simultaneous test made on these two pieces. The resistance of the two was practically the same thruout the test and both pieces drifted to failure at 410 degrees Fahrenheit. Note that this curve is plotted with total resistance and not resistivity as ordinates.

Some Practical Insulators.

The porcelain element of a practical corrugated rod or "stand-off" insulator, glazed in the usual manner, was tested with silver electrodes ceramically bonded to each end. The electrodes covered the entire end area but did not extend down over the sides. Figures 19 and 20 show respectively variation in total resistance as a function of temperature and average voltage gradient. On Figure 19 measurable drift of resistance due to internal heating was first noticed at 350 degrees Fahrenheit and at 40 Kv applied voltage but stability was reached in about 20 minutes. At 400 degrees Fahrenheit drift was measurable at 20 kv and 30 kv applied voltage, but in each case stability was reached after a time interval. At 400 degrees Fahrenheit and 40 kv, drift started and progressed with increasing speed to ultimate failure in 45-1/2 minutes. At this point the insulator would not support voltage and was found upon cooling and removal to be mechanically broken from the differential expansion. In order to avoid confusion in Figure 19 the drift curves are not shown.

A standard 23 kv heavy duty outdoor two shell switch insulator was tested completely assembled with its regular metallic parts cemented in place in the usual manner. This unit was tested with 14 kv d-c- applied between cap and pin. This is numerically the same as the r.m.s. normal service voltage to ground. Figure 21 shows the variation in total resistance with temperature. In this insulator the conduction path from top to bottom metallic elements passes thru three layers of portland cement and two layers of porcelain. It should be noted that the initial measurement made at 80 degrees Fahrenheit is considerably below the curve as drawn and also is lower than the second point at 150 degrees Fahrenheit. This peculiar performance is believed to be due to the variation in resistance of the cement. Portland cement is quite hygroscopic and when slightly moist is a fairly low resistance conductor. As the water is driven off, however, its resistance increases so that at elevated temperatures it adds in some measure to the total resistance of the insulator. The high temperature end of the curve is two pronged representing the results from two separate tests. Note that drift curves became measurable on one curve at 350 degrees Fahrenheit and on the other at 400 degrees Fahrenheit, reaching stability in each case after about 40 minutes. At 450 degrees Fahrenheit the insulators drifted to failure in 20 and 35 minutes respectively.

A similar insulator was subjected to test at 14 kv r.m.s. 60 cycles. This test was made by raising the temperature in 50 degree Fahrenheit steps and holding the voltage and temperature constant for one hour at each step. Due to the difficulties of separating conduction from charging currents, no resistance measurements were made. The unit failed after 54 minutes at 400 degrees Fahrenheit. A number of other a-c tests have been made on other porcelain samples, the results of which will be discussed later.

Discussion of Data: - Glass.

In Figure 22 are plotted the measurements of the resistivity of boro silicate glass as a function of temperature. This particular glass specimen was the glass element only of a suspension insulator. Silver electrodes with guard ring were applied to the head area. At 85 volts per mil and 350 degrees Fahrenheit, the specimen drifted to breakdown in about 3 minutes. At the instant of failure the specimen was shattered by the forces of differential expansion.

On Figure 23 the variation of resistivity of the same specimen is shown as a function of voltage gradient.

Similarly Figures 24 and 25 show the performance of a specimen made of a lead glass. This specimen drifted towards failure at 40 volts per mil at 600 degrees Fahrenheit after about 3 minutes, but upon cooling recovered and was not permanently injured. At 650 degrees Fahrenheit and 20 volts per mil the same specimen showed a definite downward drift in resistivity due to internal heating but stabilized after about 10 minutes. At 650 degrees Fahrenheit and 30 volts per mil the piece drifted to failure in about 8 minutes. In this case power was not removed quickly enough and a permanent failure occurred taking the form of a fused path thru the glass.

Discussion of Data: - Steatite.

The results of tests on two steatite specimens are shown in Figure 26. Note that for two voltage gradients, 20 and 40 volts per mil, the curves virtually coincide. Both specimens initially drifted towards failure after 15 and 17 minutes respectively at 700 degrees Fahrenheit and 40 volts per mil. The pieces were cooled back to test chamber temperature and recovered. At 750 degrees Fahrenheit both specimens failed at 20 volts per mil after 9 and 10 minutes respectively.

There is not sufficient data to plot the variation in resistivity of this steatite composition as a function of voltage for various temperature levels. In Figure 27 such data is plotted for one temperature only.

Discussion of Data:- Zircon.

Several Zircon compositions were investigated and it was found that the high temperature electrical characteristics of the several compositions varied radically. The particular zircon composition included in this paper is the one having the best characteristics of the group tried. Figure No. 28 gives the variation in resistance as a function of temperature with a voltage gradient of 40 volts per mil. Figure 29 shows the variation in resistance as a function of voltage gradient for various temperatures.

There are two characteristics of this material which are worthy of particular note. In the first place it is observed that in certain ranges increasing voltage gradient results in slight increases in the measured resistance. Such a condition was not observed on any of the other materials nor even on the other Zircon specimens having slightly different composition. Secondly it was observed that, at any fixed temperature above about 400 degrees Fahrenheit when a constant voltage was applied, an initial current was measured which diminished with time finally stabilizing at a value lower than the initial. In other words the measured resistance increased with time. This is exactly opposite to the performance of the other materials. At the lower temperatures, around 500 degrees Fahrenheit this upward drift of resistance reached stability in about one minute with a rise in resistance of about 3 to 4 percent. At higher temperatures, about 800 degrees Fahrenheit, the upward drift of resistance reached stability in several minutes with rise in resistance of about 30 percent. At 800 degrees Fahrenheit and at higher voltage gradients, 60 volts per mil, stability was reached only after 20 minutes with a rise of more than 100% of the initial value. This characteristic continued up to 900 degrees Fahrenheit, the upper limit of the test, and no breakdowns were obtained.

These two unusual characteristics of this material are believed to be due to dielectric polarization. The curves Figures 28 and 29 are plotted to show the resistance at each level for the polarized or stable condition.

Theoretical Considerations.

From an engineering standpoint it is most important that one be able to determine the temperature and voltage at which a particular insulator may be safely operated without failure. To accomplish this with some reasonable knowledge of the margin of safety, the end point conditions should be predictable. Therefore some theoretical discussion of the mechanism of breakdown is in order.

From the data it seems reasonably conclusive that, at least at elevated temperatures (250 degrees Fahrenheit and above), breakdown is a thermal phenomenon. When voltage is applied to a dielectric a leakage or conduction current flows thru the material and the I^2R loss results in internal heating above the ambient temperature. This increase in internal temperature results in a reduction of resistivity with consequent increase in internal heating, if a constant applied voltage is maintained. As the internal temperature rises above the ambient, heat is dissipated from the stressed volume. In most practical applications thermal conduction is the principal means of heat dissipation from the stressed volume. The power dissipated as heat from any point in the stressed volume is therefore a function of the internal temperature rise. If the power dissipated as heat increases more rapidly as the temperature rises, than does the power input, the time rate of temperature rise will diminish and a condition of stability will be obtained. If the reverse condition occurs the temperature will rise with increasing rapidity until the dielectric fuses or is cracked by differential expansion stresses.

Consider an elemental cube (Figure 30) in the dielectric body. Let the volume of this cube be ΔV and the edge dimensions be $\Delta x, \Delta y$ and Δz. Let the direction of voltage gradient be parallel to the Y axis thru the elemental cube. If the voltage gradient thru the cube in volts per inch is E and if the resulting current density is I amperes per square inch then, P_{T1}, the total power input to the cube is

$$P_{T1} = (E\Delta y)(I\Delta x\Delta z) = EI\Delta V$$

If the resistivity of the material is r ohms per inch cube

$$P_{T1} = \frac{E^2}{r}\Delta V$$

The power input per unit volume = $P_1 = \dfrac{P_{T1}}{\Delta V} = \dfrac{E^2}{r}$ ①

If the total power output from the cube in the form of heat is P_{T2}, then

$$P_{T2} = \int_s K\nabla T\cdot \underline{n}\, d\sigma$$

Where T is the temperature rise of the cube above the ambient and where ∇T is the temperature gradient outward from the cube, $d\sigma$ is any element of surface of the cube, n is a unit vector normal to that element of surface, and K is the thermal conductivity of the material.

The power output per unit volume = $P_2 = \dfrac{P_{T2}}{\Delta V}$

$$P_2 = \frac{K}{\Delta V}\int_s \nabla T\cdot \underline{n}\, d\sigma$$

Taking the limit as ΔV approaches zero

$$P_2 = K\nabla^2 T \quad ②$$

The term $K\nabla^2 T$ cannot be exactly evaluated from theoretical considerations alone. However, this term merely represents the power output in the form of heat from a small element in the stressed volume. In any practical insulator as soon as a voltage is applied, some element within the stressed volume begins to heat slightly faster than its immediate surroundings. This may be because the element is at the center of the volume where heat loss is the slowest or it may be because of variations in voltage gradient, or because of variations in the homogenity of the material. As soon as the element in question begins to rise in temperature above that of the surrounding stressed volume, its resistivity diminishes and consequently its rate of heating is further increased. A "hot spot" is therefore quickly established and it is this hot spot which is of primary concern. Equation (2) may be applied to represent this heat loss from the critical element and by making certain reasonable assumptions may be reduced to a more useful form. Since the surface area of any practical insulator is relatively large and since the thermal conductivity of the material under consideration is relatively small, it may be assumed thatthe rate of heat loss from the critical volume is directly proportional to the temperature rise above the ambient. For these assumptions equation (2) may be written,

$$P_2 = K\alpha T \quad ③$$

Where T is the temperature rise of the element and α is the factor of proportionality.

At any point of stability P_2 must equal P_1

When voltage is first applied T = o and consequently P_2 = o. As T increased, P_1 and P_2 both increase. If, with increasing temperature T, P_1 continuously increases faster than P_2 stability can never be reached and the temperature will continue to rise until failure occurs.

Conversely if P_2 continuously increases faster than P_1, a condition of equilibrium will ultimately be reached where $P_2 = P_1$.

The rate of increase of P_1 with respect to temperature T is

$$\frac{\partial P_1}{\partial T} = -\frac{E^2}{r^2}\frac{\partial r}{\partial T}$$

Since, for the materials under consideration, $\frac{\partial r}{\partial T}$ is negative, this shows a positive value for the product -

$$-\frac{E^2}{r^2}\frac{\partial r}{\partial T}.$$

The rate of increase of P_2 with respect to temperature is

$$\frac{\partial P_2}{\partial T} = K\frac{\partial(\nabla^2 T)}{\partial T} \approx K\alpha \qquad \textcircled{4}$$

The conditions leading to ultimate breakdown are illustrated in Figure No. 31. The power input when voltage is first applied at ambient temperature T_o is represented by P_1. As the internal temperature rises the power input increases as shown. The power output is initially zero but increases as internal temperature rises. If the P_2 curve intersects the P_1 curve, stability is reached. If the P_2 curve fails to intersect the P_1 curve runaway and breakdown ultimately occur.

If the power input (P_1) curve is concave upwards then the critical point will be reached when the starting temperature T_o is such as to make the P_2 curve reach the P_1 curve at a point of tangency. This occurs at some critical temperature T_o and with power input P_1'' as illustrated in Figure 31.

At this point

$$\frac{\partial P_1}{\partial T} = \frac{\partial P_2}{\partial T}$$

or

$$-\frac{E^2}{r^2}\frac{\partial r}{\partial T} = K\alpha \qquad \textcircled{5}$$

The initial ambient temperature T_o necessary to ultimately reach the critical condition is lower than T_c by an amount equal to P_1 divided by $K\alpha$.

If the power input curve (P_1) is concave downwards then the P_2 curve will always intersect it at some point and with some theoretical finite temperature rise above the ambient. Whether or not failure occurs then depends upon whether the temperature at this point of intersection is within the range which the dielectric can stand without fusing, cracking or charring. It is perfectly possible that the power input curve may be in some zones concave upward and in other zones concave downward with a flex point as illustrated by the broken line in Figure 31.

Equation (5) may therefore be applied only when the second derivative of power input with respect to temperature is positive at the critical point.

$$\frac{\partial^2 P_1}{\partial T^2} = -\frac{E^2}{r^2}\frac{\partial^2 r}{\partial T^2} + \frac{2E^2}{r^3}\left(\frac{\partial r}{\partial T}\right)^2$$

This term is always positive when $\frac{\partial^2 r}{\partial T^2}$ is negative. If $\frac{\partial^2 r}{\partial T^2}$ is positive the term is positive only when

$$\frac{E^2}{r^2}\frac{\partial^2 r}{\partial T^2} < \frac{2E^2}{r^3}\left(\frac{\partial r}{\partial T}\right)^2$$

$$\frac{\partial^2 r}{\partial T^2} < \frac{2}{r}\left(\frac{\partial r}{\partial T}\right)^2 \qquad \textcircled{6}$$

The values of r and of the first and second partial derivatives can be physically determined from the temperature - resistivity curve of any material. For porcelain, the steatite composition and the two glasses the relation (6) is satisfied within the range investigated. For Zircon the second derivative of r with respect to T is negative up to about 350 degrees Fahrenheit. Above 350 degrees Fahrenheit relation (6) is satisfied up to about 700 degrees Fahrenheit. Above 700 degrees Fahrenheit the power input curve is concave downward and stability can always theoretically be reached at some temperature rise. In this respect above 700 degrees Fahrenheit Zircon will behave more like a very high resistance conductor than an insulator.

Hence equation (5) can be applied to porcelain, the two glasses and the steatite composition within the range for which data exists. It can also be applied to the Zircon up to 700 degrees Fahrenheit. The value of thermal conductivity K for these materials are approximately as follows:

Porcelain	.0203	Watts/sq.in./inch/degrees Fahrenheit
Steatite	.0285	" " " " "
Borosilicate Glass	.0182	" " " " "
Lead Glass	.0182	" " " " "
Zircon	.031	" " " " "

For most of these materials the thermal conductivity increases somewhat with increasing temperature. By neglecting this change and using the above values throughout conservative results will be obtained.

In order to numerically evaluate equation (5) the value of the factor α must be determined. The points of ultimate failure with d-c voltage for all porcelain test specimens are listed in table I. The theoretical values for $-\frac{E^2}{r^2}\frac{\partial r}{\partial T}$ are shown for each case. It should again be noted that the data in table I was obtained by applying constant voltage and raising the ambient temperature in steps. In many cases failure would probably have occurred at some lower temperature had smaller steps been used. For this reason those tests on which failure occurred in less than 3 minutes have been discounted. For the remaining tests the average value of the term $-\frac{E^2}{r^3}\frac{\partial r}{\partial T}$ is o.067 with a range of from 0.0189 to 0.124. The last column in table I shows a word symbol indicating whether or not the drift curve to failure passed thru a flex point. Those tests marked "flex" showed a definite flex point in the drift curve. For those points marked "no" the drift curve continued with increasing acceleration to failure with no flex point. For cases where no flex point occurred in the drift curves the starting temperature must have been at some point above T_c. For those tests where a flex point appeared the starting temperature must have been between T_o and T_c. The values of $-\frac{E^2}{r^2}\frac{\partial r}{\partial T}$ for those tests which passed thru a flex point range from 0.0189 to .0925, with an average value of .0398. For those tests which did not show a flex point on the drift curve the value of $-\frac{E^2}{r^2}\frac{\partial r}{\partial T}$ ranged from a high of 0.124 to a low of 0.023 with an average of 0.0725. By inspection it appears that the value of the function $-\frac{E^2}{r^2}\frac{\partial r}{\partial T}$ should be about .06 at the flex point. If .06 is taken as the approximate numerical value of the function at the flex point, then this may be substituted in equation (5) and the factor $\propto$ may be evaluated as approximately 3 for porcelain. This evaluation is not very precise but it should be noted that an error of even 3 to 1 in the value of $\propto$ produces an error of only about 50 degrees Fahrenheit in the theoretical end point temperature.

For porcelain the resistivity varies but little with voltage gradient for temperature above 250 degrees Fahrenheit. A reasonably accurate general solution can therefore be obtained for temperatures above 250 degrees Fahrenheit. For temperatures below 250 degrees Fahrenheit some confusion exists probably due to the variation of resistivity with voltage gradient and sufficient data is not available for an accurate analysis. As a matter of interest equation (5) has been evaluated for porcelain below 250 degrees using the two extremes of the resistivity curve Figure 4.

This yields the theoretical internal temperature T_c at which runaway actually starts for any particular voltage gradient. In Figure 32 the values of T_c have been plotted against voltage gradient. The starting ambient temperature T_o from which the critical internal temperature T_c may ultimately be reached has also been plotted in Figure 30 taking:

$$T_c - T_o = \frac{\text{WATTS PER CU. IN. INPUT AT } T_o}{K\propto}$$

Any point to the left of the T_o curve should be safe for continuous operation. Points to the right of the T_o curve should result in failure if given sufficient time.

In table II the actual breakdown points for several practical insulators are shown. These values have also been plotted on Figure 32.

For the materials other than porcelain there is not sufficient data to make a determination of $\propto$ by the method used for porcelain. It is difficult to see why the value of $\propto$ should materially differ from that for porcelain. If we assume that $\propto$ is the same for the steatite, glass and zircon compositions as for porcelain, then theoretical breakdown curves can be plotted for these materials. Such curves for the four other materials are plotted in Figure 32

within the range of the existing data. For borosilicate glass, no data is available above 350 degrees Fahrenheit and for temperatures below 250 degrees Fahrenheit the resistivity varies greatly with voltage as indicated in Figure 22 and 23. The curve for borosilicate glass can therefore be generalized from this data over only a short range. In Figure 32 the borosilicate glass curve is shown in broken lines so that it may be distinguished from the porcelain curve.

Examination of Figures 24 and 25 will show that the lead glass curve can be generalized from existing data only within the temperature range from 350 degrees Fahrenheit to 650 degrees Fahrenheit and for voltage below 40 volts per mil.

No data is available on the steatite composition to show the variation of resistivity with voltage at the higher temperatures.. There is every indication, however, that, like porcelain, the resistivity of Steatite becomes essentially independent of voltage at temperatures above 250 degrees Fahrenheit. The plot for steatite in Figure 26 is based on this assumption.

For the zircon composition it appears as though above about 140 volts per mil resistivity will vary considerably with voltage. Also above 700 degrees Fahrenheit stability can theoretically always be reached. The generalized zircon plot is therefore quite short but does adequately indicate the relative position of this material. Above 700 degrees Fahrenheit there is some question as to whether at any particular voltage gradient, the material will stabilize before the internal temperature rise becomes excessive. The experimental evidence indicates that for d-c gradients up to 40 volts per mil the zircon composition can be successfully operated at 900 degrees Fahrenheit and possibly higher.

As a practical check on these theoretical predictions tables I, II, III and IV give the actual measured breakdown points for a number of specimens. The individual points from these tables have been plotted on the curves Figure 32 for direct comparison. As would be expected all actual breakdown points fall to the right of the theoretical curve.

Some actual breakdown points for porcelain are included for temperatures below 250 degrees Fahrenheit. It has been pointed out that at these lower temperatures the generalized curves are of doubtful value. It is interesting to note, however, that the actual low temperature breakdown points are at least of the proper order relative to the theoretical curves. Some breakdown points obtained with a-c voltages are also included in tables II and III, and are plotted on the curve Figure 32. In each case these have been listed and plotted in r.m.s. rather than crest volts since the heating effect is a function of the former. These seem to fit the curves equally as well as do the d-c points but the amount of a-c data available is relatively small. No actual resistance measurements were made with a-c and the resistivities listed in table III are taken from Curve 4.

Despite the fact that the temperature - resistivity curves were obtained from test specimens with relatively uniform voltage gradients, the theoretical breakdown curve for porcelain applies with reasonable accuracy to practical insulator shapes at the higher temperatures. This is shown by the actual breakdown tests on practical insulators as listed in table II.

It seems probable that at temperatures above 250 degrees Fahrenheit the reduction in resistivity of the porcelain results in more nearly uniform voltage gradients in the practical insulators.

No actual breakdowns were obtained on the Zircon composition even though temperatures were carried up to 900 degrees Fahrenheit at 40 volts per mill d-c. The tendency of the Zircon to increase in resistivity with time at constant ambient temperature and voltage is believed to be due to dielectric polarization. At any constant temperature and voltage the more mobile negative ions (or possibly electrons)drift away from the negative electrode leaving a super abundance of the less mobile positive ions in this area. This results in an apparent increase in the resistivity of the material. When such polarization occurs to a marked degree it would be expected that the breakdown temperature with a-c would be lower than with d-c.

Conclusions:

The electrical resistivity of all of the ceramic insulating materials tested diminishes not only with increasing temperature but also, at the lower temperatures, it diminishes with increasing voltage gradient. The rate of change of resistivity with voltage appears to diminish with increasing temperature so that for porcelain above 250 degrees Fahrenheit the resistivity is nearly independent of voltage.

From the shape and level of the temperature resistivity curves it is possible to predict the temperature at which an insulator will fail under any particular voltage gradient. While these conditions are based primarily on high temperature measurements it appears as though the thermal effect may be a major factor in insulator breakdowns even at low temperatures. The existing data does not permit definite determination at low temperature, however.

The breakdown curves, Figure 32, are believed to be applicable for 60 cycle a-c as well as d-c voltage for all of the materials except Zircon. For Zircon the a-c breakdown temperatures may be somewhat lower.

There is also some question as to whether these curves are applicable to high frequency a-c voltages. At high frequencies other forms of dielectric loss may become of important magnitude so that failure may occur at lower temperature levels. This has not been investigated.

There seems to be no appreciable difference in the high temperature electrical performance of wet process electrical porcelain as made by several well known American manufacturers.

The presence of glaze on porcelain does not seem to effect the high temperature performance.

The high temperature performance of glasses, steatite and Zircons may be expected to vary widely with different compositions. The one Zircon composition which thus far appears to be best can be operated at 900 degrees Fahrenheit and 40 volts per mil d-c without failure.

- o 0 o -

REFERENCES

1 - Insulation Failure - A. Pyroelectric Effect - J.L.R. Hayden and C.P. Steinmetz - Electrical World, Vol. 80, Page 865, 1922.

2 - High Voltage Insulation - Hayden and Steinmetz - Transactions, AIEE, 1923, P. 1029-41.

3 - A Theory of Imperfect Solid Dielectrics - M.G. Malti - Transactions, AIEE, 1927, P. 616-634.

4 - Electrical Resistivity of Insulating Materials - H.L. Curtis - Transactions, AIEE, 1927, P. 1039-47.

5 - Electric Strength of Solid and Liquid Dielectrics - W.A. Del Mar, W.F. Davidson, R.H. Marvin - Transactions,AIEE, 1927, P. 1049-1061.

6 - Theory of Thermal Breakdown of Solid Dielectrics - Moon - Transactions, AIEE, 1931, P. 1008-21.

7 - Low Loss Ceramics - R. Russell, Jr. and F.J. Berberich - Electronics, May 1944.

8 - Breakdown of Glass with Alternating Potentials - N.D. Kenney, A.M. Luery, J.D. Moriaty - Transactions, AIEE, Vol. 51, P. 404 1932.

9 - Predetermination of the A.C. Characteristics of Dielectrics - J.B. Whitehead, Alfredo Banos, Jr. - Transactions, AIEE, Vol. 51, P. 392, 1932.

List of Captions.

Figure 1. Test chamber and operating panel with specimen mounted in position.

Figure 2. Temperature vs resistivitiy, wet process electrical porcelain, voltage gradient 40 volts per mil d-c, thickness 0.8 inch, electrode area 30 square inches.

Figure 3. Voltage gradient vs resistivity, wet process electrical porcelain, thickness o.8 inch, electrode area 30 square inches.

Figure 4. Composite curve. Temperature vs resistivity wet process electrical porcelain.

Figure 5. Temperature vs resistivity, wet process electrical porcelain, specimen thickness 0.2 inch.

Figure 6. Temperature vs resistivity, wet process electrical porcelain, specimen thickness 0.3 inch.

Figure 7. Temperature vs resistivity wet process electrical porcelain, specimen thickness 0.55 inch.

Figure 8. Temperature vs resistivity, wet process electrical porcelain, specimen thickness 0.8 inch.

Figure 9. Temperature vs resistivity, wet process electrical porcelain, specimen thickness .01 inch.

Figure 10. Voltage gradient vs resistivity, wet process electrical porcelain, specimen thickness 0.075 inch.

Figure 11. Voltage gradient vs resistivity, wet process electrical porcelain, specimen thickness 0.1 inch.

Figure 12. Voltage gradient vs resistivity, wet process electrical porcelain, specimen thickness 0.2 inch.

Figure 13. Voltage gradient vs resistivity, wet process electrical porcelain, specimen thickness 0.3 inch.

Figure 14. Voltage gradient vs resistivity, wet process electrical porcelain, specimen thickness 0.55 inch.

Figure 15. Voltage gradient vs resistivity, wet process electrical porcelain, specimen thickness 0.8 inch.

Figure 16. Voltage gradient vs resistivity, wet process electrical porcelain, specimen thickness 1.0 inch.

Figure 17. Temperature vs resistivity, comparison of two manufacturers of wet process electrical porcelain, voltage gradient 20 volts per mil, specimen thickness 0.55 inch.

Figure 18. Temperature vs resistance, comparison of glazed and unglazed wet process electrical porcelain, total voltage applied 5000 volts d-c.

Figure 19. Temperature vs resistance, wet process porcelain standoff insulator.

Figure 20. Total voltage vs resistance, wet process porcelain standoff insulator.

Figure 21. Temperature vs resistance of 23 kv NEMA Standard outdoor switch and bus insulator, total voltage applied 14 kv d-c.

Figure 22. Temperature vs resistivity, boro-silicate glass, thickness 0.36 inch.

Figure 23. Voltage gradient vs resistivity, boro-silicate glass, thickness 0.36 inch.

Figure 24. Temperature vs resistivity, lead glass specimen thickness 0.50 inch.

Figure 25. Voltage gradient vs resistivity, lead glass, specimen thickness 0.50 inch.

Figure 26. Temperature vs resistivity, wet process steatite, voltage gradient 20 and 40 volts per mil, specimen thickness 0.188 inch and 0.203 inch.

Figure 27. Voltage gradient vs resistivity, wet process Steatite, temperature 84 F, specimen thickness 0.188 inch and 0.203 inch.

Figure 28. Temperature vs resistivity, zircon, 40 volts per mil, 2 square inch electrode 0.489 inch thick and 1 square inch electrode 0.196 inch thick.

Figure 29. Voltage gradient vs resistivity, zircon, 1 square inch electrode, specimen thickness 0.196 inch.

Figure 30. Elemental cube in the dielectric body.

Figure 31. Power input and power output conditions leading to ultimate breakdown.

Figure 32. Temperature vs voltage gradient for breakdown.

706

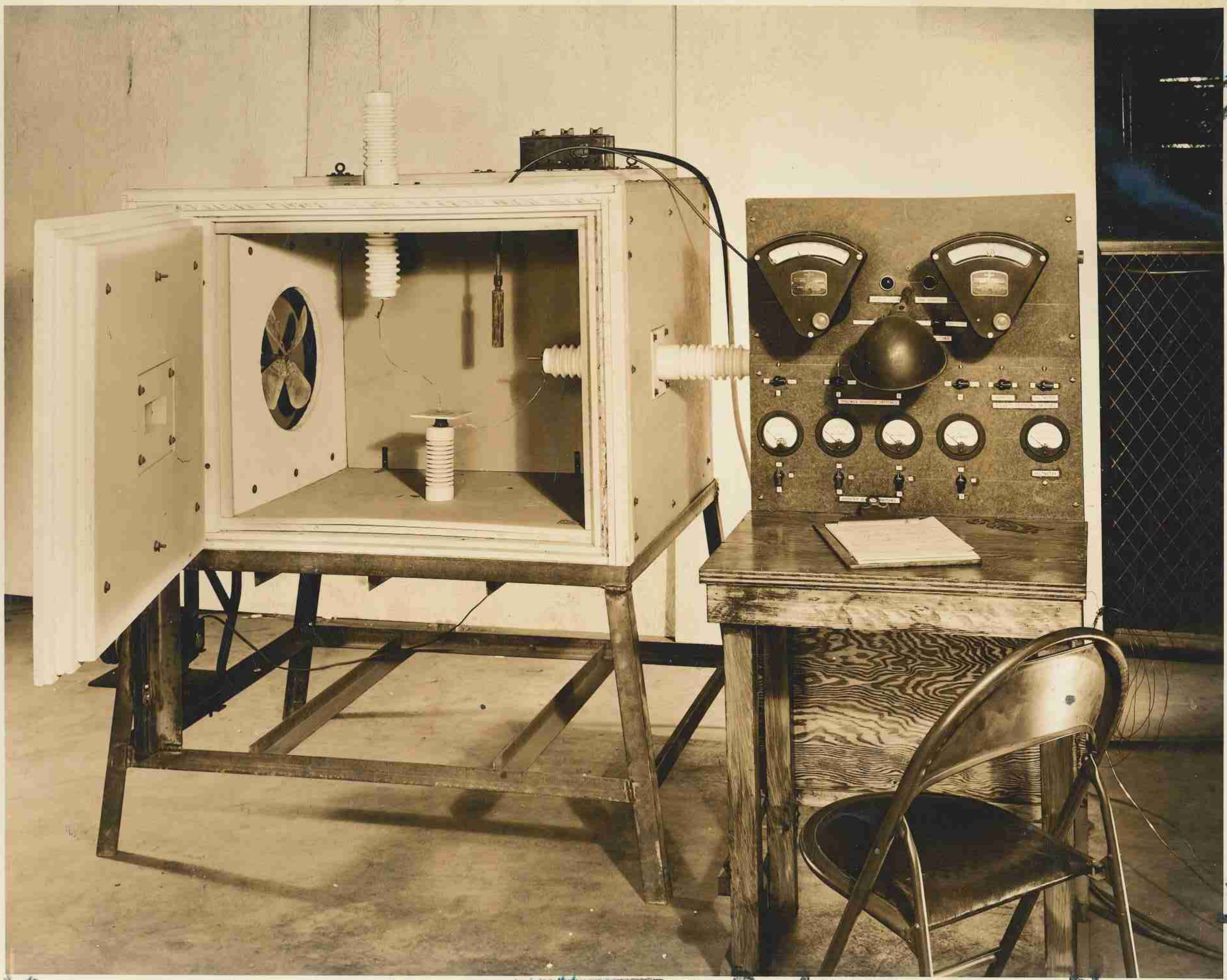

~~4 1/2~~ 21

Jul

blakeslee-lane
PHOTOGRAPHY
BALTIMORE WASHINGTON
916 N. CHARLES ST, BALTIMORE-1, MD.
VERNON 4100
FOR DUPLICATE PRINTS No. N6671-1

41.2

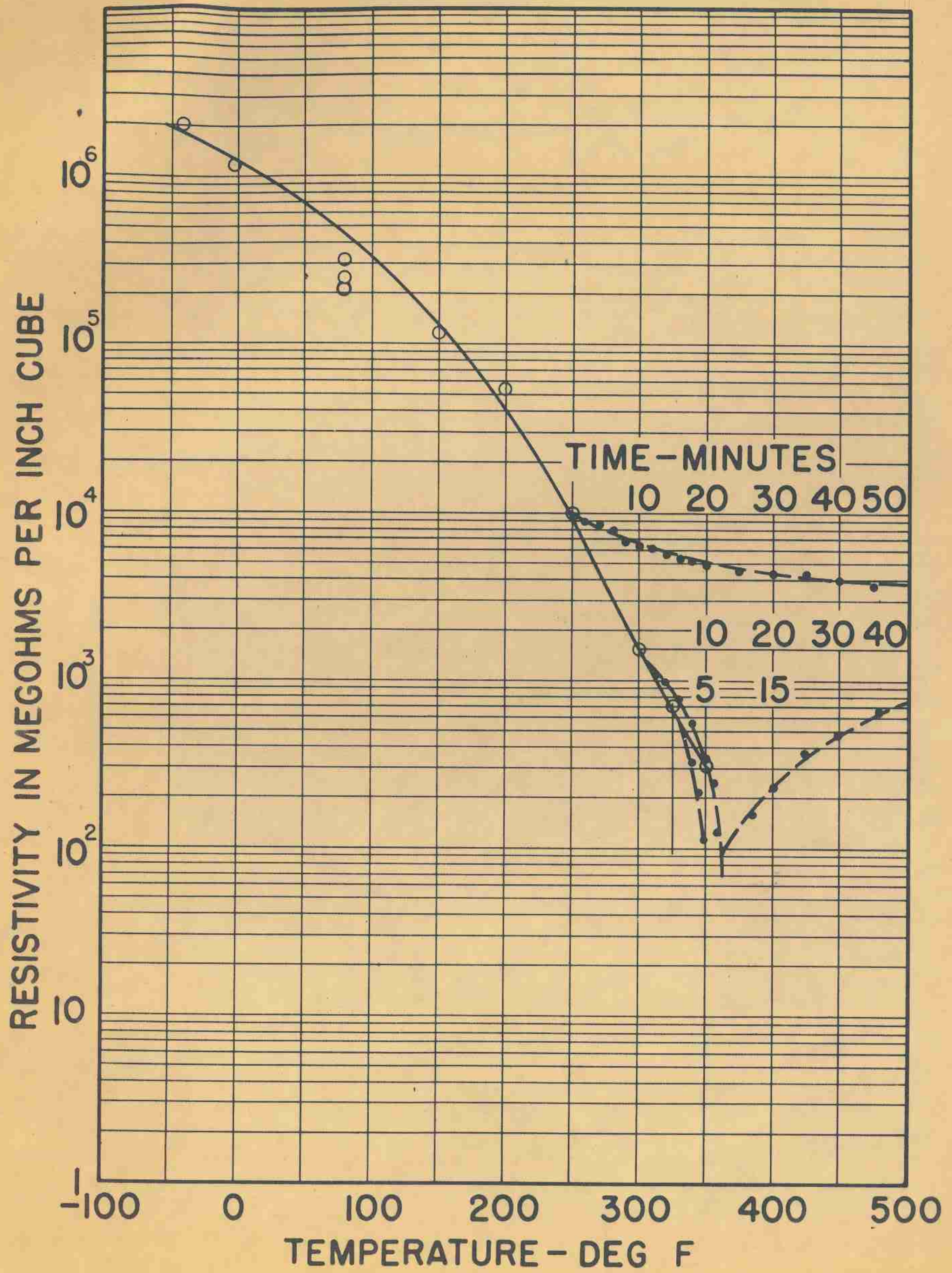

FIG. 2 (FREY & JESATKO)

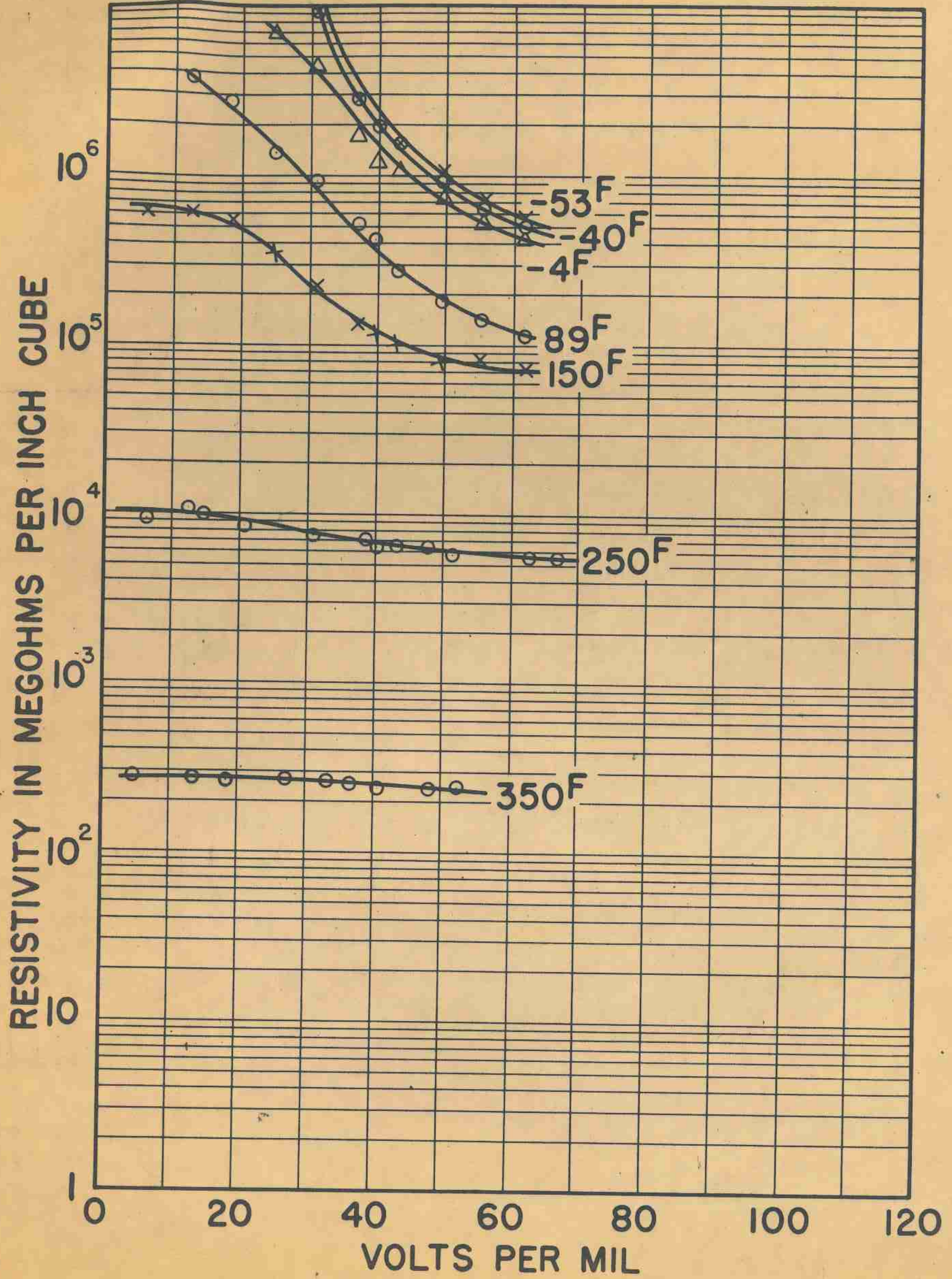

FIG. 3 (FREY & JESATKO)

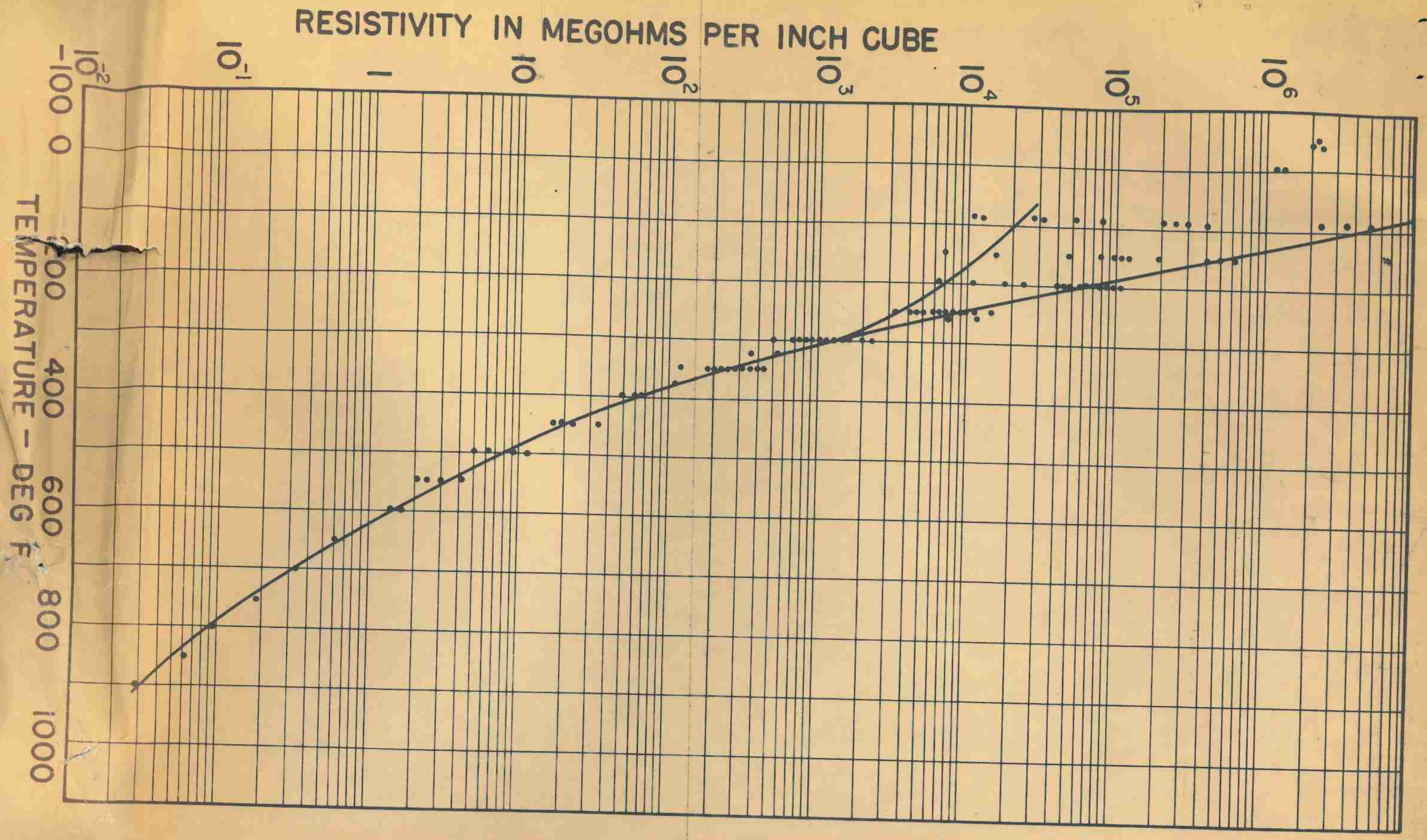

Fig. 4 (Pikey & Baker)

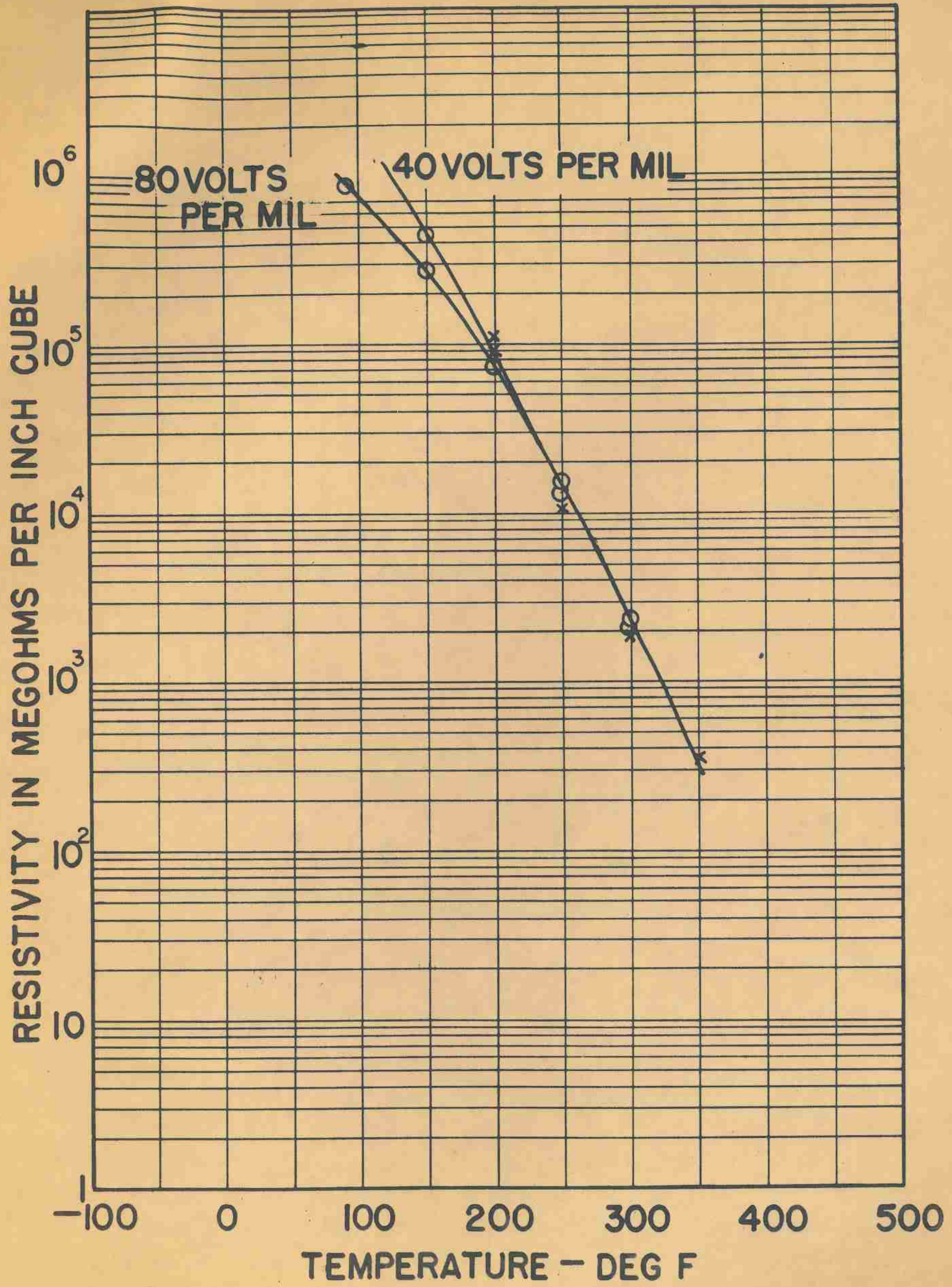

FIG. 5 (FREY & JESATKO)

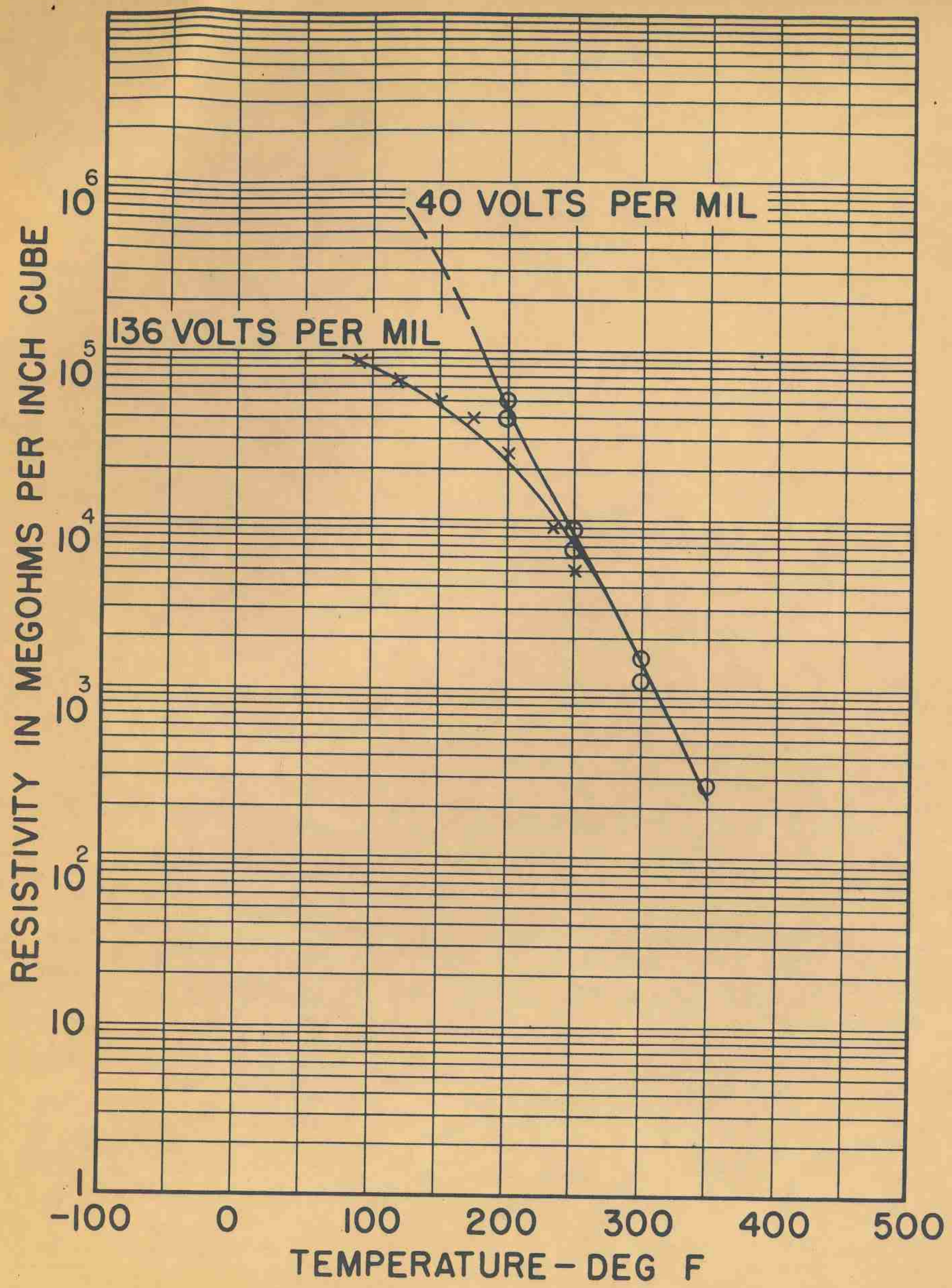

FIG. 6 (FREY & JESATKO)

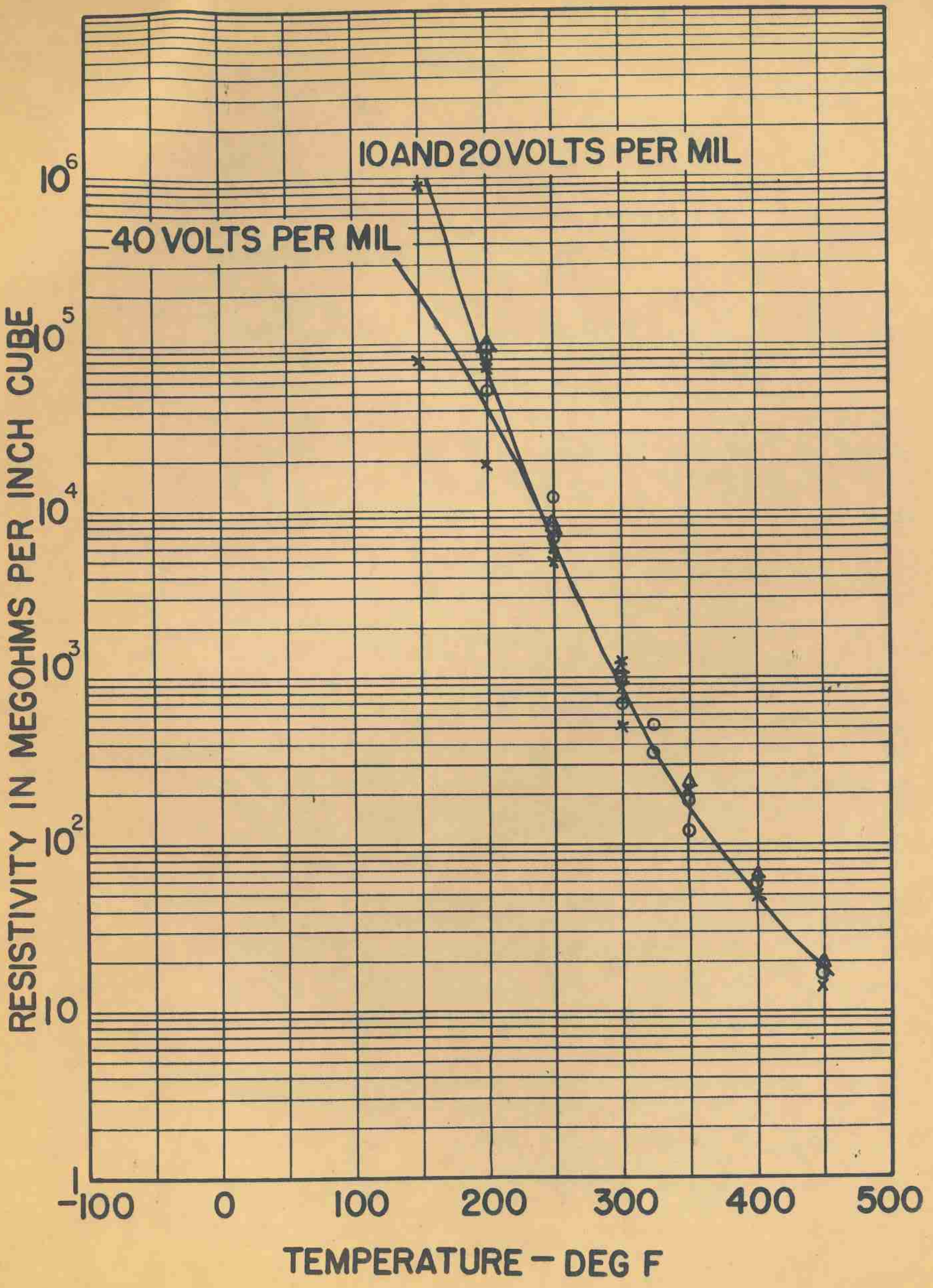

FIG. 7 (FREY & JESATKO)

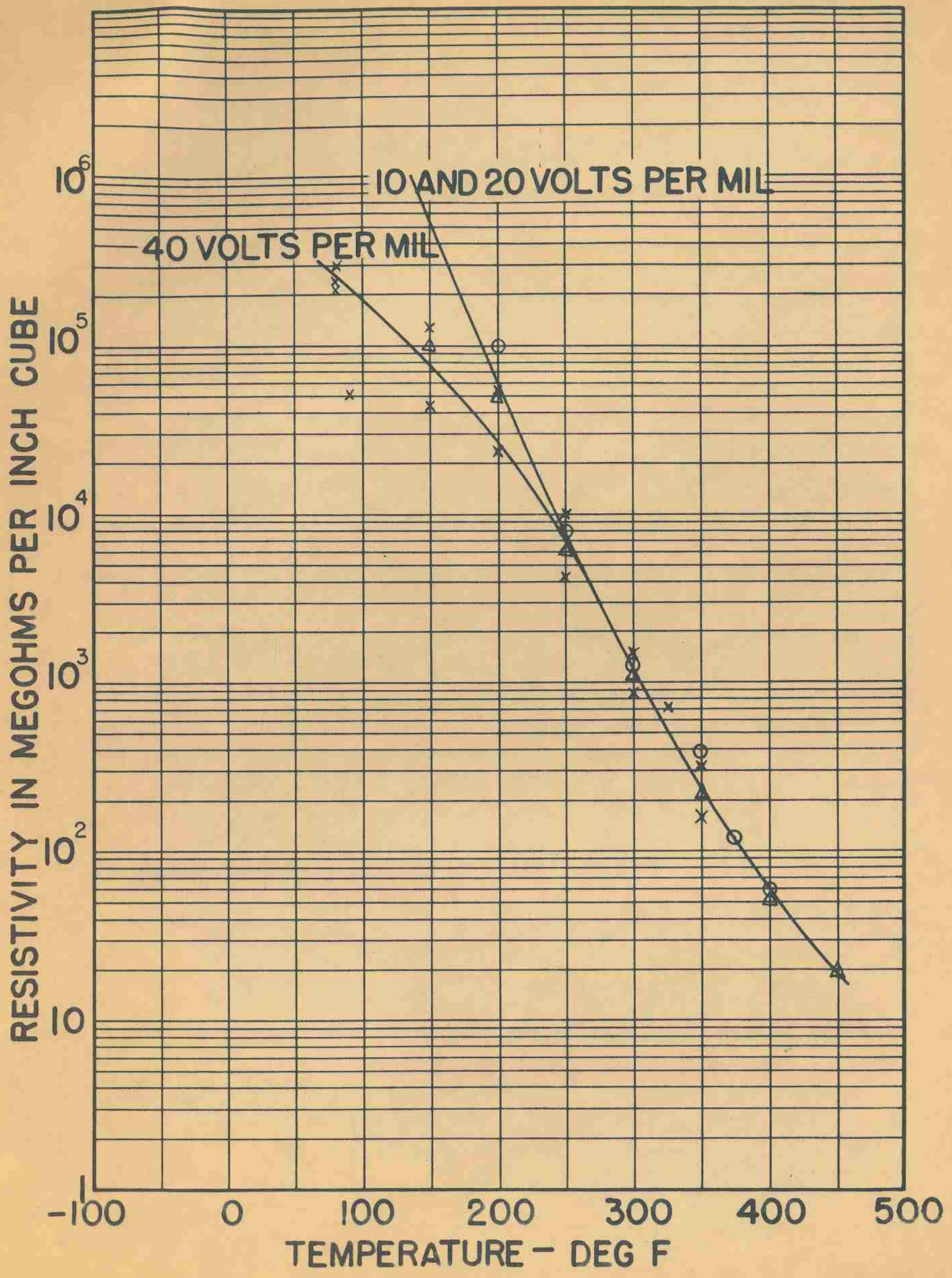

FIG. 8 (FREY & JESATKO)

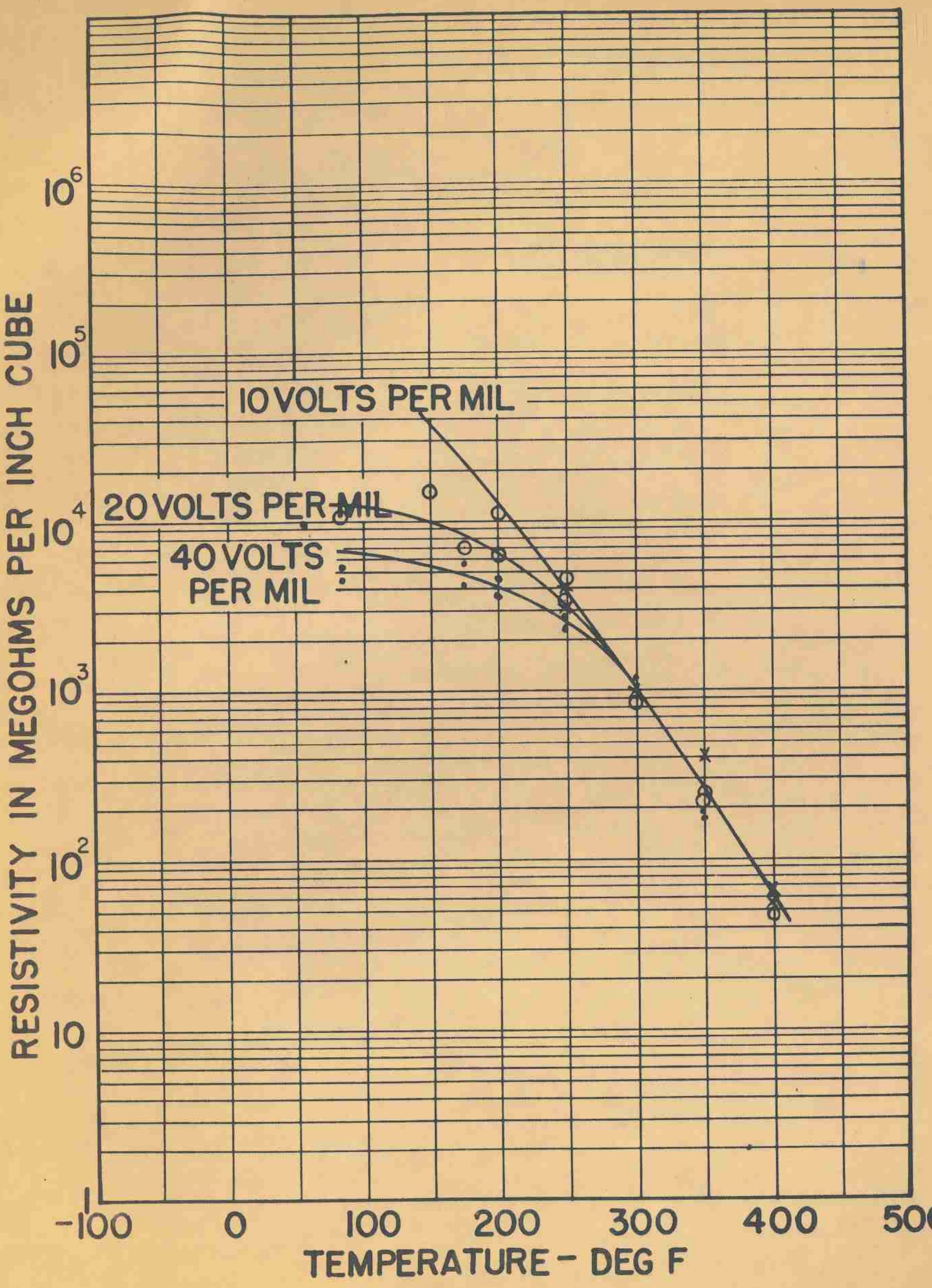

FIG. 9 (FREY & JESATKO)

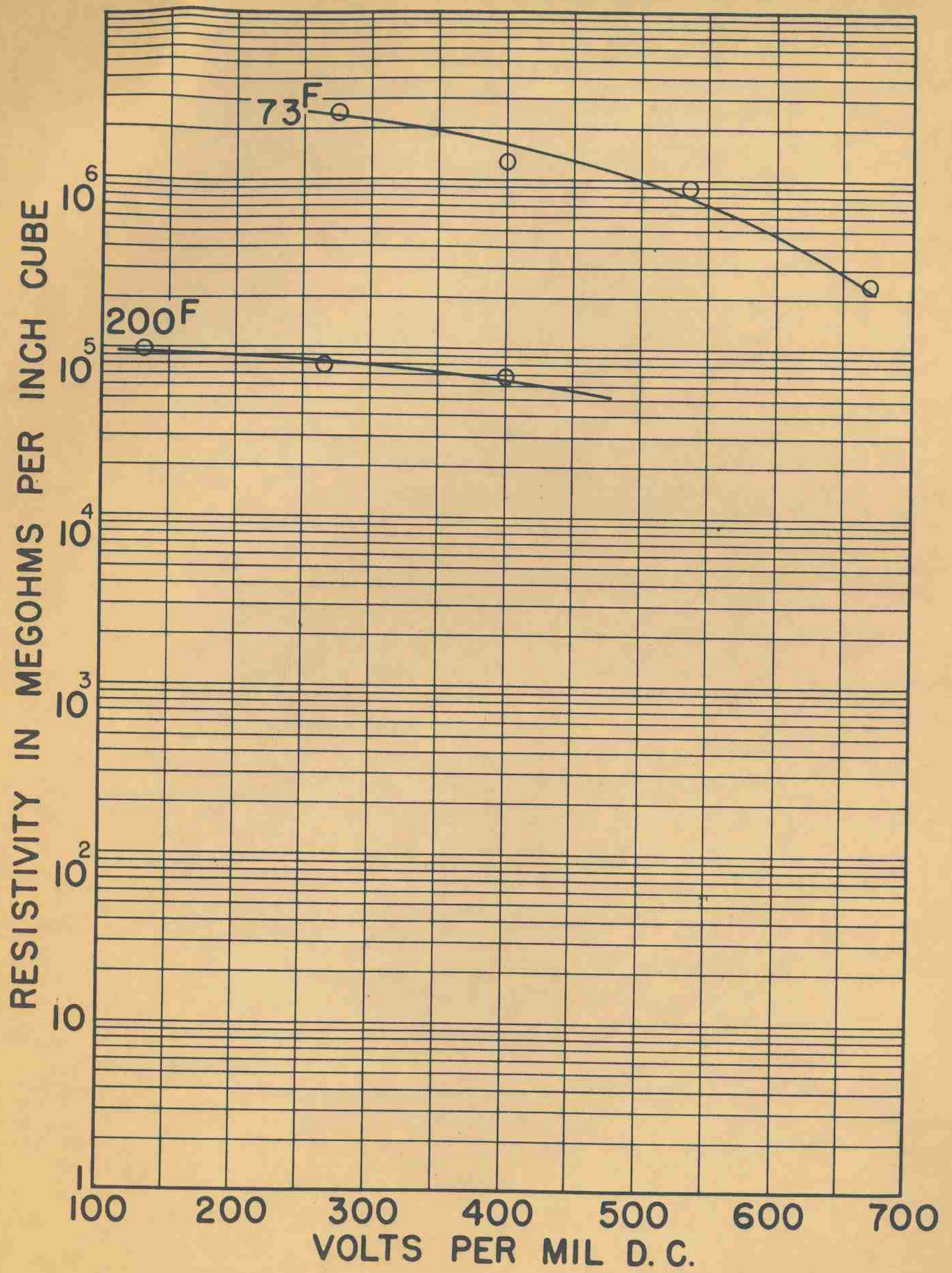

FIG. 10 (FREY & JESATKO)

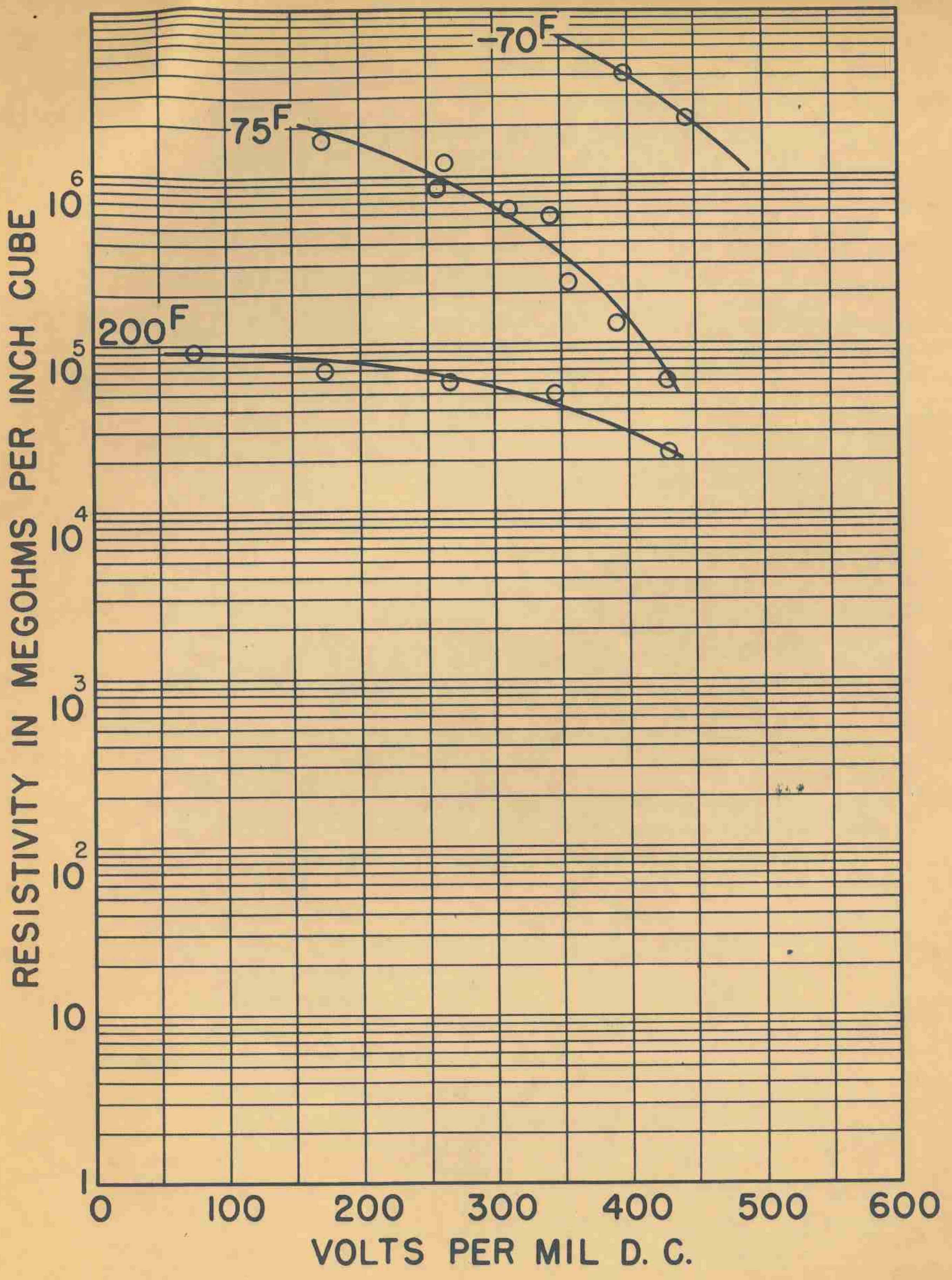

FIG. 11 (*FREY & JESATKO*)

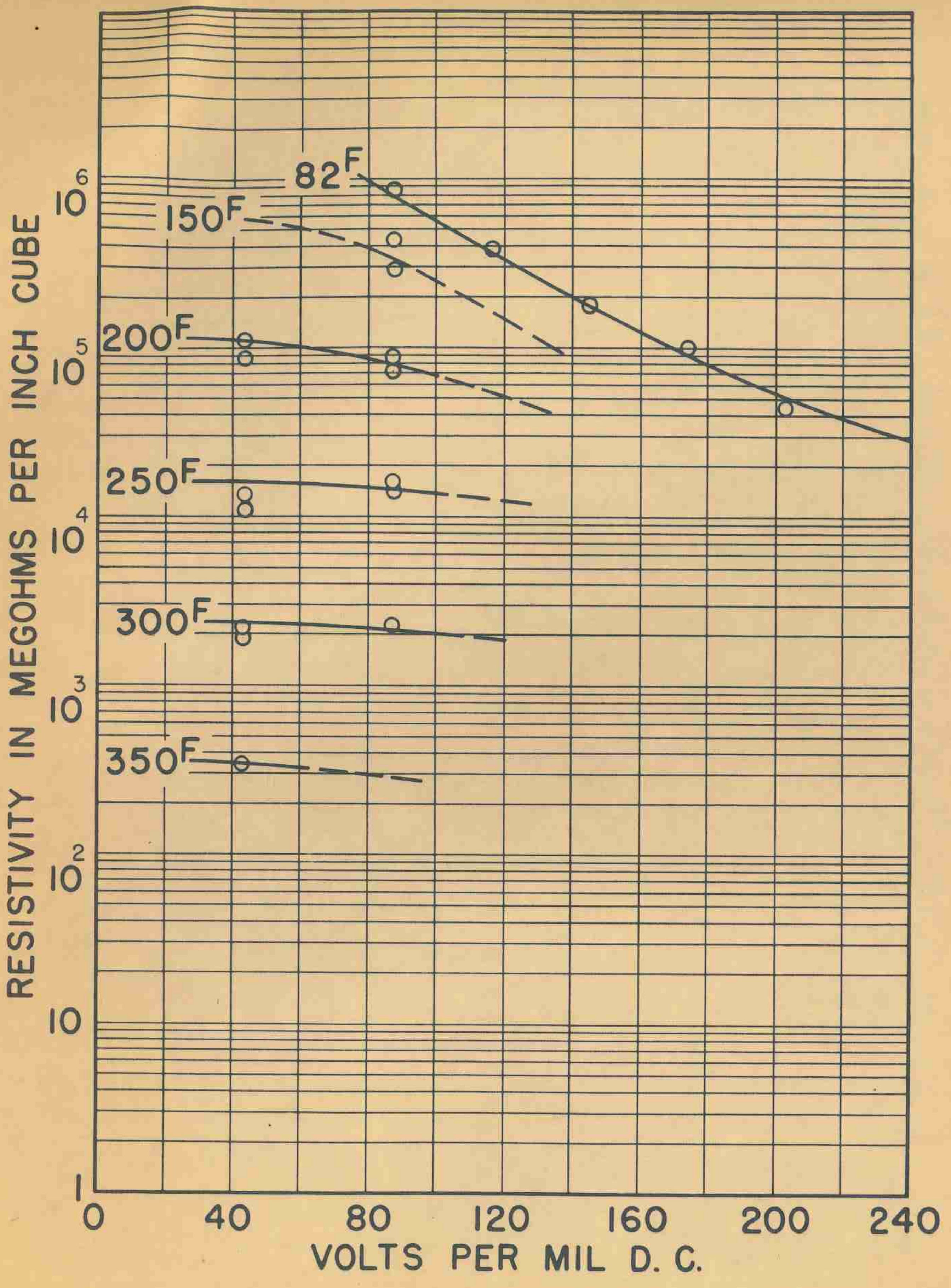

FIG. 12 (*FREY & JESATKO*)

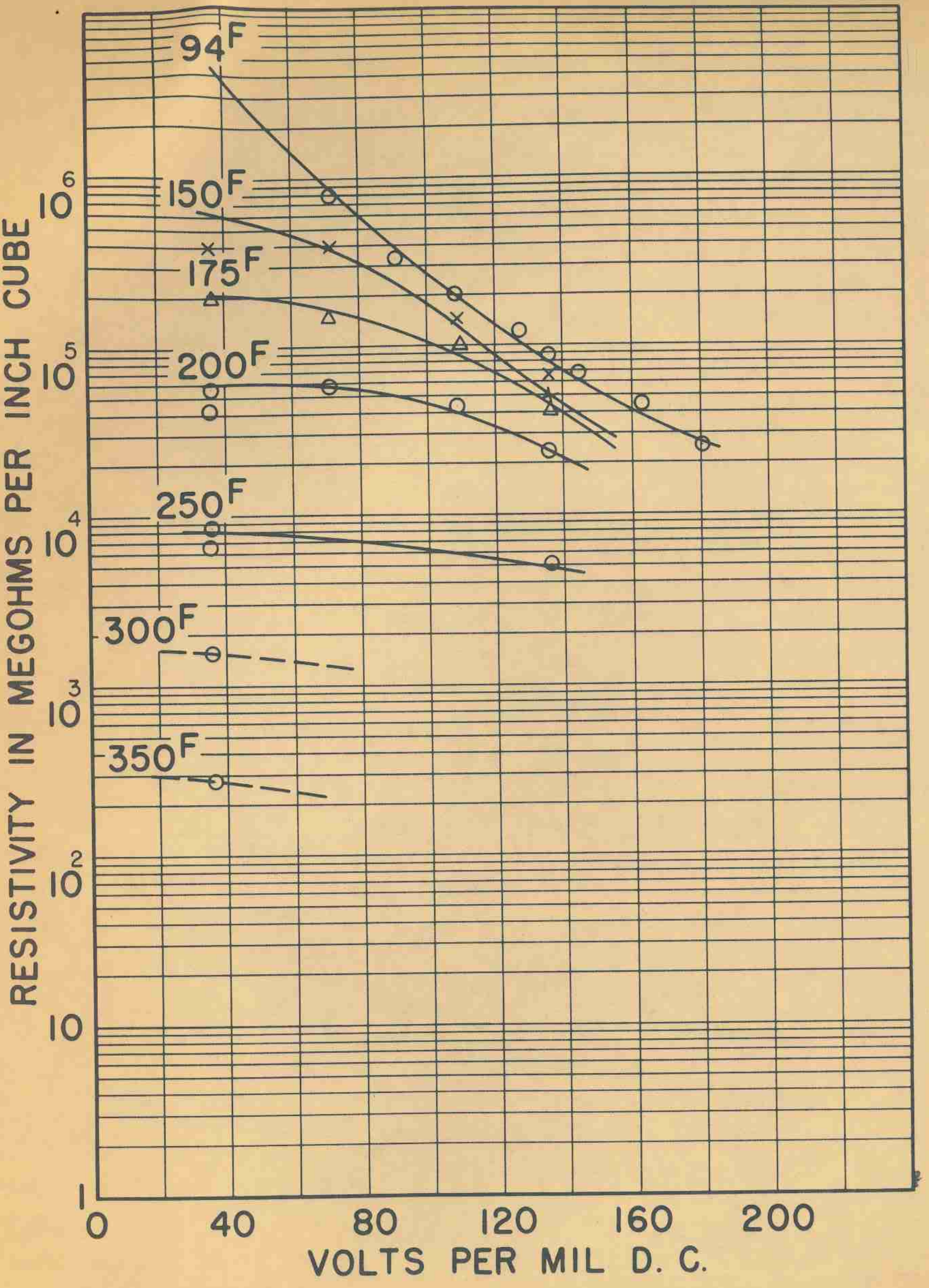

Fig. 13 (Frey & Jesatko)

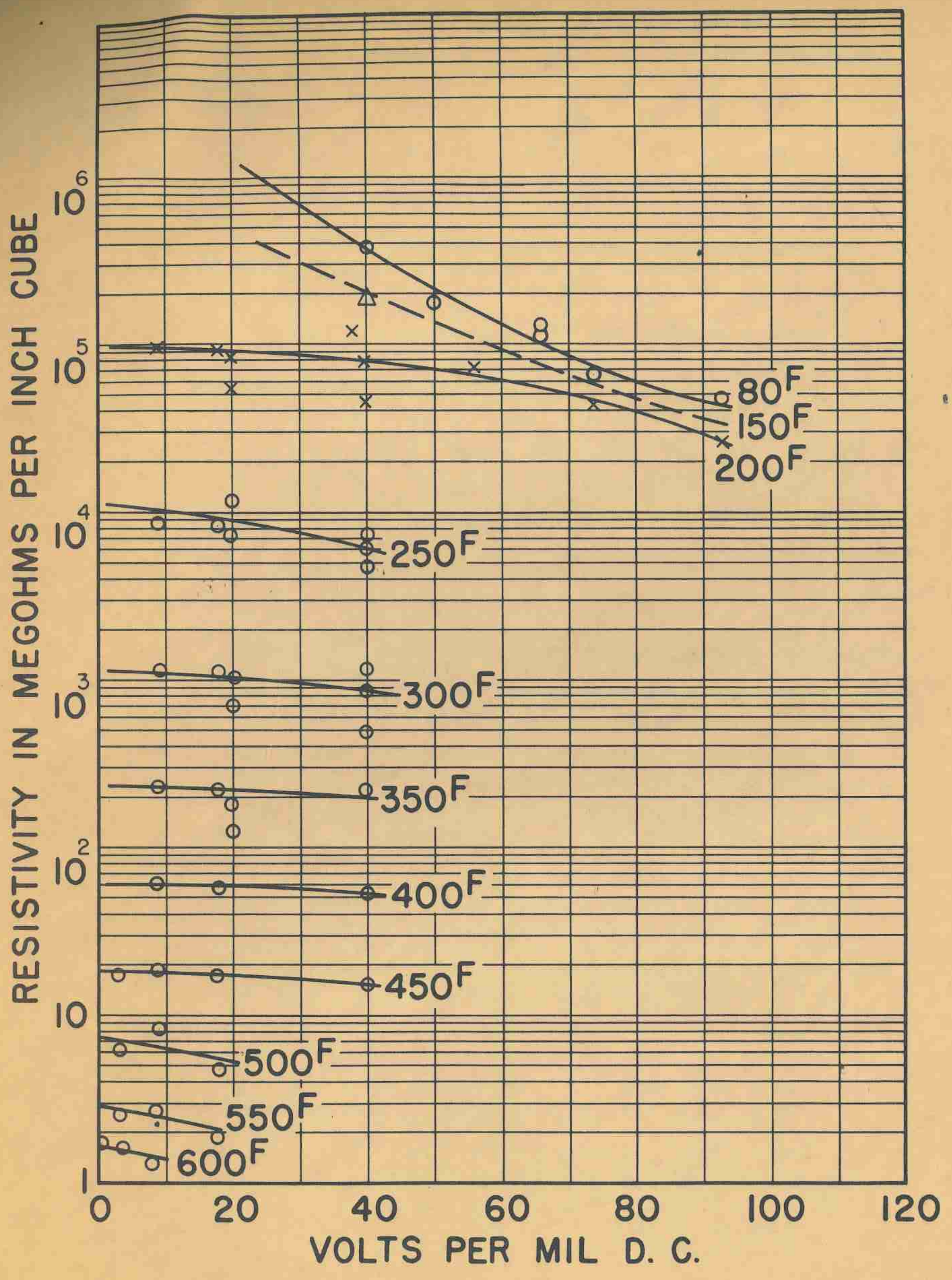

Fig. 14 (Frey & Jesatko)

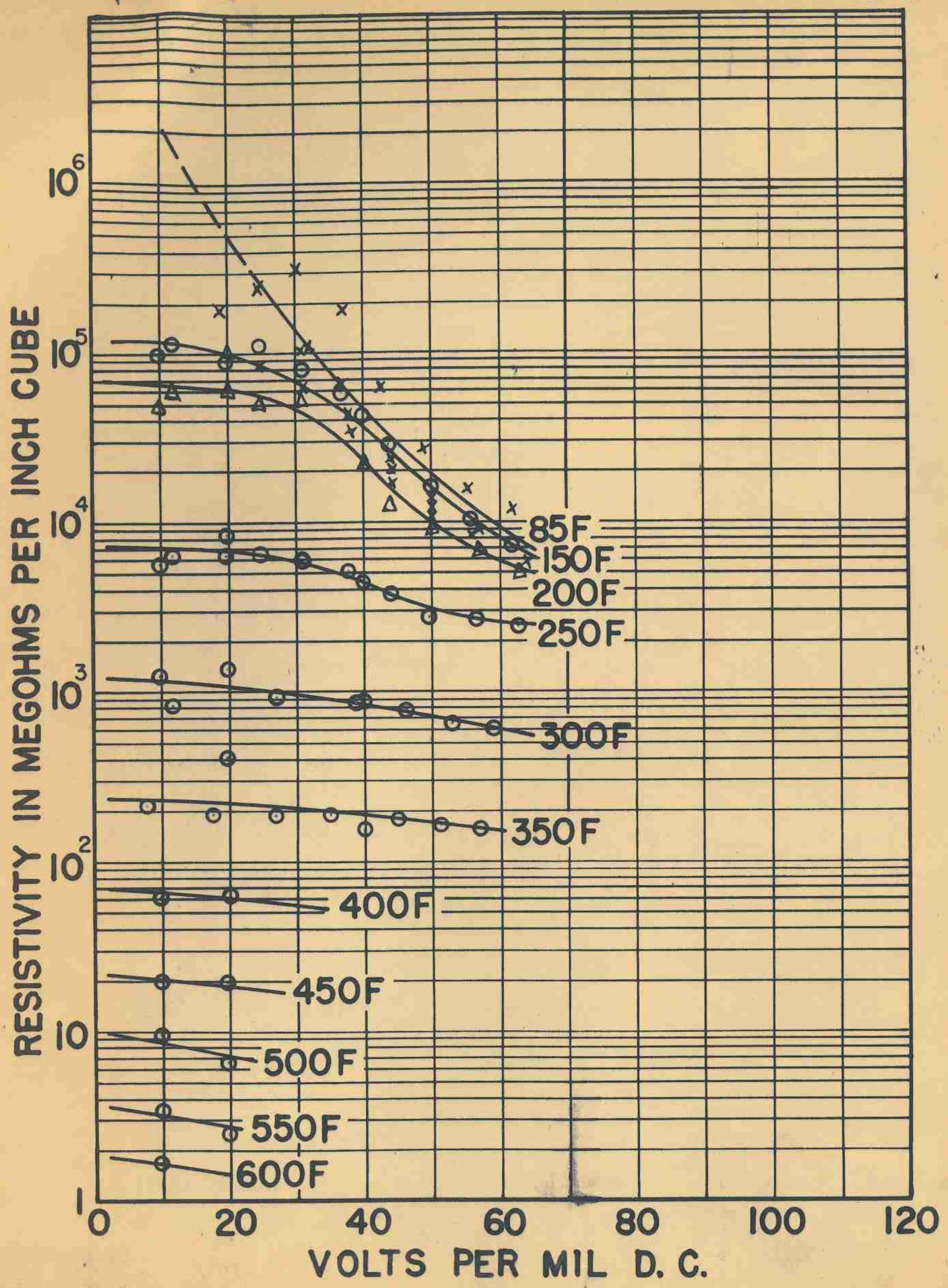

FIG. 15 (FREY & JESATKO)

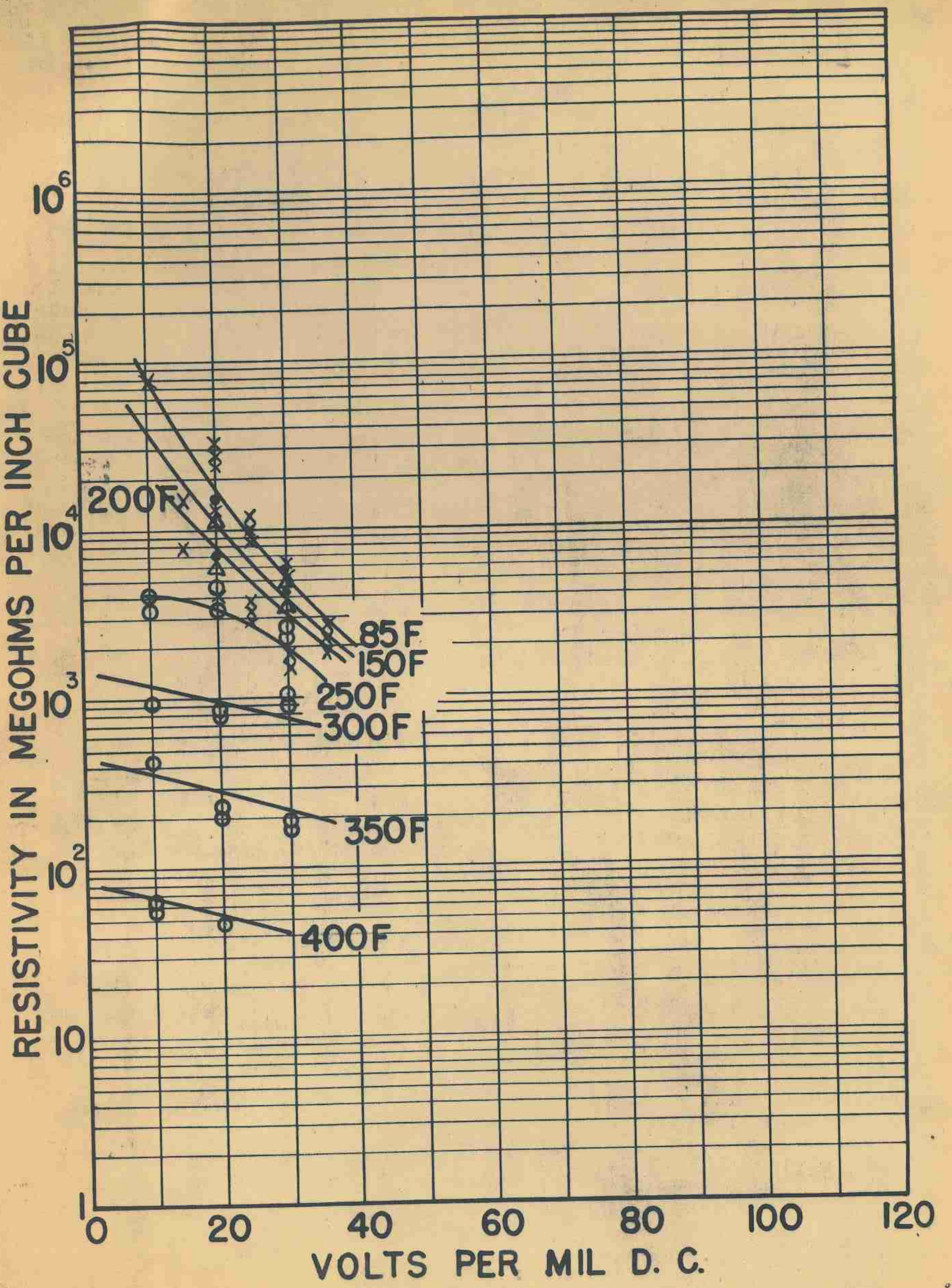

FIG. 16 (FREY & JESATKO)

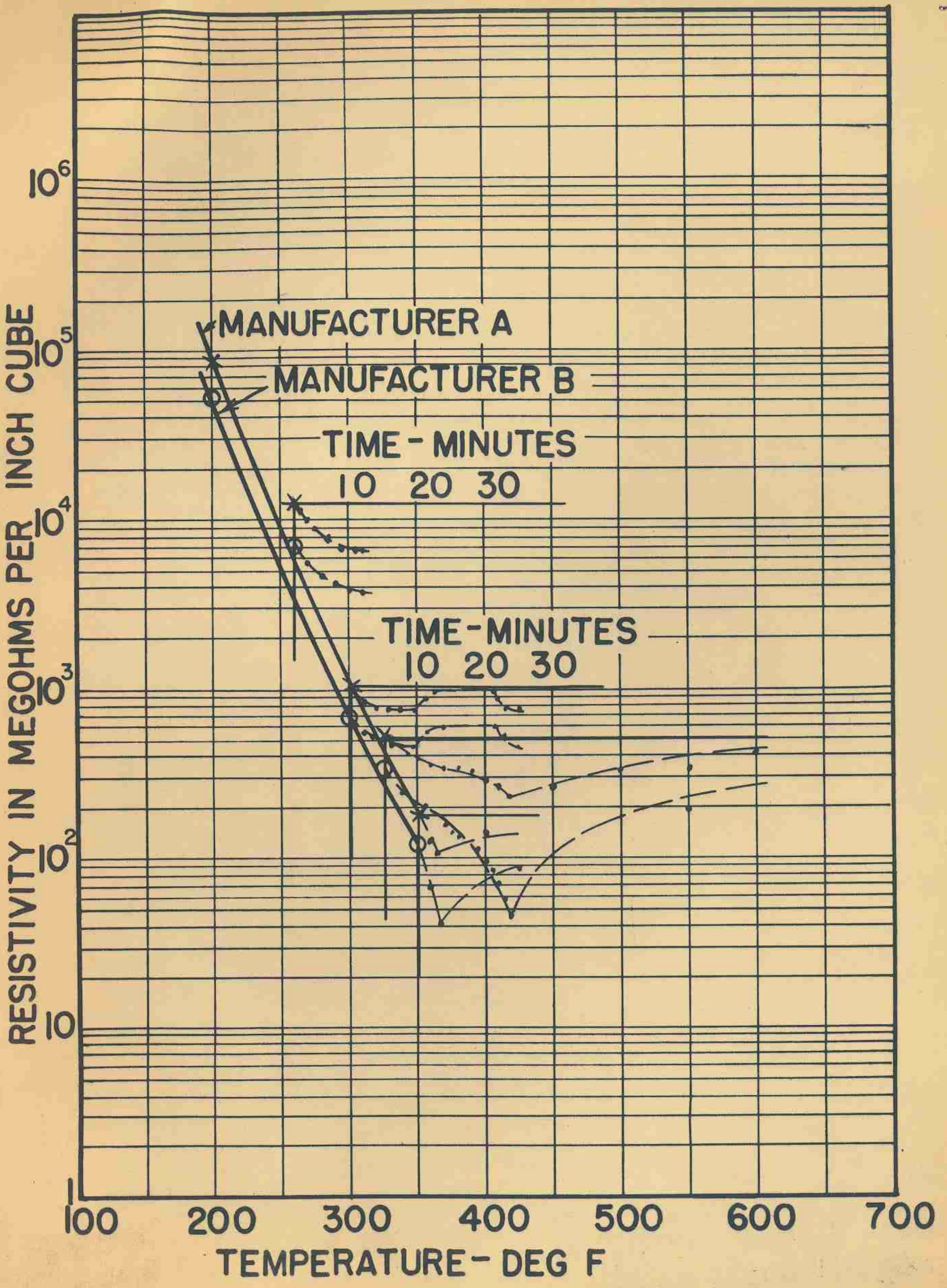

FIG. 17 (FREY & JESATKO)

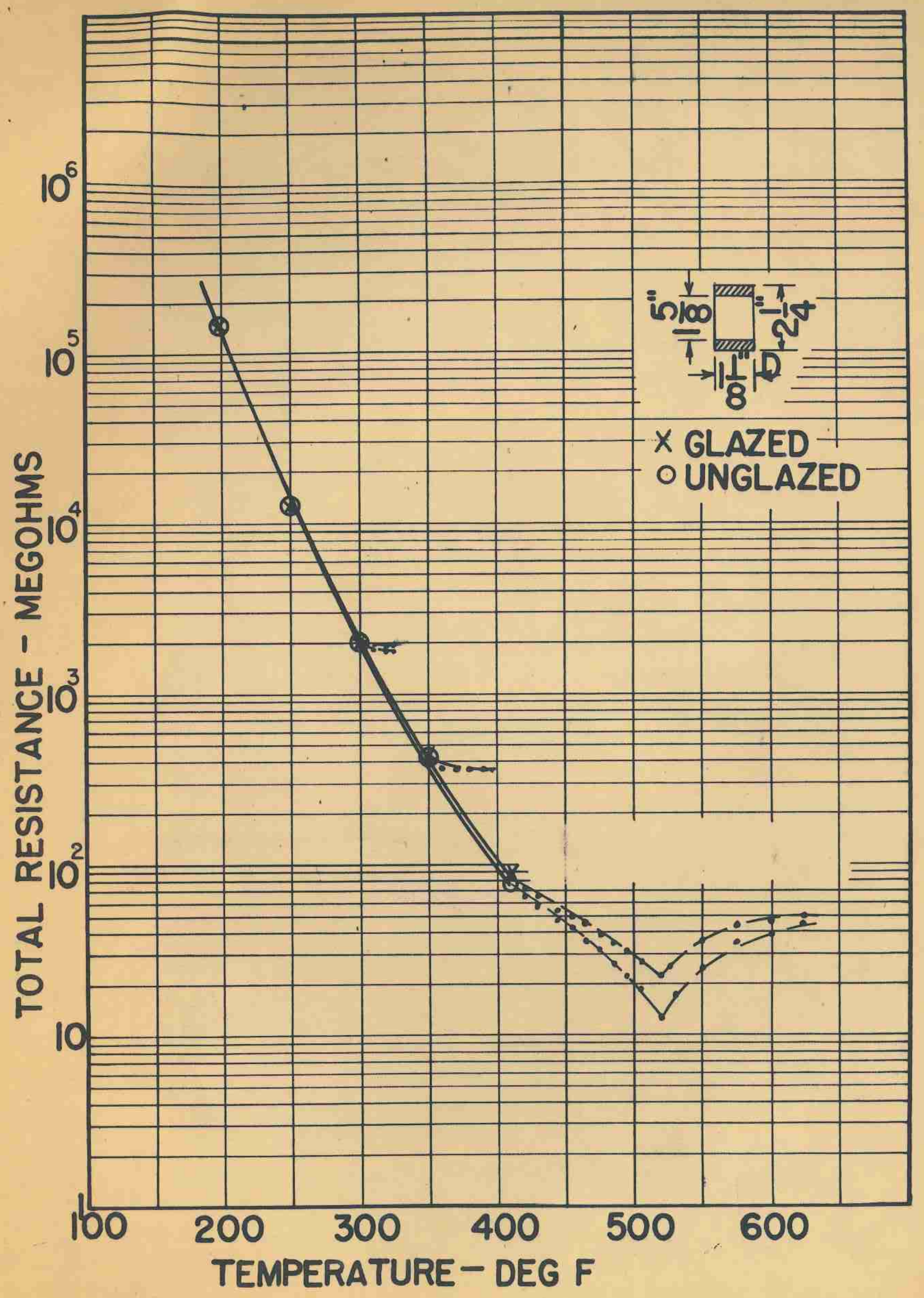

FIG. 18 (FREY & JESATKO)

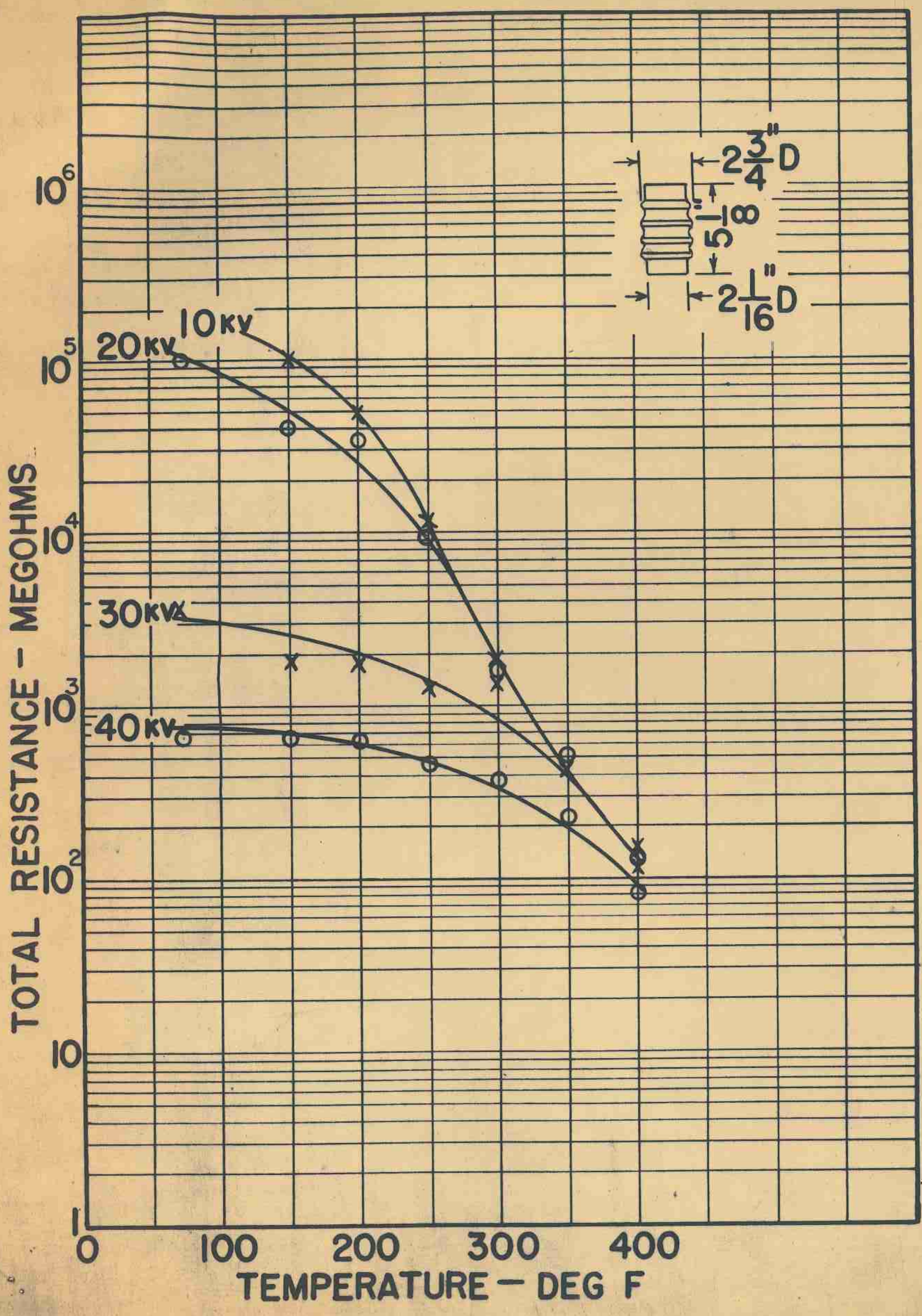

FIG. 19 (FREY & JESATKO)

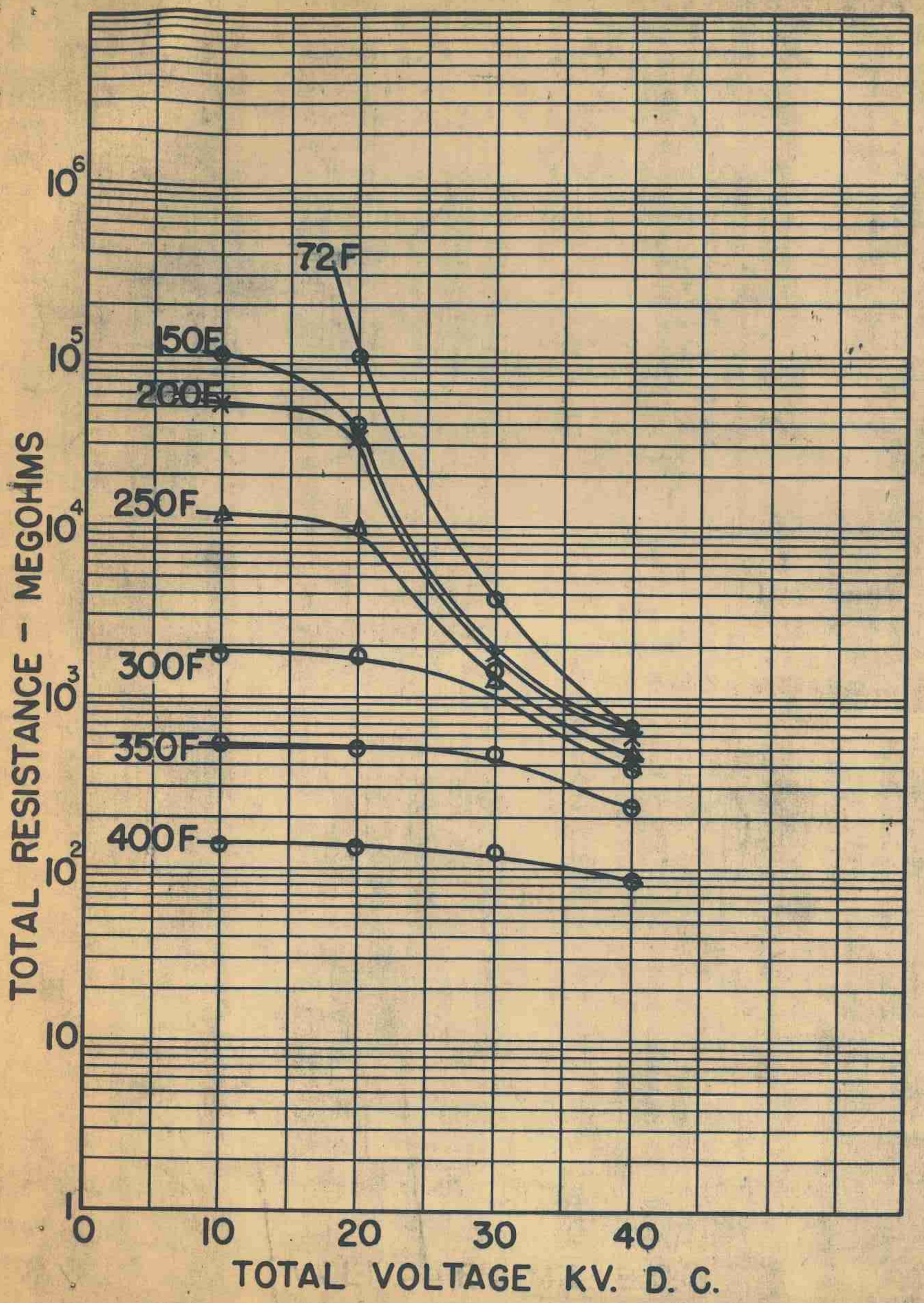

FIG. 20 (FREY & JESATKO)

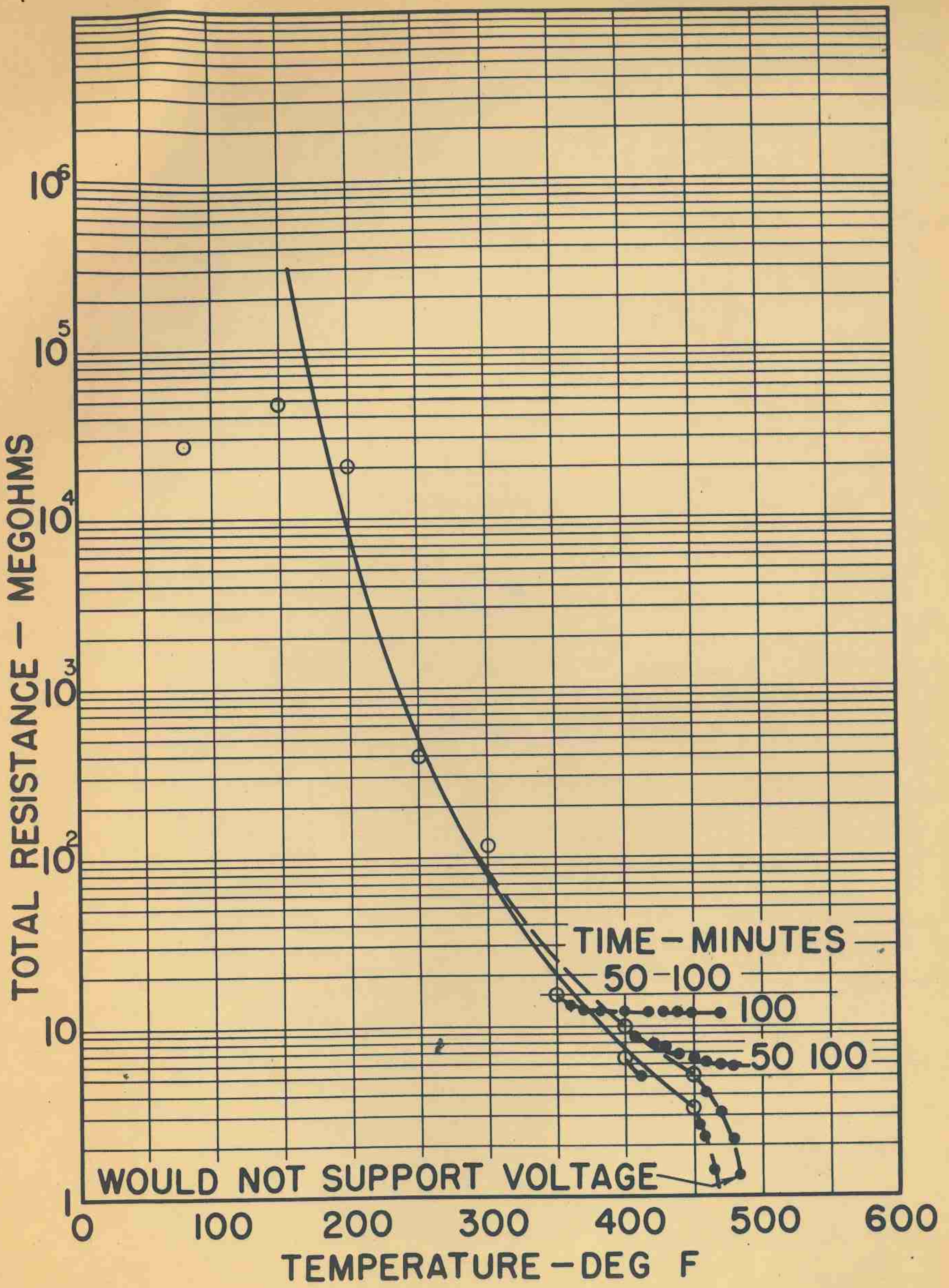

FIG. 21 (FREY & JESATKO)

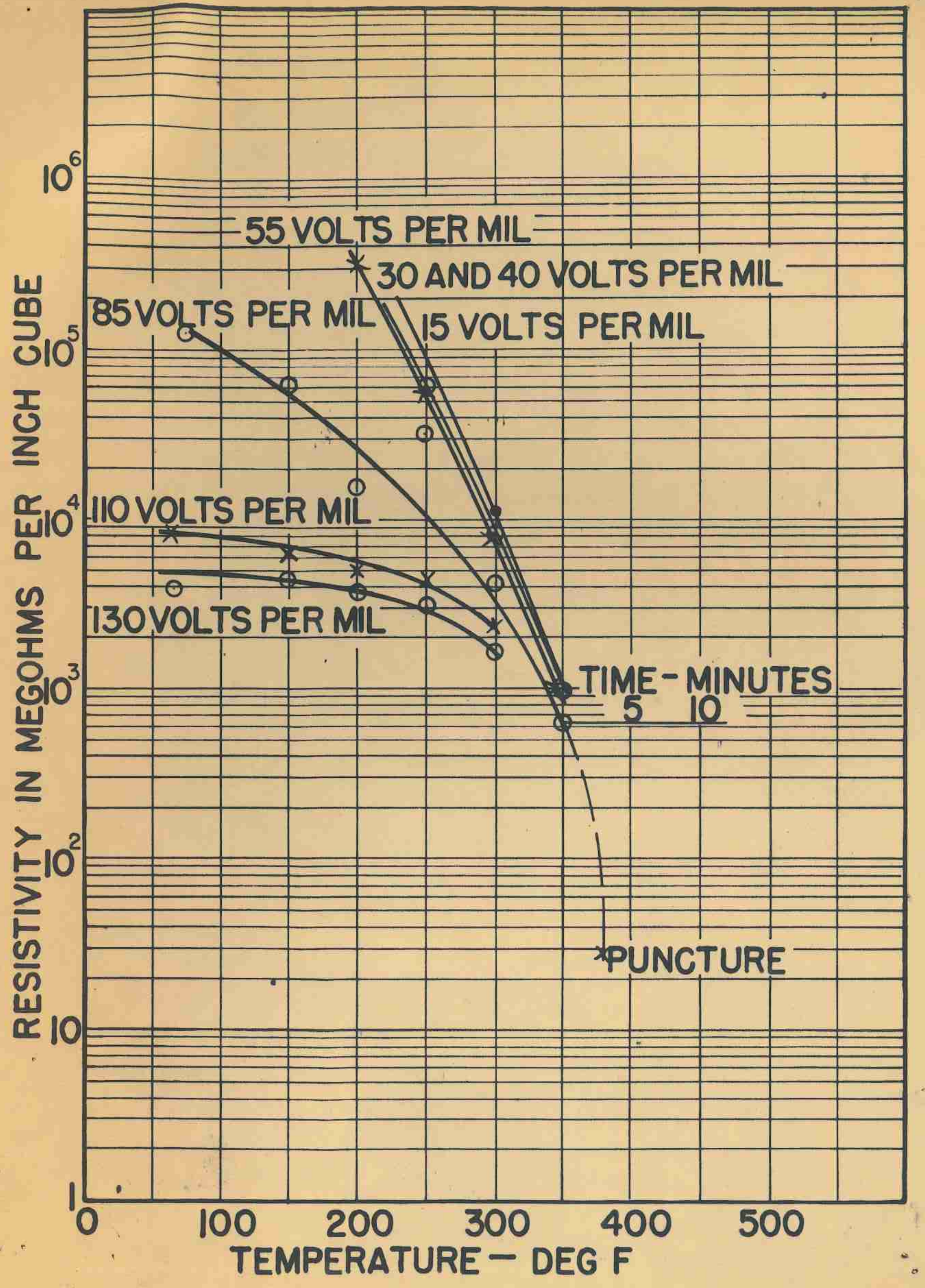

FIG 22 (FREY & JESATKO)

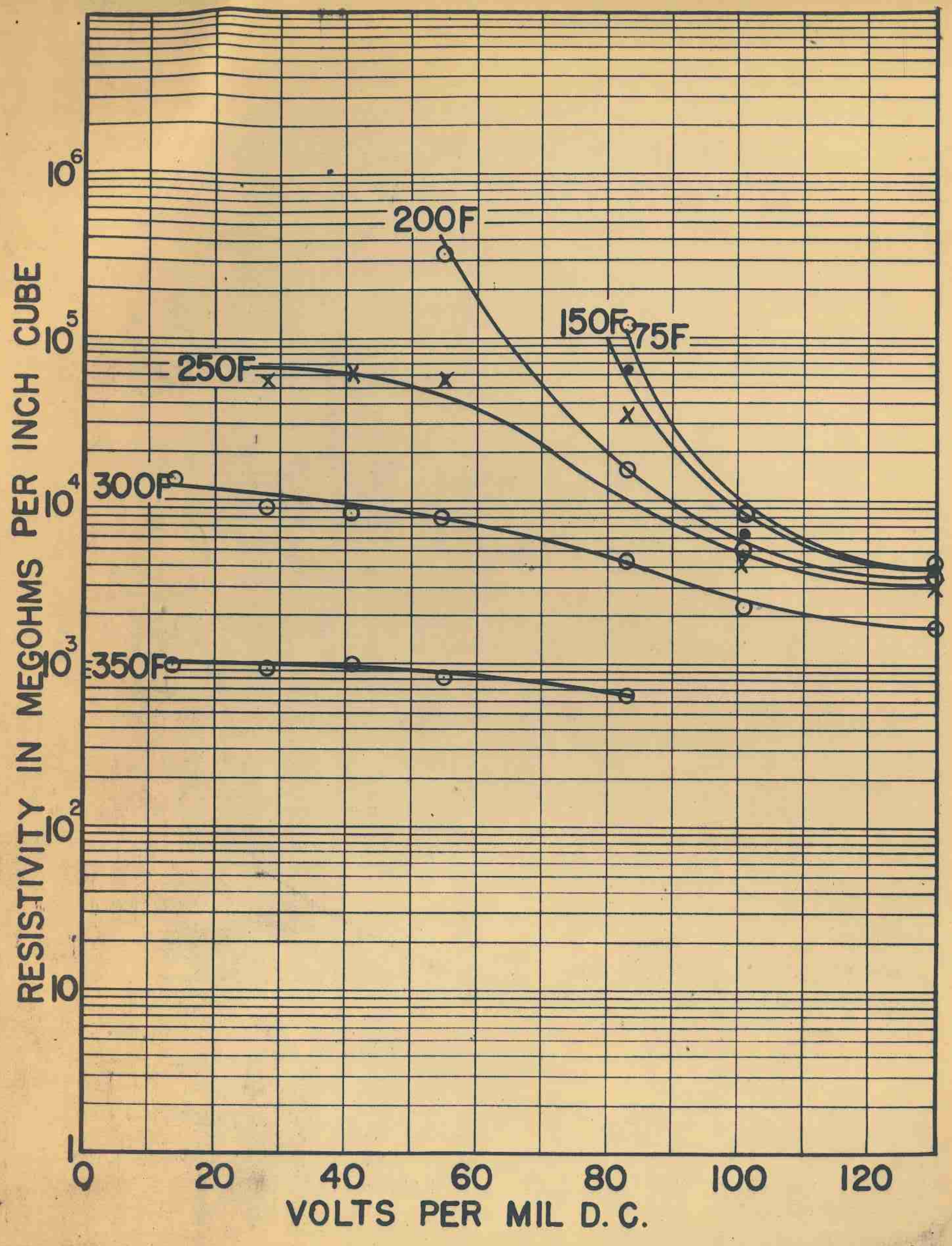

Fig. 23 (Frey & Jesatko)

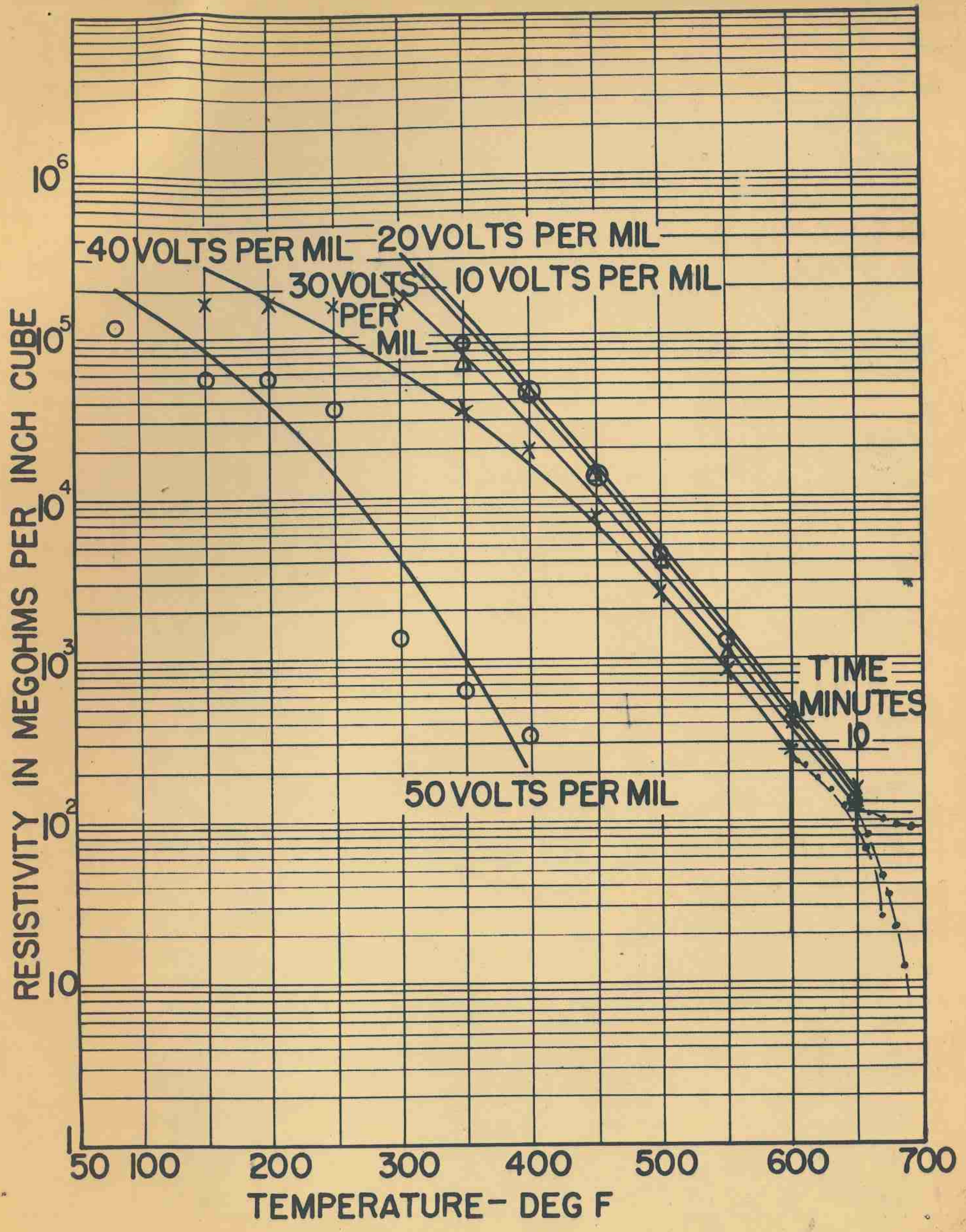

Fig. 24 (Frey & Jesatko)

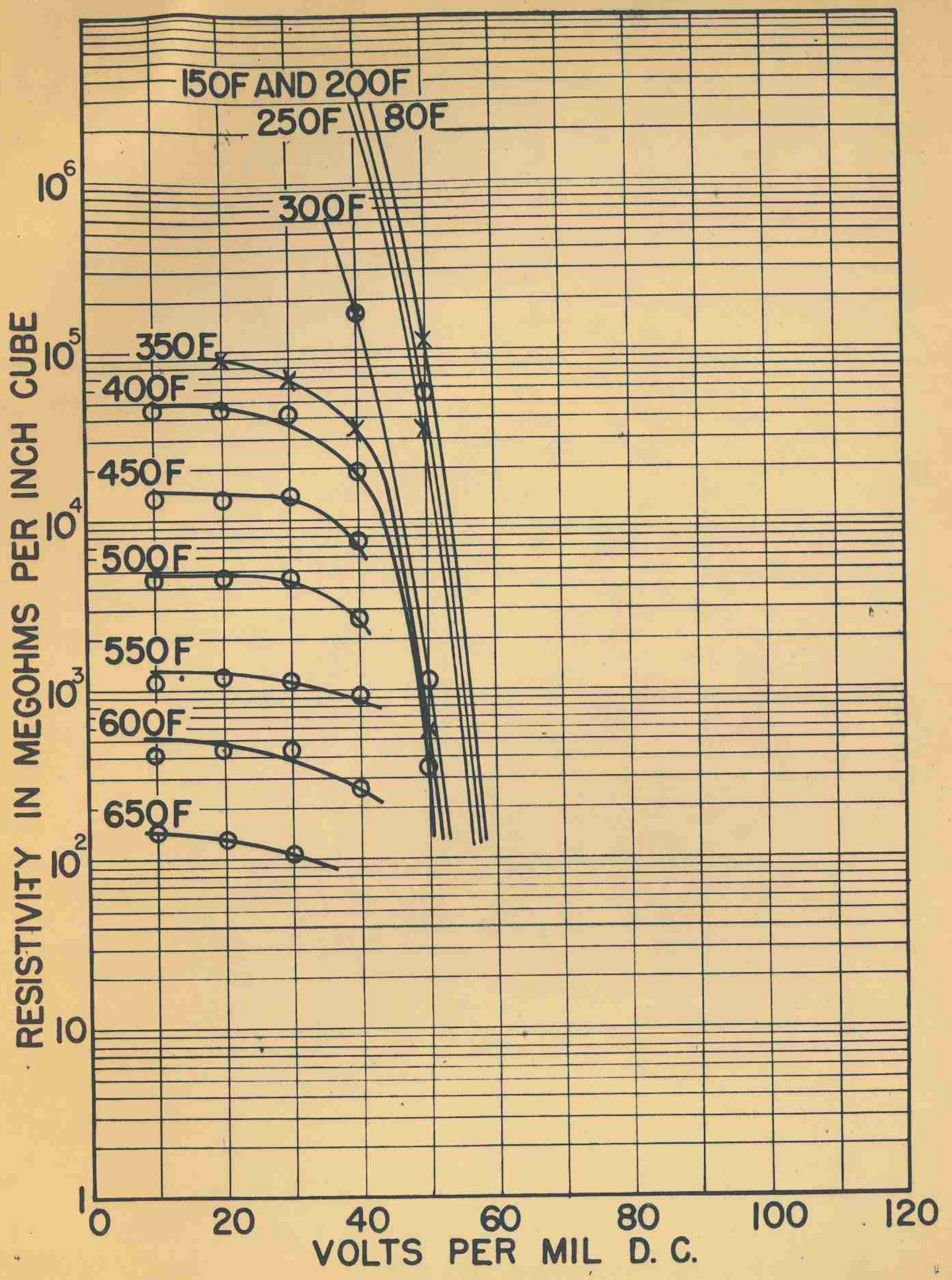

FIG 25 (FREY & JESATKO)

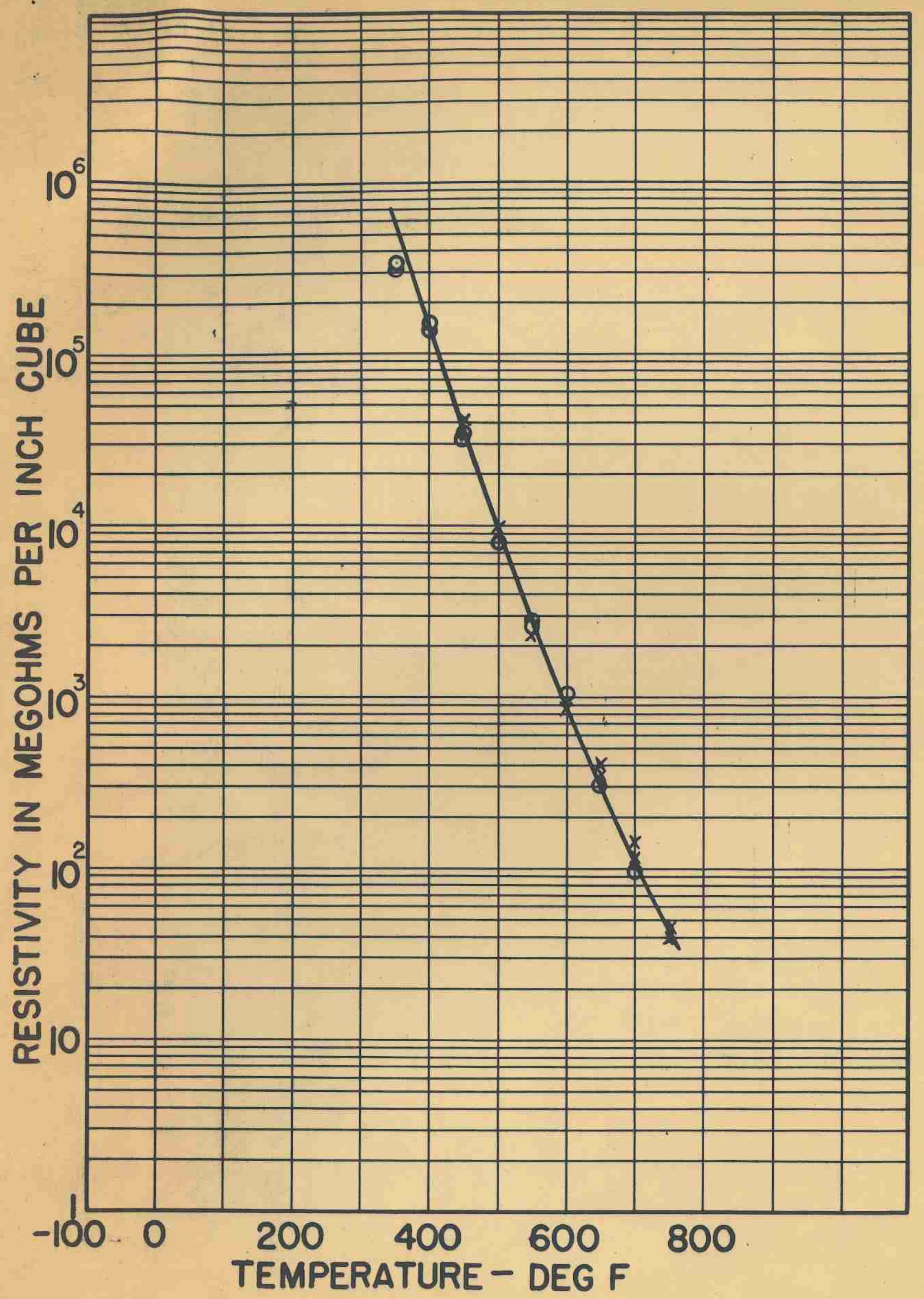

FIG. 26 (FREY & JESATKO)

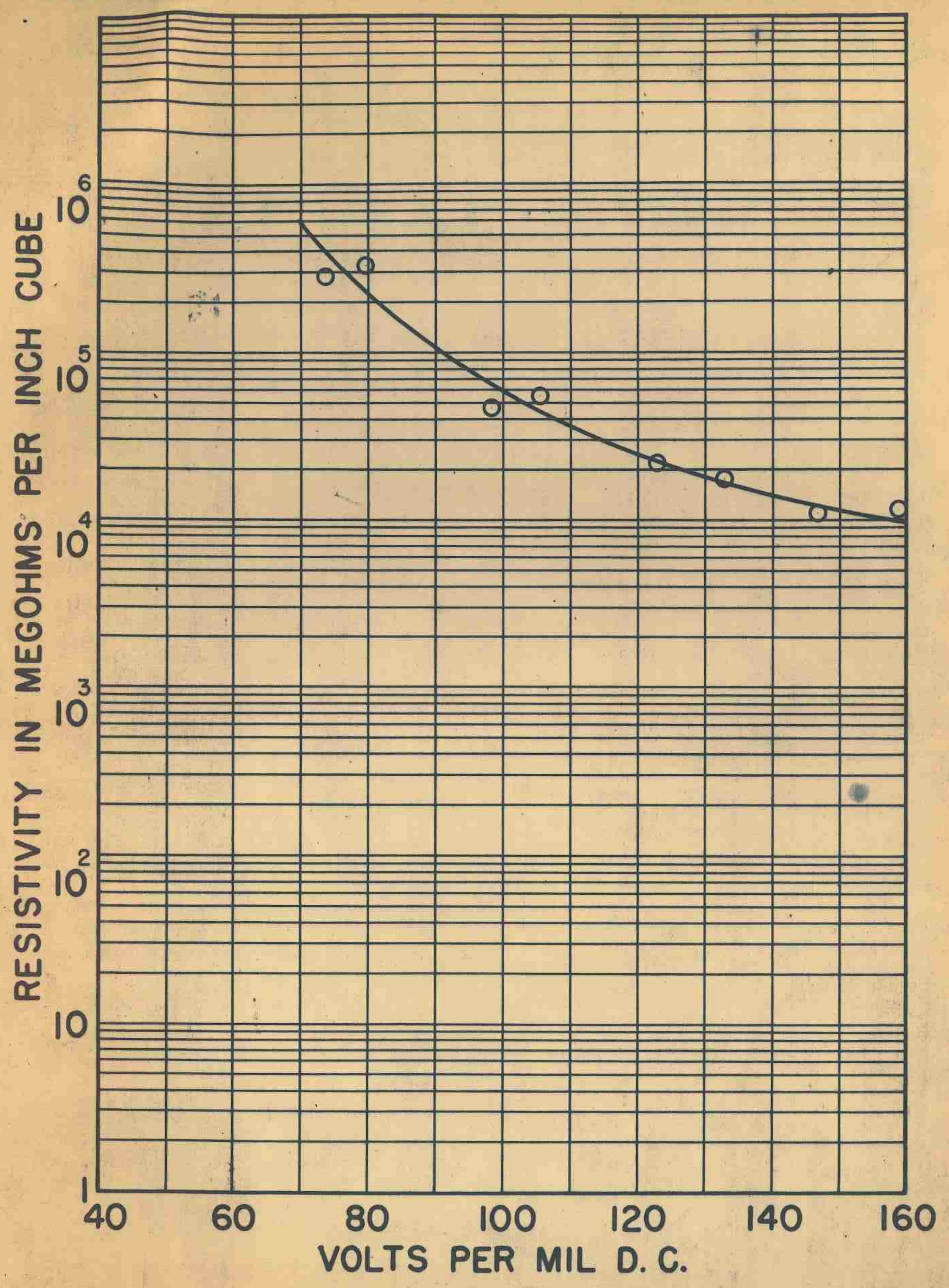

FIG. 27 (FREY & JESATKO)

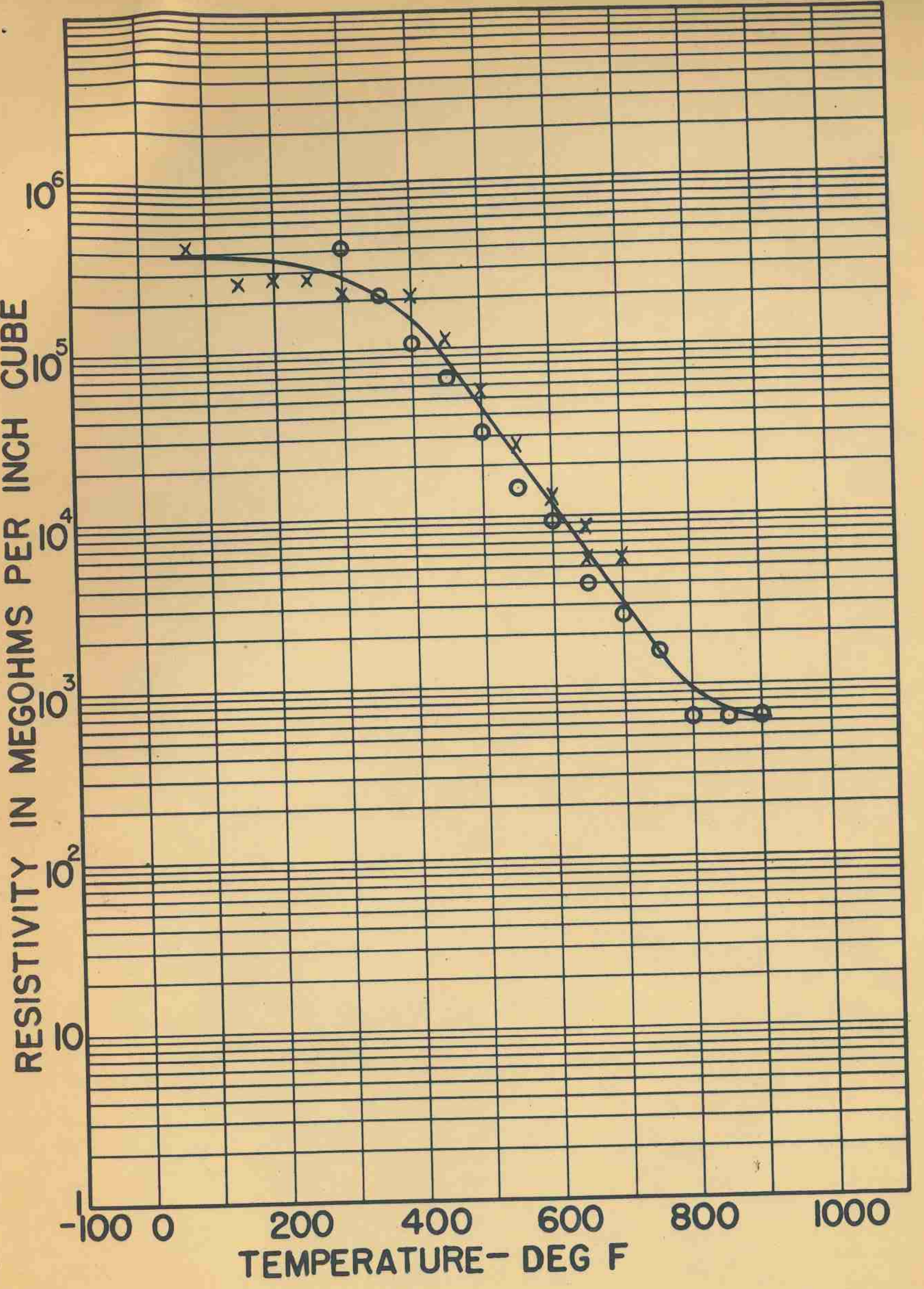

FIG. 28 (FREY & JESATKO)

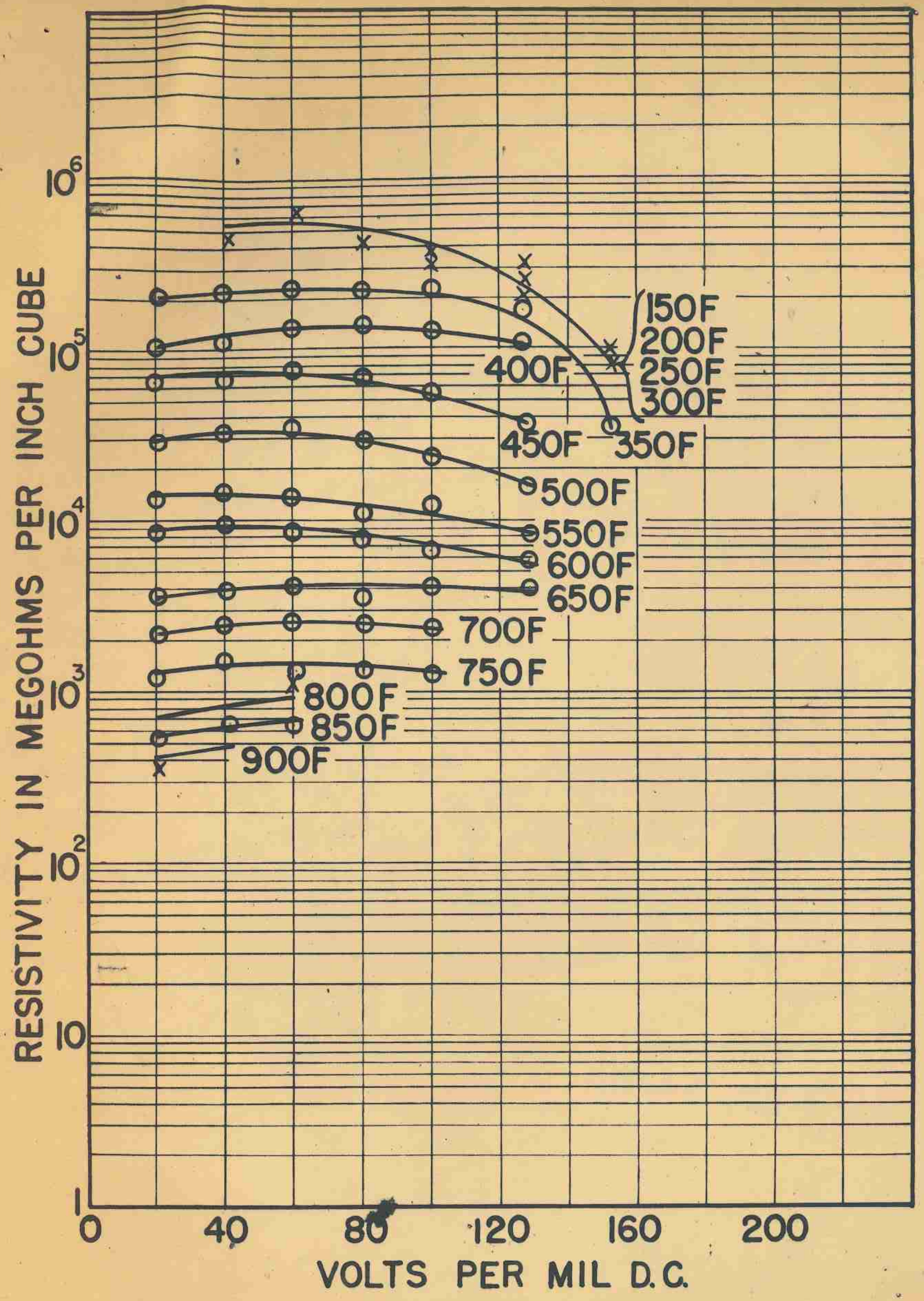

FIG. 29 (FREY & JESATKO)

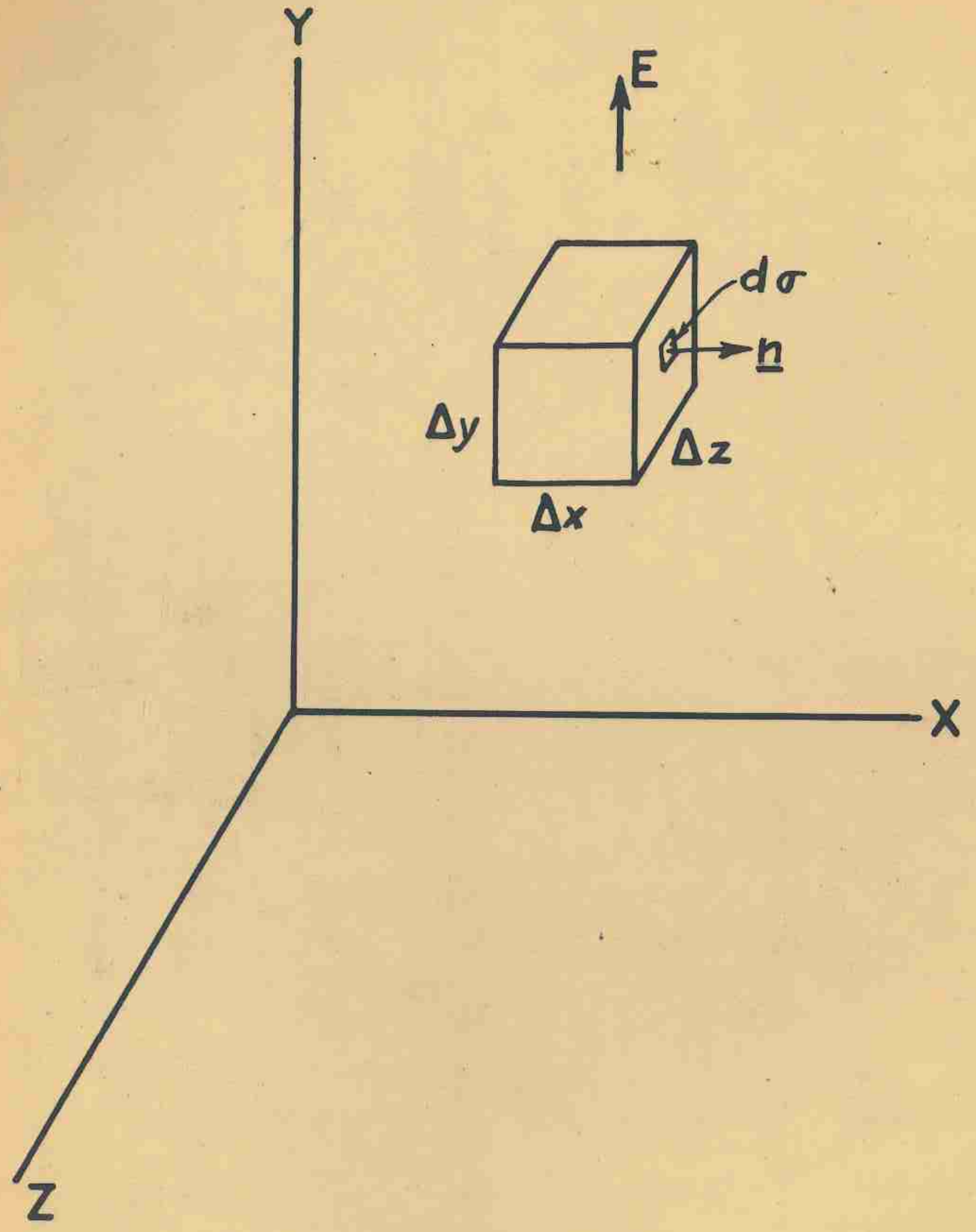
Y
E
$d\sigma$
$\underline{n}$
Δy
Δz
Δx
X
Z

FIG 30 (FREY & JESATKO)

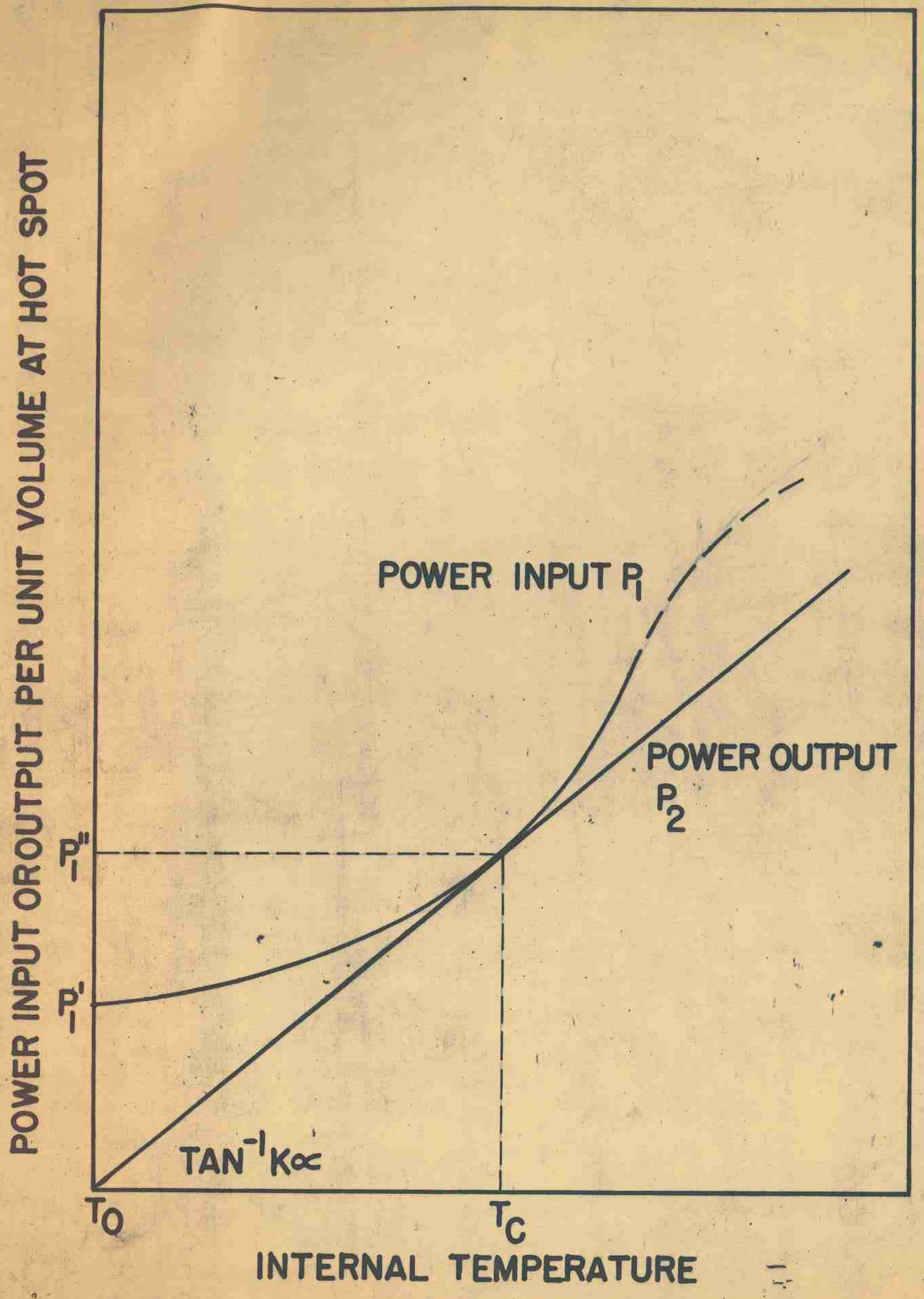

FIG. 31 (FREY & JESATKO)

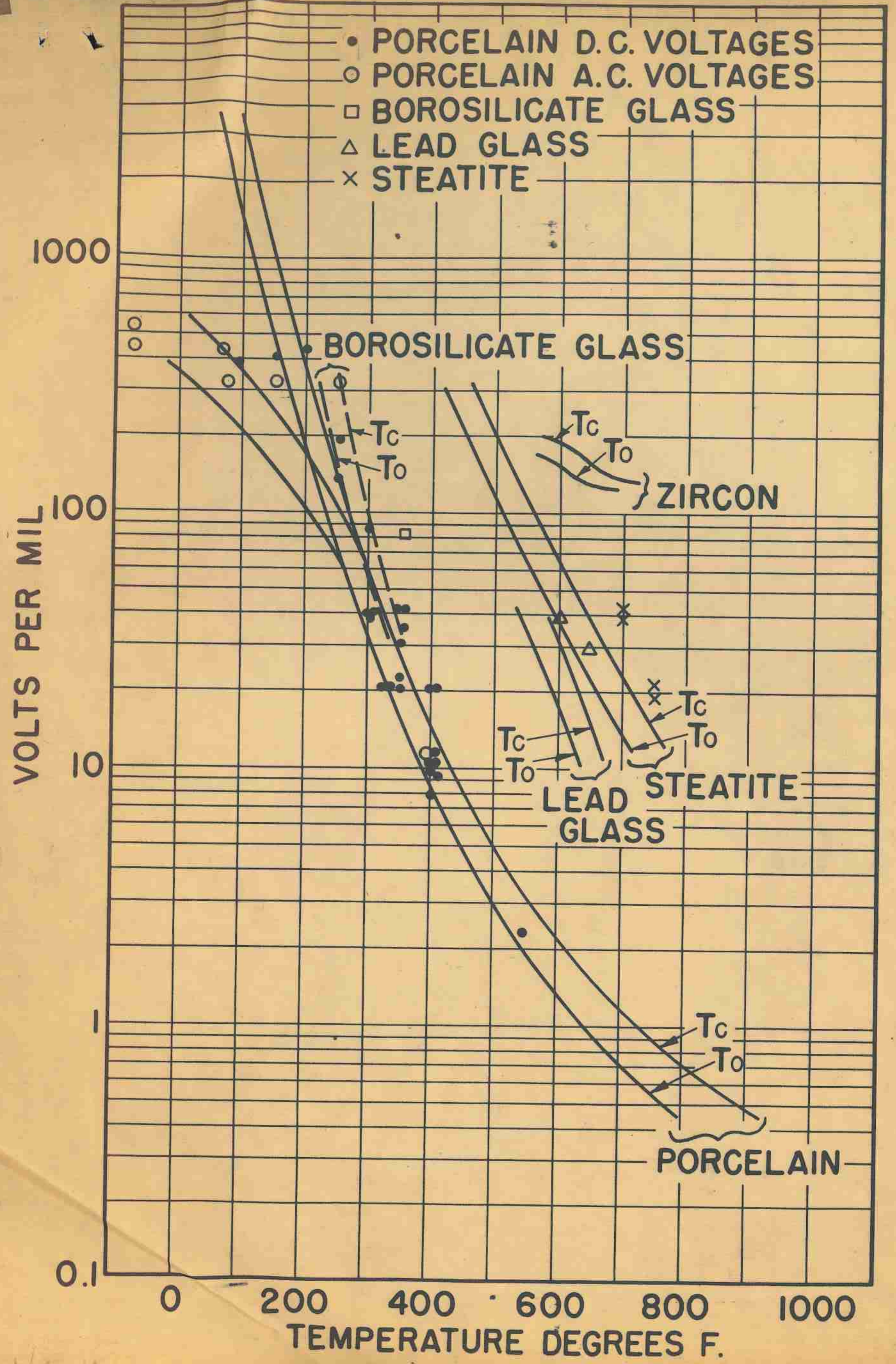

Vern Paler
Product Intro. Spec.

Alsop Engineering
High-Speed Mixer
1/4 hp motor
Oberdorfer pump
Stainless Steel

Beckman Cond. Bridge

Model RC 16B2

Slurry Mixture
40 gal H_2O - 152 l
20 g/l CAB-O-SIL 6.7 lb
3 g/l Photo-F10 #200 456 g
4 g/l NaCl - 608 g

Resistivity = 165 Ω/cm @ 21°C

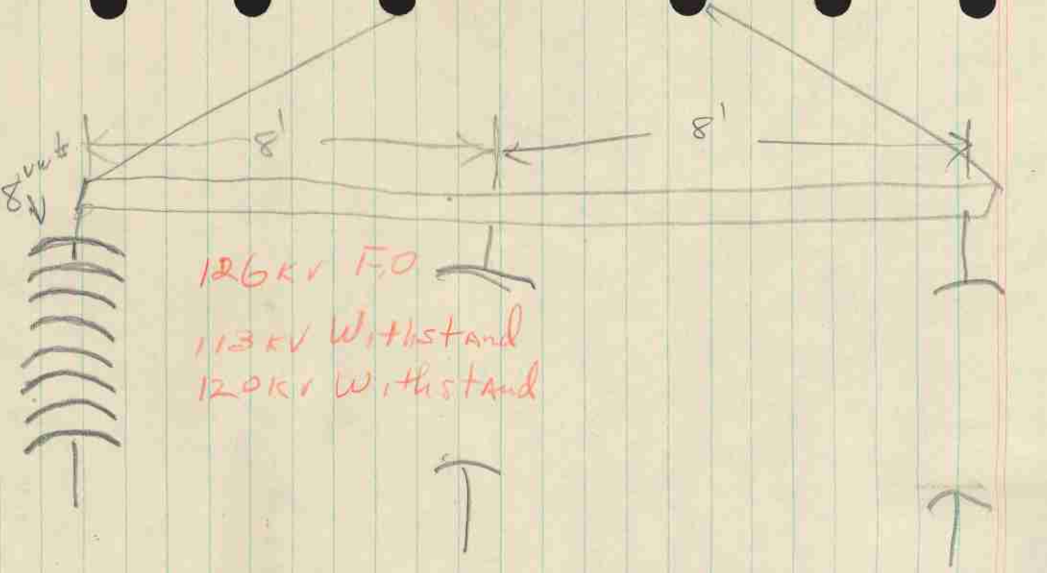

126KV F.O
113KV Withstand
120KV Withstand

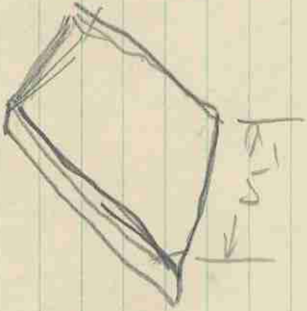

COLLECTING PAN

18 amperes - initial short-circuit current - goes to 10 amperes

1000 KVA transformer

350 KV

GENE MENDOZA

VOLTAGE Regulator
Dept.

VOLTAGE CONTROL

1. ~~Elaine - Letters~~
2. ~~Weller - data on 8707 -~~
3. Meeting uniform
4. Al - Savings & security Program
5. ~~Kay C -~~
   ✓ ~~A. Kindergarten / nursery matters~~
   ~~B. Records~~

✓ 6. Book on Motors & Generators

AIEE
Technical Paper
46-117

May 1946

Return to
B Findlay

THE ELECTRICAL PERFORMANCE OF CERAMIC DIELECTRICS AT ELEVATED TEMPERATURES

H. A. Frey
Member AIEE

J. A. Jesatko
Associate AIEE

Both of:
Locke Insulator Corp.
Baltimore, Md.

Advance Copy
Not Released for Publication

All Rights Reserved by the
American Institute of Electrical Engineers
33 West 39th Street, New York, N.Y.

A paper recommended by the AIEE committee on power transmission and distribution for presentation at the AIEE summer convention, Detroit, Mich., June 24-28, 1946. Manuscript submitted March 5, 1946; made available for printing May 8, 1946.

PRICE: *30¢ PER COPY BY MAIL*
25¢ AT HEADQUARTERS OR MEETING

Litho in U.S.A.

THE ELECTRICAL PERFORMANCE OF CERAMIC DIELECTRICS AT ELEVATED TEMPERATURES

- o 0 o -

It is well known that the electrical resistance of most of the commonly used insulating materials diminishes with increasing temperature. The actual performance of ceramic insulating materials at temperatures above the normal atmospheric level, and the factors affecting the ultimate breakdown at these temperatures, has not been the subject of much investigation. Recent requirements for insulators to operate at high temperatures and high voltages have indicated the need for such information.

There have been several insulator failures in precipitator applications which are directly attributable to the combination of high voltage and high temperature operation. Perhaps even more important are the development of certain new industrial processes which require that insulators be used at high temperatures. This investigation was undertaken for the purpose of obtaining fundamental design information on the high temperature electrical performance of ceramic materials and to develop suitable special materials for such applications.

Apparatus and Method.

It was necessary to provide a suitable test chamber in which the specimens could be mounted and held at any desired temperature while voltage was applied. Accordingly, a thermally insulated box or furnace was built. The electrical heating elements in the back of the box were separated from the test chamber by a one inch thick thermally insulating partition in order to prevent direct heating of the specimens by radiant heat. The heated air was circulated by means of a fan thru ports at each end of the test chamber. The fan also served to maintain air turbulence in the test chamber and thus prevent stratification. Temperature measurements were by commercial gas thermometer and automatic controls were provided for holding any desired temperature between minus 100 degrees Fahrenheit and 1000 degrees Fahrenheit. With this arrangement temperatures could be held within five degrees Fahrenheit of the desired level. Provision was also made for removing the heating elements from the back of the box and substituting racks of dry ice in order to obtain low temperatures.

Most of the tests were made with d-c voltage in order to eliminate the difficulty of separating conduction currents from charging currents. The voltage source was a full wave high voltage kenetron rectifier with suitable capacitors for the elimination of the sixty cycle pulse.

The d-c voltages were measured by means of a suitable known resistance connected in series with a microammeter.

Most of the test specimens were prepared in the form of plates of various thicknesses. Some specimens were made from standard suspension insulator shells using the head section, ground down to the desired thickness, as the test area.

Electrodes of circular shapes were applied to the opposite sides of each test specimen. Guard rings were also provided to eliminate the effect of surface leakage and corona, and to preserve a more nearly uniform field thru the test zone. The electrodes and guard rings were of silver ceramicly bonded to the surface of the dielectric to avoid entrapped air between the dielectric and its electrode.

Resistance measurements were made by connecting one electrode to the voltage source and grounding the opposite electrode thru a microammeter or milliammeter of proper scale range for the current involved. Suitable selector switches were provided for switching quickly from one instrument to another. The guard ring connections were shunted around the ammeters to ground. Resistance was determined from the ratio of voltage to current.

Before each measurement was made, the specimen was allowed to stand in the test chamber at zero voltage and constant temperature for a sufficient length of time to be sure that it was uniformly heated thruout its volume.

Materials:

The greater part of this investigation is concerned with porcelain, although some data has been obtained on two kinds of glass, a steatite composition, and a Zircon composition.

These are all generic names and there is considerable latitude in composition and in physical structure within each category.

The porcelain specimens involved were all made of wet process feldspathic porcelain of the type commonly known as "electrical porcelain". Samples of such porcelain as made by three different manufacturers were used.

The steatite specimens were a magnesia, alumina, silicate composition maturing at a firing temperature of about 2250 degrees Fahrenheit. The Zircon specimens were composed basically of Zirconia silicate with a calcium - zirconium - silicate flux compounded to mature at 2250 degrees Fahrenheit. This composition was developed particularly for high temperature applications.

Two types of glass specimens were included; a boro-silicate glass of the type used in the manufacture of high voltage insulators, and a lead glass also sometimes used in certain classes of insulators.

Discussion of Data - Porcelain.

Many measurements were made on a variety of specimens of varying shapes and thicknesses, at temperatures ranging from minus 70 degrees Fahrenheit to 900 degrees Fahrenheit and at voltage gradients up to 700 volts per mil. A gratifying degree of consistency in results was obtained. Typical data illustrating the results obtained are presented herein. As an example, the curve, Figure 2, is typical of the measurement made to determine the variation of resistivity with temperature and to determine the temperature at which final breakdown would occur. In plotting the curve the measured total resistances have been reduced to resistivity in megohms per inch cube. It should be noted that as the temperature was increased the resistivity steadily declined but remained stable (within the limits of measurement) at each point up to 250 degrees Fahrenheit. At 250 degrees Fahrenheit, on this particular specimen, it was found that with constant voltage the resistivity declined slowly with time, finally becoming stable at a lower level after about 45 minutes. This change in resistivity with time is indicated in Figure 2 by superimposing a time axis on the curve. The variation in resistivity with time, for a constant ambient temperature corresponding to that at zero time, is indicated by a broken line. This decline in resistance with time is undoubtedly caused by the internal heating of the specimen above the surrounding air due to the I^2R loss. It represents an average internal temperature rise of about 20 to 25 degrees Fahrenheit.

When the test chamber temperature was raised to 300 degrees Fahrenheit and held constant, the resistivity, with constant applied voltage, diminished with increasing rapidity until after 12 minutes the specimen would no longer support voltage and had, for all practical purposes, failed electrically. At this point voltage was removed but the test chamber was still held at a constant temperature of 300 degrees Fahrenheit. At intervals of 5 minutes the same voltage was momentarily reapplied and readings were quickly taken. It should be noted that as the specimen cooled internally the resistivity recovered along a typical cooling curve.

The test chamber temperature was then raised to 325 degrees Fahrenheit and the same voltage reapplied. The resistivity again declined still more rapidly with time, and within 5 minutes reached the point where voltage could not be supported. Voltage was then removed and the piece was again allowed to recover. The test chamber temperature was raised to 350 degrees Fahrenheit and a momentary reading taken as indicated on the curve. The test chamber was allowed to cool back to room temperature and the resistivity was again measured checking the value determined at the start of the test.

On this particular specimen voltage was removed in each case as soon as a runaway condition was observed as indicated by current increasing more and more rapidly. On some other specimens voltage was not promptly removed and power was delivered to the piece for several seconds after the runaway phenomenon was observed. In such cases the dielectric was cracked or a fused path developed thru it resulting in a permanent failure.

The Curve Figure 2 illustrates the variation of resistivity with temperature for one particular porcelain specimen at a constant voltage gradient. At any temperature level the resistivity may also vary with changing voltage gradient. This effect was studied on a number of porcelain specimens and Figure 3 is a typical plot of the data obtained on one particular specimen -- the same specimen appearing in Figure 2. It should be noted that at the lower temperatures resistivity diminishes rather rapidly with increasing voltage gradient but at temperatures above 250 degrees Fahrenheit, the resistivity becomes nearly independent of voltage gradient.

The results of all measurements made on porcelain to determine the variation of resistivity with temperature was plotted on one composite curve (Figure 4). At the higher temperature it was necessary to make all tests at relatively low voltage gradients in order to obtain stable measurements. Thus at 900 degrees Fahrenheit the measurements were made on a specimen approximately 0.8 inch thick with voltage applied from a 45 volt battery equivalent to about 0.05 volts per mil. At these higher temperatures the resistivity changes but little with changing voltage gradient so this limitation does not impair the usefullness of the information contained in Figure 4.

An examination of Figure 4 shows that data conforms with reasonable accuracy to a single curve for all temperatures above about 250 degrees or 300 degrees Fahrenheit. At lower temperatures the composite data spreads widely as indicated by the envelope shown. This spread of the data at the lower temperatures is due primarily to two factors. First the influence of voltage gradient on resistivity at lower temperature and second the influence of specimen thickness.

The influence of voltage gradient has already been illustrated. In testing specimens of different thicknesses it was observed that at low temperatures the apparent resistivity was lower for thick specimens than for thin ones. The influence of thickness on resistivity diminished with increasing temperature so that for temperatures above about 250 or 300 degrees F. the apparent resistivity was relatively independent of thickness. The apparent effect of thickness on resistivity is believed to be due to the variation of the true voltage gradient from the average voltage gradient. As the specimen thickness is increased it becomes more and more difficult to maintain a truly uniform voltage gradient thru it.

It has been pointed out that porcelain made by three different manufacturers was used in the investigation. No significant difference was found between the three porcelains. Figure 5 shows a typical comparison of dimensionally identical pieces as made by two manufacturers. These two pieces were tested simultaneously. The change in resistivity with time (due to internal heating and cooling) is shown on the curve in the same manner as in Figure 2. At 300 degrees Fahrenheit, voltage was applied for 10 minutes at which time the resistivity had become stable. Voltage was then removed and the specimen allowed to cool back to the test chamber temperature. Voltage was then reapplied and a duplicate heating curve was obtained. At 325 degrees Fahrenheit both specimens drifted towards breakdown. Specimen B actually refused to support voltage but specimen A was well on the way to the same condition and would doubtless have failed in another minute or two had the test been continued. It should be noted that at 325 degrees Fahrenheit, both of the resistivity drift curves pass thru a definite flex point where the shape of the drift curve changes from concave upward to concave downward. After the breakdown at 325 degrees Fahrenheit, the pieces were allowed to cool and the test chamber temperature was raised to 350 degrees Fahrenheit. At this level both specimens drifted rapidly to breakdown in about 3 minutes.

Effect of Glaze.

All data which has been discussed up to this point has been obtained on unglazed specimens. In order to determine the effect of glaze on the high temperature performance of porcelain, two cylinders were prepared 1-1/8" in diameter and 2-1/4" long. One of these cylinders was glazed with a standard glaze of the type normally applied to high voltage insulators. The other cylinder was left unglazed. Silver electrodes were applied and ceramicly bonded to each end of each cylinder. The silver coatings were carried over the ends and extended down the side walls on each end for a distance of 5/16". This was done in order to place the highest voltage gradient along the outer glazed surface. Figure 6 shows the results of a simultaneous test made on these two pieces. The resistance of the two was practically the same thruout the test and both pieces drifted to failure at 410 degrees Fahrenheit. Note that this curve is plotted with total resistance and not resistivity as ordinates.

Some Practical Insulators.

In addition to prepared test specimens a number of tests have been made on practical insulators of various types and forms. Figure 7 shows the results of two such tests made on a standard 23 KV heavy duty, two shell outdoor switch insulator. The insulator was tested with its regular metallic parts cemented in place in the usual manner. A d-c voltage of 14 KV was applied between cap and pin which voltage is numerically the same as the r.m.s. normal service voltage to ground. Note that in Figure 7 the total resistance to ground is plotted as a function of temperature. In this insulator the conduction path from top to bottom metallic elements passes thru three layers of portland cement and two layers of porcelain. It should be noted that the initial measurement made at 80 degrees Fahrenheit is considerably below the curve as drawn and also is lower than the second point at 150 degrees Fahrenheit. This peculiar performance is believed to be due to the variation in resistance of the cement. Portland cement is quite hygroscopic and when slightly moist is a fairly low resistance conductor. As the water is driven off, however, its resistance increases so that at elevated temperatures it adds in some measure to the total resistance of the insulator. The high temperature end of the curve is two pronged representing the results from two separate tests. Note that drift curves became measurable on one curve at 350 degrees Fahrenheit and on the other at 400 degrees Fahrenheit, reaching stability in each case after about 40 minutes. At 450 degrees Fahrenheit the insulators drifted to failure in 20 and 30 minutes respectively.

A similar insulator was subjected to test at 14 KV r.m.s. 60 cycles. This test was made by raising the temperature in 50 degree Fahrenheit steps and holding the voltage and temperature constant for one hour at each step. Due to the difficulties of separating conduction from charging currents, no resistance measurements were made. The unit failed after 54 minutes at 400 degrees Fahrenheit. A number of other a-c tests have been made on other porcelain samples, the results of which will be discussed later.

Discussion of Data: - Glass.

In Figure 8 are plotted the measurements of the resistivity of boro silicate glass as a function of temperature. This particular glass specimen was the glass element only of a suspension insulator. Silver electrodes with guard ring were applied to the head area. At 85 volts per mil and 350 degrees Fahrenheit, the specimen drifted to breakdown in about 3 minutes. At the instant of failure the specimen was shattered by the forces of differential expansion.

In Figure 9 the variation of resistivity of the same specimen is shown as a function of voltage gradient.

Similarly Figures 10 and 11 show the performance of a specimen made of a lead glass. This specimen drifted towards failure at 40 volts per mil at 600 degrees Fahrenheit after about 3 minutes, but upon cooling recovered and was not permanently injured. At 650 degrees Fahrenheit and 20 volts per mil the same specimen showed a definite downward drift in resistivity due to internal heating but stabilized after about 10 minutes. At 650 degrees Fahrenheit and 30 volts per mil the piece drifted to failure in about 8 minutes. In this case power was not removed quickly enough and a permanent failure occurred taking the form of a fused path thru the glass.

Discussion of Data: - Steatite.

The results of tests on two steatite specimens are shown in Figure 12. Note that for two voltage gradients, 20 and 40 volts per mil, the curves virtually coincide. Both specimens initially drifted towards failure after 15 and 17 minutes respectively at 700 degrees Fahrenheit and 40 volts per mil. The pieces were cooled back to test chamber temperature and recovered. At 750 degrees Fahrenheit both specimens failed at 20 volts per mil after 9 and 10 minutes respectively.

There is not sufficient data to plot the variation in resistivity of this steatite composition as a function of voltage for various temperature levels. In Figure 13 such data is plotted for one temperature only.

Discussion of Data - Zircon.

Several Zircon compositions were investigated and it was found that the high temperature electrical characteristics of the several compositions varied radically. The particular zircon composition included in this paper is the one having the best characteristics of the group tried. Figure No. 14 gives the variation in resistance as a function of temperature with a voltage gradient of 40 volts per mil. Figure 15 shows the variation in resistance as a function of voltage gradient for various temperatures.

There are two characteristics of this material which are worthy of particular note. In the first place it is observed that in certain ranges increasing voltage gradient results in slight increases in the measured resistance. Such a condition was not observed on any of the other materials nor even on the other Zircon specimens having slightly different composition. Secondly it was observed that, at any fixed temperature above about 400 degrees Fahrenheit when a constant voltage was applied, an initial current was measured which diminished with time finally stabilizing at a value lower than the initial. In other words the measured resistance increased with time. This is exactly opposite to the performance of the other materials. At the lower temperatures, around 500 degrees Fahrenheit this upward drift of resistance reached stability in about one minute with a rise in resistance of about 3 to 4 percent. At higher temperatures, about 800 degrees Fahrenheit, the upward drift of resistance reached stability in several minutes with rise in resistance of about 30 percent. At 800 degrees Fahrenheit and at higher voltage gradients, 60 volts per mil, stability was reached only after 20 minutes with a rise of more than 100% of the initial value. This characteristic continued up to 900 degrees Fahrenheit, the upper limit of the test, and no breakdowns were obtained.

These two unusual characteristics of this material are believed to be due to dielectric polarization. The curves Figures 14 and 15 are plotted to show the resistance at each level for the polarized or stable condition.

Theoretical Considerations.

From an engineering standpoint it is most important that one be able to determine the temperature and voltage at which a particular insulator may be safely operated without failure. To accomplish this with some reasonable knowledge of the margin of safety, the end point conditions should be predictable. Therefore some theoretical discussion of the mechanism of breakdown is in order.

From the data it seems reasonably conclusive that, at least at elevated temperatures (250 degrees Fahrenheit and above), breakdown is a thermal phenomenon. When voltage is applied to a dielectric a leakage or conduction current flows thru the material and the I^2R loss results in internal heating above the ambient temperature. This increase in internal temperature results in a reduction of resistivity with consequent increase in internal heating, if a constant applied voltage is maintained. As the internal temperature rises above the ambient, heat is dissipated from the stressed volume. In most practical applications thermal conduction is the principal means of heat dissipation from the stressed volume. The power dissipated as heat from any point in the stressed volume is therefore a function of the internal temperature rise. If the power dissipated as heat increases more rapidly as the temperature rises, than does the power input, the time rate of temperature rise will diminish and a condition of stability will be obtained. If the reverse condition occurs the temperature will rise with increasing rapidity until the dielectric fuses or is cracked by differential expansion stresses.

Consider the elemental cube (Figure 16) in the dielectric body. Let the volume of this cube be ΔV and the edge dimensions be $\Delta x, \Delta Y$ and ΔZ . Let the direction of voltage gradient be parallel to the Y axis thru the elemental cube. If the voltage gradient thru the cube in volts per inch is E and if the resulting current density is I amperes per square inch then, P_{T1}, the total power input to the cube is

$$P_{T1} = (E\Delta Y)(I\Delta x\Delta z) = EI\Delta V$$

If the resistivity of the material is r ohms per inch cube

$$P_{T1} = \frac{E^2}{r}\Delta V$$

The power input per unit volume = $P_1 = \frac{P_{T1}}{\Delta V} = \frac{E^2}{r}$ $\qquad \textcircled{1}$

If the total power output from the cube in the form of heat is P_{T2}, then

$$P_{T2} = \int_s K\nabla T \cdot \underline{n}\, d\sigma$$

Where T is the temperature rise of the cube above the ambient and where ∇T is the temperature gradient outward from the cube, $d\sigma$ is any element of surface of the cube, n is a unit vector normal to that element of surface, and K is the thermal conductivity of the material.

The power output per unit volume = $P_2 = \frac{P_{T2}}{\Delta V}$

$$P_2 = \frac{K}{\Delta V}\int_s \nabla T \cdot \underline{n}\, d\sigma$$

Taking the limit as ΔV approaches zero

$$P_2 = K\nabla^2 T \qquad \textcircled{2}$$

The term $K\nabla^2 T$ cannot be exactly evaluated from theoretical considerations alone. However, this term merely represents the power output in the form of heat from a small element in the stressed volume. In any practical insulator

as soon as a voltage is applied, some element within the stressed volume begins to heat slightly faster than its immediate surroundings. This may be because the element is at the center of the volume where heat loss is the slowest or it may be because of variations in voltage gradient, or because of variations in the homogenity of the material. As soon as the element in question begins to rise in temperature above that of the surrounding stressed volume, its resistivity diminishes and consequently its rate of heating is further increased. A "hot spot" is therefore quickly established and it is this hot spot which is of primary concern. Equation (2) may be applied to represent this heat loss from the critical element and by making certain reasonable assumptions may be reduced to a more useful form. Since the surface area of any practical insulator is relatively large and since the thermal conductivity of the material under consideration is relatively small, it may be assumed that the rate of heat loss from the critical volume is directly proportional to the temperature rise above the ambient. For these assumptions equation (2) may be written,

$$P_2 = K\alpha T \qquad \textcircled{3}$$

Where T is the temperature rise of the element and α is the factor of proportionality.

At any point of stability P_2 must equal P_1

When voltage is first applied T = o and consequently P_2 = o. As T increases, P_1 and P_2 both increase. If, with increasing temperature T, P_1 continuously increases faster than P_2 stability can never be reached and the temperature will continue to rise until failure occurs. Conversely if P_2 continuously increases faster than P_1, a condition of equilibrium will ultimately be reached where $P_2 = P_1$.

The rate of increase of P_1 with respect to temperature T is

$$\frac{\partial P_1}{\partial T} = -\frac{E^2}{r^2}\frac{\partial r}{\partial T}$$

Since, for the materials under consideration, $\frac{\partial r}{\partial T}$ is negative, this shows a positive value for the product -

$$-\frac{E^2}{r^2}\frac{\partial r}{\partial T}$$

The rate of increase of P_2 with respect to temperature is

$$\frac{\partial P_2}{\partial T} = K\frac{\partial(\nabla^2 T)}{\partial T} \approx K\alpha \qquad \textcircled{4}$$

The conditions leading to ultimate breakdown are illustrated in Figure 17. The power input when voltage is first applied at ambient temperature T_o is represented by P_1. As the internal temperature rises the power input increases as shown. The power output is initially zero but increases as internal temperature rises. If the P_2 curve intersects the P_1 curve, stability is reached. If the P_2 curve fails to intersect the P_1 curve runaway and breakdown ultimately occur.

If the power input (P_1) curve is concave upwards then the critical point will be reached when the starting temperature T_o is such as to make the P_2 curve reach the P_1 curve at a point of tangency. This occurs at some critical temperature T_c and with power input P_1'' as illustrated in Figure 17.

At this point

$$\frac{\partial P_1}{\partial T} = \frac{\partial P_2}{\partial T}$$

or

$$-\frac{E^2}{r^2}\frac{\partial r}{\partial T} = K\alpha \qquad \textcircled{5}$$

The initial ambient temperature T_o necessary to ultimately reach the critical condition is lower than T_c by an amount equal to P_1'' divided by $K\alpha$.

If the power input curve (P_1) is concave downwards then the P_2 curve will always intersect it at some point and with some theoretical finite temperature rise above the ambient. Whether or not failure occurs then depends upon whether the temperature at this point of intersection is within the range which the dielectric can stand without fusing, cracking or charring. It is perfectly possible that the power input curve may be in some zones concave upward and in other zones concave downward with a flex point as illustrated by the broken line in Figure 17.

Equation (5) may therefore be applied only when the second derivative of power input with respect to temperature is positive at the critical point.

$$\frac{\partial^2 P_1}{\partial T^2} = -\frac{E^2}{r^2}\frac{\partial^2 r}{\partial T^2} + \frac{2E^2}{r^3}\left(\frac{\partial r}{\partial T}\right)^2$$

This term is always positive when $\frac{\partial^2 r}{\partial T^2}$ is negative. If $\frac{\partial^2 r}{\partial T^2}$ is positive the term is positive only when

$$\frac{E^2}{r^2}\frac{\partial^2 r}{\partial T^2} < \frac{2E^2}{r^3}\left(\frac{\partial r}{\partial T}\right)^2$$

$$\frac{\partial^2 r}{\partial T^2} < \frac{2}{r}\left(\frac{\partial r}{\partial T}\right)^2 \qquad \textcircled{6}$$

The values of r and of the first and second partial derivatives can be physically determined from the temperature - resistivity curve of any material. For porcelain, the steatite composition and the two glasses the relation (6) is satisfied within the range investigated. For Zircon the second derivative of r with respect to T is negative up to about 350 degrees Fahrenheit. Above 350 degrees Fahrenheit relation (6) is satisfied up to about 700 degrees Fahrenheit. Above 700 degrees Fahrenheit the power input curve is concave downward and stability can always theoretically be reached at some temperature rise. In this respect above 700 degrees Fahrenheit Zircon will behave more like a very high resistance conductor than an insulator.

Hence equation (5) can be applied to porcelain, the two glasses and the steatite composition within the range for which data exists. It can also be applied to the Zircon up to 700 degrees Fahrenheit. The value of thermal conductivity K for these materials are approximately as follows:

Porcelain	.0203	Watts/sq.in./inch/degrees Fahrenheit
Steatite	.0285	" " " " " "
Borosilicate Glass	.0182	" " " " " "
Lead Glass	.0182	" " " " " "
Zircon	.031	" " " " " "

For most of these materials the thermal conductivity increases somewhat with increasing temperature. By neglecting this change and using the above values throughout conservative results will be obtained.

In order to numerically evaluate equation (5) the value of the factor α must be determined. The points of ultimate failure with d-c voltage for all porcelain test specimens are listed in table I. The theoretical values for $-\frac{E^2}{r^2}\frac{\partial r}{\partial T}$ are shown for each case. It should again be noted that the data in table I was obtained by applying constant voltage and raising the ambient temperature in steps. In many cases failure would probably have occurred at some lower temperature had smaller steps been used. For this reason those tests on which failure occurred in less than 3 minutes have been discounted. For the remaining tests the average value of the term $-\frac{E^2}{r^2}\frac{\partial r}{\partial T}$ is 0.067 with a range of from 0.0189 to 0.124. The last column in table I shows a word symbol indicating whether or not the drift curve to failure passed thru a flex point. Those tests marked "flex" showed a definite flex point in the drift curve. For those points marked "no" the drift curve continued with increasing acceleration to failure with no flex point. For cases where no flex point occurred in the drift curve the starting temperature must have been at some point above T_c. For those tests where a flex point appeared the starting temperature must have been between T_o and T_c. The values of $-\frac{E^2}{r^2}\frac{\partial r}{\partial T}$ for those tests which passed thru a flex point range from 0.0189 to .0925, with an average value of .0398. For those tests which did not show a flex point on the drift curve the value of $-\frac{E^2}{r^2}\frac{\partial r}{\partial T}$ ranged from a high of 0.124 to a low of 0.023 with an average of 0.0725. By inspection it appears that the value of the function $-\frac{E^2}{r^2}\frac{\partial r}{\partial T}$ should be about .06 at the flex point. If .06 is taken as the approximate numerical value of the function at the flex point, then this may be substituted in equation (5) and the factor α may be evaluated as approximately 3 for porcelain. This evaluation is not very precise but it should be noted that an error of even 3 to 1 in the value of α produces an error of only about 50 degrees Fahrenheit in the theoretical end point temperature.

For porcelain the resistivity varies but little with voltage gradient for temperature above 250 degrees Fahrenheit. A reasonably accurate general solution can therefore be obtained for temperatures above 250 degrees Fahrenheit. For temperatures below 250 degrees Fahrenheit some confusion exists probably due to the variation of resistivity with voltage gradient and sufficient data is not available for an accurate analysis. As a matter of interest equation (5) has been evaluated for porcelain below 250 degrees using the two extremes of the resistivity curve Figure 4.

This yields the theoretical internal temperature T_c at which runaway actually starts for any particular voltage gradient. In Figure 18 the values of T_c have been plotted against voltage gradient. The starting ambient temperature T_o from which the critical internal temperature T_c may ultimately be reached has also been plotted in Figure 18 taking:

$$T_c - T_o = \frac{\text{WATTS PER CU. IN. INPUT AT } T_o}{K\alpha}$$

Any point to the left of the T_o curve should be safe for continuous operation. Points to the right of the T_o curve should result in failure if given sufficient time.

In table II the actual breakdown points for several practical insulators are shown. These values have also been plotted on Figure 18.

For the materials other than porcelain there is not sufficient data to make a determination of α by the method used for porcelain. It is difficult to see why the value of α should materially differ from that for porcelain. If we assume that α is the same for the steatite, glass and zircon compositions as for porcelain, then theoretical breakdown curves can be plotted for these materials. Such curves for the four other materials are plotted in Figure 18 within the range of the existing data. For borosilicate glass, no data is available above 350 degrees Fahrenheit and for temperatures below 250 degrees Fahrenheit the resistivity varies greatly with voltage as indicated in Figures 8 and 9. The curve for borosilicate glass can therefore be generalized from this data over only a short range. In Figure 18 the borosilicate glass curve is shown in broken lines so that it may be distinguished from the porcelain curve.

Examination of Figures 10 and 11 will show that the lead glass curve can be generalized from existing data only within the temperature range from 350 degrees Fahrenheit to 650 degrees Fahrenheit and for voltage below 40 volts per mil.

No data is available on the steatite composition to show the variation of resistivity with voltage at the higher temperatures. There is every indication, however, that, like porcelain, the resistivity of Steatite becomes essentially independent of voltage at temperatures above 250 degrees Fahrenheit. The plot for steatite in Figure 12 is based on this assumption.

For the zircon composition it appears as though above about 140 volts per mil resistivity will vary considerably with voltage. Also above 700 degrees Fahrenheit stability can theoretically always be reached. The generalized zircon plot is therefore quite short but does adequately indicate the relative position of this material. Above 700 degrees Fahrenheit there is some question as to whether at any particular voltage gradient, the material will stabilize before the internal temperature rise becomes excessive. The experimental evidence indicates that for d-c gradients up to 40 volts per mil the zircon composition can be successfully operated at 900 degrees Fahrenheit and possibly higher.

As a practical check on these theoretical predictions tables I, II, III and IV give the actual measured breakdown points for a number of specimens. The individual points from these tables have been plotted on the curves Figure 18 for direct comparison. As would be expected all actual breakdown points fall to the right of the theoretical curve.

Some actual breakdown points for porcelain are included for temperatures below 250 degrees Fahrenheit. It has been pointed out that at these lower temperatures the generalized curves are of doubtful value. It is interesting to note, however, that the actual low temperature breakdown points are at least of the proper order relative to the theoretical curves. Some breakdown points obtained with a-c voltages are also included in tables II and III, and are plotted on the 18? curve Figure 32. In each case these have been listed and plotted in r.m.s. rather than crest volts since the heating effect is a function of the former. These seem to fit the curves equally as well as do the d-c points but the amount of a-c data available is relatively small. No actual resistance measurements were made with a-c and the resistivities listed in table III are taken from Curve 4.

Despite the fact that the temperature - resistivity curves were obtained from test specimens with relatively uniform voltage gradients, the theoretical breakdown curve for porcelain applies with reasonable accuracy to practical insulator shapes at the higher temperatures. This is shown by the actual breakdown tests on practical insulators as listed in table II.

It seems probable that at temperatures above 250 degrees Fahrenheit the reduction in resistivity of the porcelain results in more nearly uniform voltage gradients in the practical insulators.

No actual breakdowns were obtained on the Zircon composition even though temperatures were carried up to 900 degrees Fahrenheit at 40 volts per mil d-c. The tendency of the zircon to increase in resistivity with time at constant ambient temperature and voltage is believed to be due to dielectric polarization. At any constant temperature and voltage the more mobile negative ions (or possibly electrons) drift away from the negative electrode leaving a super abundance of the less mobile positive ions in this area. This results in an apparent increase in the resistivity of the material. When such polarization occurs to a marked degree it would be expected that the breakdown temperature with a-c would be lower than with d-c.

Conclusions:

The electrical resistivity of all of the ceramic insulating materials tested diminishes not only with increasing temperature but also, at the lower temperatures, it diminishes with increasing voltage gradient. The rate of change of resistivity with voltage appears to diminish with increasing temperature so that for porcelain above 250 degrees Fahrenheit the resistivity is nearly independent of voltage.

From the shape and level of the temperature resistivity curves it is possible to predict the temperature at which an insulator will fail under any particular voltage gradient. While these predictions are based primarily on high temperature measurements it appears as though the thermal effect may be a major factor in insulator breakdowns even at low temperatures. The existing data does not permit definite determination at low temperature, however.

The breakdown curves, Figure 18, are believed to be applicable for 60 cycle a-c as well as d-c voltage for all of the materials except zircon. For zircon the a-c breakdown temperatures may be somewhat lower.

There is also some question as to whether these curves are applicable to high frequency a-c voltages. At high frequencies other forms of dielectric loss may become of important magnitude so that failure may occur at lower temperature levels. This has not been investigated.

There seems to be no appreciable difference in the high temperature electrical performance of wet process electrical porcelain as made by several well known American manufacturers.

The presence of glaze on porcelain does not seems to effect the high temperature performance.

The high temperature performance of glasses, steatite and zircons may be expected to vary widely with different compositions. The one Zircon composition which thus far appears to be best can be operated at 900 degrees Fahrenheit at 40 volts per mil d-c without failure.

- o 0 o -

REFERENCES.

1 - Insulation Failure - A. Pyroelectric Effect - J. L. R. Hayden and C. P. Steinmetz - Electrical World, Vol. 80, page 865, 1922.

2 - High Voltage Insulation - Hayden and Steinmetz - Transactions, AIEE, 1923, P. 1029-41.

3 - A Theory of Imperfect Solid Dielectrics - M. G. Malti - Transactions, AIEE, 1927, P. 616-634.

4 - Electrical Resistivity of Insulating Materials - H. L. Curtis - Transactions, AIEE, 1927, P. 1039-47.

5 - Electric Strength of Solid and Liquid Dielectrics - W. A. DelMar, W. F. Davidson, R. H. Marvin - Transactions, AIEE, 1927, P. 1049-1061.

6 - Theory of Thermal Breakdown of Solid Dielectrics - Moon - Transactions, AIEE, 1931, P. 1008-21.

7 - Low Loss Ceramics - R. Russell, Jr. and F. J. Berberich - Electronics, May 1944.

8 - Breakdown of Glass with Alternating Potentials - N. D. Kenney, A. M. Luery, J. D. Moriaty - Transactions, AIEE, Vol. 51, P. 404, 1932.

9 - Predetermination of the A. C. Characteristics of Dielectrics - J. B. Whitehead, Alfredo Banos, Jr. - Transactions, AIEE, Vol. 51, P. 392, 1932.

Table I

Breakdown Points of Porcelain
Test Specimens d-c Voltage

Electrode Area Sq.In.	Spec. Thickness Inch	d-c Volts per mil	Temp. at Beginning of Failure Degree F.	Resistivity at Beginning of Failure Megohms Per In. Cube	Time Reqd. For Failure Minutes	$\frac{E^2}{r^2}\frac{\partial r}{\partial T}$ watts per cubic inch per Degree F.	Char. of Drift Curve
1	0.131	382	95	Approx. 200,000	5	.021	No
1	0.122	410	150	" 50,000	7	.094	No
1	0.075	440	200	" 58,000	Less than .02	.087	No
1	0.275	136	250	5,000	28.5	.0925	Flex
1	0.258	194	250	" 3,000	2.5	.287	No
1	0.605	40	300	495	15	.077	No
1	0.609	40	300	870	15	.0442	No
30	0.81	39.5	300	1,630	12	.023	No
1	0.172	87	300	2,150	7.5	.084	No
1	0.172	87	300	2,150	7.5+	.084	No
1	0.797	40	300	892	16	.043	Flex
2	0.535	20.6	325	516	19	.0189	Flex
2	0.528	20.6	325	348	19	.0282	Flex
0.785	0.97	30.8	350	193	3+	.108	No
0.785	0.98	30.8	350	183	3+	.114	No
1	0.791	20.2	350	405	44	.0222	Flex
0.44	0.282	35.5	350	285	4	.0975	No
0.44	0.282	35.5	350	285	4+	.0975	No
1	0.172	43.5	350	335	6	.124	No
1	0.172	43.5	350	335	6+	.124	No
1	0.81	9.87	400	60	62	.034	Flex
0.785	0.97	10.25	400	66	15.5	.0336	No
0.785	0.98	10.25	400	57	15.5	.0387	No
0.785	0.975	20.4	400	47	2.5	.186	No
0.785	0.980	20.4	400	47	2.5+	.186	No

TABLE II

Breakdown Points Of
Practical Porcelain Insulator Shapes
Alternating and Continuous Voltage

	Continuous Voltage					Alternating Voltage
	Cylinderical Smooth Walled Standoff Insulator	Cylinderical Corrugated Standoff Insulator	Standard 23 KV Heavy Duty Outdoor Switch & Bus Ins.	Tube 2-3/4x1-3/4 x 20" Long Smooth Walled	3 Units 5-3/4 x 10" Suspension Insulator	Standard 23 KV Heavy Duty Outdoor Switch and Bus Ins.
Total Porcelain Thickness	1.62	5.12	1.25	20	2.06	1.25
Total Voltage Applied Volts	15000	40000	14000	46000	46000	14000 RMS
Average d-c Volts Per Mil	9.25	7.8	11.2	2.3	22.3	11.2 RMS
Temperature at beginning of failure, degrees Fahrenheit	410	400	405	550	350	400
Total resistance at beginning of failure, megohms	79	82	3.26-5.2	24.8	82.2	Approx. 2.7
Approx. average resistivity at beginning of failure, megohms per inch cube	48.7	50.4	81-128	4.36	461	" 66
Time required for failure, minutes	21	45	17 - 35	49	112	54
$\frac{E^2}{r^2}\frac{\partial r}{\partial T}$ watts per cubic inch per degree F.	.036	.025	.0254-.0162	0.0205	0.0237	.032
Characteristics of Drift Curve	Flex	Flex	No	Flex	Flex	-

TABLE III

Breakdown Points of Porcelain
Test Specimens with a-c Voltage

Electrode Area Sq.In.	Specimen Thickness Inches	RMS Volts Per Mil	Temp. at Beginning of Failure Degrees Fahrenheit	Calculated Resistivity at Beginning of Failure Megohms Per Inch Cube	Time Reqd. for Failure Minutes	$\frac{E^2}{r^2}\frac{\partial r}{\partial T}$ Watts Per Cubic Inch Per Degree F.
1	.113	531	-70	600,000	0.25	.0118
1	.125	448	-70	1,200,000	5.5	.0042
1	.137	438	71	50,000	1.5	.077
1	.150	347	77	100,000	18	.024
1	.121	346	150	80,000	2.25	.030
1	.117	342	250	5,000	0.116	.469

TABLE IV

Breakdown Points of Glass And
Steatite Test Specimens

Material	Electrode Area Sq.In.	Spec. Thickness Inches	d-c Volts per Mil	Temp. at Beginning of Failure Degrees Fahrenheit	Resistivity at Beginning of Failure Megohms per Inch Cube	Time Reqd.for Failure Minutes	$\frac{E^2}{r^2}\frac{\partial r}{\partial T}$ Watts per cubic Inch per Degree F.	Char. of Drift Curve
Borosilicate Glass	0.6	.36	83.3	350	625	3	0.6	No
Lead Glass	0.442	.50	40	600	272	14	0.109	No
Lead Glass	0.442	.50	30	650	110	7.25	0.22	No
Steatite	0.785	0.188	21.3	750	43.9	13	0.188	Flex
Steatite	0.785	0.203	19.7	750	42.5	13	0.166	Flex
Steatite	0.785	0.188	42.5	700	104.5	1.5	0.285	No
Steatite	0.785	0.203	39.4	700	101.3	3	0.252	No

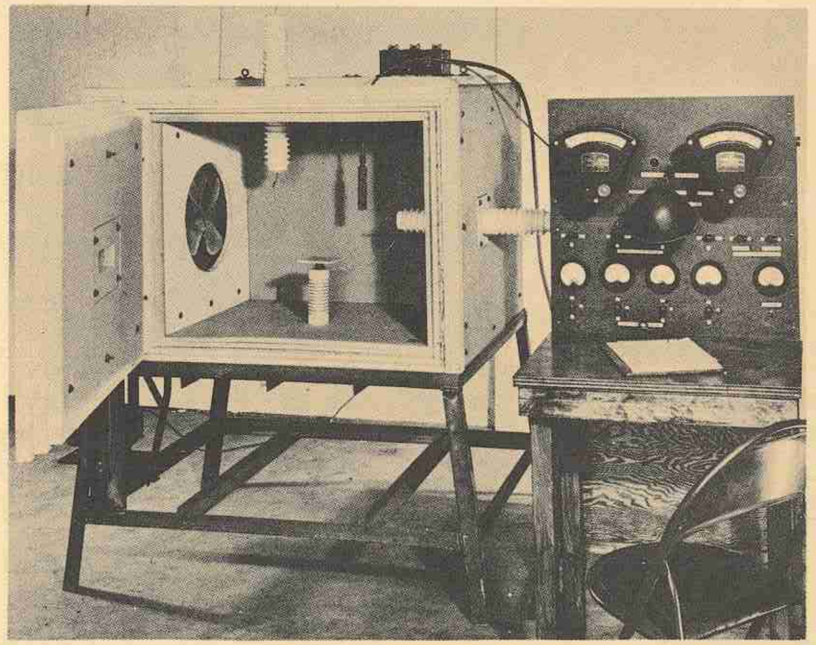

Figure 1. Test chamber and operating panel with specimen mounted in position.

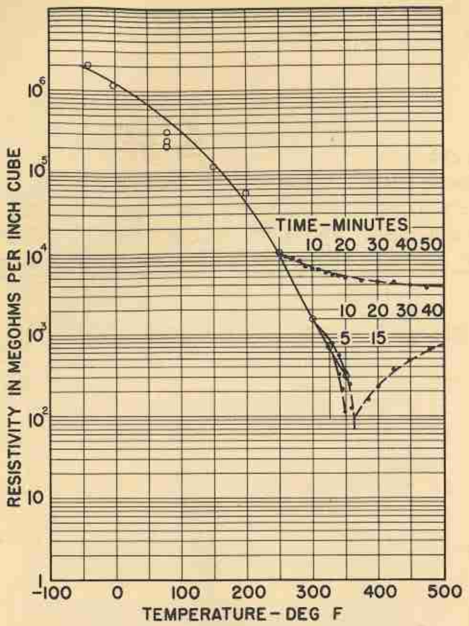

Figure 2. Temperature vs resistivity, wet process electrical porcelain, voltage gradient 40 volts per mil d-c, thickness 0.8 inch, electrode area 30 square inches.

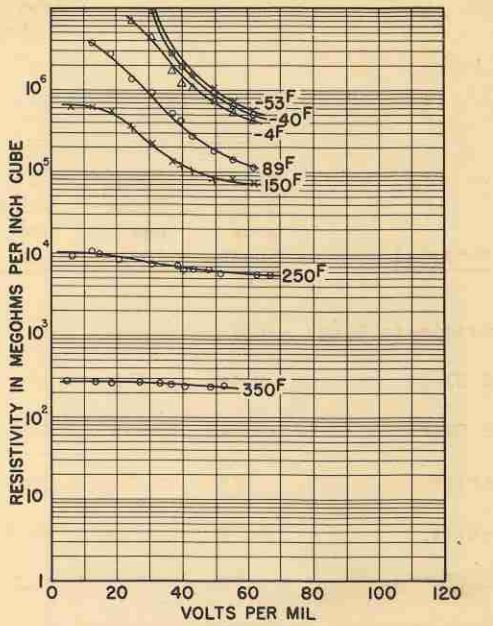

Figure 3. Voltage gradient vs resistivity, wet process electrical porcelain, thickness 0.8 inch, electrode area 30 square inches.

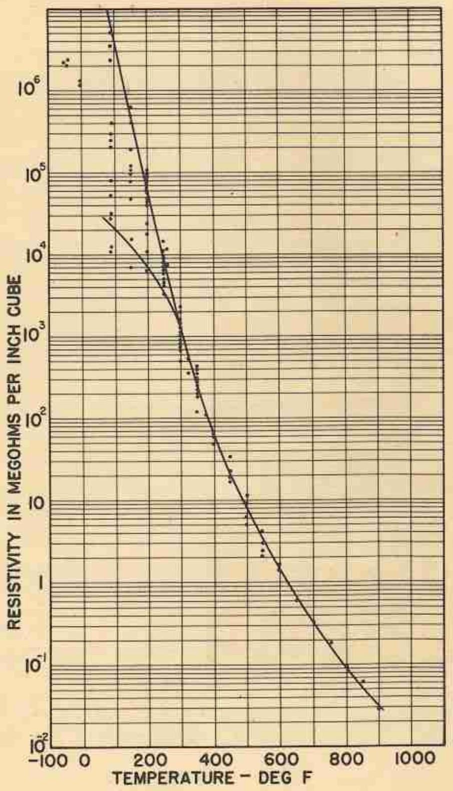

Figure 4. Composite curve. Temperature vs resistivity wet process electrical porcelain.

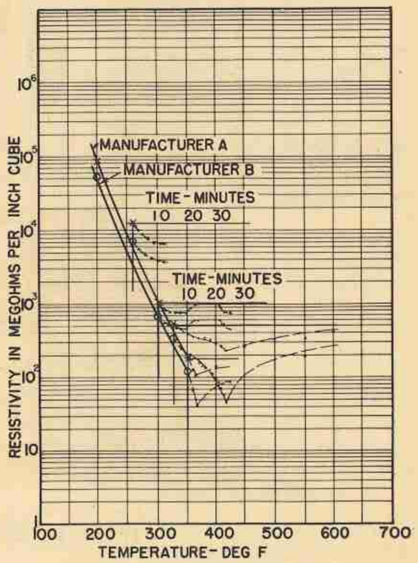

Figure 5. Temperature vs resistivity, comparison of two manufacturers of wet process electrical porcelain, voltage gradient 20 volts per mil, specimen thickness 0.55 inch.

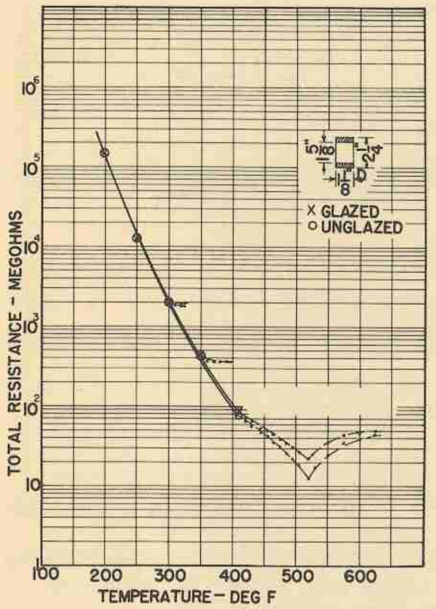

Figure 6. Temperature vs resistance, comparison of glazed and unglazed wet process electrical porcelain, total voltage applied 5000 volts d-c.

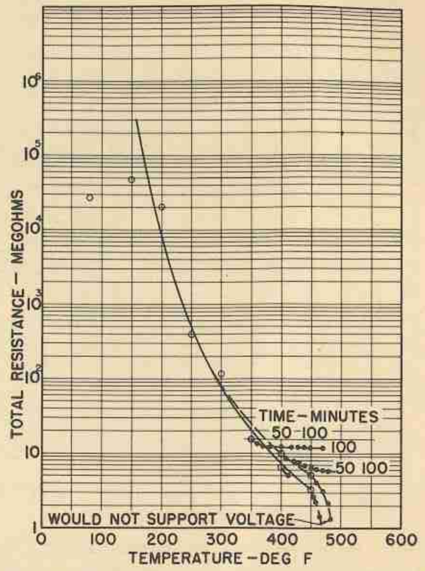

Figure 7. Temperature vs resistance of 23 kv NEMA Standard outdoor switch and bus insulator, total voltage applied 14 kv d-c.

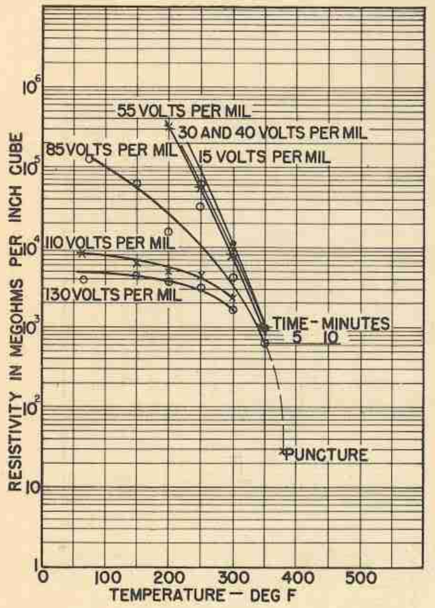

Figure 8. Temperature vs resistivity, boro-silicate glass, thickness 0.36 inch.

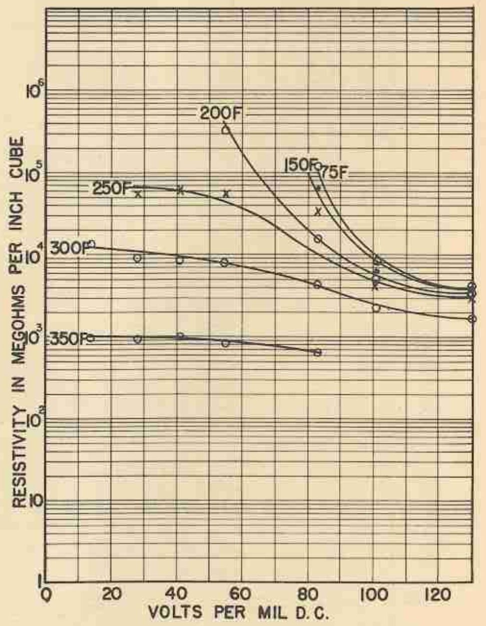

Figure 9. Voltage gradient vs resistivity, boro-silicate glass, thickness 0.36 inch.

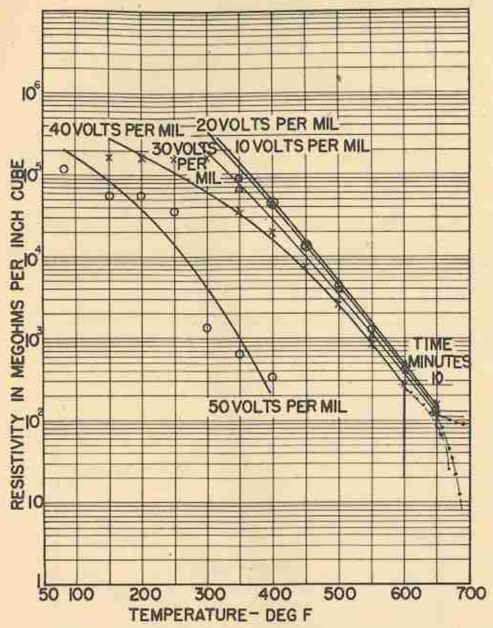

Figure 10. Temperature vs resistivity, lead glass specimen thickness 0.50 inch.

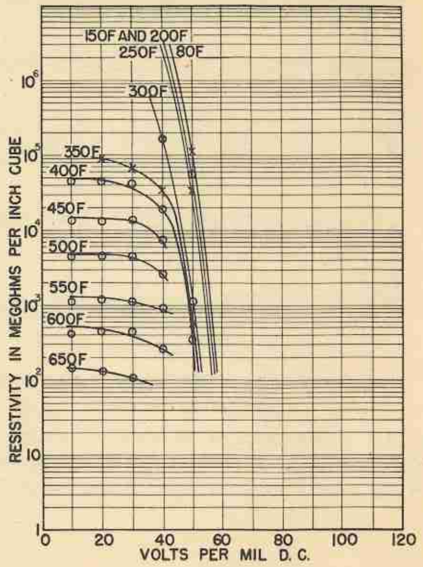

Figure 11. Voltage gradient vs resistivity, lead glass, specimen thickness 0.50 inch.

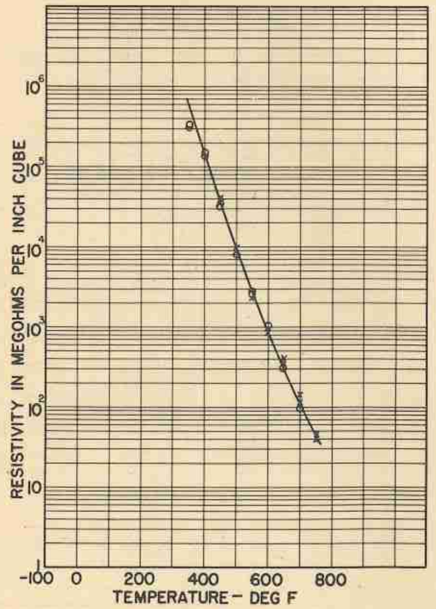

Figure 12. Temperature vs resistivity, wet process steatite, voltage gradient 20 and 40 volts per mil, specimen thickness 0.188 inch and 0.203 inch.

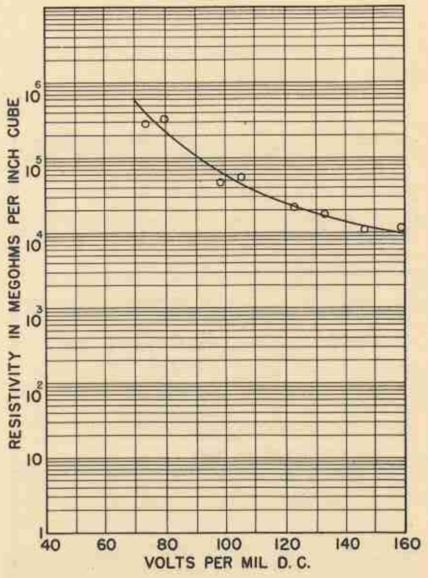

Figure 13. Voltage gradient vs resistivity, wet process Steatite, temperature 84 F. specimen thickness 0.188 inch and 0.203 inch.

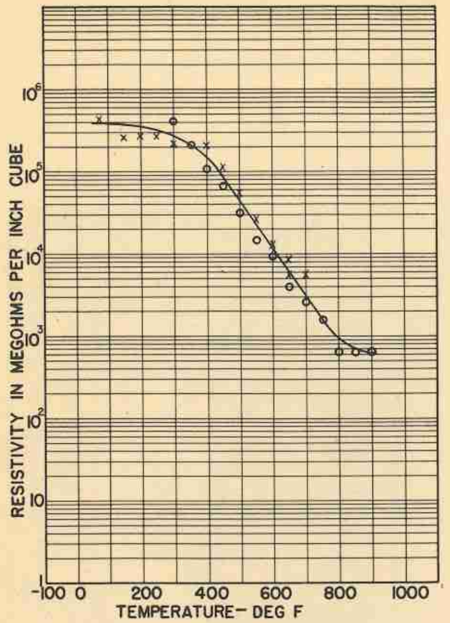

Figure 14. Temperature vs resistivity, zircon, 40 volts per mil, 2 square inch electrode 0.489 inch thick and 1 square inch electrode 0.196 inch thick.

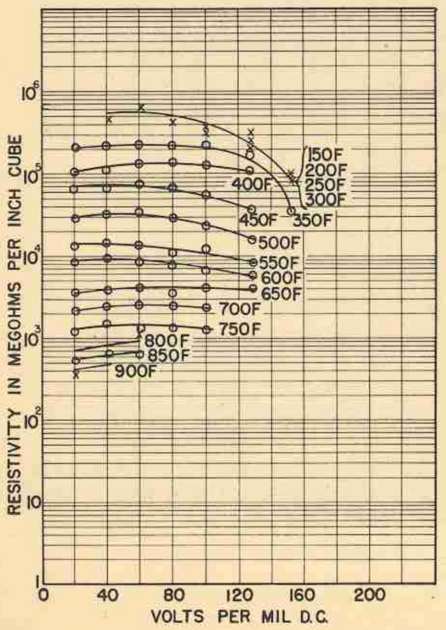

Figure 15. Voltage gradient vs resistivity, zircon, 1 square inch electrode, specimen thickness 0.196 inch.

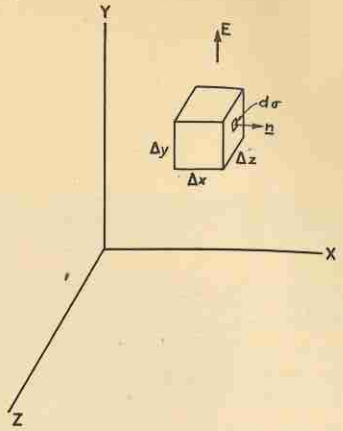

Figure 16. Elemental cube in the dielectric body.

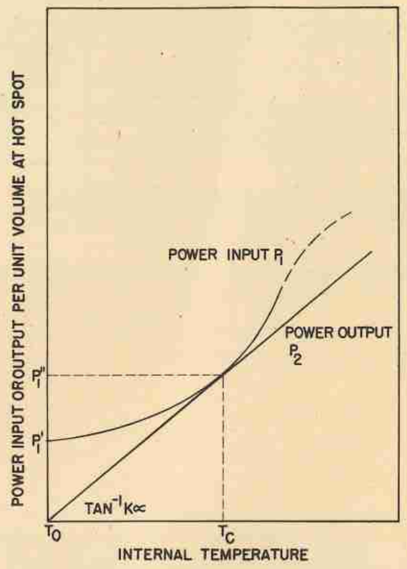

Figure 17. Power input and power output conditions leading to ultimate breakdown.

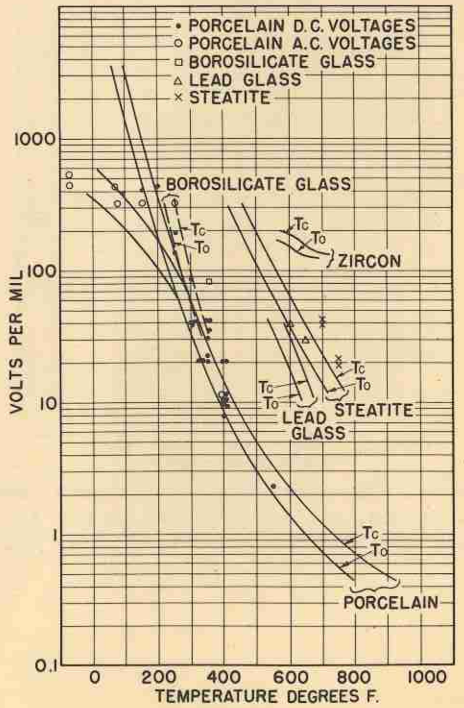

Figure 18. Temperature vs voltage gradient for breakdown.

Litho in U.S.A.

AIEE
Technical Paper
46-117

May 1946

Return to [illegible]

THE ELECTRICAL PERFORMANCE OF CERAMIC DIELECTRICS AT ELEVATED TEMPERATURES

H. A. Frey
Member AIEE

J. A. Jesatko
Associate AIEE

Both of:
Locke Insulator Corp.
Baltimore, Md.

Advance Copy
Not Released for Publication

All Rights Reserved by the
American Institute of Electrical Engineers
33 West 39th Street, New York, N.Y.

A paper recommended by the AIEE committee on power transmission and distribution for presentation at the AIEE summer convention, Detroit, Mich., June 24-28, 1946. Manuscript submitted March 5, 1946; made available for printing May 8, 1946.

__PRICE:__ 30¢ PER COPY BY MAIL
25¢ AT HEADQUARTERS OR MEETING

This is a reprint from
Electrical Engineering
Published monthly by the
American Institute of Electrical Engineers
33 West 39th St., New York, N. Y.

6/12/'36 June 1936 issue

Porcelain for High Voltage Insulators

In this paper the mechanical failure of porcelain is discussed with special reference to 3 seldom recognized characteristics: the effect of the porcelain surface on the strength, the apparent anomalous distribution of individual mechanical test values, and the effect of time on mechanical strength. A method of evaluating the result of these factors on electrical insulator performance is suggested.

By
D. H. ROWLAND
ASSOCIATE A.I.E.E.

Locke Insulator Corp.,
Baltimore, Md.

THERE CAN BE little argument as to what mechanical characteristics are desirable in high voltage insulators, but the factors which contribute to such characteristics are concealed, more often than not, by an extraordinary amount of sophistic data. Modern high voltage insulators on the average have improved enormously in the past decade. This improvement has been brought about in most cases by expensive and tedious cut and try tests conducted on assembled insulators. The procedure has been to assume that certain features of the completed units such as mechanical strength, ability to withstand immersion first in boiling water and then in ice water, imperviousness to moisture, and other qualities would insure insulators capable of standing up in service, which, after all, is the only real criterion of insulator worth. Finally specifications such as the A.I.E.E. Standards No. 41 for the testing of high voltage insulators were evolved and it may here be stated, unequivocally, that insulators which will successfully pass these specifications will give an unusually good account of themselves in the field. However, just because 2 groups of insulators of different manufacture successfully pass a certain specification it cannot be assumed that their maintenance cost in the field will be the same. How will they stand up under mechanical shock such as the impact from stones or bullets? What effect will time under load have upon their life? What is the maximum load that they will withstand? Is actual experience over a period of years the only way to find out? The purpose of this discussion is to provide engineers with a greater insight into some of the more recently investigated and rather peculiar mechanical characteristics of ceramic materials with the hope that an understanding of this work will help them to answer these questions and to point out that some of the characteristics which have been viewed with alarm by the uninitiated are really a true part of the whole scheme while other factors which have been unknown, or neglected, have been of major importance. A realization of this is bound to lead to still greater efficiency of systems dependent on the insulating qualities of such materials.

A paper recommended for publication by the A.I.E.E. committee on power transmission and distribution, and scheduled for discussion at the A.I.E.E. summer convention, Pasadena, Calif., June 22–26, 1936. Manuscript submitted March 25, 1936; released for publication April 23, 1936.

10. For numbered references see list at end of paper.

The Failure of Nonductile Materials

Ceramic materials are nonductile and as such they behave in certain ways peculiar to such materials. In addition they reserve for themselves other individual characteristics which it is important to understand in order to make use of them in the most efficient manner. Cast iron, among the metals, comes closely enough to this class of materials in some respects so that a limited analogy may be drawn between them. A few of the elementary facts regarding cast iron may be considered. First of all, when it is pulled in tension its yield point and point of failure are practically coincident. It does not neck down before failure but breaks off squarely.

If cast iron tests rods as shown in figure 1*a* are pulled they will break at the abrupt change in section *cc* because the tension is concentrated in the cross section adjacent to the sharp corner. If, however, the material is ductile, necking will take place before failure and as the thick section to the left of *cc* will tend to prevent necking it will considerably strengthen the section to the right of *cc*. To obtain the greatest strength from nonductile materials sudden changes in section must be avoided and tension specimens should be shaped as in figure 1*b*.

The point to be emphasized between cast iron on the one hand and ductile material on the other is that the former will break suddenly as shown in figure 2*a* while the latter will first neck down and then break as shown in figure 2*b*.

Effect of Surface Conditions on Mechanical Strength

All this is well known to most engineers, but probably few of them realize the effect which surface characteristics exert upon the strength of such materials. It is a fact that polishing the surface of cast iron test specimens will considerably influence their strength and the phenomenon is, in general, more pronounced the less ductile the material.

Mechanical Failure of Ceramic Materials

The complete absence of ductility in ceramic materials means first of all that strength is to a great extent dependent upon surface conditions. In order to cut glass the surface is scratched, then it is tapped, and a crack goes through to the other surface from the bottom of the scratch. Porcelain, glass, and all other nonductile materials have somewhat this same characteristic to a greater or lesser degree. Failures start at the surface with an infinitesimal crack and proceed progressively through the body of the material until they reach another exterior surface.

If a porcelain test rod is subjected to a transverse load as in figure 3*a* it is obvious that the lower surface of the rod will be thrown into tension while the upper surface is compressed. The tensile strength of porcelain is much lower than the so-called compressive strength, which will be discussed later on, so that at the bottom of some slight indentation, where the stress is greatest, a tiny crack will occur at some value in the loading. When this happens a condition exists such as shown in figure 3*b*. A sharp crack projects into the porcelain. Because of the nonductility of the porcelain the angle at the crack remains acute and the stress approaches infinity in the minute localized zone at the apex of the crack. Thus the porcelain breaks down progressively fiber by fiber until the piece is broken. On the contrary, if the rod is made of a ductile material and for some reason a crack occurs on the tension side as shown in figure 3*c* the ductility of the material allows the crack to widen and smooth out as shown by the dotted line, and this avoids a progressive breakdown.

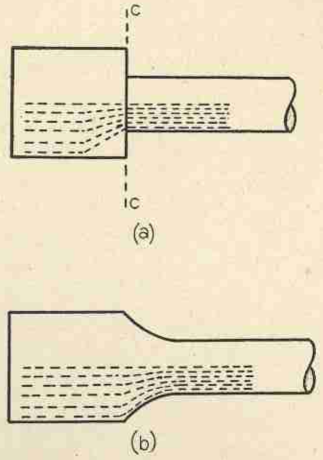

Fig. 1. Effect of shape on nonductile specimens in tension

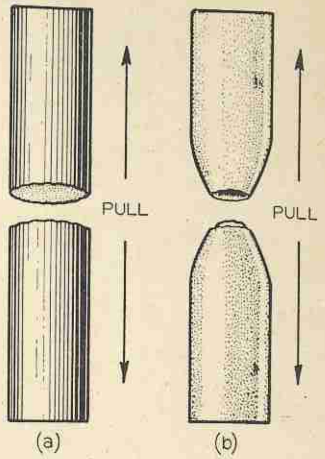

Fig. 2. Comparison of breaks in tension of nonductile and ductile materials

Unglazed Porcelain

Unglazed porcelain necessarily has a slightly rough surface from the aggregate of ground silicon dioxide which it contains. The microscopic pits (figure 4*a*) in the surface offer focal points for incipient cracks. The fact that the surface of the material is one of the governing factors from the point of view of mechanical strength can be shown easily by giving a group of specimens a coat of varnish which smooths the surface as in figure 4*b*. Strange as it may seem this thin coat of varnish will raise the modulus of rupture of one inch rods from 10 to 15 per cent.

Glazed Porcelain

Because of the slight roughness of unglazed porcelain it is the practice to cover the surface with a glaze, as it is known to the pottery industry. Glaze has a composition close to that of porcelain but with additional fluxes which give it a melting point lower than that of the porcelain. At the firing temperature it flows over the surface in the molten state and on cooling creates a smooth glossy surface which prevents the adherence of dirt. From what has been said before it is obvious that this alteration of the surface must have an effect upon the physical strength of the porcelain. First of all the glaze smooths over the slight surface roughnesses. In addition it forms a 2 ply structure made up of the glaze and the porcelain fused together. The glaze is only 0.005 inch thick, but it must be remembered that it is in a critical position so far as the breaking of the porcelain is concerned. All cracks must start at the surface and therefore the glaze must be the first to fail.

In addition to the smoothness created by the glaze and its effect on the mechanical strength, there is another factor which is vastly important. One aspect of what takes place when a piece of glazed porcelain is fired may be considered. As has been stated the glaze has a melting point considerably lower than that of the porcelain, and melts down and smooths out forming a thin film while the porcelain is in a slightly soft state. Soon after this condition is reached the temperature is reduced and the ware starts to cool and harden. At some point in this cooling process the porcelain and glaze assume, in a large measure, the physical characteristics which they have at ordinary temperatures. From there on as the material cools each part will shrink in accordance with its coefficient of expansion provided, of course, that no strains are set up through the structure. If the glaze has a greater coefficient of expansion than the porcelain it will try to shrink more than the porcelain body will allow and in doing so will put itself under a tensional stress. In fact it may be strained to the breaking point and show fine cracks or craze marks on the surface. Nearly everyone has seen these surface cracks on old sanitary ware. Frequently, however, the glaze may be under considerable stress but short of its yield point. Sometimes a piece of ware just out of the kiln may appear to be perfect but it will craze after a short period of time as a result of slight thermal or mechanical shocks.

Conversely, if the glaze has a lower coefficient of expansion than the porcelain the latter tends to shrink on cooling more than the glaze, but the glaze must come along with the great mass of porcelain so that at ordinary temperature the glaze has been pushed together and is in compression.

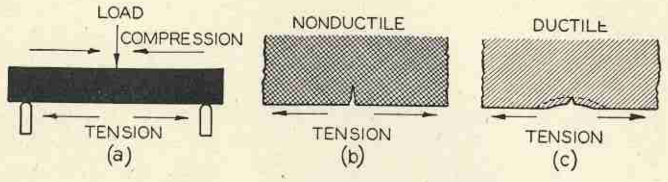

Fig. 3. Behavior of cracks in nonductile and ductile materials in tension

Glaze in Tension or Compression

In figure 5*A* is shown a transverse test specimen on supports ready to be subjected to a load. The outside surface is shown slightly shaded to represent an initial tension due to those factors which have just been described. Since action and reaction are equal and opposite the tension in the glaze must be balanced by slight compression in the porcelain. Now if a load is applied to the rod the zone above the neutral axis of the specimen is placed in compression while that below is placed in tension. In accordance with established beam theory the maximum stress in the bar induced by the load will be in the outermost fibers of the piece or in other words in the glaze. This stress on the underside will be added to that which is already present and if the load is great enough the glaze will fail (figure 5*B*) and a progressive crack will pass through the specimen at high velocity.

Where the glaze is in compression (figure 5*a*) and a load is placed on the rod (figure 5*b*) the tensile stress developed in the glaze will be that due to the load minus the initial compressive stress and so the load must be considerably greater than in the first case in order to start an incipient failure as indicated in figure 5*c*.

Effect of Compressive Stress

A question may arise regarding the effect of the compression components on mechanical failure. The apparent compressive strength of glass or porcelain is on the order of 8 times that of the apparent tensile strength. It may be stated here, categorically, that when such materials are placed under compression the initial failure occurs due to a concomitant tensile stress set up by the compression load. F. W. Preston[10] ably sums up this characteristic in the following words which pertain to glass but which are in a large measure applicable to all nonductile materials:

Fig. 4. Unglazed porcelain (a) and the effect of varnish (b)

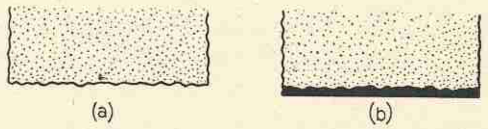

> "From what has been said before, it will be clear that the term 'compressive strength of glass' is a rather meaningless term. Compression tests may be made under strictly defined conditions, but up to date those conditions have not been defined. The failure of glass, when it occurs, will be due to minor tensile stresses developed incidentally 'and so to speak, accidentally,' and their amount depends, in general, on rather subtle factors, and on things that are difficult to specify or control accurately. From a practical point of view, the compressive strength of a glass may be almost anything. From a theoretical point of view it is infinite."

Method of Determining the Stress in a Glaze

It would be fair to ask the question, "How is it possible to tell whether the glaze is in compression or tension?" One of the most obvious methods would be to make up specimens of glaze and porcelain and measure the coefficient of expansion of each one separately by some suitable means. This method, however, does not work very well because when the ware is fired there is an interchange of ingredients between the glaze and porcelain while they are in the molten state and this alters the chemical make-up of the glaze and the adjacent porcelain.

A better method is that shown in figure 6. Suppose a thin slab is cut from the porcelain in such a way that the glaze forms one surface and the porcelain the opposite one. Such slabs should be about $^{1}/_{16}$ inch thick and 5 inches long and perhaps $^{1}/_{2}$ inch wide. To all intents and purposes they resemble the familiar bimetallic strips used for thermostats except that in this case the materials are nonmetallic. If it is supposed that the glaze and porcelain are split apart into 2 separate strips as shown in figure 6*a* and that the 2 strips are heated by some convenient means, then, if the coefficient of expansion of the glaze is greater than that of the porcelain the strips will assume some such position as that shown by the dotted sections. If it is imagined that the strips are again fused together and heated it is evident that the strip would bend as shown in figure 6*b*. If the converse is true and the porcelain coefficient is greater than that of the glaze, then under similar conditions the results will be as in parts *c* and *d* of the figure. This method gives a qualitative result as to the relative coefficients of expansion of the glaze and porcelain.

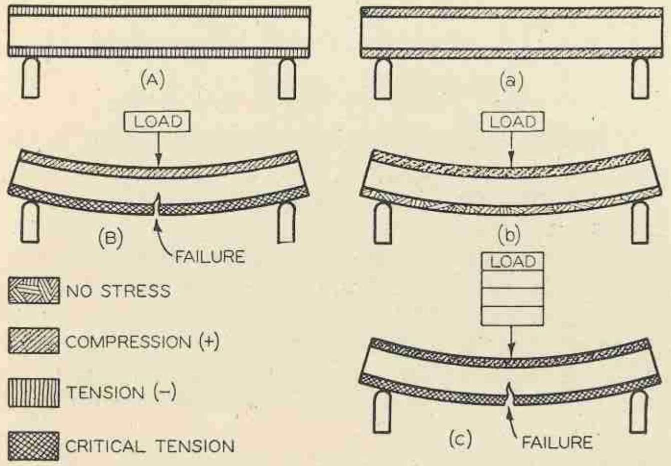

Fig. 5. Comparison of strengths of glazes initially in tension and initially in compression

If it is desired to obtain a quantitative number for the differential coefficient of expansion of the glaze and porcelain the technique involved becomes somewhat more complicated. The method used in this work was briefly this: Strips of porcelain and glaze were cut to fixed dimensions and heated to 400 degrees Fahrenheit. The movement which took place at the end of the strips was measured in thousandths of an inch and designated as (+) when the glaze had a smaller coefficient of expansion than the porcelain and (−) when the opposite condition prevailed. Thus a glaze designated as +8 would be under approximately twice as much compression as one designated as +4. Conversely, −8 would signify tension in the glaze.

Mechanical Strength of Different Porcelains and Glazes

The mechanical strength of porcelain with its glaze in various stages of compression and tension can now be considered. Table I shows strength values obtained by breaking $^{1}/_{2}$ inch rods transversely on supports 4 inches apart. The average modulus of rupture of rods with the glaze under strong compression and tension are shown and also the strengths of unglazed porcelain together with several intermediate glazes. The numbers and signs at the tops of columns indicate the amount of initial compression or tension.

Table I—Moduli of Rupture of $^{1}/_{2}$ Inch Rods Broken Transversely on Supports 4 Inches Apart

	Unglazed	Glaze +8	Glaze +1	Glaze −1	Glaze −2	Glaze −8	Glass
High value	12,900	20,950	15,500	12,340	11,100	5,380	18,950
Low value	4,860	12,850	6,000	4,470	4,230	3,075	7,660
Average	9,597	17,250	10,450	9,100	8,300	4,550	14,060

Load application 988 pounds per square inch per second in modulus of rupture. All values in pounds per square inch.

It must be conceded that any factor which can influence the strengths of test specimens by 300 or 400 per cent is something that must be considered when manufacturing high voltage insulators. Not only does the glaze influence the strength of porcelain under mechanical load but it may also add materially to the ability of the porcelain to withstand sudden thermal changes. Many theories have been advanced from time to time to explain the failure of certain insulators after a length of time in the field. The electrical failures in nearly all cases are preceded by mechanical cracks which start at the surface of the porcelain. It is believed that the evidence here presented is of sufficient weight to support another theory. Briefly it may be stated as follows: The mechanical cracking of porcelain, other things being equal, is caused by its surface characteristics and much of the deterioration of insulators in service is the result of an improper realization of the importance and adequate control of this factor.

Practical Application of the Glaze Principle

It might be interesting to touch briefly on some of the practical applications of what has already been discussed. Figure 7 shows the cross sections and silhouettes of 2 cement grips, *A* and *B* the ordinary type and *a* and *b* the effect of the reglazing process which consists of coating the porcelain surface, which is to be gripped by the cement, with a special +8 glaze, applying a layer of sized porcelain particles, and subsequently spraying or dipping a secondary coat of special +8 glaze over the particles. When insulators thus treated are fired the porcelain particles are completely covered with a glaze which is in compression and no sharp crevices exist between the particles to start progressive failure.

The effect which this treatment has upon the strength of the insulators is shown clearly in figure 8, which gives the results of a duration load test made on 16 insulators half of which were treated while the other half were made in the ordinary manner. The load on the units was started at 10,000 pounds and increased 1,000 pounds per day. The units were tested daily and figure 8 shows the loads at which they failed, the *S* points representing untreated units and the *R* points treated units. Also, a comparison between the low values is given.

Figure 9 shows a machine in which insulators can be placed to determine their ability to withstand impact. The units are mounted as shown and given a blow on their outer edge by means of the pendulum. It must be apparent that other things being equal the ability of insulators to withstand such blows is some measure of the amount of breakage that will occur in service due to stone throwing or bullets. The effect that glaze has upon this ability is shown in figure 10. The white insulators were coated with a −8 glaze and the brown with a +8 glaze and each unit was then subjected to a single blow of exactly the same amount. The results are self-evident. It must be emphasized here that the color of the glaze has nothing to do with its mechanical characteristics and that the white color used here was to prevent any chance of weak insulators getting into the factory stock.

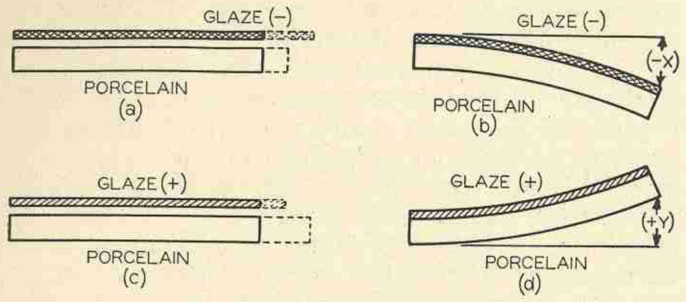

Fig. 6. Qualitative method of determining relative coefficients of expansion of porcelain and glaze

Variation in Mechanical Strength of Ceramic Material

The second important characteristic of ceramic materials and one which from time to time is the cause of considerable worry to the purchasers of insulators is the variation of mechanical strength between seemingly identical specimens. Such variations, while they may appear to be entirely anomalous to the uninitiated, are in reality predictable and form a part of the complete scheme of things. It is proposed here to give data pertaining to this subject in an effort to throw some light on the strength variations of insulators and to show that in properly manufactured insulators it is not an unknown but a known quantity and that by itself it cannot be used as a criterion of insulator quality.

Table I gives the high, low, and average moduli of rupture obtained by breaking a number of test rods. In the case of the +8 glazed and unglazed porcelain a large number of specimens were broken so that it was possible to get a good idea of the distribution of individual values which fell between the low and high values. Figure 11 shows distribution curves plotted for these 2 types of porcelain. The method used in plotting these curves was to indicate values of moduli of rupture along the abscissa and then to plot the percentage of the total number of rods which broke between fixed intervals along the abscissa as ordinates. The resulting curves are somewhat similar to sine curves and give a clear picture of the strength values which may be expected from a group of specimens. Relatively few specimens of glass were broken so that it was not feasible to plot a distribution curve, but it is evident from the high, low, and average values obtained from the small number of tests that its spread would have been greater than that of either of the porcelain curves.

The tests on the glass rods were introduced as check tests to answer any arguments which might be advanced that the reason for variations in the strength of ceramic materials lies in hidden flaws. Glass, being transparent, can be examined readily for flaws which in opaque materials cannot be so detected. The glass used was specially selected, homogeneous, smooth, and free from strains, and the results obtained indicate by comparison that the presence of flaws, strains or other concealed defects are not necessary to explain the variation in the individual test values of the porcelain specimens, but are the outcome of inherent properties of the material.

Fig. 7. Silhouettes of ordinary and specially glazed porcelain cement grips

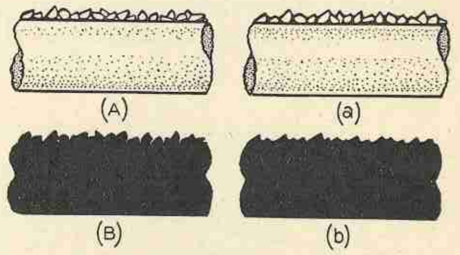

Behavior of Insulators Made From Different Materials

If the characteristics of insulators made from these 3 materials are now considered it is possible to arrive at a few conclusions regarding their behavior.

Before proceeding, the statement made by F. W. Preston, quoted earlier in this paper, regarding the mechanics of failure of glass under load should again be called to mind. Briefly it was to the effect that regardless of how glass is loaded the initial failure develops as the result of an incidental tensile stress developed somewhere on the surface. It is believed that this theory applies to porcelain and to many other nonductile materials. Certainly all the available experimental data seem to support it and in the development which follows it will be considered as axiomatic. Having accepted this, it is permissible to go one step further and to say that since all failures start at the surface of porcelain, or glass, it may be assumed, other things being equal, that the modulus of rupture of the material is a fair criterion of its ability to withstand any type of loading. This follows because the modulus of rupture is the calculated tensile stress in the outermost fibers of the test specimen at the instant of failure. In other words, it is a measure of the surface strength of the material and since we have assumed that this is the controlling factor governing the insulator strength it is possible to draw conclusions regarding the characteristic of insulators by considering the results obtained from laboratory specimens.

It is evident that for the same size and general construction insulators made with the material having the highest average modulus of rupture will have the highest average strength. This, of course, assumes that the surface of the insulators in the zone where the maximum surface tension is induced by the external stress is of the same nature as the laboratory specimens. By the same reasoning it may be concluded that the porcelain which shows the narrowest distribution curve on laboratory samples will when made into insulators show the greatest uniformity in strength values when tested at the same loading rate. Every type of material has its own particularly shaped distribution curve to which it will always adhere. Porcelain is no exception to this rule.

Since porcelain has such a strength distribution curve it at once removes the low and high test values obtained on insulators from the realm of unknown quantities. If the porcelain test rods have breaking strengths which vary in a certain way it is perfectly reasonable to suppose that insulators built of this same material will vary at least as much as the porcelain, and, if the assembly methods vary, a little bit more depending upon the manufacturing control. All this, of course, presupposes that the insulator design is such that under a mechanical load the porcelain is the first part to fail which is generally true. Now in order to find the possible low test value that would be obtained from a large quantity of insulators it is necessary only to find their average strength and to multiply this average by the ratio obtained by dividing the lowest rod value by the average rod value, or to obtain the maximum test figure to multiply by the ratio of the maximum rod value divided by the average. Since the testing of 10 insulators will give a figure very close to the true average it is apparent that this method of predicting the possible low and high test values of insulators is a very valuable tool to work with. In what follows the ratio of the low to the average values of test specimens will be referred to as the distribution factor F.

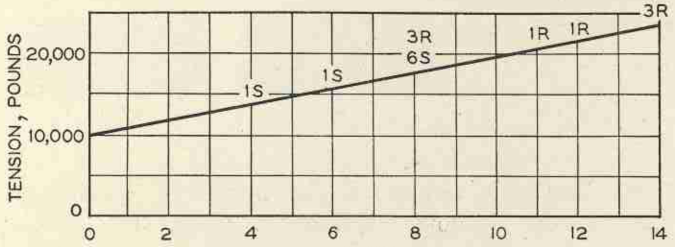

Fig. 8. Results of duration load test on porcelain insulators, showing effect of glazing treatment

S—Untreated, low value 14,000 pounds
R—Treated, low value 18,000 pounds

For glazed porcelain, based on 420 specimens, F is 0.74. These results were obtained at a rate of loading of 988 pounds per square inch per second in modulus of rupture and it would be natural to ask whether or not this ratio changes materially with different rates of load application. Table II shows F calculated for different loading rates. For comparison these factors were determined for 2 ceramic materials. At all but the fastest rate the data are obviously insufficient to establish fixed conclusions because of the small number of specimens tested. There is, however, an indication that the reduction in strength under time loading affects the high, low, and average values by the same percentage. In the calculations which follow the lowest values for F were taken for these 2 materials, 0.74 for material A, which is +8 glazed porcelain, and 0.54 for material B which is a ceramic material that has been advocated for making insulators.

Considering now groups of insulators made from these materials, what are the minimum test values to be expected if a large group of each type is tested each having a known average quick pull value of 15,000 pounds? Multiplying by their respective factors a possible low value is obtained for material A of 11,100 pounds and for material B of 8,100 pounds. A practical application of this is shown in table III, which gives a comparison of the predicted high and low values for porcelain insulators with the actual results obtained from testing 48 standard suspension units. It is indicated certainly by these results that if there are other variables, such as assembly differences, they cannot in this case be a very large factor since the observed results are accounted for by the expected inherent variation in the porcelain strength.

The Effect of Time and Load on Ceramic Materials

The third physical characteristic of porcelain to be discussed, is the effect of a duration load on mechanical strength. So far the strength of nonductile materials under relatively quick load applications has been considered. What happens with the introduction of a time factor? Unfortunately few data on the effect of time loading on the strength of nonductile materials have been published except by certain technologists in the glass industry. They have found that under long continued loads the strength of glass is materially reduced, not just perceptibly but a matter of from 30 to 60 per cent. It is reasonable to suppose that to some degree this characteristic is common to all similar materials.

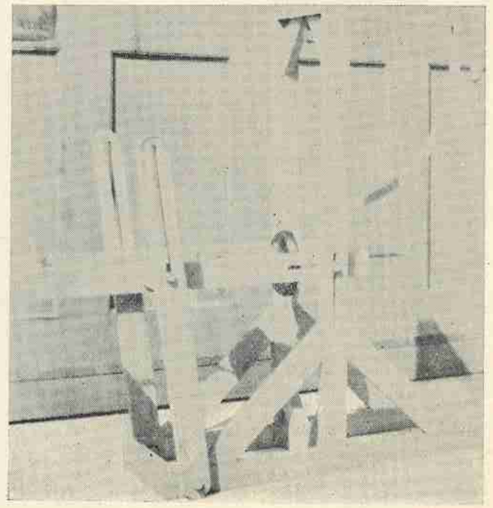

Fig. 9. Machine for testing impact resistance of insulators.

Table II—Ratio of Low Transverse Value to Average Transverse Value

Rate of Loading in Modulus of Rupture, Pounds per Second	Distribution Factor F	
	For Material A +8 Glaze	For Material B
988	0.74 (420)	0.69 (21)
3.11	0.80 (10)	0.59 (10)
1.36	0.89 (10)	0.69 (10)
0.62	0.87 (10)	0.72 (10)
0.26	0.79 (10)	0.54 (10)

Figures in parentheses indicate number of tests.

Porcelain insulators in service are subjected to continued loads of more or less severity for prolonged periods of time and certainly the load time factor is of major importance.

Load Testing Procedure

In obtaining the present data the testing machine shown in figure 12 was devised. The test specimens used were $^1/_2$ inch round rods placed on supports in the machine 4 inches apart and subjected to a transverse load at their center imposed by a weight carried on the upper beam. The gearing actuating this weight was variable so that it could be arranged to move the weight out quickly thus building up the load on the specimens at a rapid rate until failure, or the travel could be slowed down to the point where it required several days to break a rod. An automatic stop was provided to shut off the motor and apply a brake so that the breaking of the test rods and the recording of the strength values was automatic after each start. By running this machine day and night considerable progress could be made even when the loading was very slow.

Figure 13 shows the results obtained on materials A and B previously considered. The average strength values of 10 samples for each point reduced to moduli of rupture are the ordinates while the abscissa values are plotted as the reciprocal of the rate of loading in modulus of rupture in pounds per square inch per second. Thus the further to the right on the abscissa the slower the rate of loading. Most of the loss in strength occurs with the first decrease in the rate of loading and the curves then flatten out. Probably the average load that the materials would support indefinitely is that which would be represented by the asymptotes of the curves. In the case of material B it would be approximately 60 per cent of the quick load average while the value for material A would be about 80 per cent.

Although further data on this characteristic of ceramic materials are desirable, the foregoing is sufficient to emphasize the importance of studying the time load characteristics of porcelain which is to be subjected to continued loads. Certainly, other things being equal, the most desirable material to use in insulators is obviously the one which shows the lowest decrease in mechanical strength under a continued load.

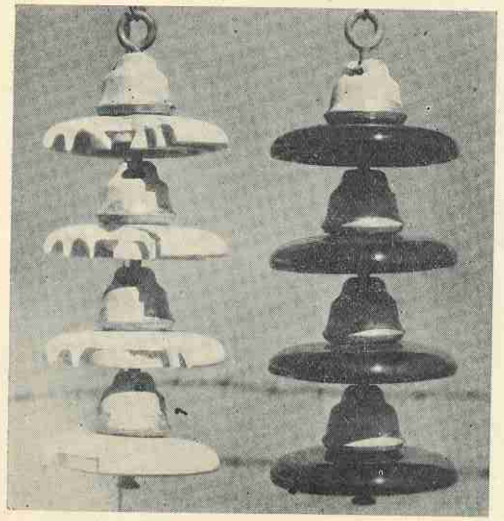

Fig. 10. Comparison of impact resistance of insulators with glazes in tension (left) and in compression (right)

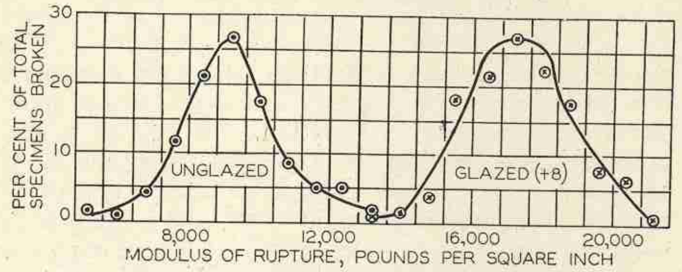

Fig. 11. Distribution curves for failure of unglazed and glazed specimens

Influence of Time on Service Life

In the earlier part of this discussion a theoretical method of arriving at the possible low strength values of insulators based on the strength of laboratory specimens was presented. The conclusions arrived at were the result of quick loading tests. Now it is possible to go a step further and to consider the effect of time. It must be assumed that the decrease in strength shown in figure 13 is approximately the lower limit and that the curves will now flatten out, and a further slowing up in the rate of load application will result in no further decrease in strength. For material B this load is about 40 per cent less than that found for the quick loading. The figure representing material A is 20 per cent lower; thus, the previously given possible low strength value for insulators if made of the particular materials in question, must be multiplied by 0.6 and 0.8 respectively. The figures thus obtained approach very closely to the load which any number of these insulators will sustain indefinitely without a single failure. As the load is increased above this figure an increasingly larger percentage of units will fail, depending upon the strength distribution curve and time factor of the dielectric used in the units.

PRACTICAL USE OF DATA

Of what value to the engineer are these figures? Most of the suspension insulators in service are working at values far below the theoretical point at which the first failure will occur. Even if they were working at a point slightly above this figure the number of failures as indicated by the distribution curve would be very few; thus, the data presented here may be of little practical value for the ordinary electrical porcelain installation. In recent years, however, the loading on the insulators has been increased in a number of cases. Certainly this is true for river crossings, radio work, and large switch insulator and bus support work. In arriving at a working load which a large number of such insulators will withstand indefinitely without the possibility of a failure the following expression may be used:

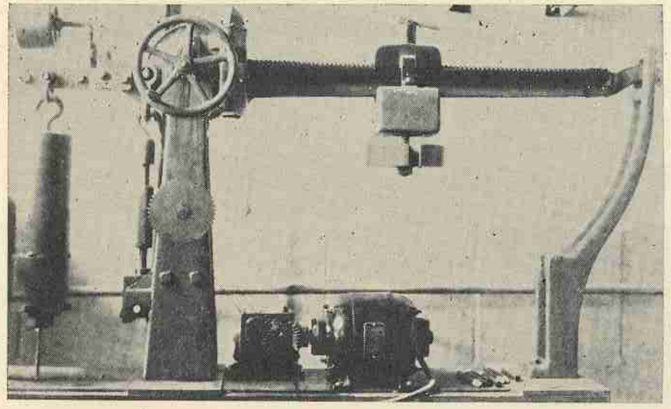

Fig. 12. Machine for time load testing

$W_A = S_a \times F \times T$

where

W_A = Working load at which no failure will occur in any number of insulators
S_a = Average quick strength of insulators
F = Distribution factor
T = Time loading factor

It should be borne in mind that the distribution factor and the time factor are 2 entirely separate and distinct entities, the former resulting from the inherent spread in the strength values obtained from breaking identical test specimens and the latter resulting from the effect of the time of loading on the strength of the material. For insulators which average 15,000 pounds made from the materials upon which the previous data were based breaking loads are obtained as follows:

$W_L = 15{,}000 \times 0.74 \times 0.8 = 8{,}900$ pounds for material A
$W_L = 15{,}000 \times 0.54 \times 0.6 = 4{,}860$ pounds for material B

In certain installations where a large percentage of the load is not of a constant nature, but occurs only for brief intervals, such as in the case of short circuits, or during switch operation, the time factor T in the above equations may be omitted.

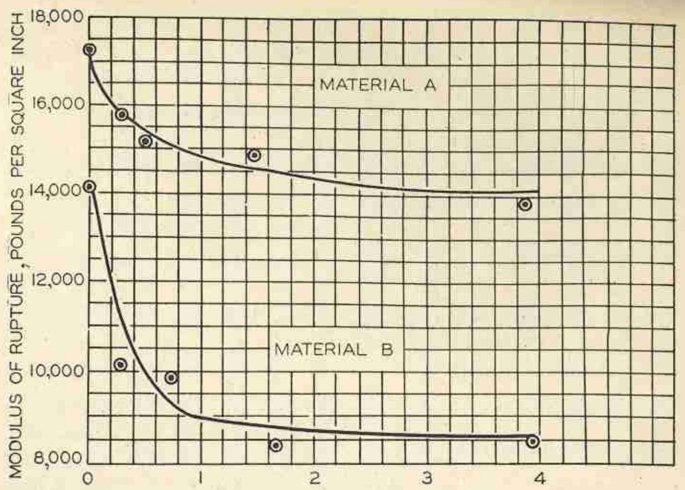

Fig. 13. Results obtained on time load tests; abscissa is the reciprocal of the rate of loading in pounds per square inch per second in modulus of rupture

Conversely, for a river crossing requiring insulators which must hold a constant 10,000 pound load the average strength is found as follows:

$10{,}000 = S_A \times 0.74 \times 0.8$
$S_A = 16{,}900$ pounds for material A

$10{,}000 = S_A \times 0.54 \times 0.6$
$S_A = 30{,}800$ pounds for material B

Hence, for such work insulators made of the particular materials in question should have these average strengths in a quick pull test.

It is conceded readily that the above rules are not infallible and that certain minor factors have been neglected; also, the accuracy of the figures is limited to some extent by the relatively small number of specimens tested. Nevertheless, it is believed that 3 of the basic factors affecting the life of ceramic insulators have been differentiated for the first time and an effort made to evaluate them in an orderly manner.

SOURCES OF ERROR

It is apparent that there are several possible sources of error in the calculations that have been given. In the first place, it must be assumed that the material in the test specimens has the same mechanical characteristics as that in the insulators. Since ceramic materials may vary widely in strength and uniformity it is obvious that the values of the factors used in this paper cannot be applied indiscriminately to several classes of material; also, in some cases the number of specimens tested was inadequate. Then too, the time loading factor may be found to be considerably lower when the loading is applied for a much longer time. Further research will be conducted to find this out.

Table III—Mechanical and Electrical Strength Values on Suspension Insulators Obtained With A.I.E.E. Standard Loading Rate

	Actual Test Values, 48 Tests	Predicted Values Using Rod Strengths With +8 Glaze. Load Rate 988 Pounds per Square Inch per Second (Modulus of Rupture)
Average	16,835	
High	20,400	20,450
Low	12,900	12,450

It is believed, however, that even with the possibilities of discrepancies as the result of these factors, the conclusions drawn are surprisingly accurate for the dielectrics that have been dealt with.

SUMMARY

Based on the study reported in this paper, the following statements may be made:

1. The present general method used for arriving at guaranteed mechanical values for insulators using ceramic dielectrics is insufficient.

2. Porcelain is an ideal insulating medium when the factors affecting its physical characteristics are properly controlled.

3. All indications point to surface strength as being of fundamental importance to the proper performance of an insulator dielectric.

4. Even with perfect porcelain one must expect an inherent variation in individual strength values when tests are conducted on a group of specimens. This is a characteristic of brittle nonductile materials. Since, regardless of the method of loading, the initial failure of a piece of this class of ceramic material is the result of a tension crack in the surface it is possible to predict the probable variations in quick strength of any insulator design by a simple calculation based upon the moduli of rupture obtained from a number of laboratory samples.

5. Uniformity of test values is not, by itself, a criterion of good porcelain.

6. Distribution curves of ultimate strength may be obtained by breaking a considerable number of test specimens and plotting the results so as to indicate the percentages of the total number which break within fixed limits. Since, regardless of the method of loading, the initial failure of a piece of glass or porcelain is caused by excessive localized tensile stress set up incidentally at some point in the surface, the distribution curves obtained from test specimens may be used to predict the range of strength values which may be expected from any insulator design.

7. Tests made with variable speeds of load application indicate a considerable drop in strength as the loading rate is decreased.

8. By evaluating the strength distribution factor and time factor a simple formula may be obtained for calculating safe insulator loads.

9. The testing of relatively few specimens is a source of error in arriving at the correct values to be used in the formula.

10. It is readily conceded that this work is not absolutely conclusive, but it is believed that for the first time the important factors which materially influence insulator life are evaluated and a simple method of approach outlined for the selection of insulators.

11. Since ceramic materials vary widely in their characteristics the factor values here used are only applicable to the particular materials studied.

REFERENCES

1. ELECTRICAL PROPERTIES OF GLASS (a book), J. T. Littleton and G. W. Morey. John Wiley and Sons, Inc., New York, N. Y., 1933.

2. THE INFLUENCE OF GLAZE ON INSULATOR STRENGTH, D. H. Rowland. *Gen. Elec. Rev.*, v. 32, March 1929, p. 136–8.

3. THE ANGLE OF FORKING OF GLASS CRACKS AS AN INDICATOR OF THE STRESS SYSTEM, F. W. Preston. American Ceramic Society *Jl.*, v. 18, June 1935, p. 175.

4. THE TIME FACTOR IN THE TESTING OF GLASSWARE, F. W. Preston. American Ceramic Society *Jl.*, v. 18, July 1935, p. 220–4.

5. RECENT IMPROVEMENTS IN HIGH VOLTAGE INSULATOR DESIGN, D. H. Rowland. *Gen. Elec. Rev.*, v. 33, July 1930, p. 384–7.

6. MECHANICAL AND THERMAL SHOCK TESTS ON CERAMIC INSULATING MATERIALS, H. M. Kraner and R. A. Snyder. American Ceramic Society *Jl.*, v. 14, Sept. 1931, p. 617.

7. MECHANICAL ELECTRICAL STRESS STUDIES OF PORCELAIN INSULATOR BODIES, Cullen W. Parmelee and John O. Kraehenbuehl. Bulletin No. 273, Engineering Experiment Stations, University of Illinois, Urbana.

8. INFLUENCE OF GLAZE COMPOSITION ON THE MECHANICAL STRENGTH OF ELECTRICAL PORCELAIN, L. E. Theiss. American Ceramic Society *Jl.*, v. 19, March 1936, p. 70–3.

9. STATISTICAL METHODS OF RESEARCH WORKERS (a book), R. A. Fisher. Oliver and Boyd, London, England, 1925.

10. GLASS AS A STRUCTURAL AND STRESS RESISTING MATERIAL, American Ceramic Society *Jl.*, v. 12, April 1933, p. 163–86.

This is a reprint from
Electrical Engineering
Published monthly by the
American Institute of Electrical Engineers
33 West 39th St., New York, N. Y.

6/12/'36 June 1936 issue

Porcelain for High Voltage Insulators

In this paper the mechanical failure of porcelain is discussed with special reference to 3 seldom recognized characteristics: the effect of the porcelain surface on the strength, the apparent anomalous distribution of individual mechanical test values, and the effect of time on mechanical strength. A method of evaluating the result of these factors on electrical insulator performance is suggested.

By
D. H. ROWLAND
ASSOCIATE A.I.E.E.

Locke Insulator Corp.,
Baltimore, Md.

THERE CAN BE little argument as to what mechanical characteristics are desirable in high voltage insulators, but the factors which contribute to such characteristics are concealed, more often than not, by an extraordinary amount of sophistic data. Modern high voltage insulators on the average have improved enormously in the past decade. This improvement has been brought about in most cases by expensive and tedious cut and try tests conducted on assembled insulators. The procedure has been to assume that certain features of the completed units such as mechanical strength, ability to withstand immersion first in boiling water and then in ice water, imperviousness to moisture, and other qualities would insure insulators capable of standing up in service, which, after all, is the only real criterion of insulator worth. Finally specifications such as the A.I.E.E. Standards No. 41 for the testing of high voltage insulators were evolved and it may here be stated, unequivocally, that insulators which will successfully pass these specifications will give an unusually good account of themselves in the field. However, just because 2 groups of insulators of different manufacture successfully pass a certain specification it cannot be assumed that their maintenance cost in the field will be the same. How will they stand up under mechanical shock such as the impact from stones or bullets? What effect will time under load have upon their life? What is the maximum load that they will withstand? Is actual experience over a period of years the only way to find out? The purpose of this discussion is to provide engineers with a greater insight into some of the more recently investigated and rather peculiar mechanical characteristics of ceramic materials with the hope that an understanding of this work will help them to answer these questions and to point out that some of the characteristics which have been viewed with alarm by the uninitiated are really a true part of the whole scheme while other factors which have been unknown, or neglected, have been of major importance. A realization of this is bound to lead to still greater efficiency of systems dependent on the insulating qualities of such materials.

A paper recommended for publication by the A.I.E.E. committee on power transmission and distribution, and scheduled for discussion at the A.I.E.E. summer convention, Pasadena, Calif., June 22–26, 1936. Manuscript submitted March 25, 1936; released for publication April 23, 1936.

10. For numbered references see list at end of paper.

700-Kv Transmission Planned for

Canadian Electrical Association told of project to deliver 6,000 Mw to Montreal and Quebec, hears plea for international development of St John River and continental grid

Transmission at 700/735 kv ac was selected by Hydro-Quebec's EHV Project Group as the best way to convey nearly 6 million kw from hydro plants on the Manicouagan and Outardes rivers 400 miles to Montreal, Project Chairman H. W. Haberl told the Canadian Electrical Association recently at Quebec. This voltage was selected, he said, as "the highest . . . possible at this time," considering that manufacturers must start to deliver equipment next year for service in 1965.

Other sessions of the four-day conference covered national and international grids, hydro and thermal generation, overhead and underground distribution, and many other utility subjects.

Backbone of the 700-kv project, Haberl explained, will be three 700-kv lines, two crossing the St. Lawrence near Quebec and following the south shore to a new receiving station at Boucherville, opposite Montreal. The third will run entirely north of the St. Lawrence and terminate at the existing Bout de l'Ile Substation on Montreal Island. All three circuits must also span the 6,000-ft-wide Saguenay.

Boucherville and Bout de l'Ile substations will be linked by a ten-mile 700-kv tie and will deliver Manicouagan power to the existing 300-kv system through nine 600-Mva banks. A similar link near Quebec will link Levis Substation with the third 700-kv circuit and existing 300 kv lines at Laurentides Substation; Levis will have four 400-Mva banks for 230-kv load.

Input to the 700-kv lines will be collected at two transformer stations in the Manicouagan-Outardes area. The first, to be known as Manicouagan because of its proximity to the 1,016-Mw Manicouagan 2, will also gather 1,123-Mw from Manicouagan 3 via four 38-mile lines, 642 Mw from Outardes 3 via two 28-mile lines, and 300 Mw from a later development. All gathering circuits will operate at 300 kv. This station will feed about 3,000 Mw to the two south-shore 700-kv lines.

The other collector station, to be built about 40 miles up the watershed near Outardes 4, from which it gets its name and 596 Mw, will also pick up 1,344 Mw from Manicouagan 5 via four 69-mile 300-kv circuits. Outardes' 2,000-Mw output will flow to Quebec and Montreal via the third 700-kv circuit; it will also have a 700-kv link with Manicouagan Collector Station.

Corona loss will be no greater than that of the existing 300-kv Bersimis lines, Haberl said. Final design will provide four-conductor bundles of the same Bersimis conductor at 18-in. spacing with phase spacings greater than 50 ft. Clearance to steel at each tower must be about 200 in. requiring strings of 35 insulators. Such lines will be rated at 2,000 amp continuous but would be "capable of much more."

Voltage Limited by Reactors

Overvoltages on lines and equipment will be reduced considerably, Haberl said, by permanently connecting 330-Mva shunt reactors to each 226-mile circuit at the collecting stations and at the receiving stations near Quebec. The shorter lines from Quebec to Montreal will have 165-Mva reactors at each end. Maximum dynamic overvoltage on load rejection, with these reactors, he said, will not exceed 1.5 times normal. Switching surges from line energization are also reduced and will not exceed 2.1 times normal. Consequently, he said, BIL requirements will be 2,000 to 2,500 kv, but without reactors they would be "very difficult."

Total current drawn by the shunt reactors will neutralize two-thirds of line-charging current, he continued, and generators and additional lower-voltage switched reactors will be used to hold down light-load voltage. Switched capacitors on receiving-end 300-kv buses will neutralize shunt-reactor current during full-load operation.

Stability requirements of the 6,000-Mw system will be met by clearing line-to-ground faults in six cycles and reclosing in 25 cycles. The shunt reactors completely discharge the 700-kv line during 25 cycles of dead time, Haberl said.

Power transformers for receiving stations with rail access will be banks of single-phase units capable

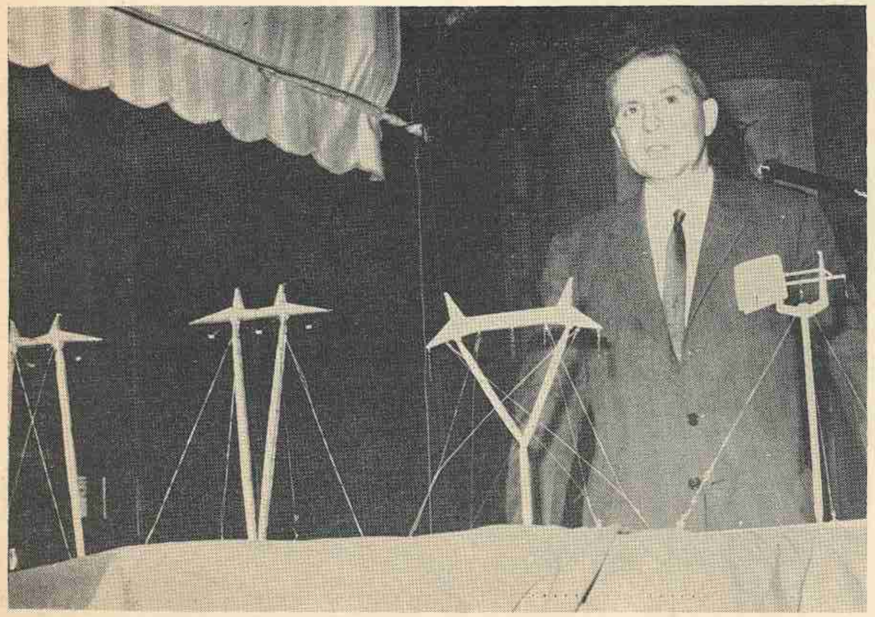

NEW GUYED-Y TOWER for 500-kv lines (second from right) is compared with more conventional guyed structures by V. F. Crowley, Shawinigan Engineering Co.

Communication Systems Dominate

Discussions of two extensive communication systems dominated the program of the Pennsylvania Electric Association Systems Operation Committee at its recent Pittsburgh meeting. One system for supervisory control of the West Penn Power Co substations covers much of western Pennsylvania. The other system for the Power Authority of New York's overall communications covers much of upstate New York. Both systems aroused deep interest from the more than 100 operators who attended.

The size of the supervisory control system of the West Penn Power Co can be pictured by the fact that it involves three distinct dispatching centers. These in turn control 27 major 138-kv step-down substations to which more than 70 minor stations report abnormalities. About $3¼ million of supervisory control equipment is involved.

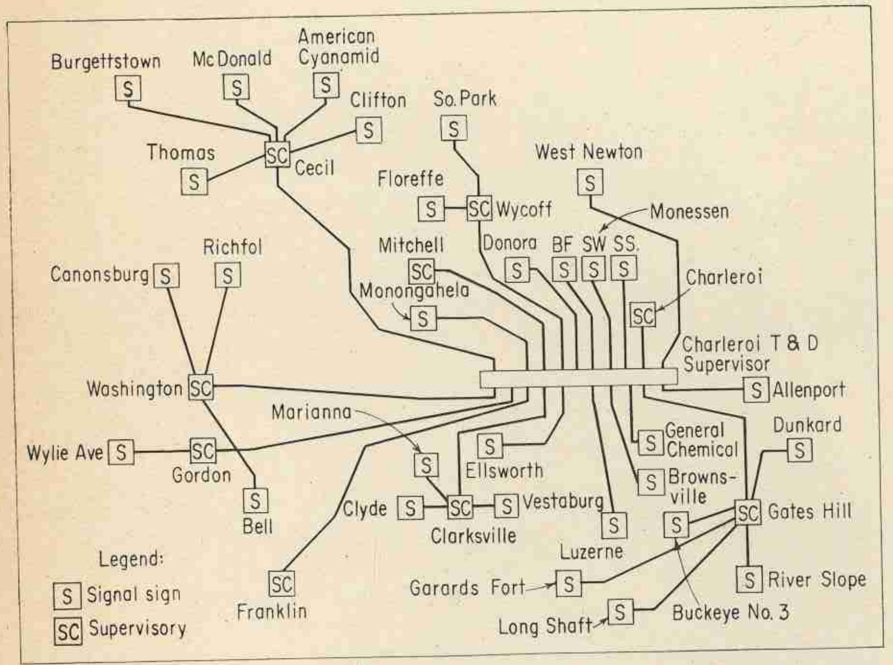

ONE CENTER controls key substations which in turn have communication channels to smaller substations; West Penn Power has three such centers

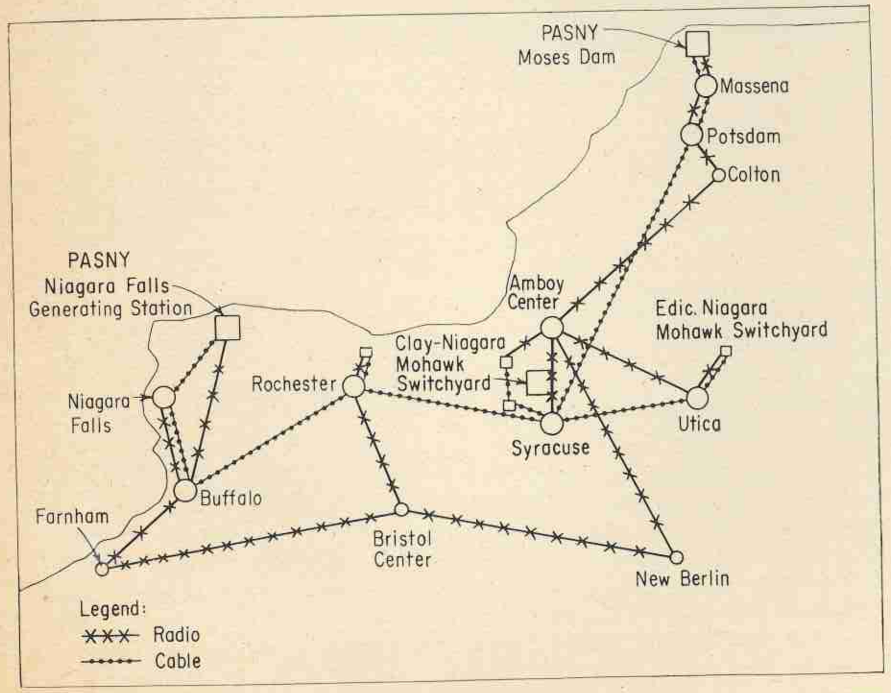

SYSTEM for upstate New York provides duplicate channels between main points on power systems of Niagara Mohawk Power, Rochester G&E, and PASNY

Three centers, manned round-the-clock, handle all switching and trouble calls of the West Penn system, according to Stanley Smith. The dispatcher in each center is given the following information on major substations: Notification of low control-battery voltage, of transformer alarms, and of pilot-wire channel trouble; telemetering of 25 and 46-kv bus voltages; and the operating position of every circuit breaker and all 138-kv motor-operated airbreak switches. The dispatcher can also close any breaker serving a line that can be sectionalized, and trip breakers to drop selected blocks of load in system emergencies.

The 25 and 46-kv switching stations are brought into the supervisory system as satellites of the 138-kv stations. Telephone channels radiate from each 138-kv station to the 25 and 46-kv stations in their vicinity. Each of these stations has an alarm bus which, when energized by any station abnormality, activates a signal back at the 138-kv station which is transmitted in turn to the dispatch center. This signal only tells the dispatcher that something has happened at a specific station.

Uses Telephone Channels

The system uses telephone channels for its communications. Bell Telephone Co of Pennsylvania supplied and correlated channel requirements with nine independent telephone companies in the area.

The first supervisory installations were placed in service in Aug 1960. Early troubles showed that separate action by Bell Telephone, the communications supplier, by Westinghouse, the supervisory control equipment supplier, and by West Penn, the user, would gain nothing but confusion. Accordingly a three-man committee was formed in which an engineer from each company took full charge of investigating

Hydro-Quebec

of 200-Mva summer loading, Haberl said. But the 100-ton shipping limit will restrict collector-station units to about 170 Mva.

Despite the industry trend to 3-phase power transformers, V. B. Ross, CGE, told another session, shipping limitations will favor single-phase units for EHV. One reason is the "enormous external phase-to-phase spacing required—27 ft for 700 kv. The problems of designing an economic tank having three bushings each 30 ft long and with adequate clearance to ground are close to being insurmountable."

Weight is saved by using high-temperature insulation, said R. A. Veitch, Canadian Westinghouse, as well as by forced-air cooling and use of grain-oriented steels.

Structures for EHV lines reflect a continuous quest for economy, said V. F. Crowley, Shawinigan Engineering Co. The most recent design, known as the "Y" tower, will be used for the first 50 miles of Ontario Hydro's 500-kv extension south of Sudbury.

In discussion, H. B. White, Alcan, indicated that rather high aluminum Y towers weigh about 61% as much as rigid self-supporting structures, vs 75% for the guyed-V.

Boosts Continental Grid

"We have heard a great deal about the interconnection of transmission systems across Canada," CEA Pres. R. E. Tweeddale told a dinner session. He suggested that concentrated study would show economies in such ties, and "ties across the international boundary would result in a complete transmission grid of the entire continent."

"The recently announced policy change with respect to the export of surplus power to the US will have a very important bearing on the electrical industry in Canada by making possible an accelerated development of our remaining hydro potentials. It is in the national interest", he continued, "to develop these as rapidly as possible."

"A total of 1.6 million kw is available from full development of the St John River," Tweeddale added. "It would involve a large dam in Maine providing downstream regulation for plants in New Brunswick and on-site installation of 700,000 kw. This would require integrated operation between systems in Maine and New Brunswick." But it could be followed, he suggested, by large-scale development of tidal power with interconnections throughout the Maritimes, Quebec, and New England.

Thus Canada has more need for EHV transmission than any other country except possibly Russia, Tweeddale continued, as a continental grid would make her hydro sites valuable for peaking.

At another session, G. A. Ewald, Public Service E&G Co, told of his company's gains from aerial-cable distribution in New Jersey. Outages with the new construction are at a rate less than a fifth those experienced with open-wire, he said, and the cost has averaged only about 3% more.

Original installations were at 4 kv but recent developments have permitted extension to 13 kv, he continued. The higher-voltage system is designed with automatic reclosers and tie switches between adjacent circuits to hold outage exposures to the equivalent of 4-kv circuits and provide service of comparable reliability. Construction of 13-kv circuits generally resembles that developed for 4 kv except that insulation is boosted to 156 mil of butyl rubber and 65 mils of neoprene strung in ceramic spacers.

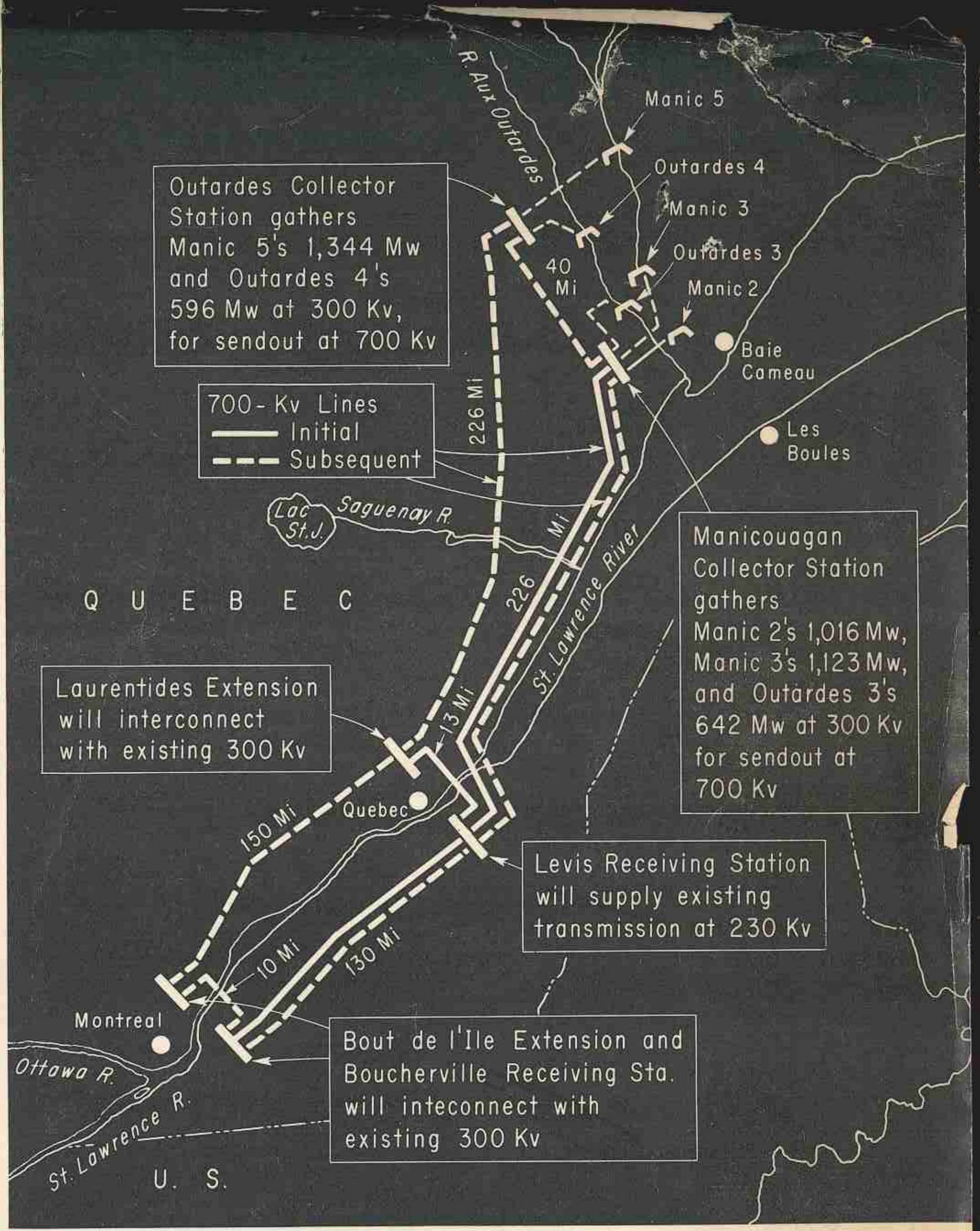

R. Aux Outardes
Manic 5
Outardes 4
Manic 3
Outardes 3
Manic 2
40 Mi
Baie Cameau
Les Boules
Outardes Collector Station gathers Manic 5's 1,344 Mw and Outardes 4's 596 Mw at 300 Kv, for sendout at 700 Kv
700-Kv Lines
Initial
Subsequent
226 Mi
226 Mi
Lac St.J.
Saguenay R.
Q U E B E C
St Lawrence River
Manicouagan Collector Station gathers Manic 2's 1,016 Mw, Manic 3's 1,123 Mw, and Outardes 3's 642 Mw at 300 Kv for sendout at 700 Kv
Laurentides Extension will interconnect with existing 300 Kv
13 Mi
150 Mi
Quebec
Levis Receiving Station will supply existing transmission at 230 Kv
10 Mi
130 Mi
Montreal
Ottawa R.
St. Lawrence R.
Bout de l'Ile Extension and Boucherville Receiving Sta. will inteconnect with existing 300 Kv
U. S.

GENERATION AT FIVE HYDRO PLANTS on Manicouagan and Outardes rivers will be collected via 300-kv links and sent at 700 kv to four receiving stations

National Power Survey Report

vide the lion's share of steam-electric peaking capacity

- Hydro installations will be used more and more for peaking
- The role of the gas turbine may be considerably expanded by recent innovations such as the jet engine application and by continuing development. Total percentage of this type equipment will probably be significant.
- Diesel engines are expected to be applied in relatively small total capabilities, but will be valuable in situations where applicable.

The report cautions that each technique must be evaluated carefully for each individual application. There is no rule of thumb broad enough to render individual analysis unnecessary.

Furthermore, it points out that an optimum ratio of peaking to base capacity would be difficult to determine. Studies have shown, however, that in most large predominantly steam systems, peaking in the order of 20-30% of total generation capacity may be justified.

The report includes lists of peak carrying equipment (see tables) to illustrate size and number of installations being made of various types of peaking equipment. These do not provide an all-inclusive list of peaking installations.

Two general methods of reducing system peaks are presented. One includes such techniques as controlled residential water heating, off-peak rates, and regulation of load by customers. The other includes such techniques as interruptible electric and steam loads, voltage reduction, and frequency reduction. The report states that voltage reduction should be looked upon as an emergency device only, and that frequency reduction is no longer practical because of widespread interconnections.

The report also notes that fuels may some day have a major influence on selection of peaking capacity. Other industries are making ever increasing demands on petroleum, and adequate reserves are diminishing. Use of coal as a fuel for power production will probably increase relative to oil and gas, and adequate reserves are available far into the future. It also cautions that innovations must not be overlooked since they may shift responsibility of meeting peaks to what is now considered efficient base steam units.

Report No. 2, prepared by a subcommittee chairmanned by Arnold Taylor of the Corps of Engineer, discusses axial-flow turbines. These are also known as bulb or tubular-type turbines. They operate as a turbine or pump in both directions of flow in low heads from 11 to 41 feet. The Rance tidal project in France will have 24 10-Mw bulb sets, and use of these units is of course considered by any proposed tidal power project such as Passamaquoddy.

The report states that this type of turbine will not be an important element in power systems but that, where sites and system electrical characteristics are favorable, it should be considered.

Report No. 3, also prepared by a subcommittee chairmanned by Arnold Taylor, deals with redevelopment of hydro projects. It cites factors which limit opportunities for redevelopment of particular hydro sites. But it suggests that studies be made on hydro stations where new units or creation of upstream storage appears to be economically feasible.

The reports may be obtained from the Office of Public Information, Federal Power Commission, Washington 25, D. C.

Multiple-Unit Diesel Units

Company	Location	Kw Size	Date in Service
Main Public Service Co	Presque Isle, Me.	4,200	1959
Iowa Electric L&P Co	Ames, Iowa	2,000	1960
Bangor Hydro Electric Co	Medway, Me.	8,000	1960
Bangor Hydro Electric Co	Bar Harbor, Me.	8,000	1961
Bangor Hydro Electric Co	East Port, Me.	2,000	1962
Edison Sault Electric Co	Manistique, Mich.	2,000	1960
Interstate Power Co	Hills, Minn.	2,000	1960
Interstate Power Co	Rushford, Minn.	2,000	1961
Public Service Co of Oklahoma	Grandfield, Okla.	2,000	1960
Public Service Co of Oklahoma	Clinton, Okla.	6,000	1962
Sierra Pacific Power Co	Reno & Carson City, Nev.	18,000	1960
Sierra Pacific Power Co	Reno & Carson City, Nev.	8,000	1961
Newport Electric Corp	Newport, R. I.	4,000	1960
Newport Electric Corp	Newport, R. I.	4,000	1961
Long Island Lighting Co	Northport, L. I., N. Y.	4,000	1960
Long Island Lighting Co	East Hampton, L. I., N. Y.	8,000	1962
Philadelphia Electric Co	Philadelphia, Pa.	6,000	1960
Pennsylvania Electric Co	Benton Air Force Base, Pa.	4,000	1960
Upper Peninsula Power Co	Dodgeville, Mich.	4,000	1961
Atlantic City Electric Co	Beesley's Point, N. J.	8,000	1961
Cheyenne Light, Fuel & Power Co (Public Service Co, Denver, Colorado)	Cheyenne, Wyoming	4,000 kw to go to 8,000 kw	1962 1963
Hilo Electric Co	Hilo, Hawaii	2,000 kw	1961
Golden Valley Electric Coop	Fairbanks, Alaska	5,330 kw	1962

700-Kv Transmission Planned for Hydro-Quebec

Canadian Electrical Association told of project to deliver 6,000 Mw to Montreal and Quebec, hears plea for international development of St John River and continental grid

Transmission at 700/735 kv ac was selected by Hydro-Quebec's EHV Project Group as the best way to convey nearly 6 million kw from hydro plants on the Manicouagan and Outardes rivers 400 miles to Montreal, Project Chairman H. W. Haberl told the Canadian Electrical Association recently at Quebec. This voltage was selected, he said, as "the highest . . . possible at this time," considering that manufacturers must start to deliver equipment next year for service in 1965.

Other sessions of the four-day conference covered national and international grids, hydro and thermal generation, overhead and underground distribution, and many other utility subjects.

Backbone of the 700-kv project, Haberl explained, will be three 700-kv lines, two crossing the St. Lawrence near Quebec and following the south shore to a new receiving station at Boucherville, opposite Montreal. The third will run entirely north of the St. Lawrence and terminate at the existing Bout de l'Ile Substation on Montreal Island. All three circuits must also span the 6,000-ft-wide Saguenay.

Boucherville and Bout de l'Ile substations will be linked by a ten-mile 700-kv tie and will deliver Manicouagan power to the existing 300-kv system through nine 600-Mva banks. A similar link near Quebec will link Levis Substation with the third 700-kv circuit and existing 300 kv lines at Laurentides Substation; Levis will have four 400-Mva banks for 230-kv load.

Input to the 700-kv lines will be collected at two transformer stations in the Manicouagan-Outardes area. The first, to be known as Manicouagan because of its proximity to the 1,016-Mw Manicouagan 2, will also gather 1,123-Mw from Manicouagan 3 via four 38-mile lines, 642 Mw from Outardes 3 via two 28-mile lines, and 300 Mw from a later development. All gathering circuits will operate at 300 kv. This station will feed about 3,000 Mw to the two south-shore 700-kv lines.

The other collector station, to be built about 40 miles up the watershed near Outardes 4, from which it gets its name and 596 Mw, will also pick up 1,344 Mw from Manicouagan 5 via four 69-mile 300-kv circuits. Outardes' 2,000-Mw output will flow to Quebec and Montreal via the third 700-kv circuit; it will also have a 700-kv link with Manicouagan Collector Station.

Corona loss will be no greater than that of the existing 300-kv Bersimis lines, Haberl said. Final design will provide four-conductor bundles of the same Bersimis conductor at 18-in. spacing with phase spacings greater than 50 ft. Clearance to steel at each tower must be about 200 in. requiring strings of 35 insulators. Such lines will be rated at 2,000 amp continuous but would be "capable of much more."

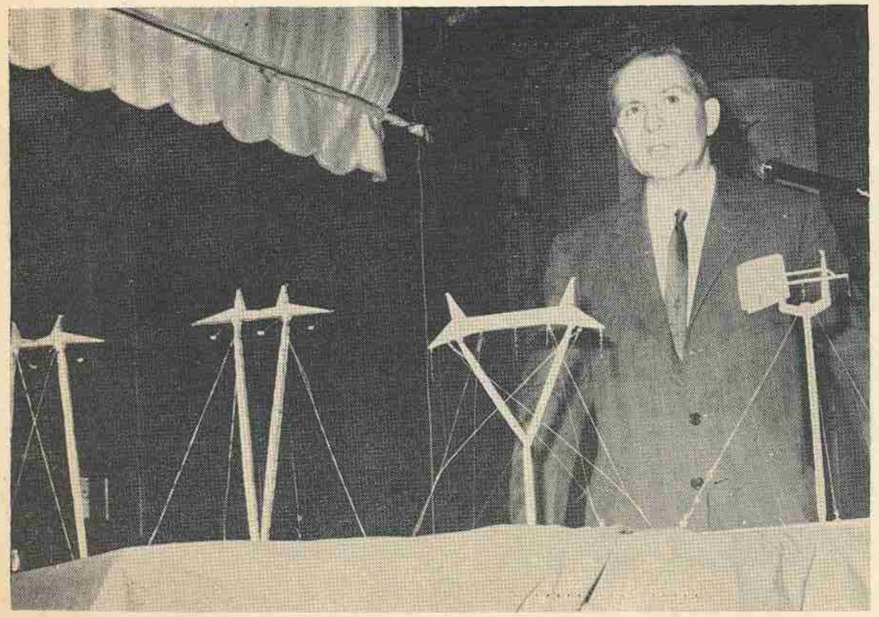

NEW GUYED-Y TOWER for 500-kv lines (second from right) is compared with more conventional guyed structures by V. F. Crowley, Shawinigan Engineering Co.

Voltage Limited by Reactors

Overvoltages on lines and equipment will be reduced considerably, Haberl said, by permanently connecting 330-Mva shunt reactors to each 226-mile circuit at the collecting stations and at the receiving stations near Quebec. The shorter lines from Quebec to Montreal will have 165-Mva reactors at each end. Maximum dynamic overvoltage on load rejection, with these reactors, he said, will not exceed 1.5 times normal. Switching surges from line energization are also reduced and will not exceed 2.1 times normal. Consequently, he said, BIL requirements will be 2,000 to 2,500 kv, but without reactors they would be "very difficult."

Total current drawn by the shunt reactors will neutralize two-thirds of line-charging current, he continued, and generators and additional lower-voltage switched reactors will be used to hold down light-load voltage. Switched capacitors on receiving-end 300-kv buses will neutralize shunt-reactor current during full-load operation.

Stability requirements of the 6,000-Mw system will be met by clearing line-to-ground faults in six cycles and reclosing in 25 cycles. The shunt reactors completely discharge the 700-kv line during 25 cycles of dead time, Haberl said.

Power transformers for receiving stations with rail access will be banks of single-phase units capable of 200-Mva summer loading, Haberl said. But the 100-ton shipping limit will restrict collector-station units to about 170 Mva.

Despite the industry trend to 3-phase power transformers, V. B. Ross, CGE, told another session, shipping limitations will favor single-phase units for EHV. One reason is the "enormous external phase-to-phase spacing required—27 ft for 700 kv. The problems of designing an economic tank having three bushings each 30 ft long and with adequate clearance to ground are close to being insurmountable."

Weight is saved by using high-temperature insulation, said R. A. Veitch, Canadian Westinghouse, as well as by forced-air cooling and use of grain-oriented steels.

Structures for EHV lines reflect a continuous quest for economy, said V. F. Crowley, Shawinigan Engineering Co. The most recent design, known as the "Y" tower, will be used for the first 50 miles of Ontario Hydro's 500-kv extension south of Sudbury.

In discussion, H. B. White, Alcan, indicated that rather high aluminum Y towers weigh about 61% as much as rigid self-supporting structures, vs 75% for the guyed-V.

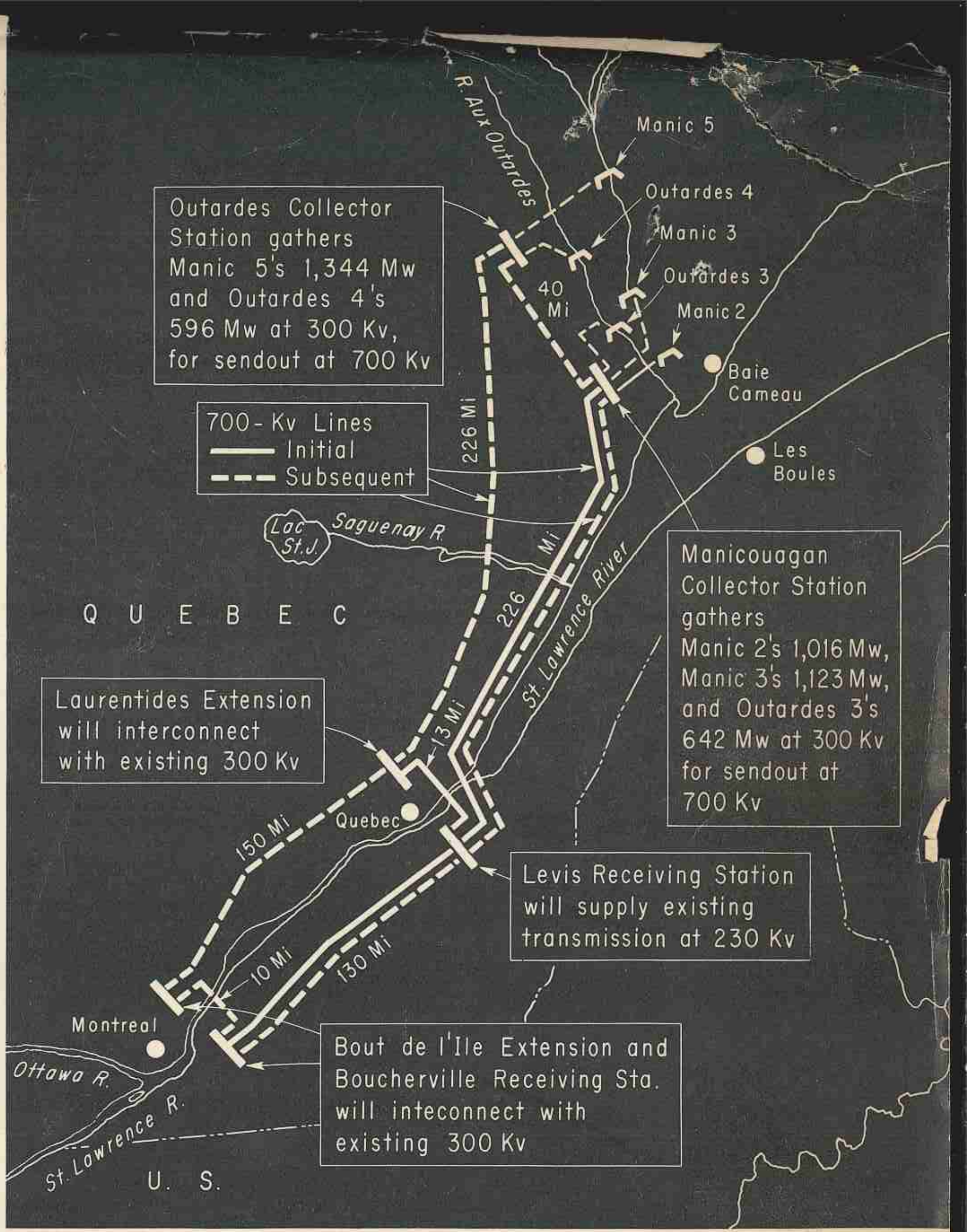
R. Aux Outardes
Manic 5
Outardes 4
Manic 3
Outardes 3
Manic 2
Baie Cameau
Les Boules
Outardes Collector Station gathers Manic 5's 1,344 Mw and Outardes 4's 596 Mw at 300 Kv, for sendout at 700 Kv
40 Mi
226 Mi
700-Kv Lines
Initial
Subsequent
Lac St.J.
Saguenay R
QUEBEC
Mi
226
St Lawrence River
Manicouagan Collector Station gathers Manic 2's 1,016 Mw, Manic 3's 1,123 Mw, and Outardes 3's 642 Mw at 300 Kv for sendout at 700 Kv
Laurentides Extension will interconnect with existing 300 Kv
13 Mi
Quebec
150 Mi
Levis Receiving Station will supply existing transmission at 230 Kv
10 Mi
130 Mi
Montreal
Ottawa R.
St Lawrence R.
Bout de l'Ile Extension and Boucherville Receiving Sta. will interconnect with existing 300 Kv
U. S.

GENERATION AT FIVE HYDRO PLANTS on Manicouagan and Outardes rivers will be collected via 300-kv links and sent at 700 kv to four receiving stations

Boosts Continental Grid

"We have heard a great deal about the interconnection of transmission systems across Canada," CEA Pres. R. E. Tweeddale told a dinner session. He suggested that concentrated study would show economies in such ties, and "ties across the international boundary would result in a complete transmission grid of the entire continent."

"The recently announced policy change with respect to the export of surplus power to the US will have a very important bearing on the electrical industry in Canada by making possible an accelerated development of our remaining hydro potentials. It is in the national interest", he continued, "to develop these as rapidly as possible."

"A total of 1.6 million kw is available from full development of the St John River," Tweeddale added. "It would involve a large dam in Maine providing downstream regulation for plants in New Brunswick and on-site installation of 700,000 kw. This would require integrated operation between systems in Maine and New Brunswick." But it could be followed, he suggested, by large-scale development of tidal power with interconnections throughout the Maritimes, Quebec, and New England.

Thus Canada has more need for EHV transmission than any other country except possibly Russia, Tweeddale continued, as a continental grid would make her hydro sites valuable for peaking.

At another session, G. A. Ewald, Public Service E&G Co, told of his company's gains from aerial-cable distribution in New Jersey. Outages with the new construction are at a rate less than a fifth those experienced with open-wire, he said, and the cost has averaged only about 3% more.

Original installations were at 4 kv but recent developments have permitted extension to 13 kv, he continued. The higher-voltage system is designed with automatic reclosers and tie switches between adjacent circuits to hold outage exposures to the equivalent of 4-kv circuits and provide service of comparable reliability. Construction of 13-kv circuits generally resembles that developed for 4 kv except that insulation is boosted to 156 mil of butyl rubber and 65 mils of neoprene strung in ceramic spacers.

~~M. Vose~~

~~" Kingsbury~~

GENERAL
ENGINEERING
LABORATORY

Contamination

TC-2C AND TC-15 MEETINGS - VÄSTERÅS, SWEDEN 1958

by

K. N. Mathes

Report No. 58GL332

December 5, 1958

RECEIVED
DEC 29 1958
H. A. FREY

GENERAL ELECTRIC

-213A (rev.) 9-56

The information contained in this report has been prepared for use by the General Electric Company and its employees. No distribution should be made outside the Company except when indicated below:

GENERAL DISTRIBUTION APPROVED

General Engineering Laboratory

TC-2C AND TC-15 MEETINGS - VÄSTERÅS, SWEDEN 1958

by

K. N. Mathes

Report No. 58GL332 December 5, 1958

GENERAL ELECTRIC
SCHENECTADY, NEW YORK

IEC TC-2C and 15 - 1958 Meetings
in
Västerås, Sweden

INTRODUCTION

Seven representatives of the United States attended the 1958 IEC TC-2C and 15 meeting in Västerås, Sweden. The organization of these meetings is listed below.

Committee	Chairman	Country	U.S. Delegate*
TC-2C Classification of Insulating Materials	R. Snadow	United Kingdom	K.N. Mathes
TC-15 Insulating Materials	Dr. R. Vieweg	Germany	Dr. A.H. Scott
Experts Committee**	E. F. Seaman (Dr. R. Vieweg, Acting)	U.S.A.	K.N. Mathes
WG-1 Electric Strength***	A. Collins	United Kingdom	Dr. G.L.M. Sommerman
WG-2 Resistivity and Insulation Resistance	Dr. A.H. Scott	U.S.A.	I.G. Easton
WG-3 Tracking	R. D. Poppe (Dr. R. Vieweg, Acting)	Norway	K.N. Mathes

(Continued)

*The official U.S. delegate is listed. Delegates assisted at other meetings where appropriate. C.E. Asbury attended the meetings of TC-2C. H. Blackmon attended some of the meetings of TC-15 and Working Groups.

**The Experts Committee was disbanded since the Working Groups have taken over most of its activity. A Steering Committee has been formed comprising the officiers of TC-15, the Chairmen of Working Groups, and three members at large - one each from countries not otherwise represented.

***WG - Working Group

(Continuation of IEC organization)

Committee	Chairman	Country	U.S. Delegate
WG-4 Voltage Endurance	J. Fabre for R. Langlois-Berthelot	France	J.R. Perkins, Jr.
WG-5 Encyclopedia	Dr. G. de Senarclens	Switzerland	J.F. Dexter
WG-6 Dielectric Constant and Loss	Dr. H. Roellig	Germany	I. G. Easton
WG-7 Temperature Properties	J. F. Dexter	U.S.A.	K. N. Mathes

Detailed reports of each meeting are attached as Appendices.* Wherever possible, the official minutes are incorporated with additional comment as needed.

The results of the meetings are summarized in the next section. Since the activities of IEC are continuing, it may be useful to refer to NEMA reports made in 1956 by Dr. T. Dakin and the author. A description of the 1958 meetings is containted also in the October issues of Electrical Manufacturing (by J. F. Dexter) and Insulation (by K. N. Mathes).

SUMMARY AND CONCLUSIONS

Insulation Standards

The continuing activity of TC-2C and TC-15 is producing accepted international standards. One of the best illustrations is IEC Publication No. 85, which provides the basis for the temperature classification of insulating materials by test and experience as well as by the traditional method of definition. Although much of the basis for this advance resulted from work in the United States, it is interesting that some of the wording of the new AIEE No. 1 is copied directly from IEC No. 85. Evaluation of motorettes, formettes and other ways of evaluating the thermal stability of insulation systems is under way in TC-2C but standards have not yet been accepted.

Such standards are needed as evidenced by the increased use of Class E (120 C) and Class F (155 C) insulation systems in Europe. Without question, the use of these two classes constitutes an upgrading of Class A (105 C) and Class B (130 C) systems. Although the use of superior materials is implied to permit the higher temperatures, no broad evidence is given that superior materials are actually used. Acceptance is based largely upon "experience" which at best is a very qualitative approach. Apparently, economic pressure for the new temperature classes is so great in Europe that the development and results of standardized tests for evaluating them cannot be awaited.

---

*If the Appendices are not attached, they may be obtained, if needed, on request to the author.

In TC-15, some progress has been made in the adoption of test methods for electrical properties of insulating materials. In addition to methods for resistivity previously adopted, a method on insulation resistance is receiving final approval. These methods are generally similar to ASTM methods. A drop-test method for tracking resistance is being balloted for final approval. The variable voltage feature of the IEC test appears to make it much superior to other tests. The IEC drop test merits more serious consideration and study in this country. Methods for electric breakdown will be submitted for final approval. The breakdown method in general is similar to ASTM D-149 except that agreement has not been obtained on electrodes. European, British, and American types of electrodes have all been included in the IEC method.

So far, it has not been possible to agree on an IEC method for measuring dissipation factor and capacitance of insulating materials. The American, British, and French methods for evaluating corona resistance are all under comparison and studies are outlined below.

France	Sample placed between parallel Mycalex plates with electrodes on the outside.	Emphasizes chemical effects
United Kingdom	Sample rests on a plate with point electrodes spaced slightly above sample. (Crossed cylinders are also being considered.)	Emphasizes erosion effect
United States	Sample is placed between 1/2 and 1" cylindrical electrodes (ASTM Direct Electrode Test).	Involves both chemical and erosion effects.

The problem of standard laboratory atmospheres and test conditions has been assigned to TC-15, WG-2. A British proposal for standard test conditions is under consideration as a basis for an international standard.

Insulation Evaluation

Although standardization itself moves slowly, rapid progress is evident in development, evaluation, and application of insulating materials in Europe. In particular, the considerable IEC activity on dielectric breakdown, tracking resistance, corona resistance, and thermal evaluation should be noted. Each of these areas is related to the life of electrical equipment. It is apparent that the European electrical industry intends to capitalize on the increased technical knowledge of insulation life by better and more efficient insulation design with less "margin of ignorance". By a continuing, consistent, active association with IEC TC-2C and TC-15, the electrical industry in the United States is becoming aware of important European trends in electrical insulation and may influence the direction in contributing to sound technology.

Encyclopedia

The "Encyclopedia" of Insulating Materials under development in WG-5 of TC-15 constitutes still another type of IEC activity in developing and publishing properties of insulating materials. So far, insulating materials have been classified and organized in "group tables" which contain qualitative comparisons of properties. The group tables have been published in French under the sponsorship of the Swiss committee. Translations into German and Russian are in progress. A preliminary English translation has been made. (AIEE is expected to publish the English edition.)

Plans are under way to develop monographs on specific insulating materials in which detailed information to guide application will be supplied. This tremendous job is expected to require about four years effort. Prototypes for the materials are being developed by the Swiss committee which will be submitted through the National Committees to be completed by major producers and users of insulating materials in each country.

The "Encyclopedia" is intended to guide the average user and not the "expert". Such a tremendous broad-scope effort probably is fully possible only under international sponsorship. Certainly the international aspect adds to the potential value.

GENERAL ELECTRIC

General Engineering Laboratory
SCHENECTADY, NEW YORK

TECHNICAL INFORMATION SERIES

AUTHOR	SUBJECT CLASSIFICATION	NO.
K.N. Mathes	Insulation	58GL332 DATE Dec. 5, 1958

TITLE

TC-2C and TC-15 Meetings - Västerås, Sweden 1958

ABSTRACT

Meeting of the International Electrotechnical Commission at Västerås, Sweden provided a means for the development of international standards and discussion of evaluation of insulating materials and systems. Thermal classification of insulating materials by functional test is accepted in theory internationally but in practice (cont)

G.E. CLASS		NO. PAGES
I	REPRODUCIBLE COPY FILED AT LIBRARY OF GENERAL ENGINEERING LABORATORY SCHENECTADY, NEW YORK	4
GOV. CLASS. None		

CONCLUSIONS

insulation systems are often uprated from Class A (105 C) to Class E (120 C) based on what appears to be only a nonobjective consideration of performance.

Special emphasis is being placed on voltage and thermal endurance of insulating materials. An "Encyclopedia" of insulating materials is also being developed.

INFORMATION PREPARED FOR General Information

TESTS MADE BY

AUTHOR Kenneth N. Mathes K N Mathes

COUNTERSIGNED J. A. Coffman JA Coffman

COMPONENT Insulation and Plastics, Chemistry and Metallurgy Laboratory

GL-16-C

~~M. Vore~~

~~" Kergelmeny~~

GENERAL
ENGINEERING
LABORATORY

Contamination

TC-2C AND TC-15 MEETINGS - VÄSTERÅS, SWEDEN 1958

by

K. N. Mathes

Report No. 58GL332

December 5, 1958

RECEIVED
DEC 29 1958
H. A. EREY

GENERAL ELECTRIC

-213A (rev.) 9-56

GENERAL ELECTRIC

FN-412-A (2-55)

EXTRA HIGH VOLTAGE TRANSMISSION

IN THE

CENTRAL STATES REGION

REPORT NO. 1

R.D. Webster
General Electric Company
Chicago Office
January 2, 1964

CONTENTS

Tab	Material
1	Discussion
2	Line Summary
3	Station Summary
4	Utility Identification
5	Map

DISCUSSION

The picture of extra high voltage transmission in the Central States Region is a complex one, and one that changes rapidly with time. It is important that we in General Electric keep abreast of this rapid changing EHV picture. To do this requires periodic reports. For these periodic reports to be effective, they must follow a format such that both report preparation and report absorption are easy. It is hoped that the format initiated by this report will meet this dual requirement.

The new format consists of a map, a line summary, a station summary, a utility identification list, plus a discussion. Let's review each of these sections.

Map (Tab 5)

The map shows EHV lines in the Central States Region as visioned today through about 1975. The solid lines shown are 345 kv. Five 230 kv lines (long dashes) are included on the map since they form an important part of the overall transmission picture. There are other 230 kv lines in the region; they are not shown because their importance to the overall picture is small. One 500 kv line is shown (short dashes).

In an attempt to keep the map reasonably readable, considerable data was omitted. This data is tabulated on the Line Summary and the Station Summary sheets.

Line Summary (Tab 2)

All line sections are listed on this summary in chronological order. Also shown (where known) is the utility that will build and own the particular line section.

Station Summary (Tab 3)

All stations are listed on this summary in chronological order. It should be noted that a given station is listed not only when it is originally installed, but also each time it is expanded. For example, the Eau Claire station is listed in 1966 when it will initially go into service with a single stepdown transformer, and it is again listed in 1969 when a second stepdown transformer will be added. Stations qualify for relisting for additions of breakers, as well as transformers.

For each station, the number of EHV breakers is noted and where already purchased, the manufacturer is indicated. Also the transformer rating and manufacturer are listed. When stations are relisted (not the original service date) only the additional breakers and transformers are tabulated.

One column of the Station Summary is titled "one line #". This is unused at present. In the future it will provide reference to individual station and line diagrams. These diagrams will provide a convenient means of showing complete information on the stations.

Existing stations are not listed on the Station Summary, although additions to existing stations are included.

Stations beyond 1969 are not listed. This is only because present information on these stations is too vague.

Utility Identification (Tab 4)

There is a list identifying the utility abbreviations used throughout the report.

It is felt that the above format will prove easy to revise periodically and thus keep all interested GE people up to date. It is recognized that there are presently many blanks in all parts of the report (map, line summary, station summary, utility identification). This is due not only to the fact that I do not have all known information, but also to the fact that much information has not yet been pinned down by the utility companies.

To make sure all known information is included in the next report, I am asking the application engineers to send me all missing information for their respective utilities. As more information is obtained from the utilities, it will, of course, be included.

There are several miscellaneous comments that should be made to complete the picture of EHV in the Central States Region.

1. The station currently shown at Forest Junction may actually be located at Ellington, which is about 20 miles west of the Forest Junction Station.
2. The station currently shown at Adams may actually be located at Rochester which is about 20 miles north of the Adams location.
3. It is expected that the Des Plaines, Lombard and Goodings Grove stations, plus possibility others in the Chicago area, will be interconnected at 345 kv; details of this will be pinned down in a subsequent report.

4. Plans north and west of Red Rock (Minneapolis) and Duluth are at present vague, and are dependent upon developments at Garrison. While much of the transmission in this area is presently shown at 230 kv, it may turn out to be 345 kv. The line locations may actually differ from those shown.

   Garrison, Fargo and Verndale are shown as single stations terminating both 230 kv and 345 kv. There may, in fact, be two separate stations at each of these locations.

   As shown 500 kv comes from Winnipeg to Grand Forks, and then steps down to 230 kv from Grand Forks to Fargo, and then steps up to 345 kv. This doesn't seem too logical.

   It is hoped to clarify all of the above points in a subsequent report.

5. The entire twin cities area (Minneapolis-St.Paul) has been represented by the Red Rock Station. In fact, Red Rock will form the 345 kv terminal of the lines shown. Already existing is a 230 kv station. In the future a 345 kv loop will go around the twin cities. Details will be pinned down in a subsequent report.

6. There is some question as to whether the Red Rock-Sioux Falls-Sioux City-Omaha line will be 230 kv or 345 kv. It is shown as 345 kv; this appears most logical.

7. Complete EHV studies have been conducted by GE for the Red Rock-Des Plaines line. Complete EHV studies are being conducted by "W" for the Red Rock-Hills-Sioux line.

8. Depending upon what the AEC does at Paducah, there may be considerable excess energy available from Joppa (southern tip of Illinois). There is some talk of building EHV lines from Joppa to the Chicago area for transmission of this energy.

The distribution list for this report is long; however, it may be necessary. Would each of you receiving this report let me know if (1) you do not wish future reports or (2) there are any other names that should be added to the distribution list.

R D Webster

R.D. Webster, MANAGER, ELECTRIC UTILITY APPLICATION ENGINEERING

RDW:gs

GE Co.
Chicago
1/2/64

LINE SUMMARY

(All lines 345 kv except as noted)

Service Date	Line Section	Ownership	Comments
Existing	Red Rock-Duluth		230 kv
	Goodings Grove-Olive		2-lines
	Sidney-Cayuga		
1965	Coffeen-Pana	CIPS	
	Coffeen-Ramsey	CIPS	
1966	Garrison-Minot		230 kv
	Minot-Grand Forks		230 kv
	Grand Forks-Fargo		230 kv
	Verndale-Duluth		230 kv
	Red Rock-Eau Claire	NSP	
	Eau Claire-Stevens Point	NSP	
	Stevens Point-Forest Junction	WEP	
	Forest Junction-Arcadian	WEP	
	Arcadian-Des Plaines	WEP-CE	
1967	Ramsey-Neoga	CIPS	
	Pana-Boody	IP	
	Boody-Kincaid		
	Kincaid-Bloomington	CE	
	Bloomington-Lombard	CE	
	Sioux-New Florence	UE	
	New Florence-Overton	UE	
	Overton-Kansas City	KCP&L	
	Kansas City-Topeka		
	Topeka-Wichita		
	New Florence-Hills	UE	
	Hills-Hazleton	IIG&E-IEL&P-IPS	
	Hazleton-Adams	Int. P.	
	Adams-Red Rock	NSP	
1968	Boody-Sidney	IP	
	Sioux-Wood River		
	Wood River-Stallings	IP	
	Stallings-Cahokia		
	Stallings-Coffeen		
	Kincaid-Bloomington	CE	
	Bloomington-Goodings Grove	CE	

Service Date	Line Section	Ownership	Comments
1969	Red Rock-Verndale		
	Verndale-Fargo		
	Fargo-Garrison		
	Red Rock-Sioux Falls		
	Sioux Falls-Sioux City		
	Sioux City-Omaha		
	Omaha-Kansas City		
	Wichita-Tulsa		
1970-1975	Winnipeg-Grand Forks		500 kv
	Omaha-Des Moines		
	Des Moines-Hills		
	Hills-Louisa		
	Louisa-Clinton		
	Clinton-Lombard		
	Wichita-Amarillo		
	Neoga-Breed		

3

4

5

STATION SUMMARY

(All Stations 345 kv except as noted)

Service Date	Station	Owner-ship	One-Line #	EHV Brkrs. No.	EHV Brkrs. MFG	EHV Transformers MVA	EHV Transformers KV	EHV Transformers MFG.	Comments
1965	Coffeen	CIPS				500	345/gen.		
	Pana	CIPS-IP				400	345/138	W	
	Ramsey	CIPS				400	345/138	W	
1966	Garrison								230 kv
	Minot								230 kv
	Grand Forks								230 kv
	Fargo								230 kv
	Verndale								230 kv
	Duluth	MP&L							230 kv
	Red Rock	NSP				325	345/115	W	50 KVAR tertiary reactor
	Eau Claire	NSP		1	GE	250	345/115	W	50 KVAR tertiary reactor
	Stevens Point	WPS							Not added till 1969
	Forest-Junction	WEP		2	AC	450	345/138		50 KVAR tertiary reactor
	Arcadian	WEP		2	AC	300	345/230		
	Des Plaines	CE							
1967	Ramsey	CIPS							
	Neoga	CIPS							
	Pana	CIPS-IP							
	Boody	IP							

(Cont'd from Tab 3 - 1)

Service Date	Station	Ownership	One-Line #	EHV Brkrs No.	EHV Brkrs MFG	EHV Transformers MVA	EHV Transformers KV	EHV Transformers MFG.	Comments
1967	Kincaid	CE				730	345/gen.		Transformers to be two half size or single-phase bank.
	Bloomington	CE							
	Lombard	CE							
	Sioux	UE				600	345/138		
	New Florence	UE							
	Overton	MissP&L				300	345/161		
	Kansas City	KCP&L				500	345/161		
	Topeka	KP&L							
	Wichita	KG&E							
	Hills					250	345/161		
	Hazleton								Not added till 1968
	Adams								
	Red Rock	NSP				325	345/115		50 KVAR tertiary reactor
						630	345/gen.		
1968	Boody	IP							
	Sidney	CIPS							
	Sioux	UE							
	Wood River	IP							
	Stallings	IP							
	Cahokia	UE				600	345/138		
	Coffeen	CIPS							
	Kincaid	CE				730	345/gen.		Transformers to be two half size or single-phase bank.
	Bloomington	CE							
	Goodings Grove	CE							
	Hazleton					250	345/161		

(Cont'd from Tab 3 - 2)

Service Date	Station	Ownership	One-Line #	EHV Brkrs No.	EHV Brkrs MFG	EHV Transformers MVA	EHV Transformers KV	EHV Transformers MFG	Comments
1969	Red Rock	NSP							
	Verndale								
	Fargo								
	Garrison								
	Sioux Falls								
	Sioux City								
	Omaha								
	Kansas City	KCP&L							
	Eau Claire	NSP				250	345/115		
	Stevens Point	WPS		2		167	345/115		
1970-1975									

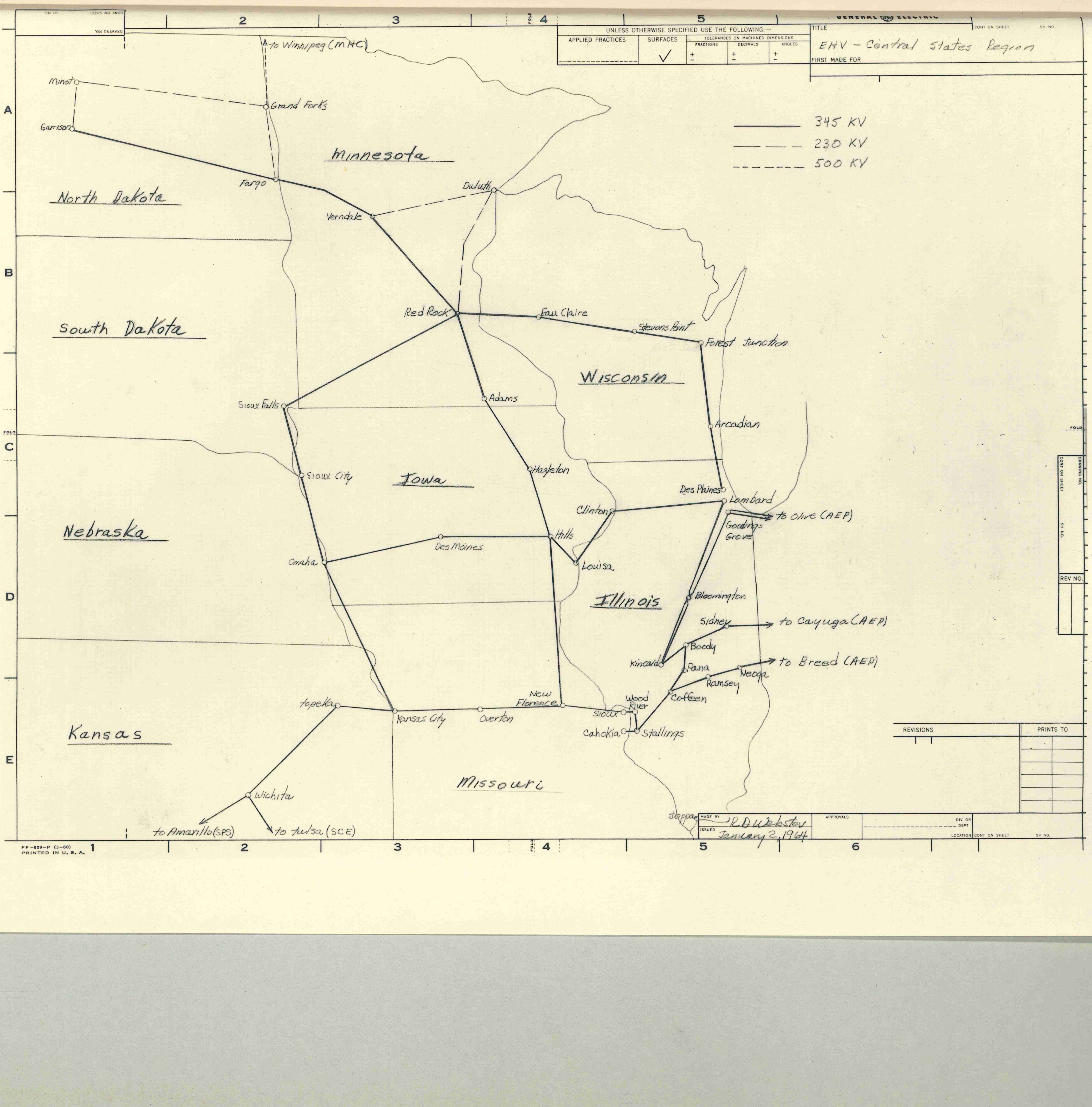
to Winnipeg (MHC)
Minot
Grand Forks
Garrison
Fargo
Verndale
Duluth
Minnesota
North Dakota
South Dakota
Nebraska
Kansas
Iowa
Wisconsin
Illinois
Missouri
345 KV
230 KV
500 KV
Red Rock
Eau Claire
Stevens Point
Forest Junction
Adams
Arcadian
Sioux Falls
Sioux City
Hazleton
Des Plaines
Lombard
to Olive (AEP)
Goodings Grove
Clinton
Hills
Louisa
Des Moines
Omaha
Bloomington
Sidney
to Cayuga (AEP)
Boody
Kincaid
Pana
to Breed (AEP)
Neoga
Ramsey
Coffeen
Wood River
Sioux
Cahokia
Stallings
New Florence
Overton
Kansas City
Topeka
Wichita
to Amarillo (SPS)
to Tulsa (SCE)
Joppa
A
B
C
D
E
1
2
3
4
5
6
FOLD

GENERAL ELECTRIC

UNLESS OTHERWISE SPECIFIED USE THE FOLLOWING:—

APPLIED PRACTICES	SURFACES	FRACTIONS	DECIMALS	ANGLES
	✓	±	±	±

TITLE EHV - Central States Region

FIRST MADE FOR

MADE BY R D Webster

ISSUED January 2, 1964

REVISIONS

PRINTS TO

FF-809-P (3-60)
PRINTED IN U. S. A.

GENERAL ELECTRIC

FN-412-A (2-55)

GENERAL ELECTRIC

RESEARCH
AND
DEVELOPMENT
CENTER

SCHENECTADY, NEW YORK

CLASS 1

THEORY OF THE TENSILE TEST

by

E.W. Hart, Metallurgy and Ceramics Laboratory

Report No. 66-C-222 June 1966

GENERAL ELECTRIC
RESEARCH AND DEVELOPMENT CENTER
SCHENECTADY, NEW YORK

TECHNICAL INFORMATION SERIES

AUTHOR Hart, EW	SUBJECT tensile testing; mechanical properties--metals; stability of plastic deformation	NO. 66-C-222 DATE June 1966
TITLE Theory of the Tensile Test		G.E. CLASS 1 GOVT. CLASS -
ADDITIONAL COPIES AVAILABLE AT Distribution Unit, Bldg. 5, Room 345 Research and Development Center P.O. Box 8, Schenectady, New York 12301		NO. PAGES 18

SUMMARY The phenomenology of the tensile test is re-examined with special attention to the influence of strain rate sensitivity of the flow stress. Explicit formulae are deduced for the measured variables of the test in terms of the phenomenological parameters of the material. The stability of the deformation is examined, and the growth of an inhomogeneity is described in the unstable deformation regime. The effect of elasticity of the specimen and the testing machine is investigated with special attention to relaxation tests.

KEY WORDS tensile testing, mechanical properties, metals, stability, plastic deformation

INFORMATION PREPARED FOR:

Metallurgy and Ceramics Laboratory

THEORY OF THE TENSILE TEST

Edward W. Hart
General Electric Research and Development Center
Schenectady, New York

I. Introduction

This is a report of the results of a study of the phenomenology of tensile deformation of metals with special attention to the effects of deformation rate sensitivity. The investigation has been restricted to phenomena and relationships that are relatively independent of special assumptions about the microscopic mechanism of deformation. Within this limitation a number of effects can be rationalized as artifacts of the tensile or creep test, dependent only on a few measurable parameters of the material and on the mechanical properties of the testing apparatus. Specially notable among these effects is the high ductility, noted for some metals at relatively high homologous temperatures, that has been termed "superplasticity."

The importance of strain rate sensitivity at elevated temperatures was first clearly indicated by Nádai and Manjoine.(1) More recently Backofen and Avery(2) have noted its relationship to the superplasticity problem. The present

---

Manuscript received June 2, 1966.

work extends the conclusions of those authors in a unified manner.

The plan of this work is as follows: In Section II the phenomenological model is introduced and the general relationships for homogeneous deformation are deduced. In Section III the problem of the stability of deformation in the tensile test is discussed and general criteria for stability are evaluated. In addition an estimate is made for the rate of progress of an inhomogeneity when the deformation is unstable. Section IV contains considerations of the effect of elasticity on tensile test results when rate sensitivity is important. The discussion in Section V is devoted to a critique of the tensile test.

II. Relationships for Homogeneous Deformation

In order to carry out any calculations some phenomenological assumption must be made concerning the relationships among true stress σ, natural plastic strain ε, and strain rate $\dot{\varepsilon}$. It will be assumed here that at any stage of deformation σ is dependent on the previous strain history, and that small changes in σ depend linearly on the corresponding small changes of ε and $\dot{\varepsilon}$. Thus, in differential form,

$$d\sigma = \sigma_{\varepsilon} d\varepsilon + \sigma_{\dot{\varepsilon}} d\dot{\varepsilon} \ . \qquad (1)$$

This differential form need not be integrable, and so the coefficients σ_{ε} and $\sigma_{\dot{\varepsilon}}$ are not simple partial derivatives but rather should be considered as general material parameters that depend on the specimen history. These parameters change their values as the deformation proceeds, and we shall make special assumptions about their nature as needed in the subsequent treatment. A similar approach was employed earlier by Hart(3) in a consideration of Lüders bands.

We shall proceed next to deduce the relationships between the measurable quantities of a tensile test and the phenomenological material parameters σ_{ε} and $\sigma_{\dot{\varepsilon}}$ for the condition of uniform deformation.

Let P be the load supported by the specimen, L be the length of the specimen, and A be the cross-section at any instant during a deformation procedure. By these symbols we denote the instantaneous values of the quantities at each instant of the deformation history. Then, by definition of the stress,

$$P = \sigma A. \qquad (2)$$

Denoting differentiation with respect to time by a dot over the symbol concerned, the time rate of change of P is readily obtained as

$$\dot{P} = \dot{\sigma}A + \sigma\dot{A}. \tag{3}$$

We shall represent $\dot{\sigma}$ by dividing Eq. 1. by dt, obtaining

$$\dot{\sigma} = \sigma_{\varepsilon}\dot{\varepsilon} + \sigma_{\dot{\varepsilon}}\ddot{\varepsilon}\ . \tag{4}$$

We need also the relationships

$$\dot{\varepsilon} = \dot{L}/L = -\dot{A}/A, \tag{5}$$

and

$$\begin{aligned}\ddot{\varepsilon} &= \ddot{L}/L - (\dot{L}/L)^2 \\ &= -\ddot{A}/A + (\dot{A}/A)^2\ .\end{aligned} \tag{6}$$

Now, dividing Eq. 3. by Eq. 2. we obtain

$$\dot{P}/P = \dot{A}/A + \dot{\sigma}/\sigma\ ,$$

and further substitutions involving Eqs. 4-6 lead to the basic relationship

$$\dot{P}/P = -(\dot{L}/L)[1 - \gamma + m] + (\ddot{L}/\dot{L})m, \tag{7}$$

where

$$\gamma \equiv (1/\sigma)\sigma_{\varepsilon}, \tag{8}$$

and

$$m \equiv (\dot{\varepsilon}/\sigma)\sigma_{\dot{\varepsilon}}\ . \tag{9}$$

The quantities γ and m are material parameters and in general vary through the deformation history.

Eq. 7. can now be specialized to describe two familiar types of tensile test:

Case A: The constant extension rate test.

For this test $\ddot{L} = 0$, and so

$$(d\ln P/d\ln L)_{\dot{L}} = \gamma - 1 - m, \tag{10}$$

where the subscript $\dot{L}$ on the derivative means that $\dot{L}$ is constant.

Case B: The constant load creep test.

For this case $\dot{P} = 0$, and since

$$(\ddot{L}/\dot{L})/(\dot{L}/L) = d\ln\dot{L}/d\ln L,$$

$$(d\ln\dot{L}/d\ln L)_P = (1 - \gamma + m)/m. \tag{11}$$

Another special case of interest is the constant stress creep test. For this purpose we divide Eq. 4 by σ and use Eqs. 5, 6, 8, and 9 to obtain

$$\dot{\sigma}/\sigma = \gamma(\dot{L}/L) + m[(\ddot{L}/\dot{L})-(\dot{L}/L)].$$

This leads us easily to

Case C: The constant stress creep test.

For this test $\dot{\sigma} = 0$, and so

$$(d\ln\dot{L}/d\ln L)_{\sigma} = 1-(\gamma/m). \tag{12}$$

III. Stability of Tensile Deformation

A Stability Criterion

The formulas of Section II are valid only if the deformation proceeds homogeneously. If on the other hand a small portion of the length of the specimen has a cross-section that differs from the cross-section of the remainder by some small amount, the formulas are in error by a small amount. If in the course of the deformation the magnitude of the cross-section difference does not increase, we shall call the deformation stable. It is only when the deformation is stable or nearly so that the error can be expected to remain small. Furthermore, we can then expect high ductility without excessive localized deformation.

To investigate the stability in greater detail we shall compute the variation in area increment rate $\delta\dot{A}$ as a function of variation in cross-section δA. Since P is the same at all points of the specimen, a variation of Eq. 2 results in the relation

$$0 = \sigma\delta A + A\delta\sigma. \tag{13}$$

In analogy to Eqs. 1, 5, and 6 we have the further equations

$$\delta\sigma = \sigma_{\varepsilon}\delta\varepsilon + \sigma_{\dot{\varepsilon}}\delta\dot{\varepsilon}, \tag{14}$$

$$\delta\varepsilon = -\delta A/A, \tag{15}$$

$$\delta\dot{\varepsilon} = -\delta\dot{A}/A + (\dot{A}/A)(\delta A/A). \tag{16}$$

Combining these relationships and making use of the definitions of γ and m, we obtain the result

$$(\delta\ln\dot{A}/\delta\ln A)_P = -(1-\gamma-m)/m. \tag{17}$$

Now, our stability criterion can be stated as follows:

The deformation is stable if

$$(\delta\dot{A}/\delta A)_P \leq 0, \tag{18}$$

and is otherwise unstable. Since in # tension $\dot{A}/A$ is negative, this condition can be restated so that the deformation is stable in tension if

$$(\delta\ln\dot{A}/\delta\ln A)_P \geq 0 \tag{18'}$$

or, in terms of the phenomenological parameters, when

$$\gamma + m \geq 1. \tag{19}$$

It is readily seen that our criterion is in agreement with the classical Considère condition for strain hardening materials with negligible rate dependence, and with the usual criterion for purely viscous materials ($\gamma = 0$) for which the limiting stable material is that which displays Newtonian viscosity, or for which $m = 1$.

The Constant Load Test

An interesting sidelight on the stability condition Eq. 18' is that the point of onset of instability can be noted directly from the measured variables in the constant load creep test. This is because the comparison of a variation along the length of a specimen, since the load is the same at each point, is analogous to successive increments of deformation in time when the deformation proceeds at constant load. We may replace δA then by $\dot{A}\delta t$. The deformation at constant P is stable then so long as

$$\frac{d}{dt}\ln\dot{A}/\frac{d}{dt}\ln A \geq 0,$$

or, more simply, if

$$\ddot{A} \geq 0. \tag{20}$$

By Eqs. 5 and 6 this leads easily to the condition

$$\ddot{L}/\dot{L} - 2(\dot{L}/L) \leq 0,$$

or

$$\ddot{L}/\dot{L} \leq 2(\dot{L}/L).$$

But the left-hand member is $d\dot{L}/dL$, and so the deformation is stable when

$$d\dot{L}/dL \leq 2(\dot{L}/L), \tag{21}$$

for creep under constant load. This condition can be applied to the plot of $\dot{L}$ vs L at constant P by simple geometrical construction.

The Growth of Inhomogeneities

The discussion of inhomogeneous deformation can be carried somewhat farther with the inclusion of a simplifying assumption concerning the values of the material parameters γ and m. We shall consider the progress of an inhomogeneity in a tensile specimen that is creeping under constant load during "stage two" of the deformation history. This stage is characterized grossly by a relatively constant (actually slightly increasing) $\dot{L}$, and can be more precisely described as a regime during which $\gamma = 0$ and m is constant. We need not assume anything about the nature of γ or m up to that stage.

The problem is then as follows:

At some initial time the specimen has uniform cross-section A_o except for a small segment that has cross-section $A_o + \delta A_o$ where δA_o is small.

After a time interval Δt the principal cross-section has changed from A_o to A and the special segment has become $A + \delta A$.

The problem is to compute the dependence of δA upon A, A_o, and δA_o.

Note first that, corresponding to Eq. 17, if the variation δ is replaced by the differential d the equation holds in similar form,

$$(d\ln\dot{A}/d\ln A)_P = -(1-\gamma-m)/m. \tag{22}$$

This can be verified also by transforming Eq. 11 to the form it takes when the variable L is transformed to A as variable through Eqs. 5 and 6.

When $\gamma = 0$, Eq. 22 is simply

$$(d\ln\dot{A}/d\ln A)_P = 1 - \frac{1}{m} . \tag{23}$$

This equation can be integrated from A_o to A to determine $\dot{A}$ in terms of A, A_o and $\dot{A}_o$. The result is easily seen to be

$$\dot{A}/\dot{A}_o = (A_o/A)^{\frac{1}{m} - 1} . \tag{24}$$

If the beginning point for the integration is displaced slightly in time by an amount δt, the changes in initial and final cross-section for the same full interval Δt are respectively $\dot{A}_o\delta t$ and $\dot{A}\delta t$. Our variation δA_o due to initial inhomogeneity can be represented by a fictitious time displacement as well and so we have that

$$\delta A/\delta A_o = \dot{A}/\dot{A}_o,$$

and so

$$\delta A = (A_o/A)^{\frac{1}{m} - 1} \delta A_o . \tag{25}$$

Therefore, if at some stage in the deformation when $\gamma = 0$, there is an inhomogeneity δA_o, after subsequent deformation, during which A_o reduces to A, the resultant inhomogeneity δA will be given by Eq. 25.

The notable feature of Eq. 25 is the very strong dependence on m. This explains why considerable ductility can be obtained even beyond the point of instability for materials of sufficiently high m, that is for m greater than about 1/3. In fact this is the principal source of the phenomenon that has been termed "superplasticity."

IV. Effect of Elasticity in Loading

General Relationships

Since most tensile testing is done with machines that possess considerable elasticity because of connecting linkages, load measuring devices, etc., and since the specimen is also elastic, it is desirable to examine some of the phenomena that result from the elasticity. Of course this problem is not a new one, and it has been discussed by other authors before. The present treatment is in large measure an augmentation of the previous treatments with special emphasis on the rate sensitivity of the specimen.

The model that we shall take for the loading apparatus is that the specimen of length L is at any instant in series with a spring of elastic constant K that is stretched by an amount $L_1 - L$. The length L_1 is then the specimen length for which there would be no load. Then if the load is P it is given by

$$P = K(L_1 - L). \tag{26}$$

The applied extension rate is $\dot{L}_1$, which is the extension rate that a perfectly weak specimen would experience.

We shall now consider the time derivative of Eq. 26

$$\dot{P} = K(\dot{L}_1 - \dot{L}). \tag{27}$$

If L_o is the nominal gauge length, and A_o the corresponding cross-section such that at any stage in the deformation,

$$LA = L_o A_o, \tag{28}$$

we may convert Eq. 27. to one involving stress and strain rates. Since

$$\dot{P} = \dot{\sigma}A + \sigma\dot{A},$$

we have

$$\dot{\sigma}A + \sigma\dot{A} = K(\dot{L}_1 - \dot{L}).$$

Then

$$\dot{\sigma} = (KL/A)[(\dot{L}_1/L) - (\dot{L}/L)] - \sigma(\dot{A}/A),$$

and since

$$\frac{\dot{A}}{A} = -\frac{\dot{L}}{L},$$

$$\dot{\sigma} = \frac{KL}{A}\left[\frac{\dot{L}_1}{L} - \left(1 - \frac{\sigma A}{KL}\right)\frac{\dot{L}}{L}\right],$$

$$= \frac{KL_o}{A_o}\left(\frac{L}{L_o}\right)^2\left[\frac{\dot{L}_1}{L} - \left(1 - \frac{\sigma A}{KL}\right)\frac{\dot{L}}{L}\right]. \tag{29}$$

Now

$$L = L_1 - P/K,$$

$$= L_1 (1 - P/KL_1).$$

But P is always much smaller than either KL or KL_1, and so we may replace L by L_1 where we wish and neglect $\sigma A/KL$ compared to 1. Then

$$\dot{\sigma} = (KL_o/A_o)(L_1/L_o)^2[(\dot{L}_1/L_1) - (\dot{L}/L)]. \tag{30}$$

If we make the transcriptions:

$$\dot{e} \equiv \dot{L}_1/L_o,$$

$$\dot{\varepsilon} \equiv \dot{L}/L,$$

$$\kappa \equiv KL_o/A_o,$$

we have finally

$$\dot{\sigma} = \kappa(L_1/L_o)^2[(L_o/L_1)\,\dot{e} - \dot{\varepsilon}], \tag{31}$$

where the only approximation has been to neglect σ compared to κ.

When Eq. 31 is applied to an interval during which the incremental strain is small, the variation of L_1 is small compared to L_1, and if L_o is taken to be the value of L_1 at the start of the interval, the equation can be used in the simpler form

$$\dot{\sigma} = \kappa(\dot{e} - \dot{\varepsilon}), \tag{32}$$

where $\varkappa$ and $\dot{e}$ are computed with the same value of L_o. This is the form that is used as the starting point by Noble and Hull.(4)

Load Relaxation Test

If in the course of a tensile test the cross-head motion is stopped, the load will relax gradually with time. This *stress relaxation experiment* can be easily analyzed to deduce m as a function of σ as follows:

Since the relaxation is generally a slow process, each stage of the process is close to steady state. Then

$$m = d\ln\sigma/d\ln\dot{\varepsilon}\ . \qquad (33)$$

Since $\dot{e} = o$,

$$\dot{\sigma} = -\varkappa\dot{\varepsilon},$$

$$d\ln\dot{\sigma} = d\ln\dot{\varepsilon},$$

and so with this geometrical constraint

$$m = (d\ln\sigma/d\ln\dot{\sigma})_{\dot{e}=o}\ . \qquad (34)$$

Therefore, if $\ln\sigma$ is plotted against $\ln\dot{\sigma}$, it is easy to determine m as slope of the curve at each point. Note that it is not necessary to assume any special power law for the dependence of σ on $\dot{\varepsilon}$ to get this result.

General Approach to Steady State

If $\dot{e} \neq o$, it is possible to estimate the approach of σ to steady state. At relatively high temperatures this is

important since it is necessary to be able to distinguish a persistent change of σ due to continuing hardening of the specimen from a change of load due to elastic behavior. We shall compute the mode of approach to steady state when m is relatively constant.

From Eq. 32,

$$\varkappa\dot{\varepsilon} = \varkappa\dot{e} - \dot{\sigma},$$

and

$$\ln\dot{\varepsilon} = \ln\dot{e} + \ln[1-(\dot{\sigma}/\varkappa\dot{e})]. \qquad (35)$$

Since near steady state $\dot{\sigma}/\varkappa\dot{e}<<1$,

$$\ln\dot{\varepsilon} \cong \ln\dot{e} - \dot{\sigma}/\varkappa\dot{e},$$

and then (dropping the approximation symbol)

$$d\ln\dot{\varepsilon} = -(1/\varkappa\dot{e})d\dot{\sigma}.$$

Substituting this expression of $\dot{\varepsilon}$ in Eq. 33, we obtain

$$-(m/\varkappa\dot{e})d\dot{\sigma} = d\ln\sigma. \qquad (36)$$

Since m, $\varkappa$, and $\dot{e}$ are constant in the range considered, Eq. 36 can be integrated.

$$-(m/\varkappa\dot{e})\dot{\sigma} = \ln(\sigma/\sigma_s), \qquad (37)$$

where σ_s is the steady state value of σ when $\dot{\varepsilon} = \dot{e}$ and so when $\dot{\sigma} = o$. Since $\sigma_s-\sigma<<\sigma_s$ we can expand the right hand number of Eq. 37 as

$$\ln(\sigma/\sigma_s) = \ln[1-(1-\frac{\sigma}{\sigma_s})],$$

$$\cong -[1-(\sigma/\sigma_s)],$$

and write Eq. 37 as

$$(m\sigma_s/\varkappa\dot{e})(\dot{\sigma}/\sigma_s) = 1 - \sigma/\sigma_s.$$

This is easily integrated to give

$$\sigma/\sigma_s = 1 - \exp[-(\varkappa\dot{e}/m\sigma_s)(t+t_o)], \qquad (38)$$

where t_o is a constant of integration. If we make the replacements $\dot{e}t \equiv \Delta e$, $\dot{e}t_o \equiv e_o$,

$$\sigma/\sigma_s = 1 - \exp[-(\varkappa/m\sigma_s)(e_o + \Delta e)], \qquad (39)$$

where Δe is the strain variable representing the increment of strain from the starting point which must be already near the steady state.

This result shows that the approach to steady state when $\dot{e} \neq o$ proceeds exponentially rather than by a power law which is the case for the relaxation when $\dot{e} = o$. The characteristic strain increment that describes the speed with which σ/σ_s approaches 1 is $(m\sigma_s/\varkappa)$. The smaller this number is , the more the test reflects the material properties since then $\dot{\epsilon}$ is closer to the imposed rate $\dot{e}$. That number is small when m is small and when $\varkappa/\sigma_s$ is large, i.e. for a hard machine.

V. Discussion

The results of Section III above show that the utility of the tensile test for the determination of material properties is severely restricted for materials with small m. In particular it is not possible then to obtain reliable data in the fully hardened state where γ has become very small. It would seem that there is good reason to place greater emphasis on the use of torsion testing methods where possible. Although such methods have not been exploited much to date, there is enough experience$^{(5)}$ with them to indicate that they can be effectively employed, and that they can be improved by further investigations.

The main problem with tensile testing is that, because of plastic flow instability and tensile fracture behavior, it is not generally possible to obtain reliable results on the steady state stress at a given strain rate. These data are readily obtained in torsion tests even with solid specimens. The early strain hardening behavior, however, is not obtained easily in torsion tests except with tubular specimens. But that range of data is explored readily by the tensile test. It would seem therefore that a judicious combination of tensile and torsion testing could produce reliable results for most materials over a wide range of testing temperatures and rates.

References

1. A. Nádai and M. J. Manjoine, J. Appl. Mech. 8, A-77 (1941).

2. W. A. Backofen, I. R. Turner, and D. H. Avery, Trans. A.S.M. 57, 980 (1964).

3. E. W. Hart, Acta Met. 3, 146 (1955).

4. F. W. Noble and D. Hull, Acta Met. 12, 1089 (1964).

5. D. S. Fields and W. A. Backofen, Proc. ASTM 57, 1259 (1957); Trans. ASM 51, 946 (1959).

GENERAL ELECTRIC

RESEARCH
AND
DEVELOPMENT
CENTER

SCHENECTADY, NEW YORK

CLASS 1

THEORY OF THE TENSILE TEST

by

E.W. Hart, Metallurgy and Ceramics Laboratory

Report No. 66-C-222 June 1966

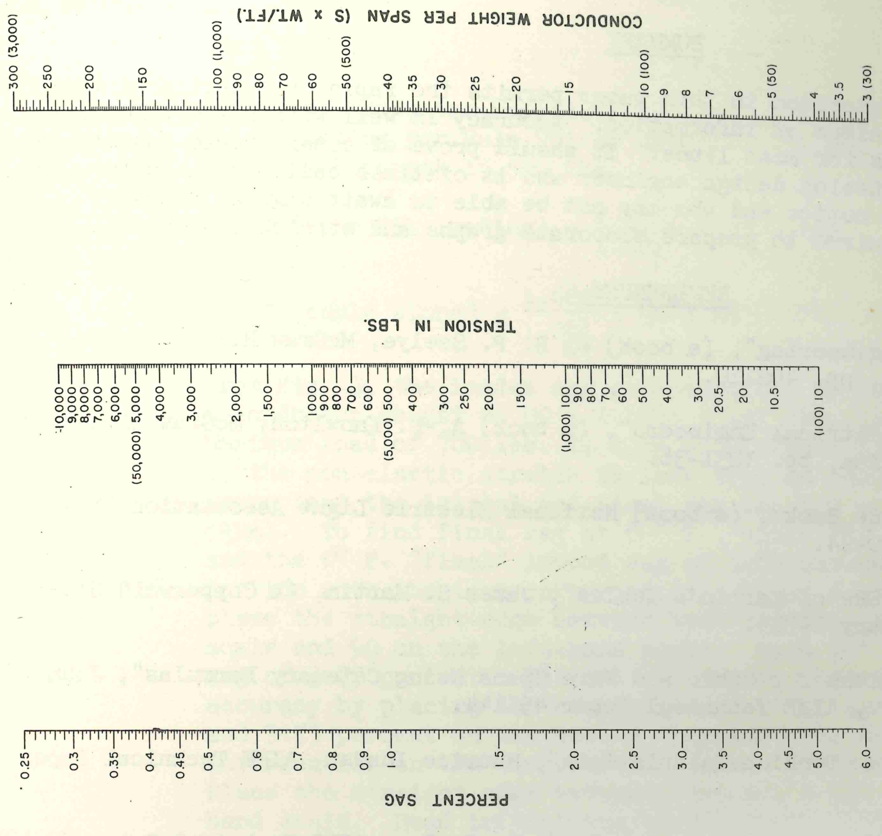

Fig. 3. Sag-Tension Chart

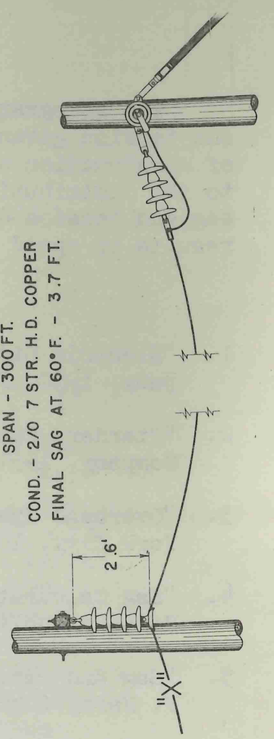

Fig. 4. Line Configuration for Broken Conductor Problem.

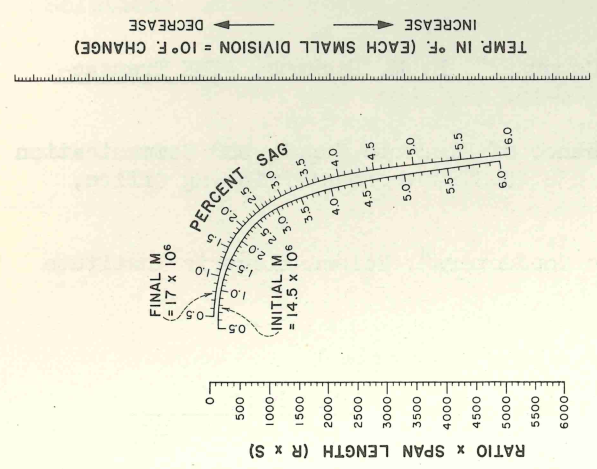

Fig. 1. Sag Calculating Chart.

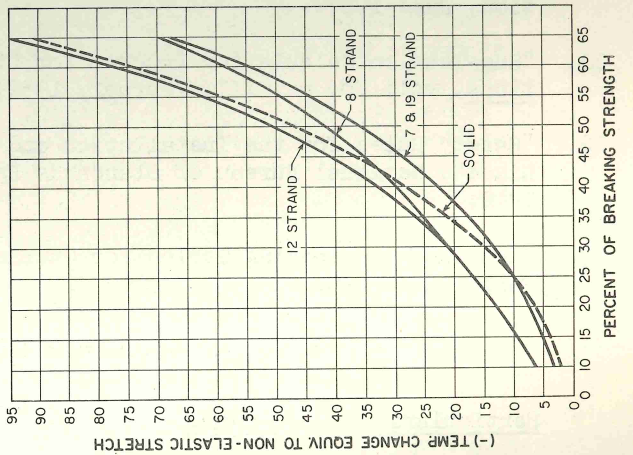

Fig. 2. Non-elastic Stretch Chart.

Conference Paper

SAG AND TENSION CALCULATIONS BY THE NOMOGRAPHIC METHOD

Robert H. Sarikas
Member AIEE
Illinois Power Company
Decatur, Ill.

A paper recommended by the AIEE Transmission and Distribution Committee for presentation at the AIEE Winter General Meeting, New York, N. Y., January 28-February 2, 1962. Manuscript submitted October 30, 1961; made available for printing December 20, 1961.

Price: $ .50 To Members
$1.00 To Nonmembers

(5¢ per copy additional if
first class mailing desired)

All Rights Reserved by the
American Institute of Electrical Engineers
345 East 47th Street, New York 17, N. Y.
Litho in U.S.A.

Paper No. **CP 62-107**

SAG AND TENSION CALCULATIONS BY THE NOMOGRAPHIC METHOD

Robert H. Sarikas

Summary. **All present techniques of sag calculation make use of the assumption that the shape assumed by a conductor supported at two points can be represented by either a parabolic or a catenary function. Application of either technique, analytically, requires the solution of two simultaneous equations if the effect of temperature change is to be taken into account. The charts provided in the paper permit these calculations to be made with a minimum of effort. Accuracy is well within the tolerance of most construction specifications.**

The method of sag-tension calculation described in this paper was developed by the author some twelve years ago when engaged in an assignment calling for numerous such computations. Its publication is prompted by the recent interest displayed by several fellow engineers working in the field of transmission and distribution line design.

All present techniques of sag calculation make use of the assumption that the shape assumed by a conductor supported at two points can be represented by either a parabolic or a catenary function. Application of either technique, analytically, requires the solution of two simultaneous equations if the effect of temperature change or stretch of the conductor is to be taken into account. Various methods of simplifying the calculation have been proposed. The Thomas Chart described in a number of references makes use of a stretch curve and a length curve diagram.[1,2,3] Points on the stretch curve are computed and it is plotted and projected to the length curve. The intersection of the two curves is the solution of the simultaneous condition. This method requires a number of large charts and laborious calculations to secure reasonable accuracy. A tabulation of catenary functions called Martin's Tables provides an extremely accurate means of computation.[4] The nomograph used in this paper was developed using such tables. Other methods using the parabolic and the catenary solution have been proposed.[5,6,7]

The calculation method, making use of nomographs or alignment charts, was first applied by Mr. D. E. Stewart in an article published more than thirty years ago.[8] The original paper did not furnish a method of determining both initial and final sag, following loaded conditions. Nor did it permit the calculation of tension if sag and conductor weight is known. The "equivalent temperature change" method of taking into account the non-elastic stretch of the conductor also represents an innovation by the author. Non-elastic stretch is the permanent set that occurs when conductors are loaded near their elastic limit. It is this permanent set that produces a final sag after heavy loading that is greater than the sag due to initial loading.

While the charts provided in this paper are only suitable for calculating sag and tension for hard-drawn copper conductors, the technique is applicable to any mono-metallic conductor such as aluminum, or composite conductor such as copperweld. The construction of similar charts for all aluminum conductor would be relatively easy. The only change required would be due to the difference in modulus of elasticity. Use of this method for calculating ACSR sags is feasible, however, it is complicated by the conditions that might arise wherein the core steel may have to carry the entire load. In such an instance there is a sudden change in the modulus of the conductor. A complete description of that phenomenon is contained in recent literature.[9] If the condition of a constant modulus is assumed, ACSR sag calculations by the nomographic method are made in the same manner as shown for copper conductors. The author has used this method for ACSR sag calculation and obtained satisfactory results. The difficulty of taking into account the change in modulus of ACSR conductor is common to almost all techniques except the ACSR Graphic method developed by Mr. Theodore Varney.[10] A recent technical paper describes the application of the digital computer to this problem.[11]

The method described in this paper is primarily for use in calculating sags and tensions in urban and rural distribution and subtransmission systems. It is also useful in checking the results of transmission line sag and tension calculations made by the usual methods. Fig. 1 shows the nomographic chart used in calculating sags. The left-hand scale is the product of R x S described below. Two center scales are provided. One is for final sag and is based on a modulus of elasticity of 17×10^6, the other center scale is for computing initial sag and is based on a modulus of 14.5×10^6. The right-hand scale is a temperature scale. Each division corresponds to a 10 degree Fahrenheit change in temperature.

Nomenclature

D = Sag in feet (supports at the same elevation)
p = Sag in percent of span length (supports at the same elevation)
S = Span length in feet
T = Temperature in degrees Fahrenheit
R = Ratio of resultant load on conductor to the weight of the unloaded conductor

Fig. 2 shows the negative temperature change, equivalent to the non-elastic stretch of various strandings of hard-drawn copper conductors for a range of maximum conductor tensions in percent of ultimate strength.

Fig. 3 is used to determine any one of the three quantities shown on the scales if two of them are known. These scales are based upon the use of catenary functions.

Use of the nomographs is explained by the solution of a number of typical problems which are encountered frequently in the design of transmission and distribution lines.

Example No. 1 - Determine Sag and Tension if Loaded Conditions are Known

Given: A subtransmission line is to be constructed with 4/0 7-strand hard-drawn bare copper cable. This line will have a 400 foot ruling span, and is to be built in a heavy loading district area as defined in Rule 251 of the National Electric Safety Code (NESC).[12] This rule specifies 1/2 inch of ice, at 0° F., with 4 lbs. of wind per square foot plus a constant of 0.29. Determine initial and final sags and tension at 30, 60, and 120 degrees Fahrenheit, also sag under heavy loading conditions. Maximum tension is to be limited to 50 percent of breaking strength.

Solution: Referring to published conductor loading tables it is found that the loading of 4/0 7 strand copper cable is as follows:[13]

Vertical (weight of conductor unloaded)	0.6533 lbs. per ft.
Heavy Loading per Rule 251 of NESC	1.6752 lbs. per ft.

Also, Breaking Strength is 9,154 lbs.

The factor R x S is calculated for the two loading conditions:

$$R \times S \text{ (Rule 251 loading)} = \frac{1.6752}{0.6533} \times 400 = 1{,}026$$

$$R \times S \text{ (cable alone)} = \frac{0.6533}{0.6533} \times 400 = 400$$

Loaded weight of the cable is 1.6752 lbs. per ft. x 400 ft. span = 670 lbs. Tension = 9,154 x 0.50 = 4,577 lbs.

The sag in percent of span under heavy loading is next calculated using Fig. 3. To obtain p (Rule 251) lay a straight-edge on the value of 4,577 lbs. on the center scale and 670 lbs. on the right-hand scale. Read 1.82 percent on the left-hand scale.

Percent final sag at 30, 60, and 120° F. are computed as follows:

Using Fig. 1, place a straight-edge at 1,026, R x S for Rule 251 loading, on the left-hand scale, and on 1.82 percent sag on the $M = 17 \times 10^6$ modulus curve in the center. Note the intersection of the temperature scale. Next move down three divisions on the right-hand (temperature) scale, corresponding to a 30° F. change and lay the straight-edge between that point and 400 on the left-hand scale, corresponding to R x S for unloaded conductor. Read the sag on the $M = 17 \times 10^6$ scale of 1.30 percent. This is the percent final sag at 30° F. To obtain final sag in percent at 60° F., count down three more divisions, a total of 60° F. from the starting conditions, on the temperature scale. Place the straight-edge between that point and 400 on the left-hand scale and read 1.50 percent sag on the $M = 17 \times 16^6$ scale in the center. Continue in the same manner in order to obtain the 120° F. sag of 1.90 percent.

To obtain percent initial sag place a straight-edge on the left-hand scale at the R x S without ice or wind and at a point on the center initial percent sag curve corresponding to any of the final unloaded conditions, say 30° F. with no ice or wind. Accuracy is improved if a low temperature condition such as 0° F. is used. Note the intersection on the temperature scale. Count up 36 degrees on the temperature scale to take into account the non-elastic stretch of the conductor. The value of 37 degrees was obtained from Fig. 2 for the conditions of 50 percent ultimate strength and 7 strand conductor. Next, place the straight-edge between the point on the temperature thus determined and R x S of 400 on the left-hand scale and read 1.11 percent sag on the $M = 14.5 \times 10^6$ center scale. This is percent initial sag at 30° F.

Determine initial sag at the other temperatures in the same manner as described for final sag, taking care to use the curve for initial modulus of 14.5×10^6. Sag in feet is calculated by multiplying percent sag by the span length which is given as 400 feet. Results are tabulated in Table 1.

Initial and final tension is obtained by the use of Fig. 3. Since the weight of conductor and percent sag is known, the tension can be read by merely placing a straight-edge between the known quantities on the left and right-hand scales and reading the unknown tension at the intersection with the center scale.

An inspection of this tabulation shows that the NESC limitations of 35% initial and 25% final tension at 60° F. have not been exceeded. In event these limitations are exceeded it will be necessary to proceed on the basis of a given initial or final tension as explained in a subsequent portion of this paper.

Example No. 2 - Determine Sag and Tension if Initial Unloaded Conditions are Known

Given: A 250 foot span of No. 2 HD solid, triple-braid, weatherproof covered, copper conductor secondary has been installed with an initial sag of 3.2 feet at 90 degrees Fahrenheit. Determine the heavy loading district Rule 251 sag and the final sag at 60 degrees.

This is perhaps the most difficult type of problem using either the nomograph or Martin's tables. It can be solved by a trial and error method in which various assumptions of loaded tension are investigated until a value is found which will provide the amount of non-elastic stretch needed to give an initial sag in agreement with the stated conditions of the problem and loaded sag corresponding to the assumed loaded tension.

Solution: From loading tables:

Weight of Conductor Unloaded	0.260 lbs. per ft.
Heavy Loading per Rule 251 of NESC	1.306 lbs. per ft.
Breaking Strength 2,850 lbs.	

$$R \times S \text{ (Rule 251 loading)} = \frac{1.306}{0.260} \times 250 = 1{,}256$$

$$R \times S \text{ (cable alone)} = \frac{0.260}{0.260} \times 250 = 250$$

$$\text{Percent initial sag at } 90^\circ \text{ F.} = \frac{3.2}{250} \times 100 = 1.28\%$$

Using Fig. 1, determine the initial sag at 0° F. by placing the straight edge at R x S = 250 on the left-hand scale and at 1.28% sag on the "initial" center scale. Note the intersection with the right-hand (temperature) scale. Count up 90 degrees corresponding to the temperature change from 90° F. to 0° F. Place a straight-edge between that point on the right-hand scale and 250 on the left-hand scale. Read 0.55% sag on the center "initial" scale. As a first trial, assume that the loaded tension is 1,500 lbs. or 52.5% of breaking strength. Set the straight-edge at 250 on the left-hand scale and 0.55% on the center "final" scale. Note the intersection on the right-hand (temperature) scale. Count down 49 degrees corresponding to the non-elastic stretch from Fig. 2 for solid copper conductors loaded to 52.5% of ultimate tension. Next, place the straight-edge on that point on the temperature scale and R x S = 1,256 on the left-hand scale. Read "final" loaded sag of 1.95%. From Fig. 3, the tension corresponding to 1.95% sag and 327 lbs. weight is found to be 2,100 lbs. which is greater than the assumed tension of 1,500 lbs. Successive trials are made in the same manner until the calculated and assumed loaded tension is in agreement. In the problem at hand this is found to be 1,850 lbs. Loaded sag is 2.2% or 5.5 ft. in a 250 ft. span. Once final loaded sag at 0° F. has been determined, it is only necessary to count down 60° F. on the right-hand scale. Set the straight-edge at 250 on the left-hand scale and read 1.6% final sag at 60° F. This corresponds to 4.0 ft. of sag.

Example No. 3 - Determine Sag and Tension if Loaded Tension is Known

Given: It is desired to limit the dead-end Rule 251 tension of a 90 foot span of 350 MCM, 19 strand, hard-drawn, bare copper cable, to 700 lbs. in order to stay within the strength limitation of an existing substation structure. What is the proper stringing tension (initial) at 80 degrees Fahrenheit? What will the final sag be at 60 degrees Fahrenheit?

Solution:

Weight of Conductor Unloaded	2.1887 lbs. per ft.
Heavy Loading per Rule 251 of NESC	1.081 lbs. per ft.
Breaking Strength 15,590 lbs.	

$$\text{R x S (Rule 251 loading)} = \frac{2.1887}{1.081} \times 90 = 182$$

$$\text{R x S (cable alone)} = \frac{1.081}{1.081} \times 90 = 90$$

From Fig. 3, the loaded sag corresponding to 700 lbs. tension and a conductor weight of 90 x 2.1887 = 197 lbs. is 3.60 percent. Maximum load of 700 lbs. is 4.5% of ultimate strength. From Fig. 2, the non-elastic stretch is less than an equivalent 2° F. This means that the initial and final sag is, for all practical purposes, equal. To find final sag at 60° F., enter Fig. 1 with R x S = 182 and the 0° F. "final" loaded sag of 3.60 percent. Note the intersection with the temperature scale. Count down 60 degrees and place the straight-edge between that point on the temperature scale and 90 on the left-hand scale. Read 60° F. final percent sag of 3.75 percent. Initial sag may be determined with sufficient accuracy by placing the straight-edge at 90 on the left-hand scale and 3.75 percent on the center "initial" sag scale. Note, the intersection on the temperature scale. Count down 20 degrees. Place the straight edge between that point and 90 on the left-hand scale. Read initial sag at 80° F. of 3.85 percent.

Example No. 4 - Broken Conductor Problem

Given: A conductor arrangement as shown in Fig. 4. What will the sag become if the conductor were to break at Point "X"? This information is needed to comply with Rule 233B3 of the National Electric Safety Code.

Solution: Broken conductor problems are readily solved by converting the increase in span length due to insulator swing, to an equivalent temperature increase. In the given figure, an analysis of the geometry shows that the conductor length between supports would be increased in length by an amount very nearly equal to length of the insulator string less the increase in distance between the points of support which in this instance is negligible, or 2.6 ft. For a span length of 300 ft. this corresponds to a change in length of 0.00867 ft. per foot of span. A temperature change of one degree Fahrenheit will cause a change in length of 0.0000094 ft. per foot of span. The change in length due to the broken conductor is, therefore, equivalent to a temperature change of $\frac{0.00867}{0.0000094} = 922$ degrees.

$$\text{Percent sag at } 60^\circ \text{ F.} = \frac{3.7 \times 100}{300} = 1.23\%$$

Entering Fig. 1 with R x S = 300 and final percent sag of 1.23%, note the intersection with the temperature scale. Count down 922 degrees. Place the straight-edge between that point and 300 on the left-hand scale. Read broken conductor sag of 5.62 percent on the "final" scale. This corresponds to 16.9 ft. of sag. The above solution neglects deflection of the unguyed pole.

Other problems that can be easily solved using the nomograph are (1) sags which will equalize the tension of dissimilar conductors when dead-ended opposite each other on the same support, thereby eliminating the need for a down-guy, (2) sag and tension of conductors dead-ended on unguyed poles or structures whose deflection is calculable.

SUMMARY

The nomographic method described in this paper permits the rapid calculation of sags and tension given only the minimum of information. Accuracy is well within the tolerance of construction specifications for most lines. It should prove of considerable assistance to the distribution or transmission design engineer who is ofttimes called upon to furnish sag and tension data on short notice and who may not be able to await digital computer results or spend the time required to prepare elaborate graphs and stretch curves.

REFERENCES

1. "Electric Distribution Engineering", (a book) by H. P. Seelye, McGraw Hill Book Company, 1930, First Edition, pp. 402-10.
2. "Standard Handbook for Electrical Engineers", (a book) A. E. Knowlton, McGraw Hill Book Company, 1957, Ninth Edition, pp. 1231-36.
3. "Overhead Systems Reference Book", (a book) National Electric Light Association, New York City, 1927, pages 320-24.
4. "Sag Calculations by the Use of Martin's Tables", James S. Martin, (A Copperweld Steel Company Publication, January 1931).
5. "Sag and Tension Calculations for Cable and Wire Spans Using Catenary Formulas", John F. Nash, John F. Nash, Jr., AIEE Technical Paper 45-144.
6. "Incremental Method for Sag-Tension Calculations", Maurice Landau, AIEE Technical Paper 51-294.
7. "A Direct Method for Sag-Tension Calculations", T. P. Harley, AIEE Technical Paper 53-182.
8. "Sag Problems Readily Solved by Aid of Alignment Chart", D. C. Stewart, Electrical World, September 20, 1930.
9. "A Simplified Sag-Tension Method for ACSR", C. A. Jordan, AIEE Transactions, vol. 71, pt. III, December 1952, pp. 1108-17.
10. "ACSR Graphic Method for Sag-Tension Calculations", Theodore Varney, (An Alcoa Publication, June 1927).
11. "Sag-Tension Calculation Program for Digital Computer", B. M. Pickens, AIEE Transactions, vol. 78, pt. III, February 1959, pp. 1308-15.
12. "Safety Rules for the Installation and Maintenance of Electric Supply and Communication Lines", National Bureau of Standards Handbook H32, U.S. Government Printing Office, 1942.
13. "Ice and Wind Loading Tables for Overhead Line Conductors", Edison Electric Institute Publication J-5.

Table 1. Calculated Sag and Tension for Example 1

Particulars	Loading	Temperature - Degrees Fahrenheit			
		0	30	60	120
Loaded Sag	Rule 251	7.3 ft.			
Initial Sag	Cable Alone		4.4 ft.	5.2 ft.	6.8 ft.
Final Sag	Cable Alone		5.2 ft.	6.0 ft.	7.6 ft.
Tension	Rule 251	4,577 lbs.			
Initial Tension	Cable Alone		2,930 lbs.	2,500 lbs.	1,910 lbs.
Final Tension	Cable Alone		2,500 lbs.	2,160 lbs.	1,710 lbs.

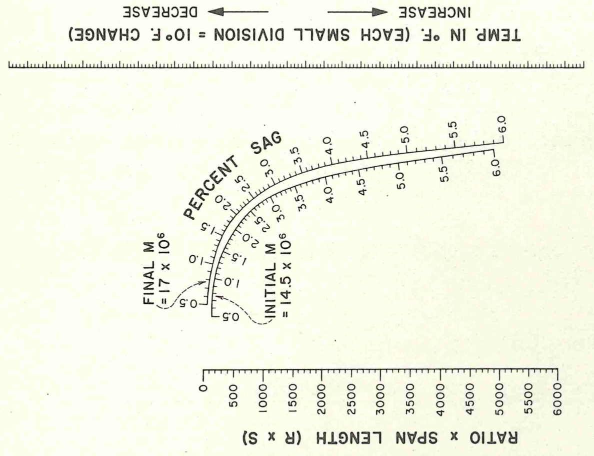

Fig. 1. Sag Calculating Chart.

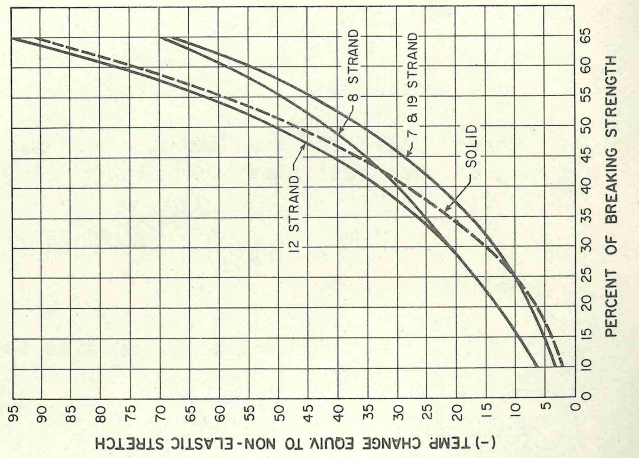

Fig. 2. Non-elastic Stretch Chart.

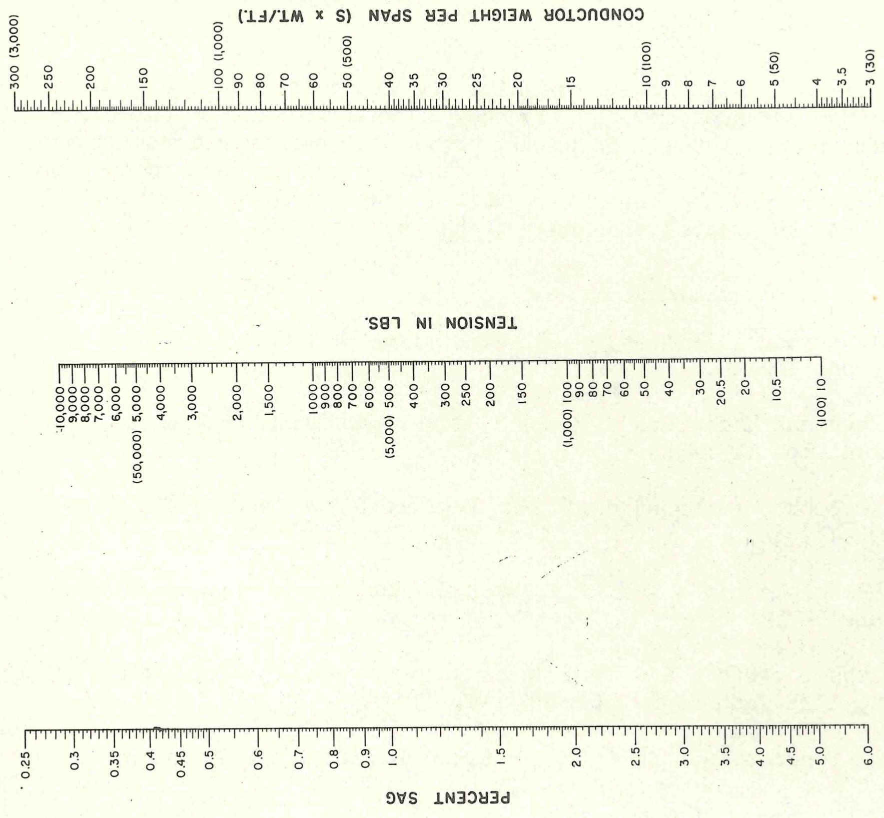

Fig. 3. Sag-Tension Chart

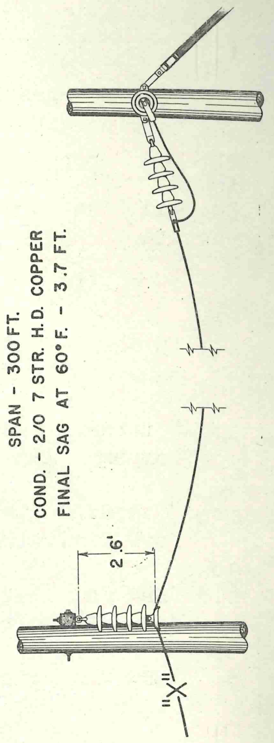

Fig. 4. Line Configuration for Broken Conductor Problem.

Conference Paper

SAG AND TENSION CALCULATIONS BY THE NOMOGRAPHIC METHOD

Robert H. Sarikas
Member AIEE
Illinois Power Company
Decatur, Ill.

A paper recommended by the AIEE Transmission and Distribution Committee for presentation at the AIEE Winter General Meeting, New York, N. Y., January 28-February 2, 1962. Manuscript submitted October 30, 1961; made available for printing December 20, 1961.

Price: $ .50 To Members
$1.00 To Nonmembers

(5¢ per copy additional if
first class mailing desired)

All Rights Reserved by the
American Institute of Electrical Engineers
345 East 47th Street, New York 17, N. Y.
Litho in U.S.A.

Paper No. **CP**
62-107

Fig. 1. Sag Calculating Chart.

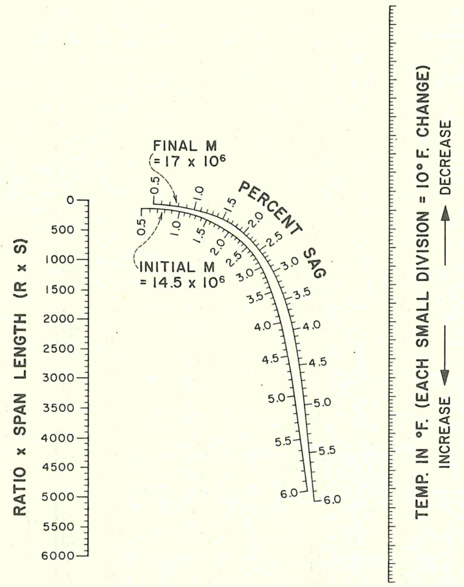

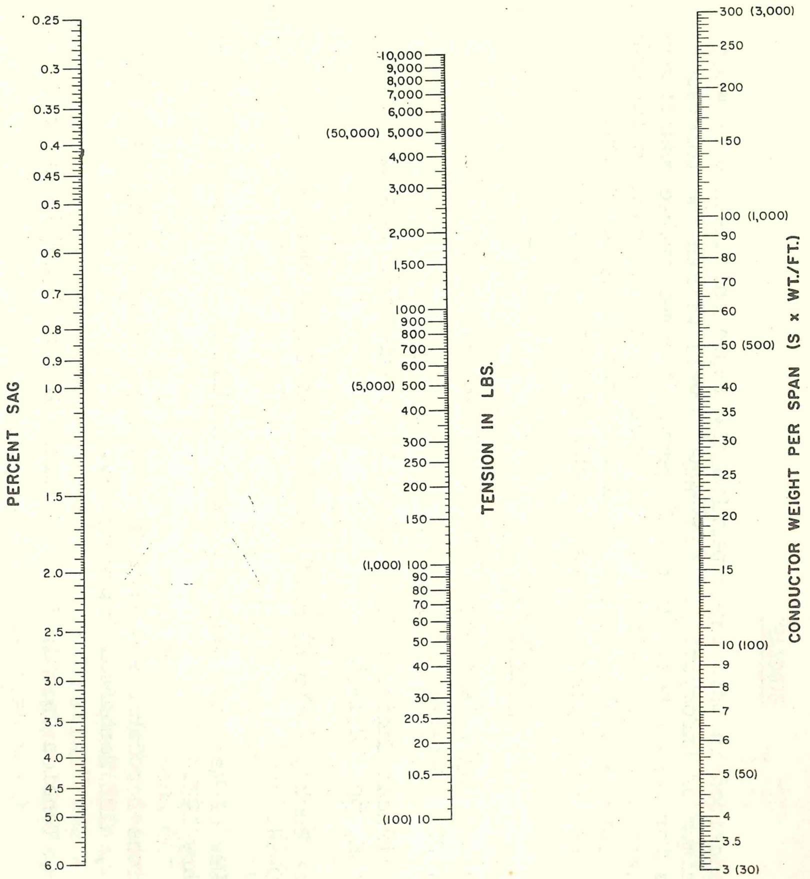

Fig. 3. Sag-Tension Chart

Fig. 2. Non-elastic Stretch Chart.

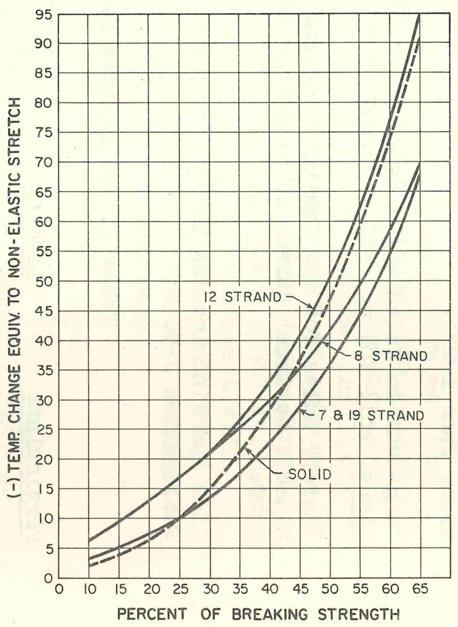

Fig. 4. Line Configuration for Broken Conductor Problem.

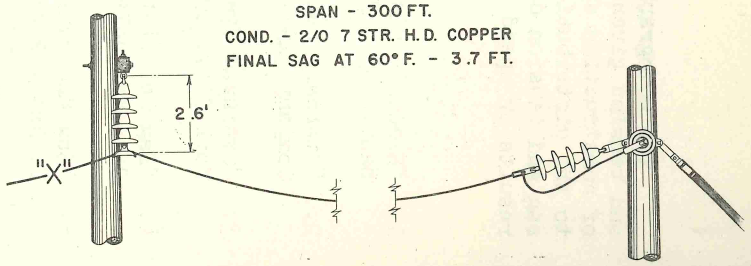
SPAN - 300 FT.
COND. - 2/0 7 STR. H.D. COPPER
FINAL SAG AT 60° F. - 3.7 FT.

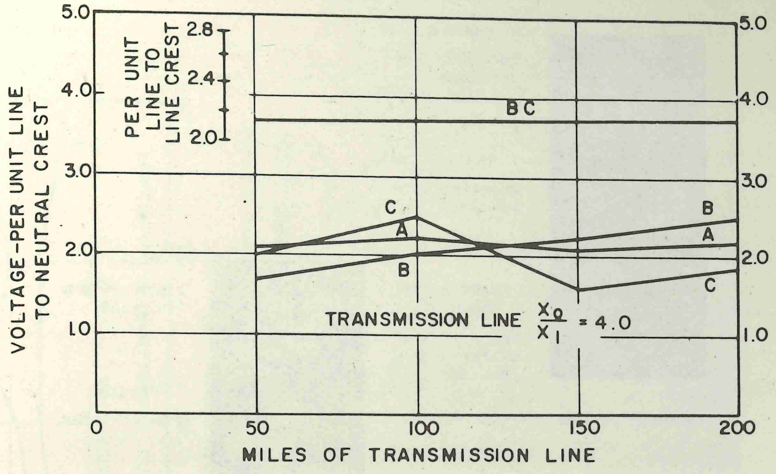

Fig. 7. Phase-to-neutral voltages giving maximum phase-to-phase voltage on open-ended line.

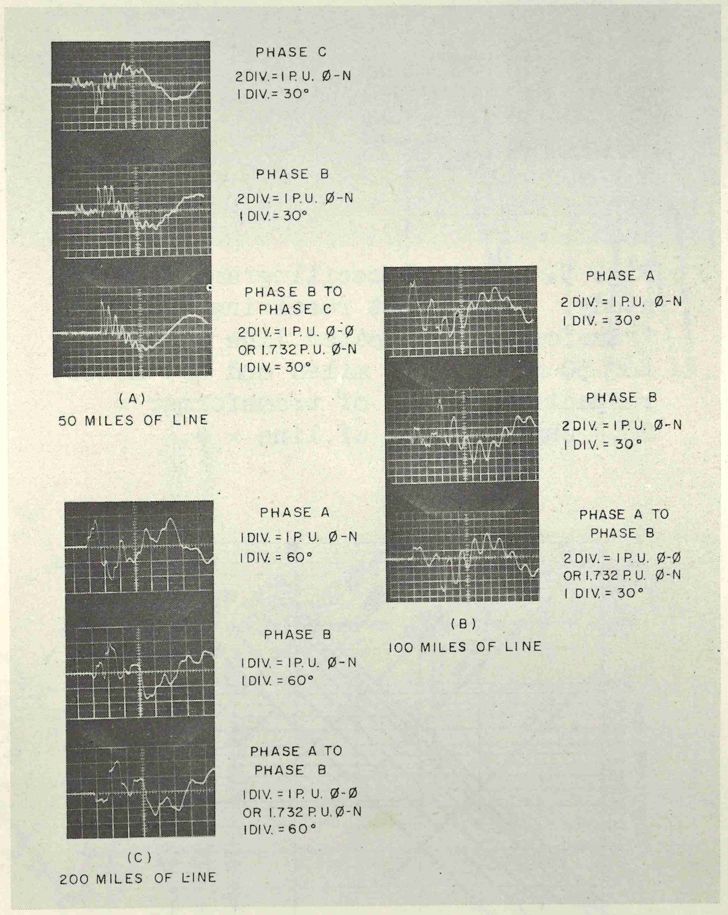

Fig. 8. Typical oscillograms from TNA study. Voltage at receiving end of open-ended line is shown for 50 miles, 100 miles and 200 miles, respectively. X_0/X_1 of line = 4.

Transactions Paper

(Reviewed and Accepted for Publication)

PHASE-TO-PHASE SWITCHING SURGES ON LINE ENERGIZATION

I. B. Johnson
Fellow AIEE
General Electric Company
Schenectady, N.Y.

R. F. Silva
Associate Member AIEE
University of Connecticut
Storrs, Conn.

D. D. Wilson
Associate Member AIEE
General Electric Company
Schenectady, N.Y.

R. F. Silva was formerly with the General Electric Company.

A paper recommended by the AIEE Transmission and Distribution Committee and approved by the AIEE Technical Operations Department for presentation at the AIEE Winter General Meeting, New York, N.Y., January 28-February 2, 1962. Manuscript submitted October 30, 1961; made available for printing December 7, 1961.

Price: $ .50 To Members
$1.00 To Nonmembers

(5¢ per copy additional if first class mailing desired)

All Rights Reserved by the
American Institute of Electrical Engineers
345 East 47th Street, New York 17, N. Y.
Litho in U.S.A.

Paper No.
62-108

Discussion in Duplicate Due February 16, 1962.

PHASE-TO-PHASE SWITCHING SURGES ON LINE ENERGIZATION

I. B. Johnson R. F. Silva D. D. Wilson

SUMMARY. Data from an investigation on a system in miniature are given on the magnitude and wave shape of phase-to-phase switching surges produced upon energization of a transformer terminated line. Included are the effects of line length, terminating impedances and switching conditions. This information is needed for the evaluation of phase-to-phase clearances and insulation, and there appears to be little, if any, information published on the matter.

INTRODUCTION

In the process of refining the protection of apparatus and systems against lightning – of operating with closer tolerances, improved arrester protection and lowered insulation strength – the adequacy of system insulation for switching surges has become of paramount importance.[1] As a consequence, some fundamental questions have been raised by the industry, and among these is the following:

1. What are representative phase-to-ground and phase-to-phase switching surges in wave shape, duration, and magnitude?

Recently a comprehensive report covering phase-to-ground switching surges was prepared by a Working Group of the AIEE Transmission and Distribution Committee. On the subject of phase-to-phase switching surges, however, there is little if any published information necessary for the evaluation of phase-to-phase clearances and insulation requirements. It is the purpose of this paper to contribute data on this subject from investigations on systems in miniature.

Specifically, magnitudes of phase-to-phase switching surges on energizing an unprotected transformer terminated line are reported in the paper for the various line lengths, terminating impedances, and switching conditions. Phase-to-neutral magnitudes corresponding to maximum phase-to-phase magnitudes are recorded as well as maximum phase-to-phase values as a function of line length.

TRANSIENT NETWORK ANALYZER CIRCUIT

Previous studies on miniature systems have presented data on the maximum possible transient voltages to ground that occur at the receiving end high voltage transformer terminals when the line is energized on the high voltage side at the sending end of the line. The exact points of closing among the poles of the circuit breaker were adjusted so as to obtain maximum line-to-ground voltage.[1,2,3] It was observed in these studies that maximum phase-to-phase voltages did not occur when maximum phase-to-ground voltages were obtained.

For the purpose of obtaining data on the maximum possible phase-to-phase switching surges, the system shown in Fig. 1(A) was set up on the Transient Network Analyzer.[4]

The three-phase model circuit is shown in Fig. 1(B). A de-energized line with a transformer connected at the receiving end was energized from an infinite source. Switching was performed with rotating drum switches designed to operate in synchronism with the supply voltage. The contacts of each drum can be adjusted independently to close at any angle on the system voltage in each phase.

The three-phase model line representation consisted of 10 mile sections, each section having the following constants with subscripts 1 and 0 indicating positive and zero sequence parameters respectively:

$L_1 = 0.02$ henry $\quad C_1 = 0.16$ microfarad

$R_1 = 1.0$ ohm $\quad C_0 = 0.10$ microfarad

$X_0/X_1 = 4.0 \quad R_0/X_1 = 0.53$

Tandem connection of several of these lumped-parameter sections approximates distributed constant typical transmission line behavior over the range of frequencies normally encountered in switching transients.

The receiving end transformer was connected in grounded wye to the line and represented in miniature by a three-phase core-type model transformer designed to have a saturation characteristic on its own volt-ampere rating comparable to that of a power transformer of modern design. The model also had a winding which was delta-connected. Since the zero sequence impedance of a transformer can vary considerably, a wide range of neutral reactance (L_N) was used to cover values which could be encountered in practice.

STUDY RESULTS

Although contacts of a circuit breaker can be adjusted to close mechanically at the same instant, actual energization can occur earlier through an arc, on various angles of the source voltage at random. Energization, therefore, can occur a phase at a time assuming that no poles remain open on a switching closure, the time interval between the energization of the phases is short enough so that only the transient oscillations generated by the closing operation need be investigated.

In determining the maximum phase-to-phase transient voltage at the receiving end of the line between any two phases, the closing contacts on the rotating drum switches were mechanically adjusted on the 60 cycle driving voltage with the limiting condition of not exceeding one half a cycle between the first and last phase to close. The exact points of closing of all three poles within half a cycle were then re-adjusted slightly to maximize this value. As an example, Fig. 2 shows one combination of pole closing angles that give maximum phase-to-phase transient voltage between B and C. Phase A is closed at 90° on the source voltage and phases B and C are closed simultaneously 90° later. At this angle of closing for phases B and C, the source voltage between phases B and C is a maximum. The transient voltage produced on energizing phase A is coupled into phases B and C through the line and the receiving end transformer, if a transformer is present. In all tests there were no initial charges on the line immediately preceding the time of switching and energization of the line. Included in the investigation of the various conditions of transformer termination was the case of no transformer termination.

Transformer Terminated Line

The maximum phase-to-phase transient voltages and the corresponding phase-to-neutral voltages on each of the phases at the receiving end of a transformer terminated line are shown in Fig. 3. The phase-to-phase transient voltages vary from 3.65 to 4.6 per unit of line-to-neutral crest voltage at the sending end as the switched line length increased from 50 to 200 miles. The phase-to-neutral voltages generally were found not to be the maximum obtainable. Limiting the phase-to-neutral transient voltage on any phase to 2.5 per unit resulted in corresponding phase-to-phase transient voltages on the order of 2.4 per unit line-to-line or 4.16 per unit line-to-neutral crest for line lengths of more than 100 miles.

The effect of varying the zero sequence impedance of the line terminating transformer is shown in Fig. 4. The maximum phase-to-phase transient voltages appear to be relatively independent of the zero sequence impedance. For a given length of line, it appears that the zero sequence impedance effect is to increase the voltage on one phase and to decrease the voltage on the other phase with little change in the corresponding maximum phase-to-phase voltage. During the study it was observed that, whether the system voltage was normal with respect to transformer saturation or lower, transformer saturation did not influence the per-unit transient voltages. The sustained voltage subsequent to the transient voltage on energization is usually lower and involves the interaction between the line capacitance and the non-linear magnetizing impedance of the transformer. For the transient voltages, single-phase transformer banks gave the same results as three-phase core-type transformers providing the zero sequence impedance is the same. Typical of the oscillograms taken during this study are those shown in Fig. 5 for energizing a transmission line of varying lengths, terminated in a transformer of X_0 = 26.4 ohms. The predominant frequency of oscillation varied from 855 cps to 235 cps for switched line lengths of 50 miles to 200 miles, respectively. In Fig. 6 a chart is provided for converting the ohmic zero sequence impedance used in the study into transformer capacity and voltage ratings. The range of zero sequence impedances used cover transformer sizes normally encountered in the voltage classes listed.

No Transformer Termination

Energizing a transmission line open-ended at the receiving end resulted in phase-to-phase transient voltages lower than the previous cases involving a transformer terminated line. The results are shown in Fig. 7. Again, corresponding phase-to-neutral voltages giving the maximum phase-to-phase transient voltage are not the maximum obtainable. The maximum phase-to-phase transient voltage is independent of the switched line length. Typical of the oscillograms taken during this study are those shown in Fig. 8 for energizing an open-ended line of varying lengths. In Fig. 8(A) for a 50 mile line, phase A, which is not shown, closed first. Voltage is coupled into phases B and C prior to the angle of closing of these two phases as shown. At the instant of closing to give the maximum phase-to-phase voltage in the bottom picture of the oscillogram shown in Fig. 8(A), the coupled voltage is of opposite polarity to the source voltage in phases B and C. The predominate frequency in the transient is the characteristic frequency of 50 miles of line; that is, approximately 960 cps. The predominate frequency of oscillation for 200 miles of line, shown in Fig. 8(C), is on the order of 250 cps.

CONCLUSIONS

1. Phase-to-phase transient voltages in excess of 2.6 per unit of normal line-to-line crest voltage or 4.5 per unit of normal line-to-neutral crest voltage may be experienced when a line terminated in a transformer is energized.

2. The maximum phase-to-phase transient voltage increases with length of line when terminated in a transformer. It appears to be relatively independent of transformer zero sequence impedance.

3. Phase-to-neutral transient voltages giving maximum phase-to-phase transient voltages are not the maximum obtainable. Limiting the phase-to-neutral transient voltage on any phase to 2.5 per unit resulted in corresponding phase-to-phase transient voltages on the order of 2.4 per unit line-to-line or 4.16 per unit line-to-neutral crest for line lengths of more than 100 miles.

4. The maximum phase-to-phase transient voltage on a transmission line open at the receiving end resulted in lower voltages than those obtained in tests on a transformer terminated line. The magnitude of 2.15 per unit line-to-line crest is independent of line length.

5. Frequencies of oscillation for the transient voltages on energizing a transformer terminated line varied from 855 cps to 235 cps for line lengths from 50 to 200 miles respectively; whereas frequencies for energizing an open-ended line from 50 to 200 miles in length varied from 960 cps to 250 cps respectively.

REFERENCES

1. "Switching Surges — I — Phase-to-Ground Voltages," AIEE Committee Report. AIEE Transactions, pt. III (Power Apparatus and Systems), vol. 80, 1961, pp. 240-261.

2. "Switching Surges on Energizing a Transformer Terminated Line," I. B. Johnson, A. J. Schultz. AIEE Transactions, pt. III (Power Apparatus and Systems), vol. 79, 1960, pp. 241-245.

3. "Switching Surges Due to Energization or Reclosing," I. B. Johnson, R. F. Silva, D. D. Wilson. Proceedings, American Power Conference, Chicago, Illinois, 1961.

4. "Model Techniques in the Transient Network Analyzer Solutions of Power Systems Problems," L. O. Barthold, R. F. Silva. Proceedings, American Power Conference, Chicago, Illinois, 1960.

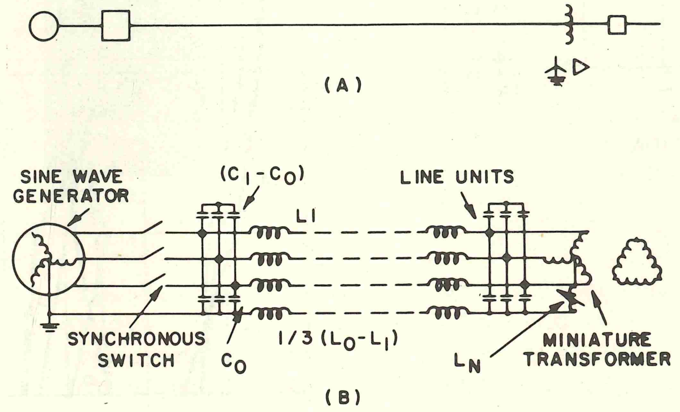

Fig. 1.

(A) System studied.

(B) Transient Network Analyzer equivalent miniature system.

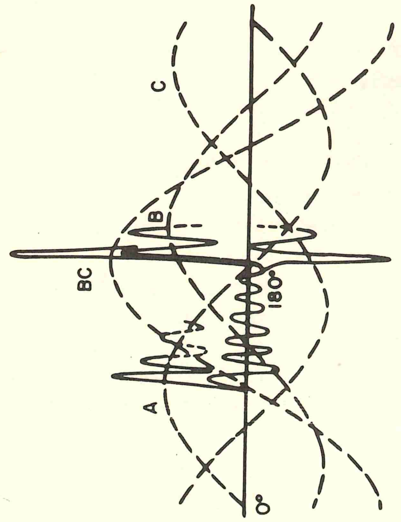

Fig. 2. Typical combination of angles of pole closing giving maximum phase-to-phase voltage on BC.

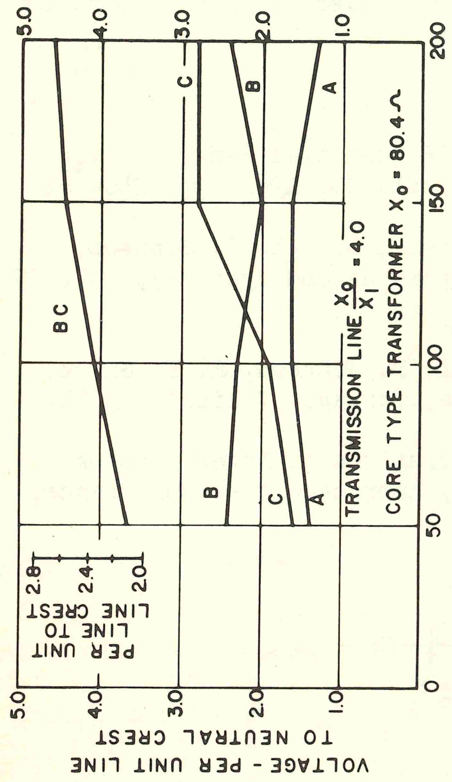

Fig. 3. Maximum phase-to-phase transient voltage at receiving end transformer due to line energization.

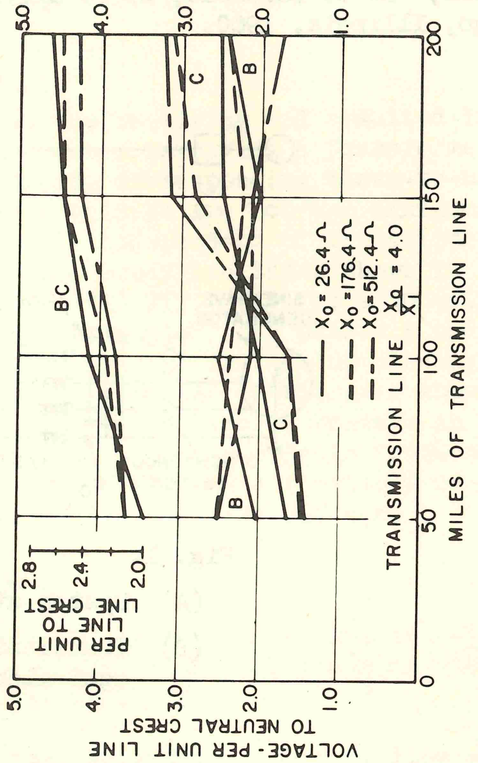

Fig. 4. Effect of transformer zero sequence impedance on transient voltages giving maximum phase-to-phase voltages.

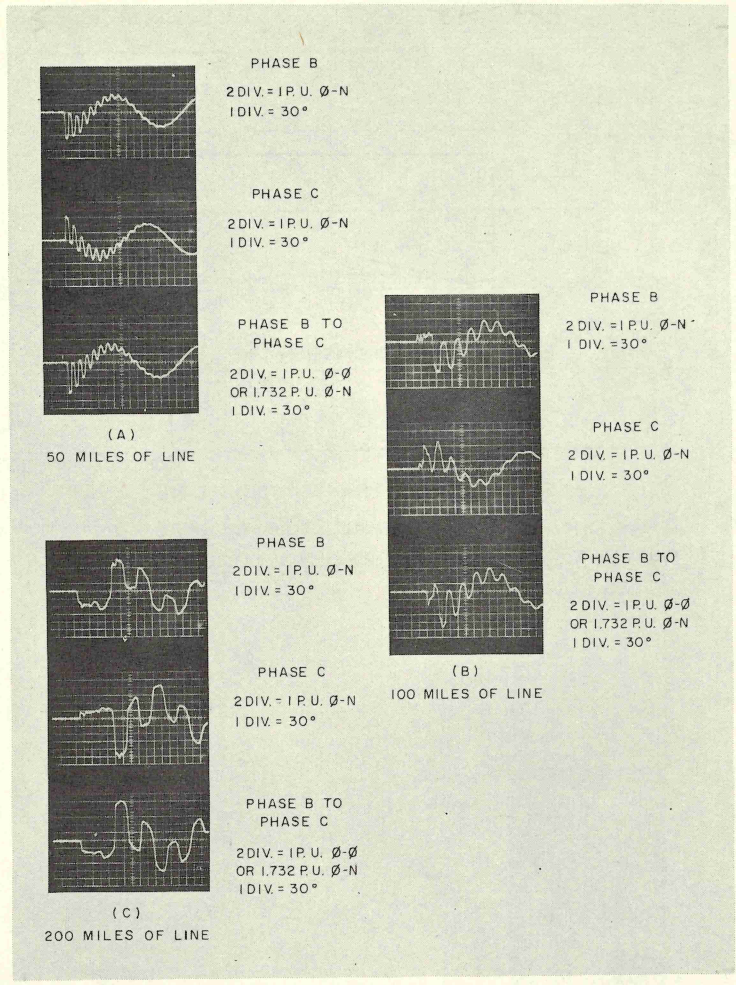

Fig. 5. Typical oscillograms from TNA study. Voltage at receiving end of transformer terminated line is shown for 50 miles, 100 miles and 200 miles, respectively. X_0 of transformer = 26.4 ohms. X_0/X_1 of line = 4.

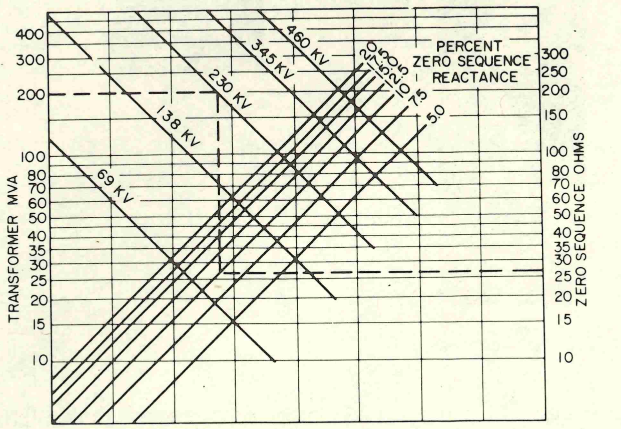

Fig. 6. Zero sequence ohms as function of transformer MVA, voltage rating, and percent zero sequence reactance. Example shown for a 200 MVA, 230 kv transformer having a 10 percent zero sequence reactance.

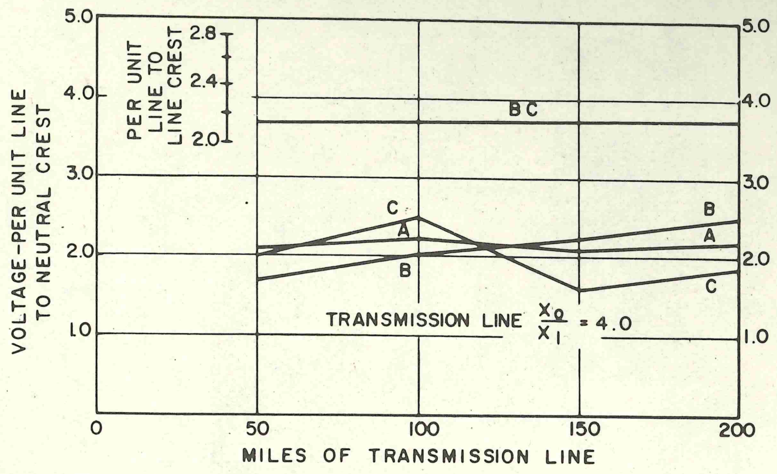

Fig. 7. Phase-to-neutral voltages giving maximum phase-to-phase voltage on open-ended line.

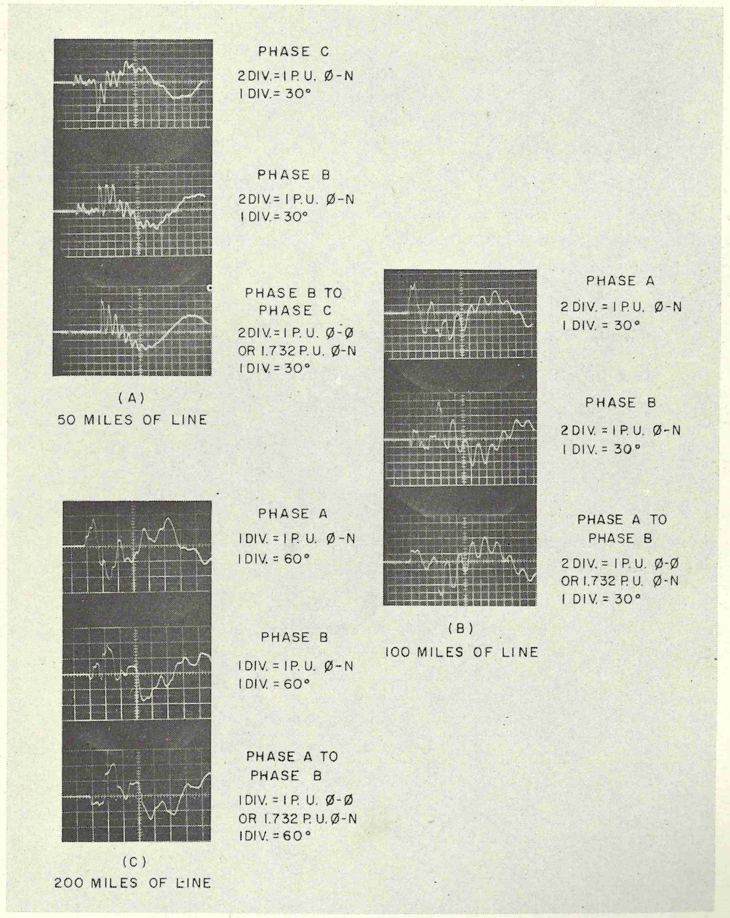

Fig. 8. Typical oscillograms from TNA study. Voltage at receiving end of open-ended line is shown for 50 miles, 100 miles and 200 miles, respectively. X_0/X_1 of line = 4.

Transactions Paper

(Reviewed and Accepted for Publication)

PHASE-TO-PHASE SWITCHING SURGES ON LINE ENERGIZATION

I. B. Johnson
Fellow AIEE
General Electric Company
Schenectady, N.Y.

R. F. Silva
Associate Member AIEE
University of Connecticut
Storrs, Conn.

D. D. Wilson
Associate Member AIEE
General Electric Company
Schenectady, N.Y.

R. F. Silva was formerly with the General Electric Company.

A paper recommended by the AIEE Transmission and Distribution Committee and approved by the AIEE Technical Operations Department for presentation at the AIEE Winter General Meeting, New York, N.Y., January 28-February 2, 1962. Manuscript submitted October 30, 1961; made available for printing December 7, 1961.

Price: $ .50 To Members
$1.00 To Nonmembers

(5¢ per copy additional if first class mailing desired)

All Rights Reserved by the
American Institute of Electrical Engineers
345 East 47th Street, New York 17, N. Y.
Litho in U.S.A.

Paper No.
62-108

Discussion in Duplicate Due February 16, 1962.

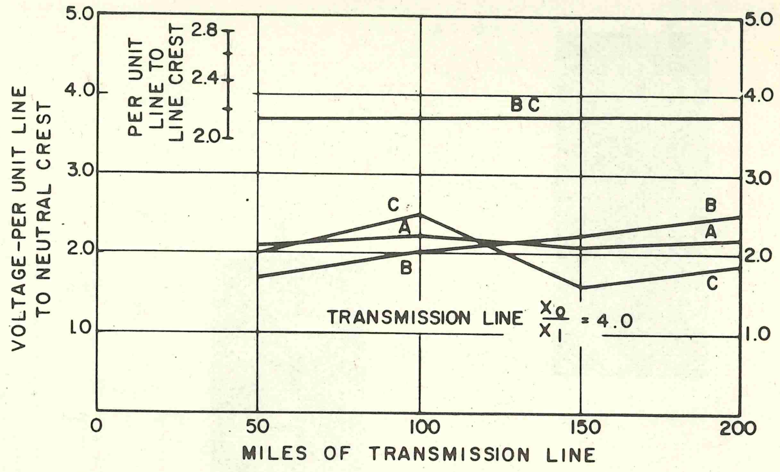

Fig. 7. Phase-to-neutral voltages giving maximum phase-to-phase voltage on open-ended line.

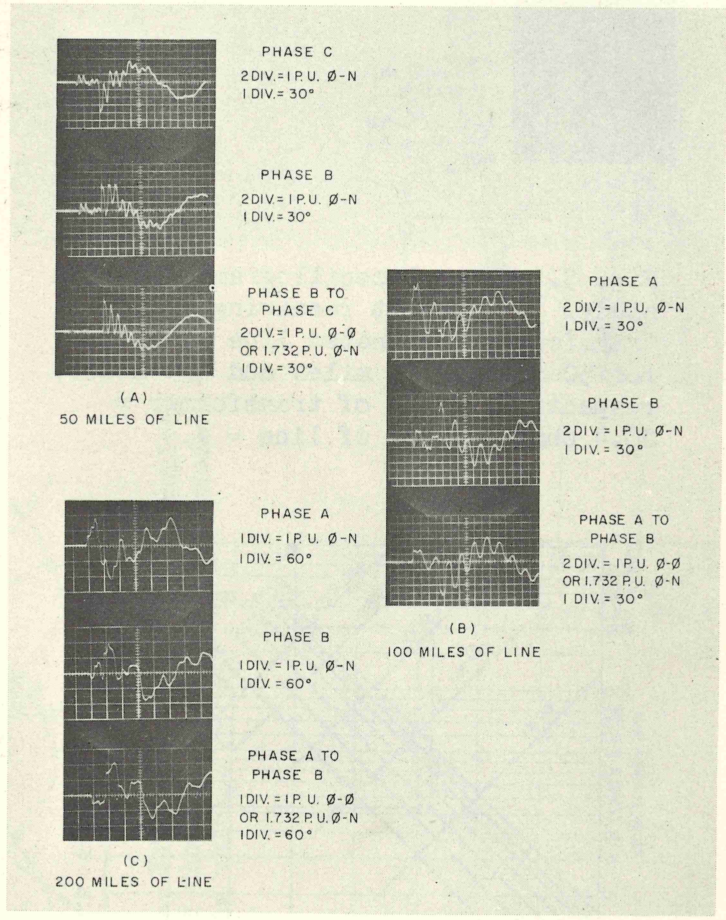

(A) 50 MILES OF LINE

(B) 100 MILES OF LINE

(C) 200 MILES OF LINE

Fig. 8. Typical oscillograms from TNA study. Voltage at receiving end of open-ended line is shown for 50 miles, 100 miles and 200 miles, respectively. X_0/X_1 of line = 4.

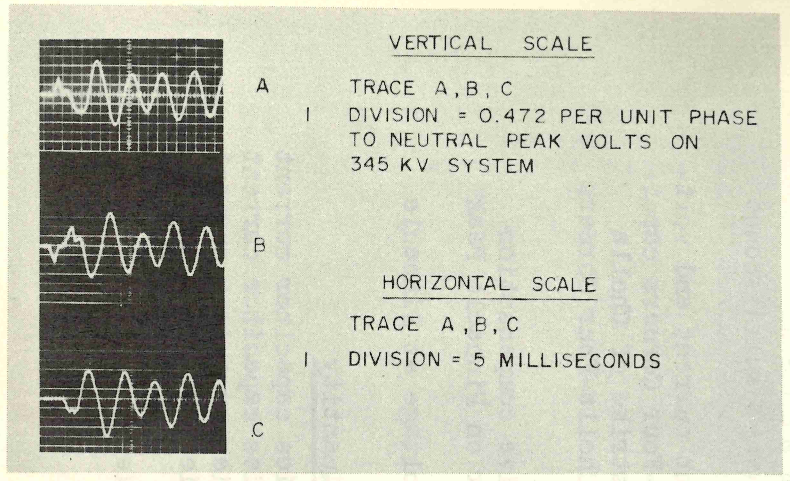

Fig. 10. Recovery voltage across Cholla 345 Kv breaker contacts, (CB5, Fig. 6) following restrike upon de-energization of Cholla-Pinnacle Peak line.

60% Series capacitive compensation
One 35 MVAR reactor on Pinnacle Peak tertiary
Two 65 MVAR reactors on Four Corners 230 Kv bus
1.00 P.U. preswitching voltage at Cholla 345 Kv bus

Trace	Quantity
A	Phase A Voltage across CB5 contacts
B	Phase B Voltage across CB5 contacts
C	Phase C Voltage across CB5 contacts

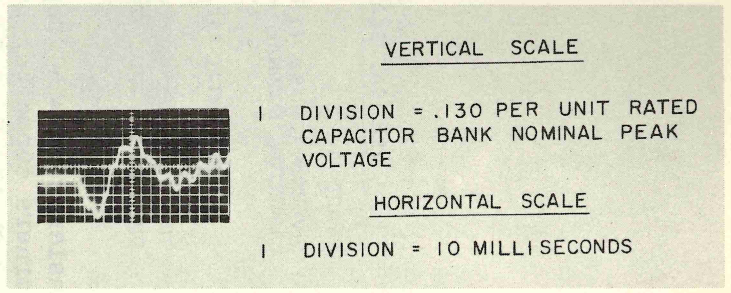

Fig. 11. Transient voltage drop across Cholla-Pinnacle Peak capacitor bank during energization of Cholla to Pinnacle Peak line with Cholla 345 Kv breaker (CB5, Fig. 6).

60% Series capacitive compensation
One 35 MVAR reactor on Pinnacle Peak tertiary
Two 65 MVAR reactors on Four Corners 230 Kv bus
Trace Series capacitor voltage drop

Transactions Paper

(Reviewed and Accepted for Publication)

A
E E
I

SWITCHING SURGE AND DYNAMIC VOLTAGE STUDY OF ARIZONA PUBLIC SERVICE COMPANY 345 KV PROPOSED TRANSMISSION SYSTEM UTILIZING MINIATURE ANALYZER TECHNIQUES

W. H. Croft
Member AIEE
Arizona Pub. Service Co.
Phoenix, Ariz.

R. H. Hartley
Member AIEE
Arizona Pub. Service Co.
Phoenix, Ariz.

R. L. Linden
Associate Member AIEE
General Electric Co.
Schenectady, N. Y.

D. D. Wilson
Associate Member AIEE
General Electric Co.
Schenectady, N. Y.

A paper recommended by the AIEE Transmission and Distribution Committee and approved by the AIEE Technical Operations Department for presentation at the AIEE Winter General Meeting, New York, N. Y., January 28-February 2, 1962. Manuscript submitted October 30, 1961; made available for printing December 8, 1961.

Price: $ .50 To Members
$1.00 To Nonmembers

(5¢ per copy additional if first class mailing desired)

All Rights Reserved by the
American Institute of Electrical Engineers
345 East 47th Street, New York 17, N. Y.
Litho in U.S.A.

Paper No.
62-109

Discussion in Duplicate Due February 16, 1962.

SWITCHING SURGE AND DYNAMIC VOLTAGE STUDY OF ARIZONA PUBLIC SERVICE COMPANY 345 KV PROPOSED TRANSMISSION SYSTEM UTILIZING MINIATURE ANALYZER TECHNIQUES

W.H. Croft R.H. Hartley R.L. Linden D.D. Wilson

SUMMARY. Investigations were conducted of switching surge phenomena on the proposed addition of the 292 mile 345 kv transmission lines to Arizona Public Service Company's system. In order to arrive at balanced design and operating conditions with regard to surge voltages, insulation levels, arrester protection and switching procedures, a study was performed on a system in miniature. Data, results and conclusions from this study are presented.

INTRODUCTION

The results and conclusions pertaining to transient overvoltage investigations, which have been made of the Arizona Public Service Company's 292 mile 345 kv transmission system, are presented because they deal with specific system parameters and conditions for which pertinent and applicable data were not available. The future development of long EHV transmission lines will be aided by publication of investigations of economically and electrically practical transmission systems which have been thoroughly investigated.

The purpose of this paper, therefore, is to document information which will be valuable to others in the planning and design of long EHV transmission lines and systems.

Early in 1959 when the initial design studies of the 345 kv system were started, experience in design and operation of systems of this voltage class was limited. In some instances available experience was not entirely applicable to the Four Corners system due to length of line between major energy sources and the lack of parallel routes of lower transmission voltages.

However, both published and unpublished data indicated the need for very serious consideration of transient overvoltages produced by such conditions as line energizing, delayed opening of one breaker under transferred trip conditions, non-simultaneous opening of phases, load rejection, and the operation of a transformer and line as an integral unit. The need for studies of this type is described in references 1-12.

Investigations of normal and abnormal system conditions were conducted by simulation of these conditions on a transient network analyzer (TNA), and records were made for reference and analysis.

SYSTEM INFORMATION

The first 345 kv transmission system in the Southwest is being constructed by the Arizona Public Service Company for the purpose of energy transmission from its Four Corners coal-fired steam-electric generating plant to Phoenix, Arizona. This system, the geographical location of which is shown in Fig. 1, will run from a point near Farmington, New Mexico, to the Pinnacle Peak Substation near Phoenix, a distance of 292 miles, with the output being fed into a 230 kv system for delivery to Phoenix area stations.

The Four Corners Plant, scheduled for operation in 1963, will initially consist of two 3600 rpm, 175 mw steam turbines with 192 mva, .64 scr, .9 pf, 20 kv liquid-cooled generator units stepping up to 230 kv. Further development to a total of at least 800 mw is planned with the third and four units being 225 mw each.

Selection of 345 kv transmission was based on economic studies which took into account such factors as the magnitude of peak loads, the time scheduling of additional units for plant expansion, ability to operate with one line out of service, ability to

operate at reduced plant capacity, the ability to provide sufficient reserve on the receiving end, and one that could be expanded for additional large blocks of power if desirable.

Line design provides for single circuit steel towers using two 795 ACSR conductors per phase with an equivalent phase spacing of 35 feet and a sub-conductor spacing of 16 inches. Since this line covers a wide range of elevation, 1700 feet to 9200 feet, the number of insulators per string varies from 18 to 20.

Initial construction of the 345 kv lines provides for two transmission lines from Four Corners to Cholla, near Holbrook, Arizona, and one line from Cholla to Pinnacle Peak. This is shown on Fig. 2, which also shows a connection to the company's Cholla-Flagstaff-Prescott 230 kv line and the Cholla 115 mw coal-fired plant scheduled for 1962 operation. When the addition of the third unit at Four Corners brings the capacity to 575 mw, the second line will be added from Cholla to Pinnacle Peak, completing a parallel line system over the entire distance. No additional transmission will be required for the fourth unit addition at Four Corners, which will raise the station capacity to 800 mw.

Series capacitors for line compensation are not required initially, but in the 575 and 800 mw levels 25% and 40% series compensation are used respectively, mainly to reduce the electrical angle between Four Corners and Phoenix for steady state stability. 60% series compensation was also investigated for limiting conditions.

Reactive control of this line is provided by the use of shunt reactors at Four Corners, Cholla and Pinnacle Peak. For the initial condition in Fig. 2, 70 mvar of reactors will be installed on the tertiary of the 345/230 kv autotransformer at Pinnacle Peak and are required for line energizing and transient overvoltage protection. 60 cmva of shunt capacitors are required at Pinnacle Peak for voltage support if the 345 kv line is out of service. A reactor of 25 mvar is required at Cholla, while at Four Corners two 65 mvar reactors are required on the 230 kv bus and 50 mvar on the tertiary of each 230/345 kv transformer.

Fig. 3 shows the proposed system for the 575 and 800 mw levels. Shunt reactor and shunt capacitor requirements compared to the 350 mw level, are expected to change. It is planned that one 65 mvar reactor at Four Corners will be moved to Cholla and the capacitors at Pinnacle Peak increased to 90 cmva. 70 mvar of reactors are used on the tertiary of the second 345/230 kv transformer at Pinnacle Peak.

Switching on the 345 kv system will be accomplished by use of 230 kv air-blast breakers at Pinnacle Peak and Four Corners, (transformers are switched with the line), and by 345 kv air-blast breakers at the Cholla 345 kv bus. High-speed comparison type relaying will be used to open both terminals simultaneously. Duplicate relaying signal facilities will be provided, one over carrier and one over microwave channels.

A preliminary study of transient conditions using miniature analyzer techniques was performed in June 1959, after preliminary system design had been completed. The results of the preliminary study were not published. Investigations of equipment connections and switching operations were made. Switching the transmission lines with transformers and shunt reactors as integral parts of the transmission line produced more favorable results than switching the lines with these units not connected. Increasing the amount of shunt reactive kva which was connected to the transformer tertiary winding reduced the overvoltages which were encountered, while omission of the shunt reactors was found to be inadvisable. Thus, with general information available pertaining to the requirements of the transmission system, it was decided to postpone a detailed examination of transient, dynamic, and steady state overvoltages until the transmission system design parameters had been more accurately determined.

INVESTIGATION OBJECTIVES

The objectives of the detailed transient overvoltage study were to check the complete design of the Four Corners transmission project at the three previously described design levels, that is, the 1963 - 350 megawatt (mw) level, the 575 mw level, and the 800 mw level. From published data[1], the transient conditions to be investigated were determined as follows:

A. Switching surges unmodified by protective devices

  1. Capacitive kilovoltampere (kva) switching

    (a) De-energization of 345 kv lines with 230/345 kv autotransformers magnetizing impedances and reactor combinations as described on Fig. 2 and Fig. 3.

    (b) Energization of lines with autotransformers and reactors as described on Fig. 2 and Fig. 3.

  2. Switching unloaded autotransformer and line as a unit with tertiary reactors (Fig. 2 and Fig. 3).

  3. Sudden loss of load at Pinnacle Peak.

B. Switching surges modified by lightning arresters.

  1. Effect of protective devices in modifying surges from (A) above.

  2. Discharge requirements of arresters upon operation by switching surges.

C. 345 kv Line energizing procedure.

  1. Cold start-up at the Four Corners Plant.

  2. Hot start-up at the Four Corners Plant.

D. Series Capacitor effects.

  1. Internal disturbances

    (a) Energization
    (b) Line dropping
    (c) Load rejection

  2. Dynamic overvoltages

    (a) Interaction of non-linear magnetizing impedance of autotransformers and system capacitance.

Criteria for Studies

1. All circuit breakers to be three cycle, with a maximum of one restrike.
2. Autotransformers (230/345 kv) to be 1175 basic impulse level (BIL) with "80 percent" (288 kv) arresters integrally mounted on the transformer.

3. Transfer tripping in 3 cycles for transformer differential protection.
4. Simultaneous tripping of 345 kv lines for fault clearing.
5. Substation ground resistance to be .5 ohms or less.
6. All poles of the circuit breakers to close within 1/2 cycle.
7. 30 cycle reclosing for transmission line faults.

METHOD OF INVESTIGATION

The described 292 mile transmission system was represented as a miniature three-phase system on the Transient Network Analyzer. By use of the model system all components could be represented including such non-linear devices as transformers and lightning arresters.[13] Internal disturbances caused by switching operations such as energization, de-energization of lines and transformers, circuit breaker restriking, load rejection, and fault conditions could be investigated and the severity of these disturbances recorded. In the cases of dynamic overvoltages, harmonic content of the voltages could be analyzed. Regions of severe voltage distortion and/or ferro non-linear oscillations caused by the interaction of transformer magnetizing impedances and system capacitance could be explored in detail. If conditions were discovered which would be deemed intolerable, corrective measures could be determined, or operating limitations considered which would reduce the severity of such conditions to tolerable levels.

In all cases of breaker closing, all three contacts of the model switch were set to close within one-half cycle on the driving voltage. In this region the contacts were adjusted to produce the maximum possible transient voltage. In instances of breaker opening such as de-energization or load rejection, the contacts of the breaker opened on consecutive current zeros, (i.e., - within 120° on the driving frequency). No other specific circuit breaker characteristics, (i.e., - arc characteristics or shunting resistors), were simulated. While restrike phenomena is not expected on the system it was intentionally initiated to explore associated system transient conditions. The restrikes studied were caused on the phase and angle of the driving voltage which maximized the transient effects.

TRANSIENT NETWORK ANALYZER, (TNA) DESCRIPTION

The 345 kv, two-conductor bundle transmission lines were represented by quasi-distributed 10- mile sections as shown in Fig. 4. Impedance and frequency base changes necessitated by the matching of model transmission line constants to the actual transmission line constants were determined consistent with established modeling techniques.[13] The other model system components incorporated these base changes.

The entire model system utilized a common voltage level (except transformer tertiaries). Therefore the magnetizing impedances of autotransformers were represented by model transformers of modern design and low air core reactance. This allowed all leakage reactances and air core reactance to be represented by linear inductance of high X/R ratio external to the transformers. The use of linear inductance of high X/R value was also utilized to represent equivalent system reactance, source (sub-transient) reactance, and shunt reactors.

The lightning arrester simulated in the study represented an 80% (288 kv) lightning arrester which very closely duplicated the characteristics of a modern EHV station-type lightning arrester. Although the maximum slow switching surge and 60 cycle sparkover is 2.76 per unit of nominal line-to-neutral peak voltage, 2.30 per unit sparkover was used to represent the minimum sparkover for the fastest voltage rise times involved, to determine current discharge duty.

Switching was performed with a drum-type switch driven in synchronism with the model system frequency. The switch allowed each phase to be controlled independently, with respect to phase voltage angle, thus enabling each phase to be opened or closed at any point on the voltage or current wave.

The entire model system was energized from a source which appeared infinite to the model system, thus all source impedances were external to the model generator.

A fast response oscilloscope (15 megacycles) and Polaroid Land camera were utilized to measure and record voltage and current phenomena. By this method of measurement all phenomena could be satisfactorily recorded and studied before proceeding with another portion of the study.

RESULTS

While verifying acceptable equipment design and operating procedures with regard to insulation, surge voltages and protective levels, it was apparent that some circuit configurations caused more severe conditions than others. The more critical conditions were often found to occur for operation of the system during its early stages of development.

Since the purpose of the investigations was to determine limiting conditions, the results which are presented are predominantly comprised of the critical conditions which were encountered. However, less severe conditions are also discussed.

The circuit configurations shown in Figs. 5, 6 and 7 were those which presented limiting conditions. Detailed findings associated with these figures will be presented.

Briefly, however, the conditions and the salient points included are as follows:

Figure 5

Operating of the 345 kv system with one line from Cholla to Four Corners, one line from Cholla to Pinnacle Peak, the Cholla 230 kv tie connected and the Four Corners generation not connected.

(1) Energization transients
  (A) Phase-to-neutral voltages.
  (B) Phase-to-phase voltage.
  (C) Lightning arrester performance.
  (D) Series capacitor voltage drops.

(2) De-energization with circuit breaker restrike.
  (A) System phase-to-neutral voltages
  (B) Recovery voltage across circuit breaker contacts
  (C) Series capacitor voltage drops

(3) Reinsertion, after transient period, of series capacitor bank which had been short circuited.

Figure 6

Operation of the 345 kv transmission system with two lines from Cholla to Four Corners, and one line from Cholla to Pinnacle Peak which is opened at Pinnacle Peak. The Cholla 230 kv tie is disconnected.

(1) Energization transients.
  (A) Phase-to-neutral voltages
  (B) Series capacitor voltage drops

(2) De-energization transients with circuit breaker restrike, with and without series compensation and with varying amounts of shunt reactance.

Figure 7

Operation of the 345 kv transmission system with two lines from Cholla to Four Corners, one line from Cholla to Pinnacle Peak and with the Cholla 230 kv tie disconnected.

(1) Solid line-to-ground faults with associated overvoltages.

(2) Line and load dropping at the Pinnacle Peak end of the system.

To detect possible regions of harmonic distortion and ferro non-linear sub-harmonic oscillations, dynamic voltages following switching were investigated over a range of preswitching voltages. The most severe system voltage and frequency conditions expected were purposely exceeded to expose borderline conditions.

A fact which is needed to interpret the data which are presented is that at full load, the generator voltage E'', (voltage behind subtransient reactance), at Four Corners is approximately 1.05 P.U., and for the main system represented at the Pinnacle Peak bus the value is slightly lower.

345 KV Transmission System Without Four Corners Generation

Circumstances which would require system operation depicted by Fig. 5 would be preparation for cold startup of the Four Corners Plant, where crank-up power must be made available from Cholla to the Four Corners Plant. Since initial conditions are without series compensation, the investigation covered this aspect. The results of investigations which produced overvoltages are presented in Table I.

The conditions shown in the data of Table I are given to indicate the magnitude of overvoltages which would occur if the system were operated in this manner. It was found that the severity of these conditions could be avoided and voltages kept within equipment rating by utilizing the shunt reactance which is located on the Four Corners 230 kv bus.

For brevity, only energizing of the Cholla to Four Corners line has been shown. Actually several other cases of line energizing disclosed that the line from Pinnacle Peak to Cholla (with no 230 kv tie at Cholla and 60 CMVA at Pinncle Peak 230 kv bus) and the line from Cholla to Four Corners (without the 345 kv tie to Pinnacle Peak) can be successfully energized with the reactor values shown on Fig. 5. In the latter case it was necessary to utilize the shunt reactance located on the Four Corners 230 kv bus.

The transient conditions which were considered of vital importance were:

(1) Transient magnitudes, duration, and wave shapes of phase-to-neutral and phase-to-phase voltages to which the circuit breakers, transformers and other equipment would be exposed.

(2) The lightning arrester performance for switching conditions which cause sparkover and the modifying effects the lightning

arrester has upon transient voltages.

(3) Voltage drops to which the series capacitor banks would be exposed.

For each condition, overvoltage locations were found which were higher than other parts of the system. The phase-to-neutral overvoltages, in general, graded downward with the proximity to the driving source voltage. To maintain clarity only the maximum values for the conditions imposed are presented in the tabulations.

In general, the transient conditions were no more severe than might be expected for the circuit elements present.[4,5,9]

The decay of transient conditions took from one to three cycles in most cases, and Fig. 8A shows the energizing transient which produced the 2.36 P.U. peak value listed in Table I. Because of the high steady state voltage conditions, harmonics of higher order than the fundamental were present. The shunt inductive reactance compensation for line charging at the Pinnacle Peak tertiary autotransformer winding was reduced to 35 mvar to maximize overvoltage effects.

Since phase-to-phase insulation strength is of importance,[14], phase-to-phase transients were explored during energization. The maximum phase-to-phase transient peak for 1.0 P.U. preswitching voltage at the Cholla 345 kv bus was 2.18 P.U. on a phase-to-phase per unit base. This value was obtained for zero percent series capacitive compensation which condition, in general, produced higher transients during energization.

Minimum lightning arrester sparkover was indicated by some of the transient switching voltages during energization. For example, when unmodified by arrester operation, a 2.36 P.U. transient peak occurred upon energizing the Cholla to Four Corners line with the Cholla 345 kv breaker (CB3, Fig. 5). Simulated lightning arrester action was performed and voltage and current recordings were made. An example is shown in Fig. 8B. The time scale is decreased, from that of other transient recordings which were made, to show wave form and rise time. The peak current represents 585 amperes on the actual system. The lightning arrester will reseal and current duty for the type of modern EHV station-type lightning arrester represented was not exceeded for anticipated operating conditions.

The voltage measurements taken across the series capacitor banks were for one section of the installation. Thus, the capacitor voltage drops are on a per unit phase-to-neutral base and represent the voltage from the center Cholla 345 kv bus to the side indicated. (Four Corners side for Fig. 5) The capacitor equipment will have voltage ratings as follows:

	Cholla - Four Corners Section		Cholla - Pinnacle Peak Section	
	Rated KV	P.U. Ø-N	Rated KV	P.U. Ø-N
25%	14.4	0.072	14.4	0.072
40%	28.8	0.145	28.8	0.145
60%	43.2	0.217	36.0	0.181

Note that 60% series compensation was studied to determine if serious borderline conditions of harmonic or subharmonic voltages were being approached for the 40% compensation. It was also studied to determine, for future consideration, the results that could be expected with this greater amount of compensation. Thus the complete range of series compensation anticipated for this system from zero to 60% was investigated.

The voltage magnitude and wave shape which would occur across a capacitor bank, during energization and restrike phenomena, were matters of interest since no data were available for a system representation of this magnitude. An example of the oscillograms obtained across the series capacitor banks during energization is shown in Fig. 9A. This example shows the conditions for 60% series capacitive compensation. No objectionable voltages across the capacitor were experienced, since the values obtained were below the nominal voltage rating. Circuit breaker restrike produced different wave shapes across the capacitor banks as evidenced by Fig. 9B, which shows the results with 25% series capacitive compensation. These voltages were also below rated values.

Capacitor reinsertion was initiated from conditions where the system was energized and at steady state prior to removal of a short circuit across the capacitor bank. This represented reinsertion after a disturbance which would cause the protective equipment to short circuit the capacitors. The anticipated protective equipment operating times were long enough for steady state conditions to be reestablished since switching transients on this system decayed in approximately three cycles. For the reinsertion under these conditions the disturbance was negligible.

The effects caused by circuit breaker restrike phenomena were maximized in the Transient Network Analyzer simulation by searching for the instant of restrike which would produce these effects. Oscillographic records were made of the recovery voltages which were measured across the breaker contacts. The highest value found for the conditions of Fig. 5 were 1.64 P.U. An example of a more severe case for different operating conditions is shown in Fig. 10 where the magnitude reached a value of 1.89 P.U.

345 KV System Operating Conditions With Four Corners Generation Disconnected from Pinnacle Peak 230 KV and the Cholla 230 KV Tie

Operating conditions which would lead to the circuit configuration of Fig. 6 could be envisioned when the Cholla tie was out either for servicing or emergency reasons and load was being transferred solely by the 345 kv system. The absence of this tie intensifies the problems encountered, and is a much more severe test of operation than with the 230 kv tie at Cholla. While this condition borders on second order contingency even in the early stages of system development, the system was designed to be independent of this tie. Operating problems are substantially reduced with the inclusion of this tie. When the Four Corners generation increases to the 575 mw or 800 mw level, then the possibility of being forced to operate in this manner would be more remote than for the 350 mw level since the second 345 kv line from Pinnacle Peak to Cholla would be installed. However, it was studied to determine operating requirements which would be necessary and also if serious overvoltage conditions would exist.

The main items of concern were the transient and steady state phase-to-neutral voltages associated with de-energization, and energization and recovery voltages in the event of circuit breaker restrike.

The results of the investigations performed are summarized in Table II.

It was considered of importance to know the effects of restrike phenomena for the circuit configuration of Fig. 6, since it was considered more severe than Fig. 5. It was envisioned that if restrike were to take place, it could occur in the following manner. The 230 kv circuit breaker at Pinnacle Peak (CB7, Fig. 6) would separate the 345 kv transmission from the main system. Following CB7 by a minimum of 3 cycles would be the opening of the Cholla 345 kv circuit breaker (CB5, Fig. 6) by means of a transferred tripping relay arrangement. At the time just prior to CB5 opening the transients caused by the CB7 operation had decayed. A restrike on CB5 was simulated and maximized to find the highest transient voltage conditions. An example of the transient voltage experienced across the circuit breaker contacts is shown in Fig. 10 where a peak magnitude of 1.89 P.U. was attained. The records indicate a rise time and transient magnitude which are below circuit breaker limits.

The severity of the restrike transients were diminished by increasing the shunt reactor size on the autotransformer tertiary at Pinnacle Peak. Testing for the requirements which would permit reenergization of the circuit configuration of Fig. 6, for example, in the event of an automatic reclosure, produced evidence which indicated the need for the two 65 mvar shunt reactors on the Four Corners 230 kv bus.

The voltage wave shapes across the series capacitor banks were different than those for the circuit configuration of Fig. 5. An example for 60% compensation is shown in Fig. 11. The magnitude of .125 P.U. phase-to-neutral voltage is less than the rated nominal voltage of the banks.

Solid Line-to-Ground Fault

The determination of the voltage magnitudes to which the unfaulted phases could rise were investigated. The prefault circuit conditions shown in Fig. 7 were used. Several fault locations were investigated to find the location which produced the most severe overvoltages. It was found that the Cholla 345 kv bus was the critical location; therefore, tests were conducted for that location. The results are given in Table III.

Results indicate that the steady state voltage on an unfaulted phase can approach 1.4 P.U. for values of driving source voltage of 1.05 P.U. which exist for full load conditions. Since the system is effectively grounded,15, the results of this investigation check with previous generalized calculations which have been made concerning faults on effectively grounded systems.16 Circuit breakers, rated 230 kv and higher, manufactured to ASA C37.6-1961, ("Preferred Ratings for Power Circuit Breakers") are intended for application only on "effectively grounded" systems. It appears that for the anticipated system conditions of this line-to-ground fault study, the voltage capability of the circuit breakers would not be exceeded if they were made in conformance with ASA C37.6.

Conditions Upon Separation of Four Corners Generation From Main System Generation

The transient and steady state conditions resulting from the separation of the Four Corners generation from the main system (Pinnacle Peak) were investigated without the series capacitive compensation to determine the severity and nature of overvoltages which could be encountered. The preswitching circuit conditions are shown in Fig. 7. The driving source voltage and frequency were varied over a wide range primarily to search for borderline circumstances where excessive dynamic overvoltages might be encountered. The results are presented in Table IV.

The transient voltages caused by the opening of the 230 kv circuit breaker at Pinnacle Peak (CB7,Fig. 7) were not significantly higher than the steady state values.

There was no evidence of subharmonic oscillations. The voltage wave shape, however, did contain higher order harmonics which caused distortion, and was more pronounced at the higher excitation values, which was expected. The decrease in overvoltage between the last two records in Table IV despite an increase in excitation voltage was caused by a reduction in the concurrent harmonics at the peak of the voltage wave. Steady state voltages which were encountered upon separation of the transmission system by the Pinnacle Peak 230 kv circuit breaker (CB7, Fig.7) reached 1.23 P.U. on the Pinnacle Peak transformer high voltage winding. A transferred trip scheme would next open the Cholla 345 kv circuit breaker (CB5, Fig. 7) after the first separation. The steady state voltages which were then experienced on the Cholla 345 kv bus were 1.24 P.U.

The results show that the maximum rated equipment design voltage of 1.05 P.U. is exceeded. Operating time at voltages in excess of the maximum rated equipment design voltage,17, should be kept to a minimum. It did not appear that the value of 1.4 P.U. voltage would be exceeded considering the operating precautions which will be taken to prevent overspeed. 18 The anticipated overvoltage for the conditions imposed does not exceed the value which could be experienced during the solid line-to-ground fault conditions which were presented just prior to these data. The investigation shows that operation of the system under these conditions would require operation with the shunt reactors shown in Fig. 7 connected to limit overvoltages.

SUMMARY AND CONCLUSIONS

1. The maximum phase-to-ground surge voltages, unmodified by lightning arrester operation, as obtained on the various circuit configurations studied when using a limited amount of shunt reactors were as follows:

Switching Operation	Per Unit Ø-N Voltage	
	Peak Transient	Steady State
Line Energization	2.36	1.21
Line Deenergization With Restrike	1.75 Ø-N 1.89 across contacts	-
Load Rejection	Approx. same as Steady State	1.00 P.U.Freq. 1.40 1.10 P.U.Freq. 1.60
Series Capacitor Reinsertion	1.25	1.25
Solid Phase-to-Ground Fault	-	1.56

2. For the conditions listed in (1), the maximum phase-to-phase transient voltage was found to be 2.18 P.U. on a phase-to-phase nominal voltage base.

3. Series capacitive compensation produced minor effects on the transient disturbances from switching operations.

4. For anticipated operating conditions lightning arrester rating (seal off), was not exceeded. However, for situations representing double contingencies, steady state voltages with harmonic distortion were found to be in excess of arrester rating, and if provision were to be made to prevent the voltage from

exceeding 1.4 per unit under these conditions, then additional shunt reactors would be required in these situations.

5. Transient surge voltages would be limited by an 80% (288 kv) arrester with ample margin to protect transformers using 1175 BIL insulation.

6. Discharge duties in the arrester from surge voltage operation were measured and found to be adequately within the capabilities of the modern station type lightning arrester represented in the investigations.

7. To limit the duration of sustained abnormal overvoltages on load rejection and fault conditions, transferred tripping of the lines to remove these conditions as quickly as possible was considered desirable.

8. It was found that shunt reactive compensation in the range of 70 to 80 percent of the line charging capacitance was needed for dynamic overvoltage control depending on the circuit configuration under consideration.

9. These studies verified the advisability of using 1175 BIL for the transformers of this 345 kv system. A lower BIL would appear to inflict undue penalties in the form of inflexible operating conditions and possibly the extra investment for more shunt reactors to reduce overvoltages.

10. While many of the tests for line dropping and line-to-ground faults extended beyond practical limits, they do indicate what could happen under these conditions. There were two lightning arrester ratings which could have been applied, either the 276 or the 288 kv. In evaluating the possibilities of abnormal conditions, and the consequences of arrester failure under these remote circumstances, the choice was made to utilize the 276 kv arrester. This confirmed original design ratings.

11. The circuit breakers will be applied in line with standards. Results of this study indicate that the reactor sizes selected, as well as other major apparatus ratings and characteristics will permit system operation within the overvoltage criterion provided for an effectively grounded system. The only exception would be under second order contingencies where machines would considerably overspeed.

12. In line with accepted operating philosophy concerning long distance EHV lines, most of the reactors used in this study must be left on continuously. These reactors are actually part of the transmission system and cannot be switched individually for either overvoltage suppression or load flow compensation.

Table I. Transient Conditions on 345 Kv System Without Four Corners Generation, as Shown in Figure 5.

One 345 Kv Line Pinnacle Peak to Cholla
One 345 Kv Line Cholla to Four Corners
230 Kv Tie at Cholla Closed
25 MVAR Reactor on Cholla 230 Kv Bus

Switching Operation	Series Compensation %	Shunt Reactors, MVAR, Connected at Pinnacle Peak Tertiary	Per Unit Preswitching Voltage and Location	Per Unit Ø-N Voltage Transient	Per Unit Ø-N Voltage Steady State	Location of Voltage Listed
Energization						
CB3 Closing	0	70	1.00 CHH	2.32	1.13	FCH
	0	70	1.10 CHH	2.36	1.21	FCH
	25	35	1.00 E" PP	1.98	1.17	FCH
	25	35	1.05 E" PP	2.19	1.25	FCH
	25	35	1.05 E" PP	0.03	0.006	CH-FC Cap. Bank
	60	35	1.00 E" PP	1.75	1.11	FCH
	60	35	1.05 E" PP	0.097	-	CH-FC Cap. Bank
Capacitor Reinsertion	25	35	1.00 E" PP	1.16	1.16	FCH
	25	35	1.05 E" PP	1.25	1.25	FCH
	60	35	1.00 E" PP	1.13	1.11	FCH
	60	35	1.05 E" PP	1.27	1.22	FCH
Deenergizing						
CB3 Opens and Restrikes	25	35	1.00 E" PP	1.39	-	FCH
	25	35	1.00 E" PP	0.045	-	CH-FC Cap. Bank
	60	35	1.00 E" PP	1.51	-	FCH
	60	35	1.00 E" PP	1.61	-	Across CB3 Contacts
	60	35	1.05 E" PP	1.64	-	FCH
	60	35	1.05 E" PP	1.53	-	Across CB3 Contacts

Abbreviations:

FCH	Four Corners 345 Kv
CHH	Cholla 345 Kv
CH-FC Cap. Bank	Series Capacitor Bank Associated with Cholla to Four Corners Line
E" PP	Voltage Behind Subtransient Reactance at Pinnacle Peak
CB3	345 Kv Circuit Breaker at Cholla on Cholla to Four Corners Line

Table II. Transient Conditions on 345 Kv System - Four Corners Isolated From Pinnacle Peak As Shown in Figure 6.

Two 345 Kv Lines Four Corners to Cholla
One 345 Kv Line Cholla to Pinnacle Peak
230 Kv Tie at Cholla Open

Switching Operation	Series Compensation %	Shunt Reactors, MVAR, Connected	Per Unit Preswitching Voltage and Location	Per Unit Ø-N Voltage		Location of Voltage Listed
				Transient	Steady State	
Deenergization						
CB7 Open	0	(A),(1)	1.05 E" FC	-	1.23	PPH
CB5 Open	0	(A),(1)	1.05 E" FC	-	1.24	CHH
CB7 Opens Followed by CB5 Which Restrikes	0	(A),(1)	1.00 E" FC	1.75	-	PPH
	0	(A),(1)	1.00 E" FC	1.72	-	Across CB5 Contacts
	0	(A),(1)	1.10 E" FC	1.70	-	PPH
	0	(A),(1)	1.15 E" FC	1.70	-	PPH
	60	(A),(2)	1.00 E" FC	1.89	-	Across CB5 Contacts
	60	(A),(2)	1.05 E" FC	1.44	-	PPH
Energization						
CB5 Closing	25	(B),(2)	1.00 E" FC	2.22	1.26	PPH
	25	(B),(2)	1.05 E" FC	2.27	1.31	PPH
	60	(A),(2)	1.00 CHH	1.80	1.07	PPH
	60	(A),(2)	1.00 CHH	0.113	0.018	CH-PP Cap. Bank
	60	(A),(2)	1.05 CHH	1.89	1.13	PPH
	60	(A),(2)	1.05 CHH	0.125	0.019	CH-PP Cap. Bank
	60	(A),(1)	1.05 CHH	1.77	1.06	PPH
	60	(A),(1)	1.05 CHH	0.095	0.012	CH-PP Cap. Bank

Abbreviations:

PPH	Pinnacle Peak 345 Kv
CHH	Cholla 345 Kv
CH-PP Cap. Bank	Series Capacitor Bank Associated with Cholla to Pinnacle Peak Line
E" FC	Voltage Behind Subtransient Reactance at Four Corners
Shunt Reactors	(A) Two 65 MVAR on Four Corners 230 Kv Bus (B) One 65 MVAR on Four Corners 230 Kv Bus (1) Two 35 MVAR on Pinnacle Peak Tertiary (2) One 35 MVAR on Pinnacle Peak Tertiary (Note) 50 MVAR Reactors Always Connected to Four Corners 230-345 Kv Autotransformers
CB5	345 Kv Circuit Breaker at Cholla on Cholla to Pinnacle Peak Line
CB7	230 Kv Circuit Breaker at Pinnacle Peak on Cholla to Pinnacle Peak 345 Kv Line

---

Table III. Overvoltage Conditions on 345 Kv System During Solid Line to Ground Fault at Cholla 345 Kv Bus. System as Shown in Figure 7.

Two 345 Kv Lines Four Corners to Cholla
One 345 Kv Line Pinnacle Peak to Cholla
230 Kv Tie at Cholla Open
Two 35 MVAR Shunt Reactors Pinnacle Peak Tertiary
Two 65 MVAR Shunt Reactors Four Corners 23 Kv Bus
One 50 MVAR Shunt Reactor on Each Four Corners Tertiary

Circuit Condition	Per Unit Preswitching Voltage and Location	Overvoltage Per Unit Ø-N		Location of Overvoltage
		Transient	Steady State	
Solid Line-to-ground fault applied at CHH Bus	1.00 E" FC and PP	-	1.30	CHH
	1.05 E" FC and PP	-	1.39	CHH
	1.10 E" FC and PP	-	1.44	CHH
	1.15 E" FC and PP	-	1.49	CHH
	1.20 E" FC and PP	-	1.56	CHH

Abbreviations:

CHH	Cholla 345 Kv
E" FC and PP	Voltage Behind Subtransient Reactance at Four Corners and Pinnacle Peak

Note E" at Four Corners at Full Load is Approximately 1.05 p.u.

Table IV. Overvoltage Conditions on 345 Kv System Following Separation of Four Corners Generation From Pinnacle Peak Load Area. Circuit as Shown in Figure 7.

Two 345 Kv Lines Four Corners to Cholla
One 345 Kv Line Pinnacle Peak to Cholla
230 Kv Tie at Cholla Open
Reactors: One 50 MVAR on Each Four Corners Tertiary
Two 65 MVAR on Four Corners 230 Kv Bus
Two 35 MVAR on Pinnacle Peak Tertiary

Switching Operation	Series Compensation %	Per Unit Preswitching Voltage and Location	Overvoltage Per Unit Ø-N Transient	Overvoltage Per Unit Ø-N Steady State	Location of Overvoltage
		P.U. Freq. 1.00			
CB7 Opens	0	1.00 E" FC	-	1.18	PPH
	0	1.05 E" FC	-	1.23	PPH
	0	1.10 E" FC	-	1.28	PPH
	0	1.15 E" FC	-	1.31	PPH
	0	1.20 E" FC	-	1.40	PPH
		P.U. Freq. 1.10			
	0	1.00 E" FC	-	1.42	PPH
	0	1.10 E" FC	-	1.60	PPH
	0	1.20 E" FC	-	1.57	PPH

Abbreviations:

PPH	Pinnacle Peak 345 Kv
E" FC	Voltage Behind Subtransient Reactance at Four Corners
CB7	230 Kv Circuit Breaker at Pinnacle Peak on Pinnacle Peak to Cholla 345 Kv Line

REFERENCES

1. Switching Surges - I - Phase-to-Ground Voltages, AIEE Committee Report. AIEE Transactions, Part III, Vol. 80, 1961, pp. 240-261.

2. Surge Transfer in 3-Winding Transformers, P.A. Abetti and H.F. Davis. AIEE Transactions, Part III-B, Vol. 73, 1954, pp. 1395-1407.

3. Surge Transfer Through 3-Phase Transformers, A.R. Hileman. AIEE Transactions, Vol. 77, Part III, 1958, pp. 1543-1554.

4. Switching Surges Due to Energization or Reclosing, I.B. Johnson, R.F. Silva, and D.D. Wilson. American Power Conference Proceedings, 1961.

5. Switching Surge Voltages in High-Voltage Stations, I.B. Johnson and A.J. Schultz. AIEE Transactions, Vol. 73, Part III-A, 1954, pp. 69-79.

6. Switching Surges and Arrester Performance on High-Voltage Stations, L.O. Barthold, I.B. Johnson, and A.J. Schultz. AIEE Transactions, Vol. 75, Part III, 1956, pp. 481-490.

7. Switching Surges and Arrester Performance on High-Voltage Systems, I.B. Johnson. CIGRE Paper No. 306, 1958.

8. Transmission Line Switching Surges as Modified by Transformer Impedances and Arrester Operation, D.F. Shankle and E.R. Taylor, Jr. AIEE Transactions, Vol. 77, 1958, pp. 1596-1604.

9. Switching Surges on Energizing A Transformer Terminated Line, I.B. Johnson and A.J. Schultz. AIEE Transactions, Vol. 79, Part III, 1960, pp. 241-245.

10. Switching Surges and Arrester and Gap Performance During 220 Kv Line Dropping Tests, W.N. Rothenbuhler and D.D. Wilson. Submitted for presentation at 1962 AIEE Winter General Meeting.

11. Fault Arc Deionization and Circuit Breaker Reclosing on EHV Lines -- Field, Laboratory and Analytical Results, American Electric Service Corporation-General Electric Company Task Force. Scheduled for presentation at 1962 Meeting of CIGRE.

12. Surge Phenomena in Large Unit-Connected Steam Turbine Generators, P.A. Abetti, I.B. Johnson, and A.J. Schultz. AIEE Transactions, Vol. 71, Part III, 1952, pp. 1035-1047.

13. Model Techniques in the Transient Network Analyzer Solution of Power Systems Problems, L.O. Barthold and R.F. Silva. American Power Conference Proceedings, March 1960.

14. Phase-to-Phase Switching Surges on Line Energization, I.B. Johnson, R.F. Silva, and D.D. Wilson. AIEE Conference Paper No. 61-670, May 1961.

15. AIEE Neutral Grounding Devices, Standard No. 32, May 1947, Part 32-1.05.

16. Determination of Ground-Fault Current and Voltages on Transmission Systems, E.M. Hunter, E. Pragst, and P.H. Light. General Electric Review, Vol. 42, No. 8, pp. 353-356, Vol. 42, No. 11, pp. 479-485. August and November 1939.

17. American Standard Guide for Preferred Voltage Ratings for A-C Systems and Equipment. C84.1 - 1954.

18. Improving Transient Stability by Use of Dynamic Braking, W.H. Croft and R.H. Hartley. AIEE Conference Paper No. 61-798, June 1961.

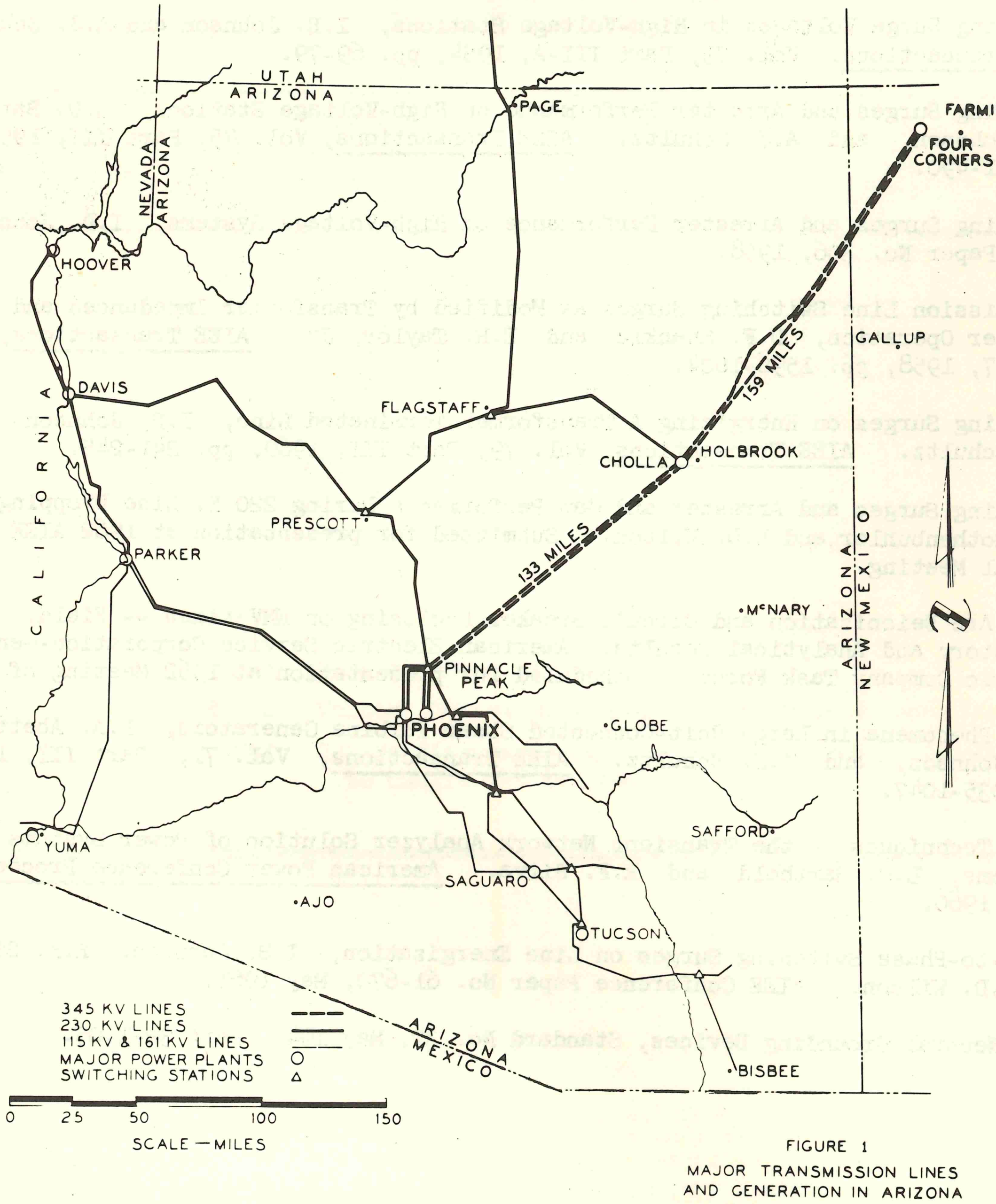

UTAH
ARIZONA
PAGE
FARMINGTON
FOUR CORNERS
NEVADA
ARIZONA
HOOVER
159 MILES
GALLUP
DAVIS
FLAGSTAFF
HOLBROOK
CHOLLA
PRESCOTT
133 MILES
PARKER
CALIFORNIA
McNARY
ARIZONA
NEW MEXICO
PINNACLE PEAK
PHOENIX
GLOBE
SAFFORD
YUMA
SAGUARO
AJO
TUCSON
ARIZONA
MEXICO
BISBEE
345 KV LINES
230 KV LINES
115 KV & 161 KV LINES
MAJOR POWER PLANTS
SWITCHING STATIONS
0
25
50
100
150
SCALE — MILES
FIGURE 1
MAJOR TRANSMISSION LINES AND GENERATION IN ARIZONA

Fig. 1 . Geographical relationship of 292 Mile 345 Kv transmission facilities to other major transmission lines.

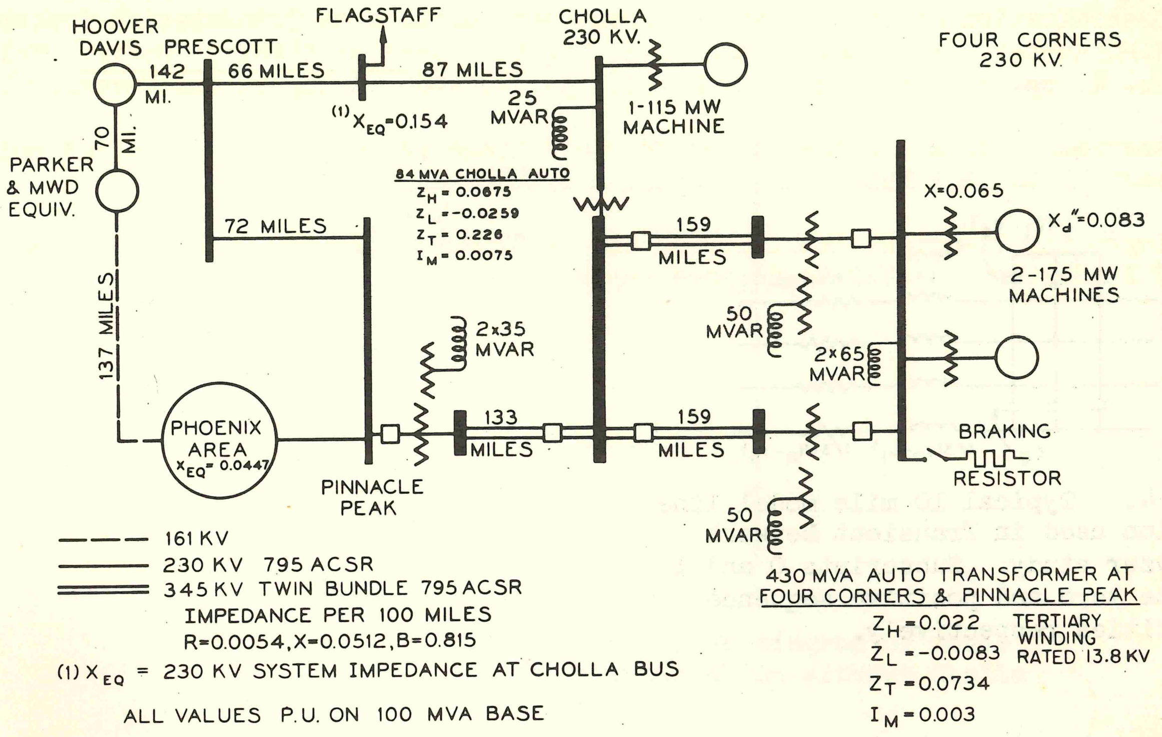

HOOVER
DAVIS
PRESCOTT
FLAGSTAFF
CHOLLA 230 KV.
FOUR CORNERS 230 KV.
142 MI.
66 MILES
87 MILES
(1) X_{EQ}=0.154
25 MVAR
1-115 MW MACHINE
PARKER & MWD EQUIV.
70 MI.
84 MVA CHOLLA AUTO
Z_H = 0.0875
Z_L = -0.0259
Z_T = 0.226
I_M = 0.0075
72 MILES
159 MILES
X=0.065
X_d''=0.083
2-175 MW MACHINES
137 MILES
2x35 MVAR
50 MVAR
2x65 MVAR
PHOENIX AREA X_{EQ}= 0.0447
133 MILES
159 MILES
BRAKING RESISTOR
PINNACLE PEAK
50 MVAR
161 KV
230 KV 795 ACSR
345 KV TWIN BUNDLE 795 ACSR
IMPEDANCE PER 100 MILES
R=0.0054, X=0.0512, B=0.815
(1) X_{EQ} = 230 KV SYSTEM IMPEDANCE AT CHOLLA BUS
ALL VALUES P.U. ON 100 MVA BASE
430 MVA AUTO TRANSFORMER AT FOUR CORNERS & PINNACLE PEAK
Z_H=0.022
Z_L=-0.0083
Z_T=0.0734
I_M=0.003
TERTIARY WINDING RATED 13.8 KV

Fig. 2. 1963, 345 Kv transmission facilities for 350 MW Four Corners generation.

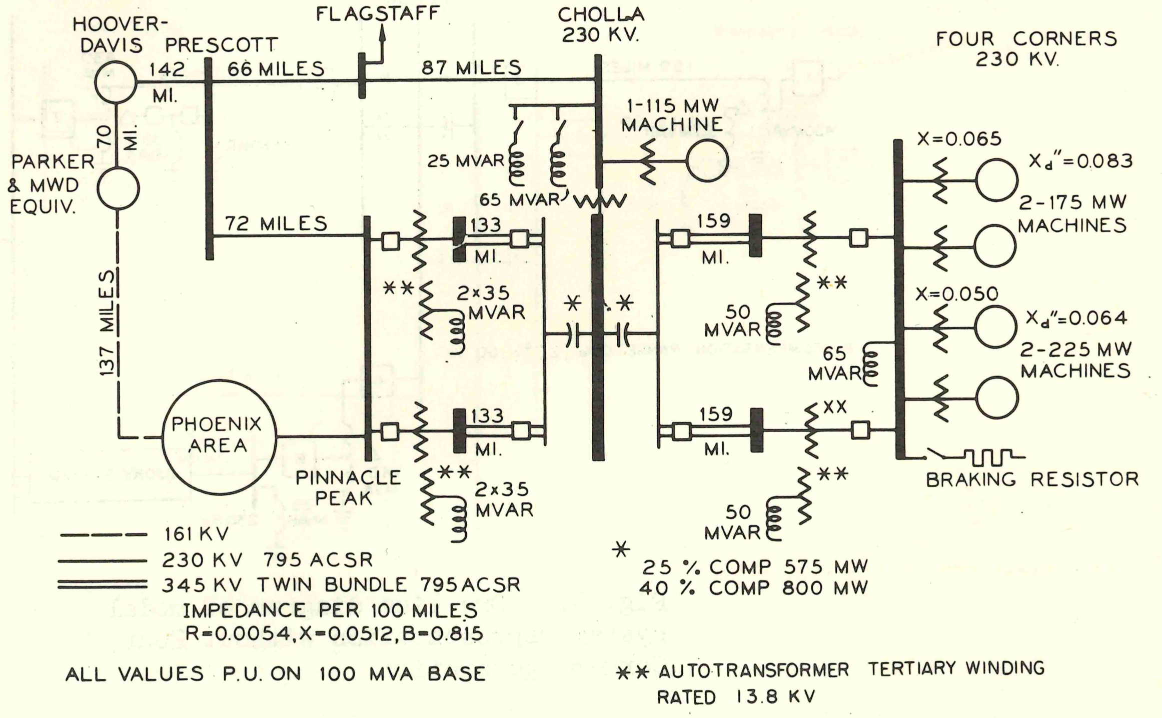

HOOVER-DAVIS
PRESCOTT
FLAGSTAFF
CHOLLA 230 KV.
FOUR CORNERS 230 KV.
142 MI.
66 MILES
87 MILES
1-115 MW MACHINE
25 MVAR
65 MVAR
PARKER & MWD EQUIV.
70 MI.
X=0.065
X_d''=0.083
2-175 MW MACHINES
72 MILES
133 MI.
159 MI.
**
2x35 MVAR
* *
50 MVAR
**
X=0.050
X_d''=0.064
2-225 MW MACHINES
137 MILES
65 MVAR
PHOENIX AREA
133 MI.
159 MI.
XX
PINNACLE PEAK
**
2x35 MVAR
**
BRAKING RESISTOR
50 MVAR
161 KV
230 KV 795 ACSR
345 KV TWIN BUNDLE 795ACSR
IMPEDANCE PER 100 MILES
R=0.0054, X=0.0512, B=0.815
ALL VALUES P.U. ON 100 MVA BASE
* 25 % COMP 575 MW
40 % COMP 800 MW
** AUTOTRANSFORMER TERTIARY WINDING RATED 13.8 KV

Fig. 3. 345 Kv transmission facilities for 575 MW and 800 MW Four Corners generation.

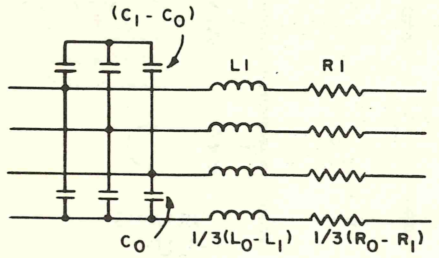
(C1 - C0)
L1
R1
C0
1/3(L0 - L1)
1/3(R0 - R1)

Fig. 4. Typical 10 mile model line section used in Transient Network Analyzer study. Subscripts 0 and 1 denote zero and positive sequence quantities respectively.

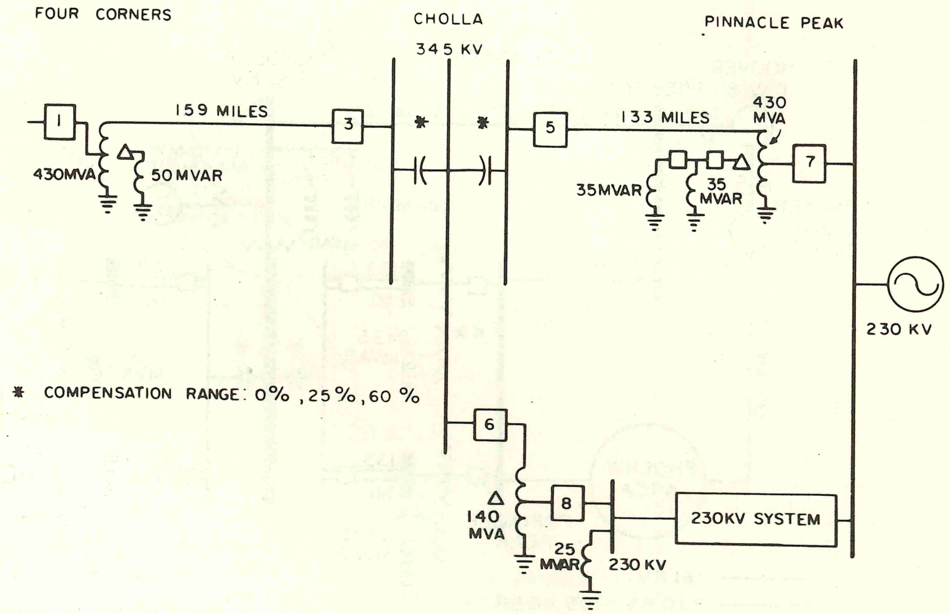
FOUR CORNERS
CHOLLA
345 KV
PINNACLE PEAK
1
159 MILES
3
*
*
5
133 MILES
430 MVA
7
430MVA
50 MVAR
35MVAR
35 MVAR
230 KV
* COMPENSATION RANGE: 0%, 25%, 60%
6
140 MVA
8
25 MVAR
230 KV
230KV SYSTEM

Fig. 5. One line diagram of model system representation without Four Corners generation.

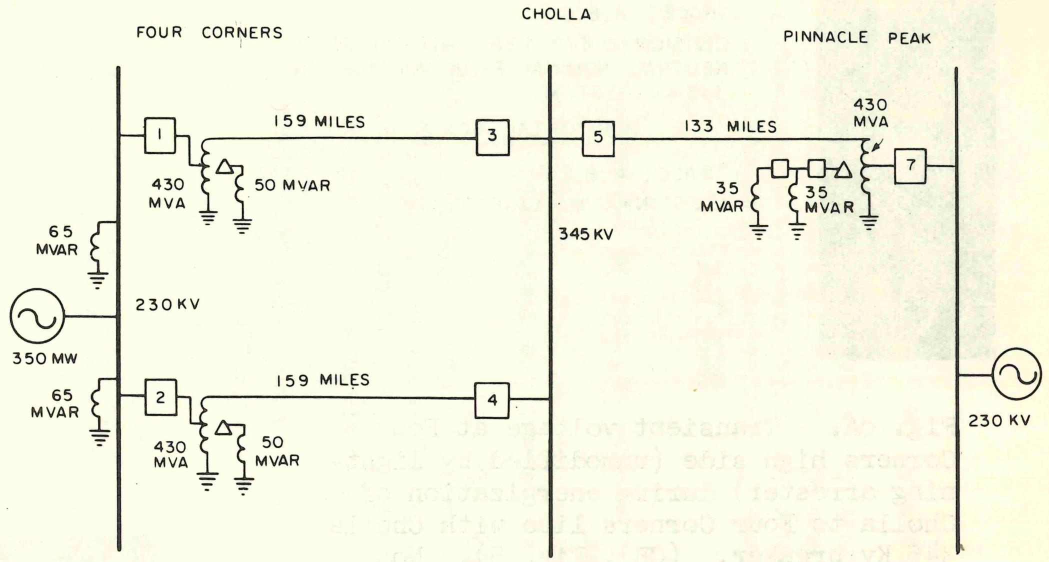
FOUR CORNERS
CHOLLA
PINNACLE PEAK
1
159 MILES
3
5
133 MILES
430 MVA
7
430 MVA
50 MVAR
35 MVAR
35 MVAR
345 KV
65 MVAR
230 KV
350 MW
65 MVAR
2
159 MILES
4
430 MVA
50 MVAR
230 KV

Fig. 7. One line diagram of model system representation without Cholla 230 Kv tie.

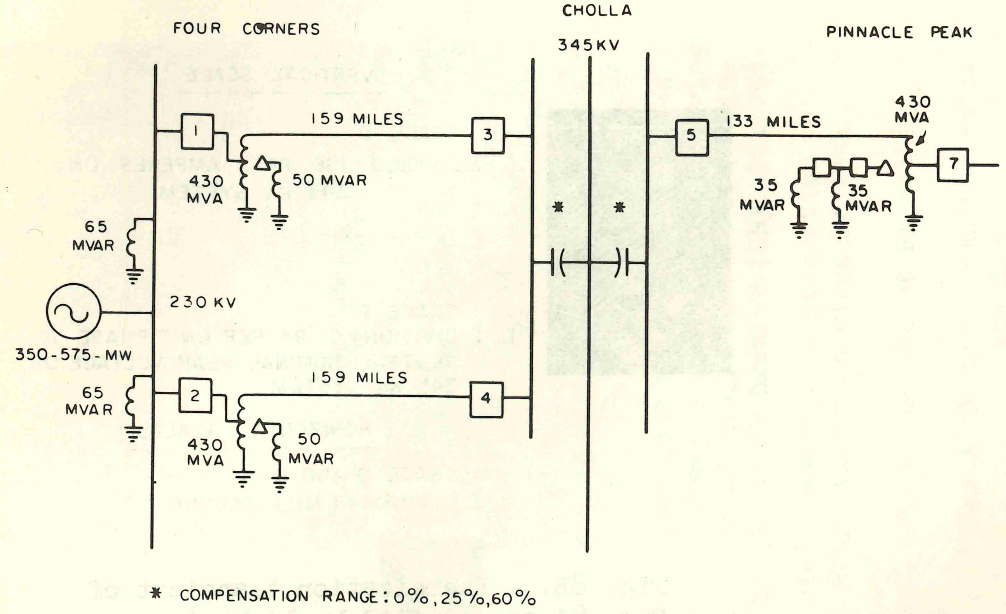
FOUR CORNERS
CHOLLA
345 KV
PINNACLE PEAK
1
159 MILES
3
5
133 MILES
430 MVA
7
430 MVA
50 MVAR
35 MVAR
35 MVAR
*
*
65 MVAR
230 KV
350-575-MW
65 MVAR
2
159 MILES
4
430 MVA
50 MVAR
* COMPENSATION RANGE: 0%, 25%, 60%

Fig. 6. One line diagram of model system representation without Pinnacle Peak and Cholla 230 kv ties.

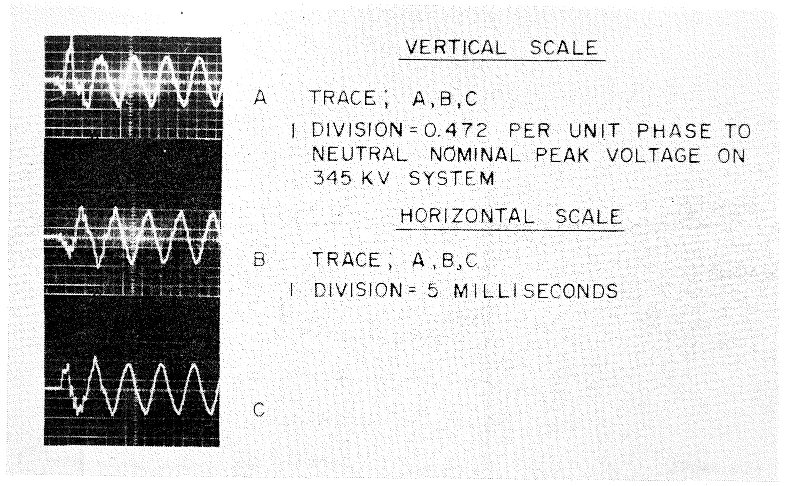

Fig. 8A. Transient voltage at Four Corners high side (unmodified by lightning arrester) during energization of Cholla to Four Corners line with Cholla 345 Kv breaker. (CB3, Fig. 5). No series capacitors; two 35 MVAR reactors on Pinnacle Peak tertiary; 1.10 P.U. preswitching voltage at Cholla 345 Kv bus.

Trace	Quantity
A	Phase A ∅ - N volts
B	Phase B ∅ - N volts
C	Phase C ∅ - N volts

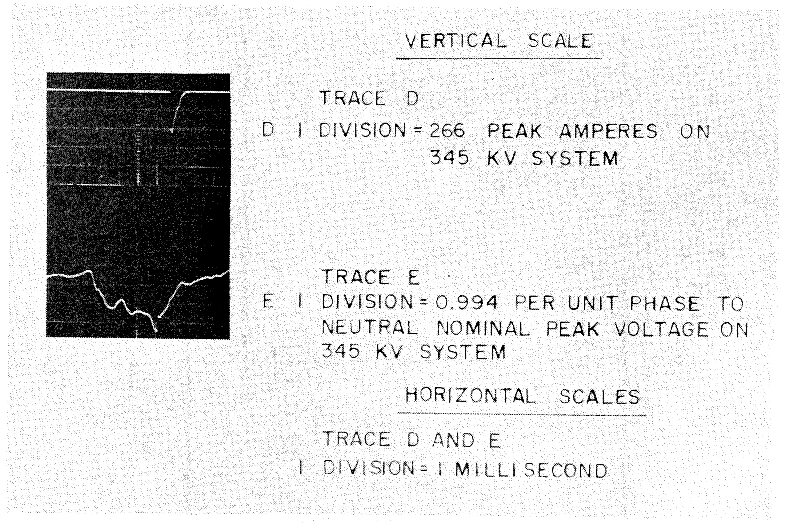

Fig. 8B. Energization transient of Fig. 8A as modified by lightning arrester operation.

Trace	Quantity
D	Phase A Lightning arrester current
E	Phase A Lightning arrester voltage

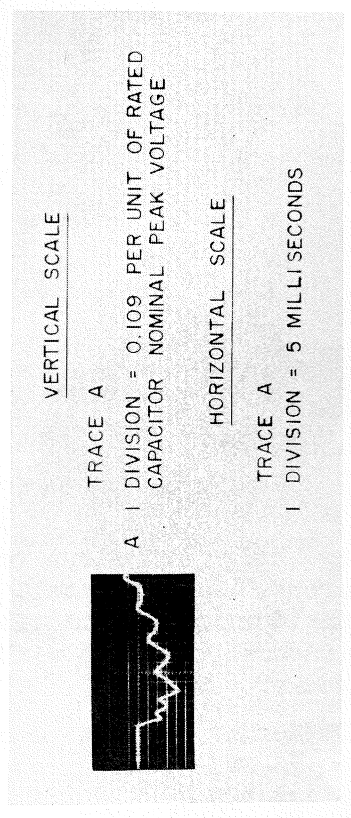

Fig. 9A. Transient voltage drop across Cholla-Four Corners capacitor bank during energization of Cholla-Four Corners line with Cholla 345 Kv breaker (CB3, Fig. 5)

60% series capacitive compensation
One 35 MVAR reactor on Pinnacle Peak tertiary
1.05 P.U. source voltage at Pinnacle Peak
Trace A Phase A Series capacitor voltage drop

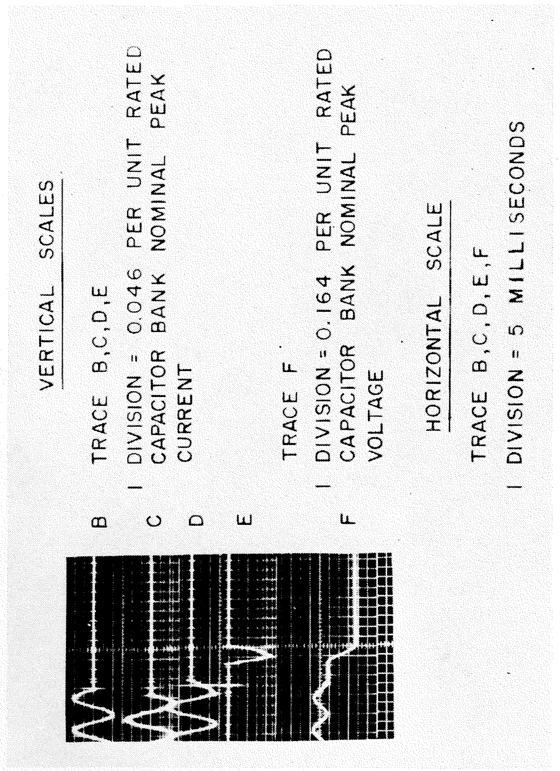

Fig. 9B. Transient current and voltage drop of Cholla-Four Corners capcitor bank during restrike of Cholla 345 Kv breaker on Cholla-Four Corners line (CB3, Fig. 5)

25% series capacitive compensation
One 35 MVAR reactor on Pinnacle Peak tertiary
1.00 P.U. source voltage at Pinnacle Peak

Trace	Quantity
B	Phase A Series capacitor current
C	Phase B Series capacitor current
D	Phase C Series capacitor current
E	Phase A Series capacitor current during restrike
F	Phase A Series capacitor voltage drop

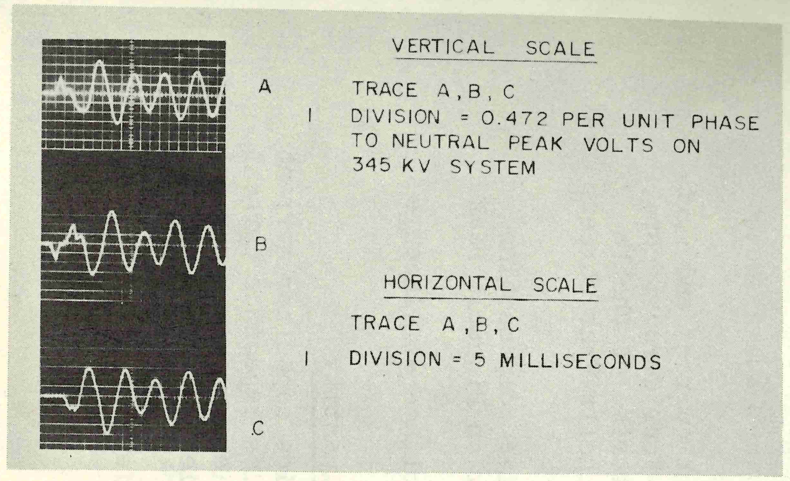

Fig. 10. Recovery voltage across Cholla 345 Kv breaker contacts, (CB5, Fig. 6) following restrike upon de-energization of Cholla-Pinnacle Peak line.

60% Series capacitive compensation
One 35 MVAR reactor on Pinnacle Peak tertiary
Two 65 MVAR reactors on Four Corners 230 Kv bus
1.00 P.U. preswitching voltage at Cholla 345 Kv bus

Trace	Quantity
A	Phase A Voltage across CB5 contacts
B	Phase B Voltage across CB5 contacts
C	Phase C Voltage across CB5 contacts

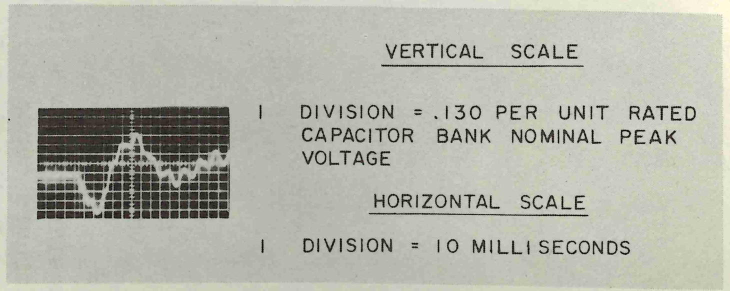

Fig. 11. Transient voltage drop across Cholla-Pinnacle Peak capacitor bank during energization of Cholla to Pinnacle Peak line with Cholla 345 Kv breaker (CB5, Fig. 6).

60% Series capacitive compensation
One 35 MVAR reactor on Pinnacle Peak tertiary
Two 65 MVAR reactors on Four Corners 230 Kv bus
Trace Series capacitor voltage drop

Transactions Paper

(Reviewed and Accepted for Publication)

SWITCHING SURGE AND DYNAMIC VOLTAGE STUDY OF ARIZONA PUBLIC SERVICE COMPANY 345 KV PROPOSED TRANSMISSION SYSTEM UTILIZING MINIATURE ANALYZER TECHNIQUES

W. H. Croft
Member AIEE
Arizona Pub. Service Co.
Phoenix, Ariz.

R. H. Hartley
Member AIEE
Arizona Pub. Service Co.
Phoenix, Ariz.

R. L. Linden
Associate Member AIEE
General Electric Co.
Schenectady, N. Y.

D. D. Wilson
Associate Member AIEE
General Electric Co.
Schenectady, N. Y.

A paper recommended by the AIEE Transmission and Distribution Committee and approved by the AIEE Technical Operations Department for presentation at the AIEE Winter General Meeting, New York, N. Y., January 28-February 2, 1962. Manuscript submitted October 30, 1961; made available for printing December 8, 1961.

Price: $ .50 To Members
$1.00 To Nonmembers

(5¢ per copy additional if first class mailing desired)

All Rights Reserved by the American Institute of Electrical Engineers
345 East 47th Street, New York 17, N. Y.
Litho in U.S.A.

Paper No.
62-109

Discussion in Duplicate Due February 16, 1962.

PUB. NO. HV 1-1968

STANDARDS PUBLICATION

HIGH-VOLTAGE INSULATORS

750
44
3000
30000
3300

NATIONAL ELECTRICAL MANUFACTURERS ASSOCIATION 155 EAST 44TH STREET, NEW YORK, N. Y. 10017

TABLE OF CONTENTS

Page

Part 1—TEST METHODS 1

Part 2—SUSPENSION-TYPE INSULATORS 2

Part 3—SPOOL-TYPE INSULATORS 5

Part 4—STRAIN-TYPE INSULATORS 5

Part 5—LOW- AND MEDIUM-VOLTAGE PIN-TYPE INSULATORS 6

Part 6—HIGH-VOLTAGE PIN-TYPE INSULATORS 8

Part 7—HIGH-VOLTAGE LINE-POST-TYPE INSULATORS 8

Part 8--CAP- AND PIN-TYPE APPARATUS INSULATORS 9

Part 9—POST-TYPE APPARATUS INSULATORS 12

Part 20—APPARATUS INSULATORS 13

- Table 20-1—Summary of Characteristics of Apparatus Insulators--Cap and Pin Type 14
- Table 20-2—Summary of Characteristics of Mixed Apparatus Insulators—Cap and Pin Type 16
- Table 20-3—Summary of Characteristics of Apparatus Insulators—Post Type 18
- Figure 20-1--Transition Plate (Upright) TR Number 151 20

FOLD BEFORE TEARING

Affix
Stamp
Before
Mailing

National Electrical Manufacturers Association
155 East 44th Street
New York, New York (10017)

KEEP YOUR NEMA STANDARDS PUBLICATIONS UP TO DATE

If you will fill out and return the postal card shown above, we will be glad to inform you when this NEMA Standards Publication is superseded by a later edition. There is no extra charge for this service.

It would be appreciated if you will return one card for each copy of this publication which is in your possession. Each card should be filled out in full with your complete mailing address.

Gentlemen: Pub. No. HV 1-1968

Please notify me when the NEMA Standards Publication for High-voltage Insulators is superseded by a new edition. There is no extra charge for this service.

NAME____

COMPANY______________________________________

STREET ADDRESS_________________________________

CITY__________________ STATE________ ZIP CODE_____

. . . .

(FOR NEMA USE ONLY) 1 2 3 4 5 6 7 8

HIGH-VOLTAGE INSULATORS

Part 1
TEST METHODS

The "USA Standard Test Methods for Electrical Power Insulators," C29.1-1961 (NEMA Publication No. HV 10-1961), was approved as a NEMA Standard on May 15, 1961 and constitutes Part 1 of this NEMA Publication No. HV 1.

Copies of C29.1-1961 (NEMA Publication No. HV 10-1961) are available from the:

USA Standards Institute (formerly the
American Standards Association, Inc.)
10 East 40th Street
New York, N.Y. 10016

National Electrical Manufacturers Association
155 East 44th Street
New York, N.Y. 10017

Part 2
SUSPENSION-TYPE INSULATORS

The following constitute Part 2 of this NEMA Publication No. HV 1:

1. USA Standard for Wet-Process Porcelain Insulators (Suspension Type), C29.2-1962 (approved as a NEMA Standard 3-21-1962). The following note which was approved as a NEMA Standard 11-11-1965 should be added to Fig. 11, Impact Testing Machine:

> 4. For impact testing of Class 52-9 insulators, invert the steel bob from the position shown in the figure and shorten the steel tube to maintain the 35-inch pendulum length.

2. USA Standard Supplement C29.2a-1965 (approved as a NEMA Standard 9-25-1963 and 1-13-1965). For the Class 52-8 insulator shown in Fig. 7a, the time load value should be changed from "20,000 lb" to "24,000 lb" (approved as a NEMA Standard 11-11-1965).

3. HV 1-2.01 Quality Conformance Test for Suspension Insulator Line Hardware (see page 3).

4. Figure 7b (see page 4).

Copies of C29.2-1962 and C29.2a-1965 are available from the:

USA Standards Institute
10 East 40th Street
New York, N.Y. 10016

HV 1-2.01 QUALITY CONFORMANCE TEST FOR SUSPENSION INSULATOR LINE HARDWARE

A. General

When applicable, the following quality conformance tests on line hardware, such as clamps, fittings and accessory hardware generally used with suspension insulators in the transmission and distribution of electrical energy, shall be used.

B. Ball and Socket Dimensions

Dimensions and tolerances of ball and socket connections, where used, shall be determined after galvanizing by ball and socket gages shown in USA Standard C29.2-1962.

Ten specimens shall be selected at random and checked with the correct gage. Failure of one specimen to meet the gage requirements shall constitute failure of the lot to meet this standard.

C. Galvanizing

A piece representative of each type of hardware shall be selected at random and tested in accordance with the latest revision of the "ASTM Method of Test for Uniformity of Coating By the Preece Test (Copper Sulphate Dip) on Zinc-Coated (Galvanized) Iron or Steel Articles*," A 239. If a specimen fails to withstand six (except for bolts, cap screws, cotter bolts, and nuts, only four required) one-minute copper sulphate dips, three additional pieces of the same type of hardware shall be selected at random from the same lot and tested. Failure of more than one specimen from the first and second sample combined to withstand the required number of dips shall constitute failure of the lot to meet this standard.

D. Tension Test

A device shall be selected at random and tested for tension in a manner simulating the service installation with properly matching connecting elements: For suspension and strain clamps, the load may be applied through stiff bars directly against the cable seat. The load may be raised rapidly to about 75 percent of the rated tension value and then continued to ultimate at a rate per minute not more than 30 percent nor less than 15 percent of the rated ultimate tension value. Should the ultimate mechanical strength fail to equal or exceed the rating, three additional samples shall be tested. Failure of any of these three samples below the rated mechanical strength shall constitute failure of the lot to meet this standard.

---

* Copies are available from the American Society for Testing and Materials, 1916 Race Street, Philadelphia, Pa. 19103.

NEMA Standard 9-29-1954.

Fig. 7b
Dead-end Suspension Insulator, Class 52-9

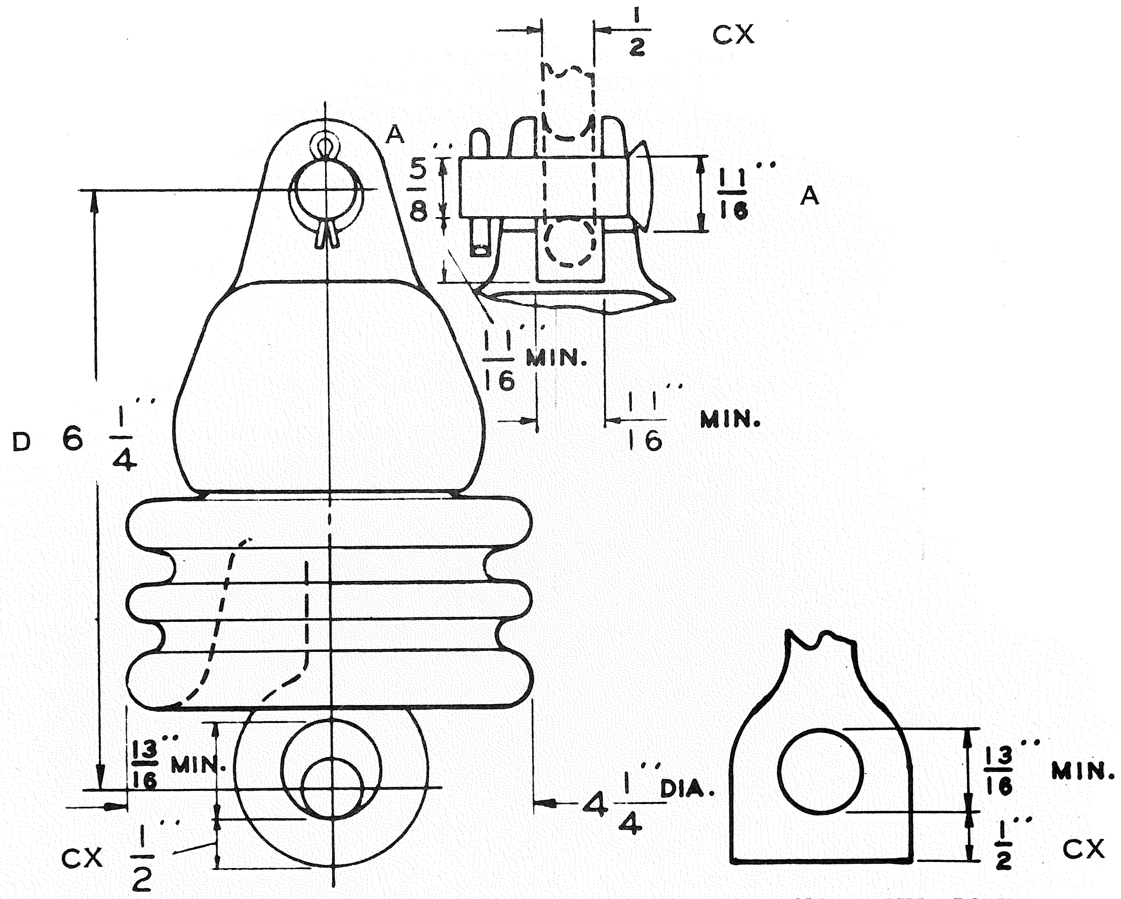

ALTERNATE EYE BOLT

	Rating	See USA Standard C29.1-1961, Section
Dimensions		
Leakage distance, in.	6.75	2.5.2
Mechanical Values		
Combined mechanical and electrical strength, lb	10,000	5.2
Mechanical impact strength, in.-lb	45	5.1.2.2
Tension proof, lb	4,000	7.2.1
Time load, lb	6,000	5.3
Electrical Values		
Low-frequency dry flashover, kv	60	4.2
Low-frequency wet flashover, kv	30	4.3
Critical-impulse flashover, positive, kv	100	4.7
Critical-impulse flashover, negative, kv	90	4.7
Low-frequency puncture, kv	80	4.11
Radio-Influence-Voltage Data		
Low-frequency test voltage, rms to ground, kv	7.5	4.9
Maximum riv at 1,000 kc, microvolts	50	4.9

Allowable Variations

The letters appearing on the figure above stand for the following tolerances. A single letter indicates a plus or minus tolerance, e.g., A = ± 1/64". When two letters are used, the first is a plus tolerance, and the second a minus, e.g., CX = + 1/16" - 0.

A = 1/64"　B = 1/32"　C = 1/16"　D = 1/8"　X = 0

NEMA Standard 11-11-1965.

Part 3
SPOOL-TYPE INSULATORS

The "USA Standard for Wet-Process Porcelain Insulators (Spool Type)," C29.3-1961, was approved as a NEMA Standard on September 29, 1960 and constitutes Part 3 of this NEMA Publication No. HV 1.

Copies of C29.3-1961 are available from the:

USA Standards Institute
10 East 40th Street
New York, N.Y. 10016

Part 4
STRAIN-TYPE INSULATORS

The "USA Standard for Wet-Process Porcelain Insulators (Strain Type)," C29.4-1961, was approved as a NEMA Standard on September 29, 1960 and constitutes Part 4 of this NEMA Publication No. HV 1.

Copies of C29.4-1961 are available from the:

USA Standards Institute
10 East 40th Street
New York, N.Y. 10016

Part 5
LOW- AND MEDIUM-VOLTAGE PIN-TYPE INSULATORS

The "USA Standard for Wet-Process Porcelain Insulators (Low- and Medium-Voltage Pin Type)," C29.5-1961, was approved as a NEMA Standard on September 29, 1960. NEMA subsequently approved the following revisions in C29.5-1961:

1. The addition of the following sentence to Note I in Figures 1 to 5, inclusive (approved as a Suggested Standard for Future Design 9-29-1961, reaffirmed 1-13-1965):

   > On radio freed insulators, the 60-cycle and impulse flashover ratings are reduced 10 percent from the tabulated values.

2. The addition of neck diameters and groove dimensions to Figures 2, 3, 4 and 5 as shown on pages 6 and 7 of this NEMA Publication No. HV 1 (approved as a NEMA Standard 1-13-1965).
3. The following revised flashover values for Class 55-2, 55-3, 55-4 and 55-5 insulators (approved as a NEMA Standard 8-20-1966):

	Flashover, Kv			
	Low-frequency		Critical Impulse	
Insulator Class	Dry	Wet	Positive	Negative
55-2	45	25	70	85
55-3	55	30	90	110
55-4	65	35	105	130
55-5	80	45	130	150

C29.5-1961, together with the foregoing revisions, constitutes Part 5 of this NEMA Publication No. HV 1.

Copies of C29.5-1961 are available from the:

USA Standards Institute
10 East 40th Street
New York, N.Y. 10016

Fig. 2
Pin Insulator, Class 55-2

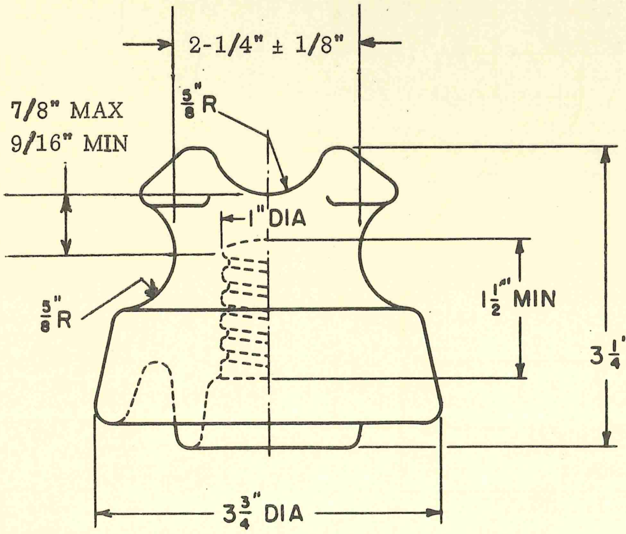

Fig. 3
Pin Insulator, Class 55-3

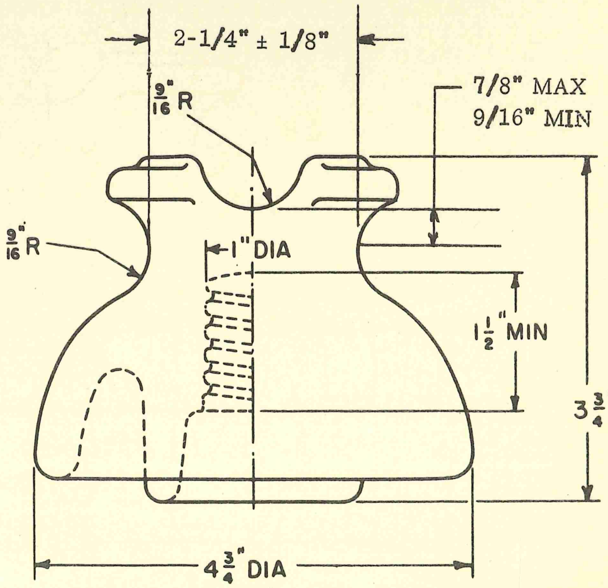

Fig. 4
Pin Insulator, Class 55-4

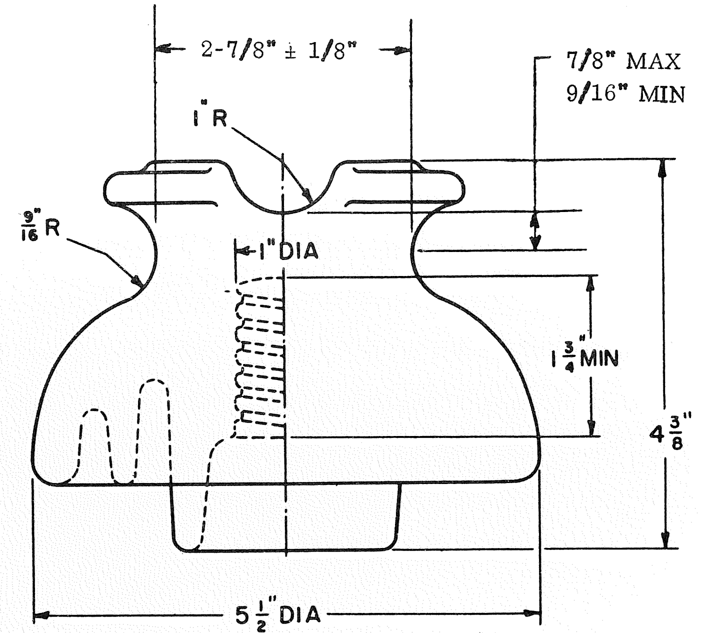
2-7/8" ± 1/8"
7/8" MAX
9/16" MIN
1" R
9/16" R
1" DIA
1 3/4" MIN
4 3/8"
5 1/2" DIA

Fig. 5
Pin Insulator, Class 55-5

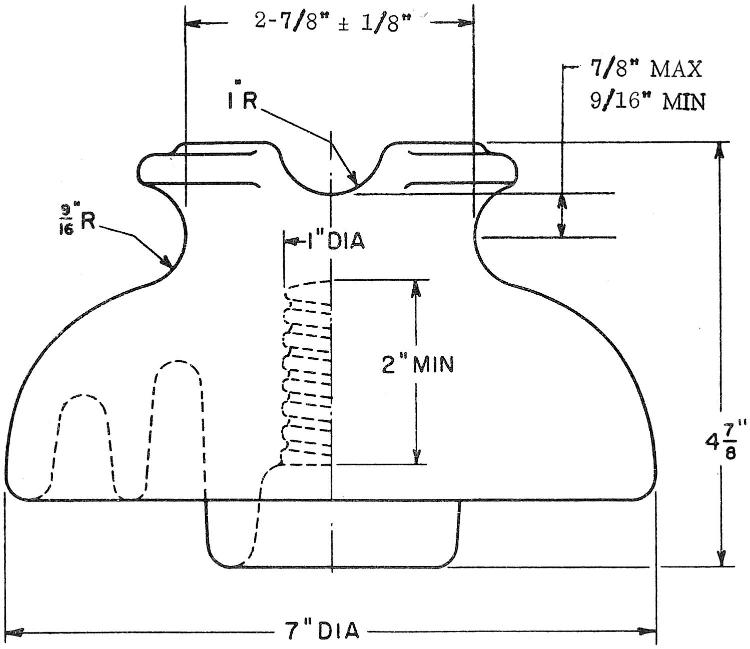
2-7/8" ± 1/8"
7/8" MAX
9/16" MIN
1" R
9/16" R
1" DIA
2" MIN
4 7/8"
7" DIA

Part 6
HIGH-VOLTAGE PIN-TYPE INSULATORS

The "USA Standard for Wet-Process Porcelain Insulators (High-Voltage Pin Type)," C29.6-1961, was approved as a NEMA Standard on September 29, 1960 and constitutes Part 6 of this NEMA Publication No. HV 1.

Copies of C29.6-1961 are available from the:

USA Standards Institute
10 East 40th Street
New York, N.Y. 10016

Part 7
HIGH-VOLTAGE LINE-POST-TYPE INSULATORS

The following constitute Part 7 of this NEMA Publication No. HV 1:

1. USA Standard for Wet-Process Porcelain Insulators (High-Voltage Line-Post Type), C29.7-1961 (approved as a NEMA Standard 9-29-1960).

2. USA Standard Supplement C29.7a-1966 (approved as a NEMA Standard 1-13-1965).

Copies of C29.7-1961 and C29.7a-1966 are available from the:

USA Standards Institute
10 East 40th Street
New York, N.Y. 10016

Part 8

CAP- AND PIN-TYPE APPARATUS INSULATORS

The following constitute Part 8 of this NEMA Publication No. HV 1:

1. USA Standard for Wet-Process Porcelain Insulators (Apparatus, Cap and Pin Type), C29.8-1961 (approved as a NEMA Standard 9-29-1960). *

2. USA Standard Supplement C29.8a-1965 (approved as a NEMA Standard 1-13-1965). *

3. Figures 16 and 17 as shown on pages 10 and 11.

* On August 20, 1966, NEMA approved the following revisions in C29.8-1961 and C29.8a-1965:

a. In Figures 1, 2, 3, 4, 5 and 6, change "PD 0.4665-0.4600" to "PD 0.4715-0.4650" for tapped holes 1/2-13 unified form special.

b. In Figures 7, 8, 10, 11, 12, 13 and 15, change "PD 0.5832-0.5760" to "PD 0.5882-0.5810" for tapped holes 5/8-11 unified form special.

c. In Figures 9 and 14, change "PD 0.7027-0.6950" to "PD 0.7077-0.7000" for tapped holes 3/4-10 unified form special.

On November 16, 1967, NEMA approved the following revisions in C29.8-1961 and C29.8a-1965:

d. Delete paragraphs 9.3.1, 9.3.2 and 9.3.5.

e. In the tabulations following Figures 1 through 15, delete all references to low-frequency dry flashover, low-frequency wet flashover, critical-impulse flashover (positive), and critical-impulse flashover (negative).

Copies of C29.8-1961 and C29.8a-1965 are available from the:

USA Standards Institute
10 East 40th Street
New York, N.Y. 10016

NOTE—See Part 20 of this NEMA Publication No. HV 1 for a summary of the characteristics of cap- and pin-type insulators.

Fig. 16
Apparatus Insulator, Cap and Pin Type

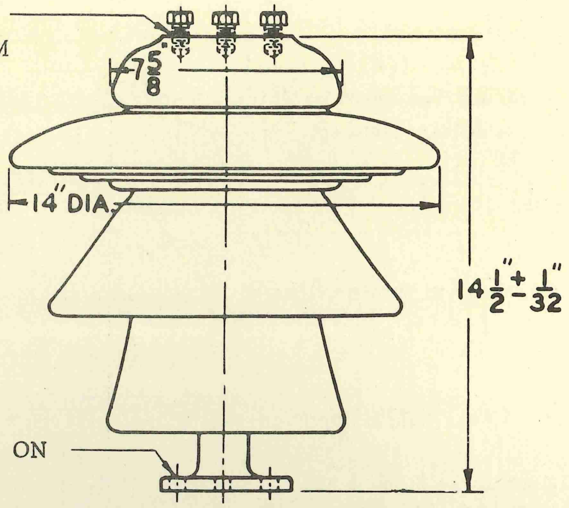

4 TAPPED HOLES 1/2-13 UNIFIED FORM SPECIAL, PD 0.4715-0.4650, LENGTH OF ENGAGEMENT 0.50 (TAP AFTER HDG) ON 3" BOLT CIRCLE

4 9/16" DIA HOLES ON 3" BOLT CIRCLE

TECHNICAL REFERENCE NO. 164

	Rating				See USA Standard C29.1-1961, Section
Number of Units per Stack	1 (TR 164)	2 (TR 166)	3 (TR 167)	4 (TR 168)	
Dimensions					
Leakage distance, in.	33	66	99	132	2.5.2
Dry arcing distance, in.	14 3/4	29	44	58	2.5.3
Mechanical Values					
Cantilever strength—upright, lb	4,000	2,000	1,000	1,000	5.1.4.1
Cantilever strength—underhung, lb	3,500	2,000	1,000	1,000	5.1.4.1
Tensile strength, lb	12,000				5.1.4.3
Torsional strength, in.-lb	30,000				5.1.4.2
Compression strength, lb	60,000				5.1.4.4
Tension proof, lb	2,000				7.2.2
Electrical Values					
Low-frequency dry withstand, kv	115	205	280	385	4.4
Low-frequency wet withstand, kv	75	160	230	315	4.5
Impulse withstand, kv	210	350	550	750	4.8
Low-frequency puncture, kv	225				4.11
Radio-Influence-Voltage Data					
Low-frequency test voltage, kv	22	44	73	103	4.9
Maximum riv at 1,000 kc, microvolts	100	200	200	500	4.9

NOTES

1. If high-resistance coatings are applied to the insulator, such coatings shall be considered as effective leakage surfaces, and the distance over them shall be included in the leakage distance.
2. Flashover and withstand ratings are predicated on the use of a sub-base 3 1/2 inches in height or its equivalent.

NEMA Standard 7-7-1965, revised 8-20-1966; 11-16-1967.

Fig. 17
Apparatus Insulator, Cap and Pin Type

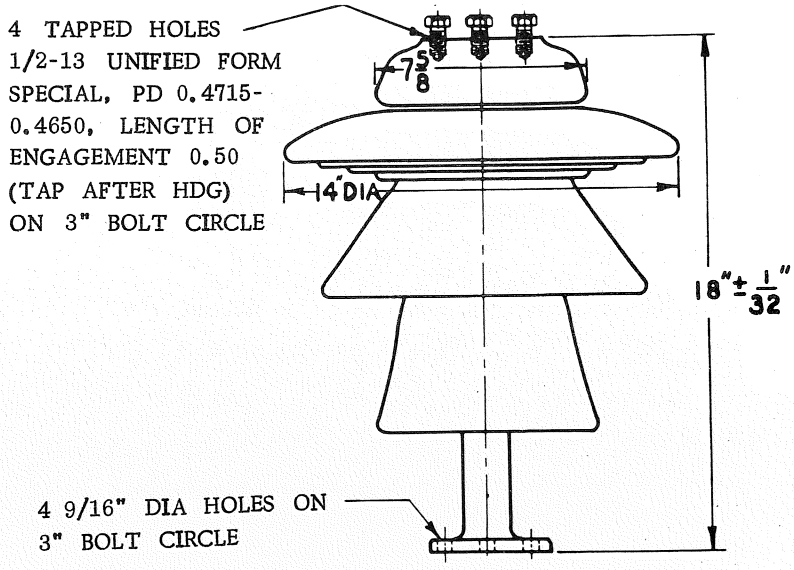
4 TAPPED HOLES 1/2-13 UNIFIED FORM SPECIAL, PD 0.4715-0.4650, LENGTH OF ENGAGEMENT 0.50 (TAP AFTER HDG) ON 3" BOLT CIRCLE
7 5/8
14" DIA
18" ± 1/32"
4 9/16" DIA HOLES ON 3" BOLT CIRCLE

TECHNICAL REFERENCE NO. 165

	Rating			See USA Standard C29.1-1961, Section
Number of Units per Stack	1 (TR 165)	2 (TR 169)	3 (TR 170)	
Dimensions				
Leakage distance, in.	36	72	108	2.5.2
Dry arcing distance, in.	17	34	51	2.5.3
Mechanical Values				
Cantilever strength--upright, lb	3,000	1,000	1,000	5.1.4.1
Cantilever strength--underhung, lb	2,000	1,000	1,000	5.1.4.1
Tensile strength, lb	12,000			5.1.4.3
Torsional strength, in.-lb	30,000			5.1.4.2
Compression strength, lb	60,000			5.1.4.4
Tension proof, lb	2,000			7.2.2
Electrical Values				
Low-frequency dry withstand, kv	120	250	335	4.4
Low-frequency wet withstand, kv	100	200	275	4.5
Impulse withstand, kv	250	450	650	4.8
Low-frequency puncture, kv	225			4.11
Radio-Influence-Voltage Data				
Low-frequency test voltage, kv	30	73	88	4.9
Maximum riv at 1,000 kc, microvolts	200	200	200	4.9

NOTES

1. If high-resistance coatings are applied to the insulator, such coatings shall be considered as effective leakage surfaces, and the distance over them shall be included in the leakage distance.

2. Flashover and withstand ratings are predicated on the use of a sub-base 3 1/2 inches in height or its equivalent.

NEMA Standard 7-7-1965, revised 8-20-1966; 11-16-1967.

Part 9

POST-TYPE APPARATUS INSULATORS

The following constitute Part 9 of this NEMA Publication No. HV 1:

1. USA Standard for Wet-Process Porcelain Insulators (Apparatus, Post Type), C29.9-1961 (approved as a NEMA Standard 9-29-1960). *

2. USA Standard Supplement C29.9a-1965 (approved as a NEMA Standard 7-7-1965). *

* On August 20, 1966, NEMA approved the following revisions in C29.9-1961 and C29.9a-1965:

a. In Figures 1, 2, 3, 4, 5 and 6, change "PD 0.4665-0.4600" to "PD 0.4715-0.4650" for tapped holes 1/2-13 unified form special.

b. In Figures 7, 8, 9 and 10, change "PD 0.5832-0.5760" to "PD 0.5882-0.5810" for tapped holes 5/8-11 unified form special.

c. In Figures 11, 12 and 13, change "PD 0.7027-0.6950" to "PD 0.7077-0.7000" for tapped holes 3/4-10 unified form special.

On November 16, 1967, NEMA approved the following revisions in C29.9-1961 and C29.9a-1965:

d. Delete paragraphs 9.3.1, 9.3.2 and 9.3.5.

e. In the tabulations following Figures 1 through 13, delete all references to low-frequency dry flashover, low-frequency wet flashover, critical-impulse flashover (positive), and critical-impulse flashover (negative).

Copies of C29.9-1961 and C29.9a-1965 are available from the:

USA Standards Institute
10 East 40th Street
New York, N.Y. 10016

NOTE—See Part 20 of this NEMA Publication No. HV 1 for a summary of the characteristics of post-type apparatus insulators.

Part 20
APPARATUS INSULATORS

Tables 20-1, 20-2 and 20-3 on pages 14 to 19, inclusive, contain a summary of the characteristics of cap- and pin-type insulators and post-type insulators. The information in these tables is given to assist in the application of apparatus insulators.

The following notes apply to Table 20-1:

▲ The data shown on these lines are Authorized Engineering Information (approved by NEMA October 7, 1959) relating to insulators which have been used in limited or special applications: for other information on these insulators see USA Standard C29.8-1961 (see Part 8 of this NEMA Publication No. HV 1).

The data shown on lines not marked ▲ are NEMA Standards taken from the USA Standard C29.8-1961 (see Part 8 of this NEMA Publication No. HV 1).

† Values for a single unit apply for the stack.

NOTE I—If high resistance coatings are applied to the insulators, such coatings shall be considered effective leakage surfaces, and the distance over them shall be included in the leakage distance.

NOTE II—Withstand ratings for stacks containing TR numbers 140, 141, 142 and 144 are predicated on the use of a sub-base 3 1/2 inches high, or its equivalent.

NOTE III—The following bolt circle and tapping are standard:

3-inch bolt circle—4 tapped holes 1/2-13 unified form special, PD 0.4715-0.4650, length of engagement 0.50 (tap after hdg)

5-inch bolt circle—4 tapped holes 5/8-11 unified form special, PD 0.5882-0.5810, length of engagement 0.625 (tap after hdg)

7-inch bolt circle—4 tapped holes 3/4-10 unified form special, PD 0.7077-0.7000, length of engagement 0.75 (tap after hdg)

10-inch bolt circle—8 tapped holes 5/8-11 unified form special, PD 0.5882-0.5810, length of engagement 0.625 (tap after hdg)

Table 20-1
Summary of Characteristics of Apparatus Insulators—Cap and Pin Type

Technical Reference Number		Number of Units per Stack	Height per Stack, Inches	Diameter, Inches	Maximum Cap Diameter, Inches	Bolt Circle Diameter, Inches	Cantilever Strength, Pounds		Tensile Strength, Pounds	Torsional Strength, Inch-pounds	Compression Strength, Pounds
Stack	Unit						Upright	Underhung			
...	1	1	7 1/2	7	5	3	2000	1000	5000	6000	10000
...	4	1	10	8	5	3	2000	1000	5000	7000	10000
...	7	1	12	10 1/2	6	3	2000	1000	5000	8000	10000
...	10	1	15	13	6	3	2000	1000	7000	10000	15000
...	13	1	18	14	7 5/8	3	2000	1000	8000	12000	15000
16	147	2	29	14	8	3	1500	1000	†	†	†
...	41	1	8	9	6 1/2	5	4000	3000	10000	12000	20000
...	44	1	10	10	6 3/4	5	4000	3000	10000	14000	20000
...	46	1	12	12	8	5	4000	3000	10000	16000	20000
...	49	1	15	14	8 1/4	5	4000	3000	14000	20000	30000
▲ ...	53	1	20	17	9 3/8	5	4000	2500	15000	20000	30000
56	140	2	29	17	9 3/4	5	3000	2350	†	†	†
19	140	3	43 1/2	17	9 3/4	5	1700	1470	†	†	†
25	140	4	58	17	9 3/4	5	1200	1070	†	†	†
123	141	4	58	18	10 7/8	5	2000	1750	†	†	†
126	140	5	72 1/2	17	9 3/4	5	910	840	†	†	†
27	141	5	72 1/2	18	10 7/8	5	1450	1350	†	†	†
128	140	6	87	17	9 3/4	5	750	700	†	†	†
28	141	6	87	18	10 7/8	5	1170	1100	†	†	†
129	142	6	87	18	10 7/8	7	1170	1100	†	†	†
▲ 131	141	7	101 1/2	18	10 7/8	5	1000	950	†	†	†
133	142	7	101 1/2	18	10 7/8	7	1000	950	†	†	†
▲ 136	141	8	116	18	10 7/8	5	900	860	†	†	†
135	142	8	116	18	10 7/8	7	900	860	†	†	†
▲ 153	142	9	130 1/2	18	10 7/8	7	770	740	†	†	†
▲ 157	142	10	145	18	10 7/8	7	680	660	†	†	†
...	147	1	14 1/2	14	8	3	3000	2000	12000	15000	25000
...	140	1	14 1/2	17	9 3/4	5	7000	4000	20000	40000	60000
...	141	1	14 1/2	18	10 7/8	5	10000	6000	25000	90000	75000
...	142	1	14 1/2	18	10 7/8	7	10000	6000	25000	90000	75000
▲ ...	144	1	14 1/2	19 1/2	12	10	13000	8000	25000	90000	75000

See Page 13 for notes applying to Table 20-1.

	Radio-influence-voltage Data					Low-frequency Withstand, Kv			Technical Reference Number	
Tension Proof, Pounds	Low-frequency Test Voltage, Kv	Max. riv, Microvolts at 1000 Kc	Low-frequency Puncture, Kv	Leakage Distance, Inches	Dry-arcing Distance, Inches	Dry	Wet	Impulse Withstand, Kv	Stack	Unit
1250	5	50	80	7 1/2	5 1/4	36	30	95	...	1
1250	10	50	115	12	7 1/4	50	45	110	...	4
1250	15	100	145	20	9 1/2	70	60	150	...	7
1750	22	100	195	28	13 1/2	95	80	200	...	10
2000	30	200	225	36	17	120	100	250	...	13
....	44	200	...	52	28	175	145	350	16	147
2000	5	50	90	8	5 1/4	36	30	95	...	41
2000	10	50	115	14	7 1/4	50	45	110	...	44
2000	15	100	145	18	9 1/2	70	60	150	...	46
2000	22	100	195	28	13 1/2	95	80	200	...	49
2000	30	200	225	36	17	120	100	250	▲ ...	53
....	44	200	...	66	29	205	160	350	56	140
....	73	200	...	99	44	280	230	550	19	140
....	103	500	...	132	58	385	315	750	25	140
....	103	500	...	132	58	385	315	750	123	141
....	125	500	...	165	73	465	385	900	126	140
....	125	500	...	165	73	465	385	900	27	141
....	146	500	...	198	87	545	455	1050	128	140
....	146	500	...	198	87	545	455	1050	28	141
....	146	500	...	198	87	545	455	1050	129	142
....	180	1000	...	231	102	610	525	1300	▲ 131	141
....	180	1000	...	231	102	610	525	1300	133	142
....	210	1000	...	264	116	680	590	1470	▲ 136	141
....	210	1000	...	264	116	680	590	1470	135	142
....	240	2000	...	297	130	745	650	1640	▲ 153	142
....	270	2000	...	330	144	810	710	1800	▲ 157	142
2000	22	100	195	26	13 3/4	95	70	190	...	147
2000	22	100	215	33	14 3/4	115	75	210	...	140
2000	22	100	215	33	14 3/4	115	75	210	...	141
2000	22	100	215	33	14 3/4	115	75	210	...	142
2000	22	100	215	30	14 1/2	115	75	210	▲ ...	144

Table 20-2
Summary of Characteristics of Mixed Apparatus Insulators—Cap and Pin Type

Technical Reference Number							Cantilever Strength, Pounds				
Stack	Unit, See Note	Number of Units per Stack	Height per Stack, Inches	Diameter, Inches	Maximum Cap Diameter, Inches	Bolt Circle Diameter, Inches	Upright	Underhung	Tensile Strength, Pounds	Torsional Strength, Inch-pounds	Compression Strength, Pounds
22	X	3	49	†	†	†	1450	1250	†	†	†
26	III	4	58	†	†	†	1700	....	†	†	†
132	IV	7	102 7/8	†	†	†	1450	....	†	†	†
33	V	8	117 3/8	†	†	†	1170	....	†	†	†
137	VI	8	117 3/8	†	†	†	1240	....	†	†	†
154	VII	9	131 7/8	†	†	†	1090	....	†	†	†
158	VIII	10	146 3/8	†	†	†	970	....	†	†	†

The above data are Authorized Engineering Information (approved by NEMA March 9, 1960) relating to insulators which have been used in limited or special applications; for other information on these insulators, see USA Standard C29.8-1961 (see Part 8 of this NEMA Publication No. HV 1).

†Unit characteristics appear in Table 20-1.

NOTE I —If high resistance coatings are applied to the insulators, such coatings shall be considered effective leakage surfaces, and the distance over them shall be included in the leakage distance.

NOTE II —Withstand ratings are predicated on the use of a sub-base 3 1/2 inches high, or its equivalent, except for TR number 53.

NOTE III—Three TR number 140 and one TR number 141.

Tension Proof, Pounds	Radio-influence-voltage Data: Low-frequency Test Voltage, Kv	Radio-influence-voltage Data: Max. riv, Microvolts at 1000 Kc	Low-frequency Puncture, Kv	Leakage Distance, Inches	Dry-arcing Distance, Inches	Low-frequency Withstand, Kv: Dry	Low-frequency Withstand, Kv: Wet	Impulse Withstand, Kv	Technical Reference Number: Stack	Technical Reference Number: Unit, See Note
†	88	200	†	102	46	335	275	650	22	X
†	103	500	†	132	58	375	305	725	26	III
†	180	1000	†	225	102	610	525	1300	132	IV
†	210	1000	†	258	116	680	590	1470	33	V
†	210	1000	†	255	116	680	590	1470	137	VI
†	240	2000	†	288	131	745	650	1640	154	VII
†	270	2000	†	321	145	810	710	1800	158	VIII

NOTE IV —Five TR number 142 and two TR number 144 with transition plate TR number 151.

NOTE V —Six TR number 142 and two TR number 144 with transition plate TR number 151.

NOTE VI —Five TR number 142 and three TR number 144 with transition plate TR number 151.

NOTE VII —Six TR number 142 and three TR number 144 with transition plate TR number 151.

NOTE VIII —Seven TR number 142 and three TR number 144 with transition plate TR number 151.

NOTE IX —See Fig. 20-1, page 20, for drawing of transition plate TR number 151.

NOTE X —Two TR number 140 and one TR number 53 (on top).

Table 20-3
Summary of Characteristics of Apparatus Insulators—Post Type

Technical Reference Number	Height per Stack, Inches	Diameter, Inches	Maximum Cap Diameter, Inches	Bolt Circle Diameter, Inches	Cantilever Strength, Pounds		Tensile Strength, Pounds	Torsional Strength, Inch-pounds	Compression Strength, Pounds
					Upright	Underhung			
202	7 1/2	7	5	3	2000	2000	5000	6000	10000
205	10	7	5	3	2000	2000	5000	7000	10000
208	14	7	6	3	2000	2000	5000	8000	10000
210	18	7 1/2	6	3	2000	2000	7000	10000	15000
214	22	8	7 5/8	3	2000	2000	8000	12000	15000
216	30	9 1/8	8	3	1500	1500	12000	15000	25000
222	10	7 1/2	6 1/2	5	4000	4000	10000	12000	20000
225	12	8	6 3/4	5	4000	4000	10000	14000	20000
227	15	9	8	5	4000	4000	10000	16000	20000
231	20	10	8 1/4	5	4000	4000	14000	20000	30000
▲ 267	24	10	9 3/8	5	4000	4000	15000	20000	30000
▲ 278	30	11	9 3/4	5	3000	3000	20000	40000	60000
▲ 286	45	10	9 3/4	5	1700	1470	20000	40000	60000
▲ 287	45	....	......	5	2900	2900	25000	90000	75000
▲ 288	54	....	......	5	1450	1450	20000	40000	60000
▲ 289	54	....	......	5	2450	2450	25000	90000	75000
▲ 291	62	11	10 1/2	5	1200	1070	20000	40000	60000
▲ 295	62	....	......	5	2000	2000	25000	90000	75000
▲ 304	80	....	......	5	910	910	20000	40000	60000
▲ 308	80	....	......	5	1450	1450	25000	90000	75000
▲ 312	92	....	......	5	750	750	20000	40000	60000
▲ 316	92	....	......	5	1170	1170	25000	90000	75000
▲ 324	106	....	......	5	1000	1000	25000	90000	75000
▲ 330	122	....	......	5	900	900	25000	90000	75000

▲ The data shown on these lines are Authorized Engineering Information (approved by NEMA November 13, 1963) relating to insulators which have been used in limited or special applications; for other information on these insulators, see USA Standard C29.9-1961 (see Part 9 of this NEMA Publication No. HV 1).

The data shown on lines not marked ▲ are NEMA Standards taken from USA Standard C29.9-1961 (see Part 9 of this NEMA Publication No. HV 1).

NOTE I—If high resistance coatings are applied to the insulators, such coatings shall be considered effective leakage surfaces, and the distance over them shall be included in the leakage distance.

Tension Proof, Pounds	Radio-influence-voltage Data: Low-frequency Test Voltage, Kv	Radio-influence-voltage Data: Max. riv, Microvolts at 1000 Kc	Leakage Distance, Inches	Dry-arcing Distance, Inches	Low-frequency Withstand, Kv: Dry	Low-frequency Withstand, Kv: Wet	Impulse Withstand, Kv	Technical Reference Number
1250	5	50	10 1/2	6	36	30	95	202
1250	10	50	15 1/2	7 1/4	50	45	110	205
1250	15	100	24	10 1/2	70	60	150	208
1750	22	100	37	14 1/2	95	80	200	210
2000	30	200	43	17	120	100	250	214
2000	44	200	72	26	175	145	350	216
2000	5	50	10 1/2	6	36	30	95	222
2000	10	50	15 1/2	7 1/4	50	45	110	225
2000	15	100	24	10 1/2	70	60	150	227
2000	22	100	37	14 1/2	95	80	200	231
2000	30	200	43	17	120	100	250	▲ 267
2000	44	200	72	26	175	145	350	▲ 278
2000	73	200	99	39	280	230	550	▲ 286
2000	73	200	99	39	280	230	550	▲ 287
2000	88	200	116	45	335	275	650	▲ 288
2000	88	200	116	45	335	275	650	▲ 289
2000	103	500	132	51	385	315	750	▲ 291
2000	103	500	132	51	385	315	750	▲ 295
2000	125	500	165	64	465	385	900	▲ 304
2000	125	500	165	64	465	385	900	▲ 308
2000	146	500	198	76	545	455	1050	▲ 312
2000	146	500	198	76	545	455	1050	▲ 316
2000	180	1000	231	90	610	525	1300	▲ 324
2000	210	1000	264	102	680	590	1470	▲ 330

NOTE II—The following bolt circle and tapping are standard:

3-inch bolt circle—4 tapped holes 1/2-13 unified form special,
PD 0.4715-0.4650,
length of engagement 0.50 (tap after hdg)

5-inch bolt circle—4 tapped holes 5/8-11 unified form special,
PD 0.5882-0.5810,
length of engagement 0.625 (tap after hdg)

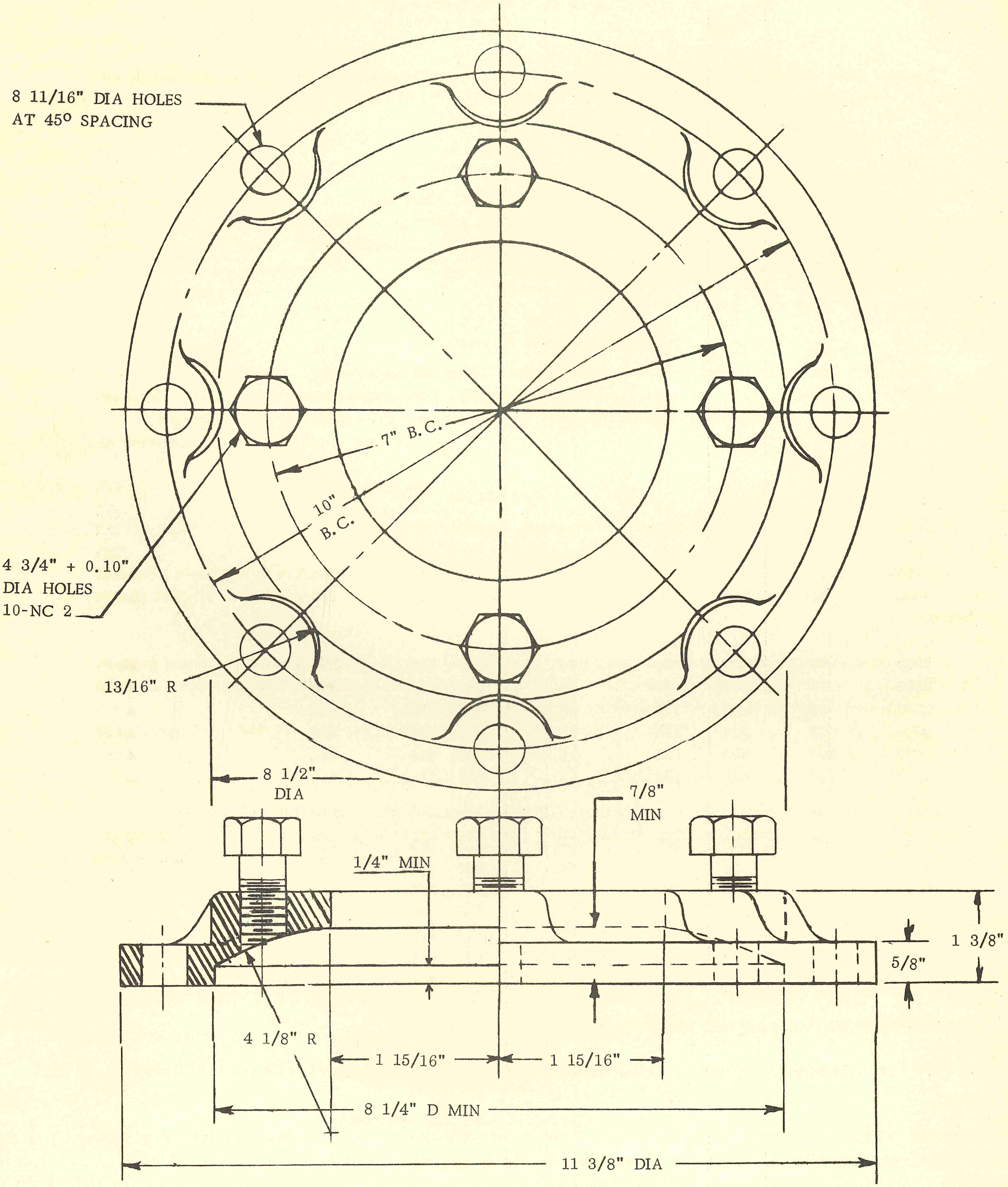
8 11/16" DIA HOLES
AT 45° SPACING
7" B.C.
10" B.C.
4 3/4" + 0.10"
DIA HOLES
10-NC 2
13/16" R
8 1/2" DIA
7/8" MIN
1/4" MIN
1 3/8"
5/8"
4 1/8" R
1 15/16"
1 15/16"
8 1/4" D MIN
11 3/8" DIA

Fig. 20-1
TRANSITION PLATE (UPRIGHT) TR NUMBER 151

NEMA STANDARDIZATION

The purpose of NEMA Standards, their classification and status are set forth in certain clauses of the NEMA By-Laws, which are quoted below:

Purpose of Standards

National Electrical Manufacturers Association Standards are adopted in the public interest and are designed to eliminate misunderstandings between the manufacturer and the purchaser and to assist the purchaser in selecting and obtaining the proper product for its particular need. Existence of a National Electrical Manufacturers Association Standard does not in any respect preclude any member or non-member from manufacturing or selling products not conforming to the Standard.

(By-Law--Art. V, Sec. 1)

Definition of a Standard

A Standard of the National Electrical Manufacturers Association defines a product, process or procedure with reference to one or more of the following: nomenclature, composition, construction, dimensions, tolerances, safety, operating characteristics, performance, quality, rating, testing and the service for which designed.

(By-Law--Art. V, Sec. 2, Subsection A)

Classes of Standards

National Electrical Manufacturers Association Standards are of two classes:

1. NEMA Standard, which relates to a product commercially standardized and subject to repetitive manufacture, which standard has been approved by at least 90 per cent of the members of the Subdivision eligible to vote thereon;

2. Suggested Standard for Future Design, which may not have been regularly applied to a commercial product, but which suggests a sound engineering approach to future development, which standard has been approved by at least two-thirds of the members of the Subdivision eligible to vote thereon.

(By-Law--Art. V, Sec. 2, Subsection B)

Authorized Engineering Information

Authorized Engineering Information consists of explanatory data and other engineering information of an informative character not falling within the classification of NEMA Standard or Suggested Standard for Future Design.

(By-Law--Art. V, Sec. 6, 1st Sentence)

Identification of Status

At the end of each standard in this publication appear the words "NEMA Standard" or Suggested Standard for Future Design," which indicate the status of the standard. These words are followed by a date which indicates when that standard was adopted in its present form by the Association.

The classification "Authorized Engineering Information" is designated similarly.

NOTE--These standards may be copied without change provided due credit is given to the National Electrical Manufacturers Association.

HIGH VOLTAGE INSULATOR SECTION
OF THE
NATIONAL ELECTRICAL MANUFACTURERS ASSOCIATION

MEMBER COMPANIES

Acme Steel & Malleable Iron Works
Buffalo, N. Y.

Brewer-Titchener Corp., The
Cortland, N. Y.

Chance, A. B., Co.
Centralia, Mo.

General Electric Co.
Baltimore, Md.

I-T-E Circuit Breaker Co.
Philadelphia, Pa.

Joslyn Manufacturing and Supply Co.
Lima, N. Y.

Knox Porcelain Corp.
Knoxville, Tenn.

Lapp Insulator Company, Inc.
LeRoy, N. Y.

McGraw-Edison Power Systems Division
Macomb, Ill.

Ohio Brass Co.
Mansfield, Ohio

Preformed Line Products Co.
Cleveland, Ohio

Westinghouse Electric Corp.
Derry, Pa.

Printed in U.S.A.